DOCTOR OF PHILOSOPHY

Novel Variants of the DNA Damage Checkpoint Protein Hus1 in Fission Yeast and Human Cells

Al Mahmoud, Widad

Award date:
2014

Awarding institution:
Bangor University

Novel Variants of the DNA Damage Checkpoint Protein Hus1 in Fission Yeast and Human Cells

Widad Abdulsamad Mansour Al-Mahmoud

School of Biology Science

University of Bangor

A thesis submitted for the degree of

Doctor of Philosophy

June 2014

Declaration and Consent

Details of the Work

I hereby agree to deposit the following item in the digital repository maintained by Bangor University and/or in any other repository authorized for use by Bangor University.

Author Name: Widad Abdulsamad Mansour Al-Mahmoud

Title: Novel Variants Identification of the DNA Damage Checkpoint Protein Hus1 in Fission Yeast and Human Cells

Supervisor/Department: Thomas Caspari / School of Biology Science

Funding body (if any):

Qualification/Degree obtained: PhD

This item is a product of my own research endeavours and is covered by the agreement below in which the item is referred to as "the Work". It is identical in content to that deposited in the Library, subject to point 4 below.

Non-exclusive Rights

Rights granted to the digital repository through this agreement are entirely non-exclusive. I am free to publish the Work in its present version or future versions elsewhere.

I agree that Bangor University may electronically store, copy or translate the Work to any approved medium or format for the purpose of future preservation and accessibility. Bangor University is not under any obligation to reproduce or display the Work in the same formats or resolutions in which it was originally deposited.

Bangor University Digital Repository

I understand that work deposited in the digital repository will be accessible to a wide variety of people and institutions, including automated agents and search engines via the World Wide Web.

I understand that once the Work is deposited, the item and its metadata may be incorporated into public access catalogues or services, national databases of electronic theses and dissertations such as the British Library's EThOS or any service provided by the National Library of Wales.

I understand that the Work may be made available via the National Library of Wales Online Electronic Theses Service under the declared terms and conditions of use (http://www.llgc.org.uk/index.php?id=4676). I agree that as part of this service the National Library of Wales may electronically store, copy or convert the Work to any approved medium or format for the purpose of future preservation and accessibility. The National Library of Wales is not under any obligation to reproduce or display the Work in the same formats or resolutions in which it was originally deposited.

Statement 1:

This work has not previously been accepted in substance for any degree and is not being concurrently submitted in candidature for any degree unless as agreed by the University for approved dual awards.

Signed …….. (candidate)

Date ……..

Statement 2:

This thesis is the result of my own investigations, except where otherwise stated. Where correction services have been used, the extent and nature of the correction is clearly marked in a footnote(s).

All other sources are acknowledged by footnotes and/or a bibliography.

Signed ……. (candidate)

Date …….

Statement 3:

I hereby give consent for my thesis, if accepted, to be available for photocopying, for inter-library loan and for electronic repositories, and for the title and summary to be made available to outside organisations.

Signed ……. (candidate)

Date …….

NB: Candidates on whose behalf a bar on access has been approved by the Academic Registry should use the following version of **Statement 3:**

Statement 3 (bar):

I hereby give consent for my thesis, if accepted, to be available for photocopying, for inter-library loans and for electronic repositories after expiry of a bar on access.

Signed …… (candidate)

Date ……

Statement 4:

Choose **one** of the following options

a) I agree to deposit an electronic copy of my thesis (the Work) in the Bangor University (BU) Institutional Digital Repository, the British Library ETHOS system, and/or in any other repository authorized for use by Bangor University and where necessary have gained the required permissions for the use of third party material.	
b) I agree to deposit an electronic copy of my thesis (the Work) in the Bangor University (BU) Institutional Digital Repository, the British Library ETHOS system, and/or in any other repository authorized for use by Bangor University when the approved **bar on access** has been lifted.	
c) I agree to submit my thesis (the Work) electronically via Bangor University's e-submission system, however I **opt-out** of the electronic deposit to the Bangor University (BU) Institutional Digital Repository, the British Library ETHOS system, and/or in any other repository authorized for use by Bangor University, due to lack of permissions for use of third party material.	

Options B should only be used if a bar on access has been approved by the University.

In addition to the above I also agree to the following:

1. That I am the author or have the authority of the author(s) to make this agreement and do hereby give Bangor University the right to make available the Work in the way described above.

2. That the electronic copy of the Work deposited in the digital repository and covered by this agreement, is identical in content to the paper copy of the Work deposited in the Bangor University Library, subject to point 4 below.

3. That I have exercised reasonable care to ensure that the Work is original and, to the best of my knowledge, does not breach any laws – including those relating to defamation, libel and copyright.

4. That I have, in instances where the intellectual property of other authors or copyright holders is included in the Work, and where appropriate, gained explicit permission for the inclusion of that material in the Work, and in the electronic form of the Work as accessed through the open access digital repository, *or* that I have identified and removed that material for which adequate and appropriate permission has not been obtained and which will be inaccessible via the digital repository.

5. That Bangor University does not hold any obligation to take legal action on behalf of the Depositor, or other rights holders, in the event of a breach of intellectual property rights, or any other right, in the material deposited.

6. That I will indemnify and keep indemnified Bangor University and the National Library of Wales from and against any loss, liability, claim or damage, including without limitation any related legal fees and court costs (on a full indemnity bases), related to any breach by myself of any term of this agreement.

Signature: …… Date : ……..

Dedication

To the memory of my parents and elder son…

To my loving, supporter and encouraging, husband ‘Safa’…

To my lovely flowers: Manar, Mustafa and Mariam…

To my sincere sister ‘Suaad’ and to all my family…

I dedicate my work with my wholeheartedly felt love and thanks for all of you,

Widad

Acknowledgment

I would thank the Iraqi Government represented by Iraqi Ministry of Higher Education and Scientific Research who have funded this PhD project.

I express my wholeheartedly felt thanks to my supervisor, Dr Thomas Caspari for his appreciative supervision, kindness and cheerfulness, which surmounted all the obstacles during my project.

I would express my sincere thanks to my research committee, my internal examiner Dr Edgar Hartsuiker for his valuable and kindly inputs on my research project, and the chairmen, Dr Torsten Bossing for his efforts during the first part of my project and Dr Henk Ronald Braig for his advices during the last months of my study.

Many thanks for Dr Fumiko Esashi, Oxford University, for her kind gift of the Flp-In system, the plasmids and the cell line. I especially appreciate Dr Claudia Barros for her kindly help in teaching the imaging by Confocal Microscope.

My sincere thanks also go to Dr Rolf Kraehenuehl and Dr Ellen Vernon for sharing their invaluable knowledge on yeast and human cells research and for daily encouragement.

I would appreciate the kindly help, daily presence and encouragement of the D2 laboratory technician Natalia Harrison. Heartfelt thanks to my PhD colleague's Dylan Jones, Karim Ashour, Mashael Alhusayni, Mohammed Gammash, Saad Aljohani, Salah Adam, Jessica Fletcher and Rabiaa Oun for their daily presence and kindly assistance. Many thanks for everyone have provided any assistance for me during this challenging time.

On a more personal note, I am too grateful to my husband, my lovely children and all my family for their constant love and endless support, encouragement and patience.

Abstract

Hus1 is a highly conserved DNA damage sensor protein, which assembles with Rad9 and Rad1 in the Rad9-Rad1-Hus1 (9-1-1) ring. Although the functions of the 9-1-1 complex are intensively studied, little is known about the Hus1 protein itself. Using *Schizosaccharomyces pombe* and human cells as a model, this PhD project reveals for the first time the existence of N-terminally truncated protein variants of Hus1. Only growing *S. pombe* cells express two variants using leaky ribosomal scanning where ribosomes initiate at the internal start sites AUG32 and AUG46 respectively. Both variants are required for a cell cycle arrest when DNA replication forks are damaged by conveying the signal from the 9-1-1 ring to the checkpoint kinase 1 (Chk1).

The work in human cells confirms the expression of three shorter hHUS1 splice variants (hHUS1-005, hHUS1-011 and hHUS1-004) at RNA level in embryonic kidney cells (HEK293) and cervical cancer cells (HeLa) as well as in different human tissues. Using a monoclonal anti-HUS1 antibody, which recognises all variants in engineered cell lines, the Hus1 protein variants could not be detected at the endogenous level. Nevertheless, the treatment of HEK293 cells, and to a lesser extent HeLa cells, with Hydroxyurea (HU), Methyl methanesulfonate (MMS) and UV light produces a smaller hHUS1 protein, which is predicted to be the hHUS1-005 variant. This variant resembles the *S.pombe* Hus1-32 variant in size and partly in protein sequence. The engineered EGFP-hHUS1-005 protein localises to the cytoplasm and to filamentous structures within the nucleus in HEK293 cells.

In summary, my work provides evidence for a novel role of the truncated Hus1 variants in the activation of the DNA damage checkpoint when DNA replication forks break. It also presents evidence for the expression of related splice variants in human cells, thus suggesting that the biology of the Hus1 variants is conserved.

Abbreviations

2D	Two dimensions
53BP1	Tumor suppressor p53-binding protein 1
5-FOA	5-Fluoroorotic acid
Aph	Aphidicolin
APS	Ammonium Persulfate
ATM	Ataxia telangiectasia mutated
ATR	Ataxia telangiectasia and Rad3-related
BamHI	*Bacillus amyloliquefaciens H*
BAX	Bcl-2-associated X protein
BER	Base Excision Repair
BGH	Bovine growth hormone (BGH) for polyadenylation signal
bp	base pair
BRCA2	breast cancer 2
BSA	Bovine Serum Albumin
CCDS	Consensus Coding Sequence
Cdc2	Cell division cycle 2
CDC25C	Cell division cycle 25C
CDK	Cyclin dependent kinases
cDNA	Complementary DNA
Cds1	CDP-diacylglycerol synthase 1
ChK1	Checkpoint kinase 1
ChK1S345ph	Checkpoint kinase 1-phosph Serin345
CMV	Cytomegalovirus
CPT	Camptothecin
Crb2	Crumbs homolog 2
DAPI	4′,6-Diamidino-2-phenylindole dihydrochloride
DTT	DL-Dithiothreitol
DDT	DNA Damage Tolerance
DEPC	Diethylpyrocarbonate
DMEM	Dulbecco's Modified Eagle's Medium
DMSO	Dimethyl sulfoxide
DNA	Deoxyribonucleic acid
dNTP	Deoxyribonucleotide triphosphate
DSBs	Double strand breaks
dsDNA	double stranded Deoxyribonucleic acid
dsRNA	double stranded RNA
E.coli	*Escherichia coli*
EDTA	Ethylenediamine tetraacetic acid
EGFP	Enhanced Green Fluorescent Protein
EGTA	Ethylene glycol-bis(2-aminoethylether)-N,N,N′,N′-tetraacetic acid
EMM	Edinburg Minimal Media
Exo1	Exonuclease 1
FANCD2	Fanconi Anaemia Complementation group D2
FBS	Fetal Bovine Serum
FRT	Flippase recognition target

GAPDH	Glyceralaldehydephosphate-dehydrogenase
GFP	Green Fluorescent Protein
GGR	Global Genome Repair
H2AX	H2A histone family, member X
H2O2	Hydrogen peroxide
H3S10ph	Histon H3 phospho- serin10
HCl	Hydrochloric acid
H-DBAS	Human-Transcriptome Database for Alternative Splicing
HEK293	Human Embryonic Kidney 293 cells
HeLa	Cervix cells obtained from the patient “Henrietta Lacks”
HR	Homologous Recombination
HU	Hydroxyurea
HUS1	Hydroxyurea sensitive
HUS1B	Hydroxyurea sensitive B
IGD	Human Intronless Gene Database
IPTG	Isopropylthio-β-galactoside
KAc	Potassium acetate
kDa	Kilo Dalton
LBA	Luria Bertani Agar
LiOAc	Lithium acetate
LiOAc/TE	Lithium acetate/ Tris-EDTA
MAPK	Mitogen-Activated Protein Kinase
MDC1	Mediator of DNA damage checkpoint protein 1
ME	Malt Extract
MEA	Malt Extract Agar
MgCl2	Magnesium Chloride
min	Minute
MMC	mitomycin C
MMR	Mismatch Repair
MMS	Methyl methane sulfonate
MRC1	Mannose Receptor, C Type 1 gene
mRNA	Messenger ribonucleic acid
Na2EDTA.2H2O	Ethylenediaminetetraacetic acid disodium salt dihydrate
$Na_2HPO_4.7H_2O$	Sodium phosphate dibasic heptahydrate
NaCl	Sodium Chloride
NaH2PO4	Sodium phosphate monobasic
NaOH	Sodium Hydroxide
NBS1	Nibrin
NCBI	National Center for Biotechnology Information database
NEB	New England Biolabs
NER	Nucleotide Excision Repair
NH4OAc	Ammonium acetate
NHEJ	Non Homologous End Joining
nu	Nucleotides
ORF	Open Reading Frame
p16INK4B	cyclin-dependent kinase inhibitor 2A
P21WAF1/CIP1	Cyclin-dependent kinase inhibitor 1
p38 MAPK	p38 mitogen-activated protein kinases
p53	Tumor suppressor p53
PBS	phosphate- buffered saline

PCR	Polymerase Chain Reaction
PEG/LiOAc/TE	Polyethylene glycol standard/ Lithium acetate/ Tris-EDTA
PEG4000	Polyethylene glycol standard
PEM	PIPES/ EGTA/ MgCl2
PEMS	PIPES/ EGTA/ MgCl2/Sorbitol
PER2	Period circadian protein homolog 2
PFA	Paraformaldehyde
Phl	Phleomycin
PIPES	piperazine-N,N'-bis(ethanesulfonic acid)
PreOGP	Pre- Osteogenic growth peptide
PRR	Post-Replication Repair
RAD proteins	Radioresistance proteins
RASV	Representative Alternative Splice Variant
Rb	Retinoblastoma protein
RFP	Red Fluorescent Protein
RGB	Red, Green and Blue channels
RMCE	recombinase-mediated cassette exchange
RNA	Ribonucleic acid
RNA Pol III	RNA polymerase III
RNAse Type I A	Ribonuclease Type I A
ROS	Reactive oxygen species
rpm	Revolutions per minute
Rqh1	RecQ type DNA helicase I
RT-PCR	Reverse-Transcriptase Polymerase Chain Reaction
S.pombe	*Schizosaccharomyces pombe*
SCE	Sister chromatid exchange
SDS	Sodium dodecyl sulfate
SDSA	Synthesis-dependent strand annealing
SDS-PAGE	Sodium dodecyl sulfate-Polyacrylamide gel electrophoresis
SEC	Size Exclusion Chromatography
Sgs1	small growth suppressor 1
shRNA	short hairpin RNA or small hairpin RNA
siRNA	small interfering RNA
SMC1	Structural Maintenance of Chromosome
sORF	short Open Reading Frame
ssDNA	Singl stranded Deoxyribonucleic acid
TAE	Tris-Acetate-EDTA
TCA	Trichloroacetic acid
TCR	Transcription-Coupled Repair
TE	Tris-EDTA
Tel1	Telomere I
TEMED	Tetramethylethylenediamine
Tet	Tetracyclin
TLS	Translesion synthesis
TRI	Trizol
UTR	Un-Translated Region
UV	Ultraviolet
UVB	Ultraviolet B
V	Volt
w/v	Weight/ Volume

Wt	Wild type
X-Gal	5-Bromo-4-chloro-3-indolyl β-D-galactopyranoside
YEA	Yeast Extract Agar
YEL	Yeast Extract Liquid

Contents

List of Figures:

Chapter1

Chapter2

Chapter 3

Chapter 4

Chapter 5

Chapter 6

Chapter 7

List of Tables:

Chapter 2

Chapter 7

Chapter 1: Introduction

1.1 Aims of the Project

The elements of the DNA damage checkpoint pathways are intensively researched resulting in a sound understanding of the underlying processes. After the recent discovery of the N-terminally truncated protein variant of the DNA damage checkpoint protein Rad9 (Janes, et.al. 2012) in fission yeast (*S.pombe*), and the identification of a similarly truncated variant of the human DNA damage checkpoint kinase Chk1 (Pabla, et.al. 2012), it became clear that cells operate a second layer of the checkpoint pathways by utilizing these alternative proteins.

This project was informed by the observation of several smaller variants of the *S. pombe* checkpoint protein Hus1 (Caspari, et.al. 2000). The aims of the work are **(1)** to investigate the cellular mechanisms resulting in the production of these N-terminally truncated Hus1 variants, **(2)** to identify some of their cellular roles and **(3)** to find out whether they also exist in human cells.

1.2 Introduction

Genomic information is susceptible to various types of exogenous and endogenous damages, which result in genetic mutations or chromosomes aberrations and, eventually, may trigger cell death or cause cancer in multicellular organisms (Shackelford, et.al. 1999; Kastan & Bartek, 2004). In order to overcome these problems, cells evolved DNA damage checkpoints and DNA repair mechanisms to maintain their genome integrity (Wang, 1998; Niida & Nakanishi, 2006). Important insights resulted from different studies on prokaryotic and eukaryotic cell lines. In this PhD study, I used yeast cells (*S.pombe*) (Palermo & Walworth, 2007) and human cells (HeLa and HEK293 cell lines) (Thomas & Smart, 2005) as eukaryotic genetic models. That was to get more insights into the biology of the Hus1 variants, which are produced by *S. pombe* (Caspari, et.al. 2000), and to verify the ability of

human cells to produce similar Hus1 alternative splice variants. The human genome contains two *hus1* genes, *hHUS1* and *hHUS1B*, which are closely related. Currently the Ensemble database curates three protein coding splice variants for *hHUS1*, *hHUS1-005*, *hHUS1-011 and hHUS1-004*; whereas the hHUS1B cannot give rise to similar variants due to the absence of introns, (http://www.ensembl.org, accessed 12 June 2014).

In the following paragraphs, I will introduce the principles of DNA damage checkpoint signalling in fission yeast and human cells.

1.3 Cell cycle phases

Cells have to pass the accurate genomic information to their daughter cells to ensure their survival with no genome aberrations. Consequently, cells have to maintain their progression through cell cycle phases, G1, S, G2 and M phase in a coordinated manner (Nurse, 1990). The main two phases are DNA replication (S) and mitosis (M). In the first one, cells perform DNA synthesis, whereas in mitosis, the genomic information is passed to the daughter cells equally and faithfully. These two phases are separated by the gap phases G1 and G2 before and after S phase, respectively. In both gap phases, the cells are very active and perform RNA and protein synthesis. Collectively, scientists referred to the G1, S and G2 phases as interphases, which means between mitosis (Harper & Brooks, 2005). These phases are conserved in eukaryotic cells from the unicellular (yeast) to multicellular organisms (human) (Palermo & Walworth, 2007). Cells, which starve for nutrients or differentiate, can exit the cell cycle in G1 into the resting phase known as G0 (G zero).

1.4 Cell cycle progression in unperturbed cells

A group of proteins Serine/Threonine kinases called Cyclin-Dependent kinases (CDKs) control unperturbed cell cycle progression in all eukaryotic cells. Such proteins regulate cell cycle progression events and control entry into S and M phase (Lee & Nurse, 1988; Nurse, 1990). Cyclin-dependent kinase (CDK1) was first identified in fission yeast mutants, which entered mitosis too early (Nurse, 1975). The affected gene was called *cdc2* in *S.pombe* (fission yeast), *cdc28* in *S.cerevisae* (budding yeast). The *cdc2* homologues were identified

later in human cells and named CDK. From the 11 known human CDKs, only four (CDK1, 2, 3 and 4) have a well-characterised role in cell cycle progression (Russell & Nurse, 1986; Lee & Nurse, 1988; Malumbres & Barbacid, 2005).

Cyclin-dependent kinases have to form a protein complex with their partners, the Cyclins, in order to perform their cell cycle control. While CDK expression levels are independent of the cell cycle phases, it was shown that cyclins expression is restricted to defined stages of the cycle (this was the way in which they were discovered) (Evans, et.al. 1983). Interestingly, in fission yeast three of the four mitotic cyclins can be removed from the cell since only the G2 cyclin B (Cdc13) is sufficient to drive a coordinated cell cycle with Cdc2 (Coudreuse & Nurse, 2010). Moreover, CDK-Cyclin complexes have a reversible phosphorylation feature, which is important for cell cycle control in both perturbed and unperturbed cells (Morgan, 2007). That allows their negative regulation by Wee1 and Myt1-mediated phosphorylation at their active site at tyrosine 15 (Y15) and threonine 14 (T14) of CDK (Figure 1-1) (Russell & Nurse, 1987). Conversely, CDK-cyclin complexes are positively controlled by their Cdc25- mediated de-phosphorylation mainly at Y15 (Russell and Nurse, 1986). In addition, the conserved Threonine site (T160) of CDK2 is modified by CDK-activating kinases (CAKs) (Yata & Esashi, 2009). In unperturbed cells, CDKs play an essential role to regulate basic cell growth mechanisms. It was shown that such proteins are responsible for DNA replication and cell division. CDKs activate DNA replication at pre-loaded origins of replication at the G1-S transition (Diffley, 2004). Moreover, they prevent DNA replication re-initiation in S and G2 phase (Kiang, et.al., 2009) and block onset of M phase as long as cells are in S and G2 (Zarzov, et.al., 2002). It was shown that specific CDK-Cyclin complexes control the mammalian cell cycle. CDK4/Cyclin D, CDK6/Cyclin D and CDK2/Cyclin E regulate the progression through the G1 phase and the restriction point in G1. At the restriction point, CDK/cyclin E becomes active thereby committing cells to DNA replication. The CDK2/Cyclin A complex regulates the initiation of DNA replication and its completion. The onset of mitosis is triggered by the effect of CDK1, which has the ability to bind to Cyclin A and Cyclin B in G2 phase (Wohlbold & Fisher, 2009).

Taken together, CDKs play an important role in undamaged cells and are the main targets of the DNA damage checkpoints, which arrest cell cycle progression in the presence of DNA lesions. That will be discussed later in this chapter (Figure1-1).

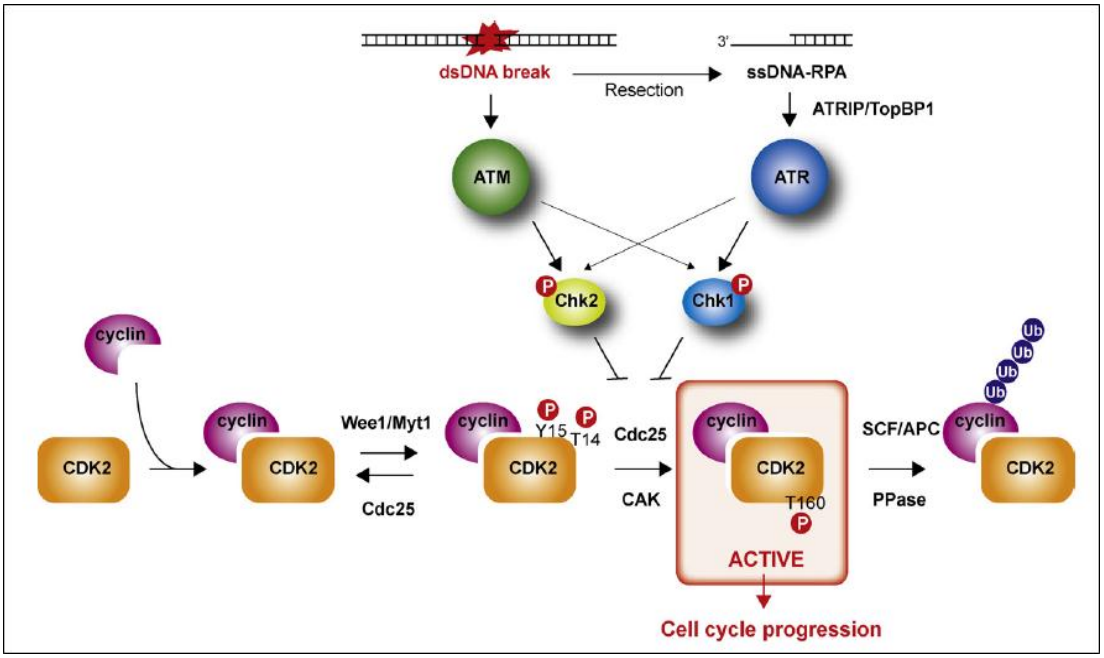

Figure 1-1: CDK2 regulates cell cycle progression in undamaged cells and in response to DNA damage. CDK2 has to form a complex with its corresponding Cyclin proteins. The CDK2-Cyclin complex is inactivated by Wee1/Myt1- mediated phoshprylation at Y15 and T14. This inhibition is removed by de-phosphorylation of CDK2 at Y15 by Cdc25 phosphatase, which enhances its kinase activity of whilst bound to Cyclin B to regulate entry into mitosis. In damaged cells, the ATR-Chk1 and ATM-Chk2 kinase cascades activate Wee1 and inactivate Cdc25 to keep cells in G2 until the damage is removed. (Adapted from Yata & Esashi, 2009).

1.5 DNA damage

1.5.1 Identification and causes

DNA damage represents any structural modifications of the DNA helix components caused by different agents leading to inconsiderable or intensive DNA lesions (Kaufmann

& Paules, 1996). DNA damage sources can be classified mainly into two groups: environmental and endogenous agents (Paulovich, et.al. 1997).

Environmental agents include two categories. Firstly, physical agents such as ionizing and UV radiation. Secondly, chemical agents, which are represented by alkylating agents (e.g. methylating and ethylating agents in addition to cancer chemotherapeutic drugs), cross linking agents (e.g. cisplatin and nitrogen mustard), hormone metabolites, some types of antibiotics (e.g. Bleomycin), Topoisomerase inhibitors (e.g. camptothecin and etoposide) and some types of bacterial toxins (Kastan & Bartek, 2004; Friedberg, et.al. 2006).

On the other hand, endogenous sources of DNA damage are represented by cellular respiration activities (Shrivastav, et.al. 2008) or by DNA metabolite enzymes or products of cellular metabolism. For example, when DNA polymerases are not error-free during the replication process, they will cause mutations (Kaufmann & Paules, 1996). In addition, inactivation of topoisomerases will result in sever chromosomal aberrations when replication forks collide with them (Kastan & Bartek, 2004).

1.5.2 DNA damage types

Since there are numerous DNA damaging agents, the type of lesion will be varied according to the causative agent. DNA damage types can be categorized into two main groups: nitrogenous bases alterations and phosphodiester backbone modifications (Friedberg, et.al. 1995). Nitrogenous bases may undergo structural modifications, or be cross-linked with another base within the same or opposite DNA strand or even when the DNA double helix suffers from depurination or de-pyrimidation (Friedberg, et.al. 2006). On the other hand, DNA single or double strand breaks or nick gaps will occur when the phosphodiester bonds are affected (Paulovich, et.al. 1997; Yamashita, et.al, 2002). Consequently, the cellular genome will exhibit lethal chromosomal breaks in the absence of efficient repair (Sonoda, et.al. 2001a) resulting in loss of heterozygosity and translocations (Hochwagen & Amon, 2006). Double strand breaks (DSBs) occur due to various reasons such as replication fork-blocking lesions, cellular respiration activities, nuclease-mediated genome re-arrangements, Ig gene conversion, meiosis, chromosomal migration towards cells

poles during mitosis, exposure to ionizing radiations or as a result of cancer chemotherapy (Bree, et.al. 2004; Shrivastav, et.al. 2008). Figure (1-2) demonstrates most common DNA damaging agents, lesions and repair mechanisms (Schärer, 2003).

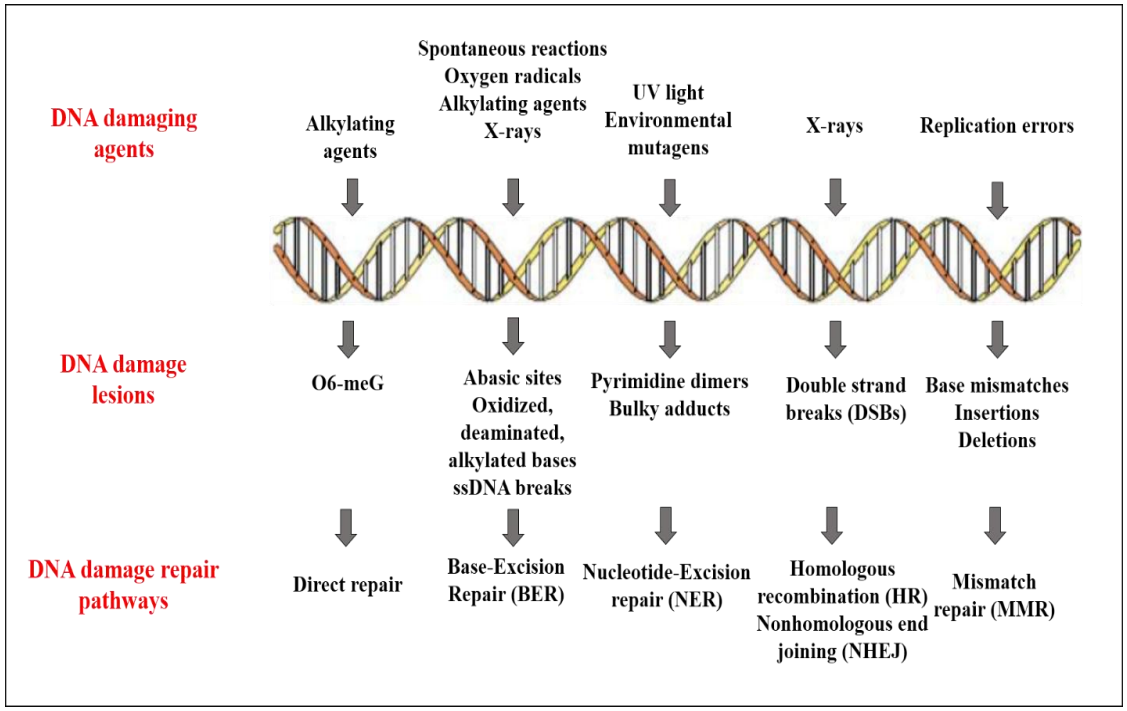

Figure 1-2: Most common DNA-damaging agents, lesions and repair pathways. (Adapted from Schärer, 2003).

1.5.3 DNA Damage Fate

1.5.3.1 DNA damage repair

Cells have to deal with each type of damage in a specific manner to ensure their genomic integrity (Hochegger & Takeda, 2006). Cells react differently as a response to the DNA damage, as follow: **(1)** removal of the DNA damage and re-establishment of the DNA duplex integrity; **(2)** DNA damage and replication checkpoints activation to trigger cell cycle arrest until the DNA damage is repaired; **(3)** adopting a new transcriptional profile; **(4)** trigger apoptosis when the DNA damage gets very severe (Sancar, et.al. 2004). Persisting damage may be transformed into a secondary lesion, if the initial repair mechanism fails (Kaufmann

& Paules, 1996; Paulovich, et. al. 1997; Sonoda, et.al. 2001a). For example, single-stranded DNA breaks may be converted into double-stranded breaks during DNA replication.

Cells are directed to choose an appropriate repair mechanism according to DNA damage structure. The DNA excision repair system encompasses three pathways, which utilise common as well as specific repair factors. These mechanisms include Nucleotide Excision Repair (NER), Base Excision Repair (BER) and Mismatch Repair (MMR) (Fleck & Nielsen, 2004; Wood, et.al. 2005) (Figure1-3).

Friedberg and his colleagues (2006) mentioned that the excision repair system includes three processes. Firstly, base excision repair (BER), which deals with chemical base alterations (e.g. base deamination or methylation). The mechanism of repair includes DNA scanning, examination of each base for any structural abnormalities, then excision of the damaged base. These steps are followed by replacing the excised bases (Morgan, 2007).

BER appears to be the most frequent repair mechanism within the group of DNA excision repair system. It deals with the chemically modified bases produced by oxidative, alkylating or deamination agents. It is initiated by damage-specific DNA glycosylases, which hydrolyse the N-glycosyl bonds of the chemically modified base. Short-patch BER removes only the damaged base, whereas long-patch BER excises a longer stretch of DNA containing the modified base. As in the case of long-patch BER, NER is able to excise short oligonucleotides flanking the pyrimidine dimers, which result from UV irradiation. This is accomplished by a different set of enzymes and divided into two sub-pathways: Global Genome Repair (GGR) and Transcription-Coupled Repair (TCR). The first one removes the damaged sites in the whole genome, whereas the second one is specific for the transcript strand of active genes. Finally, the MMR pathway deals with incorrectly inserted bases during DNA replication. These are excised as single nucleotides mediated by a third set of enzymes (Friedberg, 2003; Fleck & Nielsen, 2004; Friedberg, et.al. 2006). Generally, all excision processes result in gap formation within the damaged DNA strand, which is then refilled by DNA polymerases using the intact DNA strand as a template. Finally, DNA ligases will reseal the broken DNA strands (Kaufmann & Paules, 1996; Morgan, 2007).

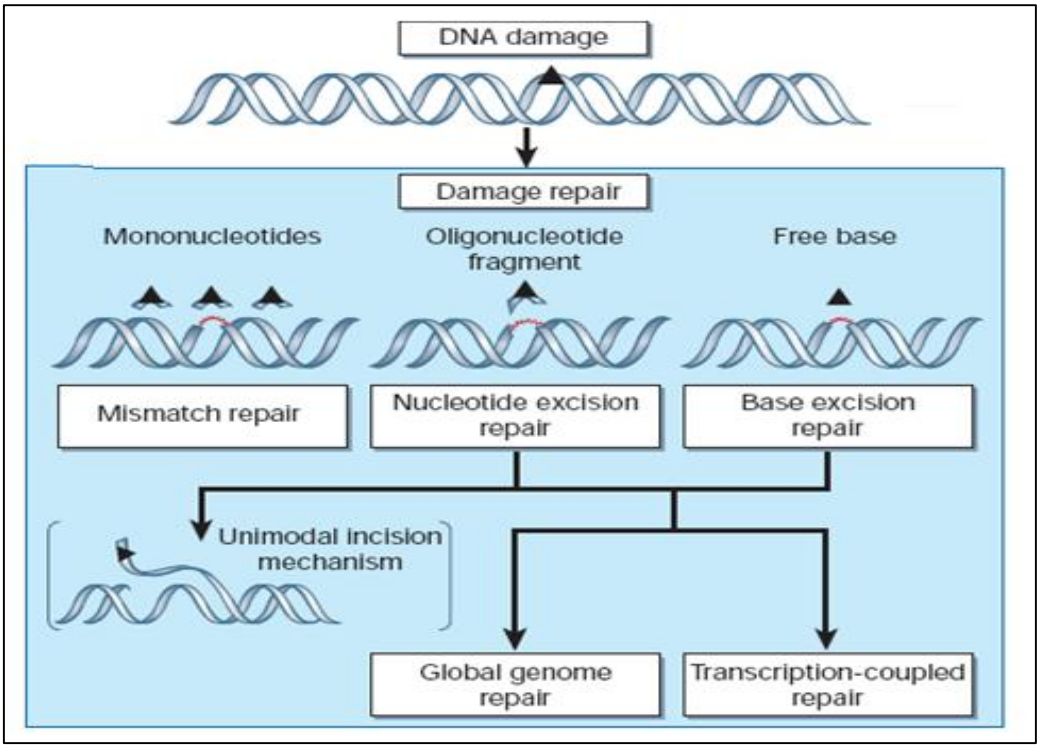

Figure 1-3: Excision repair system, which is accomplished through one of three manners, Base Excision repair (BER), Nucleotide Excision repair (NER) or Mismatch repair (MMR). The NER system consists of two sub-pathways: Global Genome Repair (GGR) and Transcription Coupled Repair (TCR). (Modified from Friedberg, 2003).

DNA breaks are extremely recombinogenic (Paulovich, et.al. 1997). Two main DNA repair systems deal with the broken chromosomes: Homologous Recombination (HR) or Non-Homologous End Joining (NHEJ) (Kaufmann & Paules, 1996; Morgan, 2007; Shrivastav, et.al. 2008). The main cell cycle regulator Cdc2 (CDK1) controls the cellular decision between the two pathways. While NHEJ is active throughout the cell cycle and especially in G1, HR is restricted to S and G2, since it requires the presence of a sister chromatid which is produced in S phase (Fleck & Nielsen, 2004; Wohlbold & Fisher, 2009).

Researchers studied the two recombination processes (HR and NHEJ) thoroughly and demonstrated that one key difference between them is their repair accuracy. HR is known to be "error-free", whereas NHEJ is described as "error-prone" (Shrivastav, et.al. 2008). This is because the first one requires a homologous strand (a homologous chromosome or sister

chromatid), which is used as an intact template. In contrast, NHEJ can re-seal the ends of the broken strand without any requirements for homology (Sonoda et. al. 2001a; Wyman, et.al, 2004; Raji & Hartsuiker, 2006). The variations in accuracy is partly due to the fact that in NHEJ nucleases resect and degrade a few bases at either DNA end before re-joining, which can lead to the loss of genetic information. In contrast, during HR, the broken ends are converted to 3`-single stranded DNA, which is known as end resection. This is followed by the invasion of the intact homolog DNA molecule by the damaged strand, which enables cells to restore the lost information (Hiom, 2000; Friedberg, et.al. 2006).

1.5.3.1.1 Non-Homologous End Joining pathway

Non-Homologous End Joining (NHEJ) is the dominant DSB repair mechanism in human cells and was discovered during the analysis of V (D) J (variable [division] joining) recombination in B and T-cells (Karran, 2000; van Gent & van der Burg, 2007).

Once DSBs are recognised, cells need to choose between Non-Homologous End Joining (NHEJ) and Homologous Recombination (HR). HR will only be selected if a sister chromatid is available as a template for the repair procedure. If not, cells proceed with NHEJ. The key regulator of NHEJ is the Ku heterodimer, which consists of two subunits, Ku70 and Ku80. The Ku heterodimer encircles the DNA end and recruits DNA-PKcs kinase (DNA-protein kinase catalytic subunit) to the break (Wymann & Kannar, 2006). This event is followed by recruitment of the MRN complex and other nucleases such as Artemis, which can process the ends for re-ligation by DNA ligase IV/ XRCC4 (Figure1-4) (Fleck & Nielsen, 2004; Hochegger & Takeda, 2006; van Gent & van der Burg, 2007). In addition, the resection of the break into ssDNA is actively suppressed by 53BP1, which is a paralogoue of Crb2 in fission yeast. Human 53BP1 recruits the protein Rif1 to the break, which blocks the association of CtIP with the damaged DNA and thereby end resection (Zimmermann, et.al. 2013). After cells replicated their chromosomes, this inhibition is counteracted by the protein BRCA1, which promotes jointly with the endonuclease CtIP the resection and invasion of the sister chromatid (Escribano-Diaz, et.al. 2013). This switch from NHEJ in G1 to HR in S and G2 is regulated by CDK enzymes. In humans, the MRN complex recruits CDK2-cyclin A to the break (Buis, et.al. 2012), whereas Cdc2-cyclin B regulate this

transition by modifying Crb2 (Esashi & Yanagida, 1999; Mahyous, et.al. 2014). In yeast, NHEJ is not as active as in human cells since yeast cells do not have paralogous of DNA-PK_{CS}, BRCA1 and Artemis (Shrivastav, et.al. 2008), but the pathway is present and can be stimulated by an increase in Cdc2 kinase activity (Manolis, et. al. 2001; Mahyous, et.al. 2014).

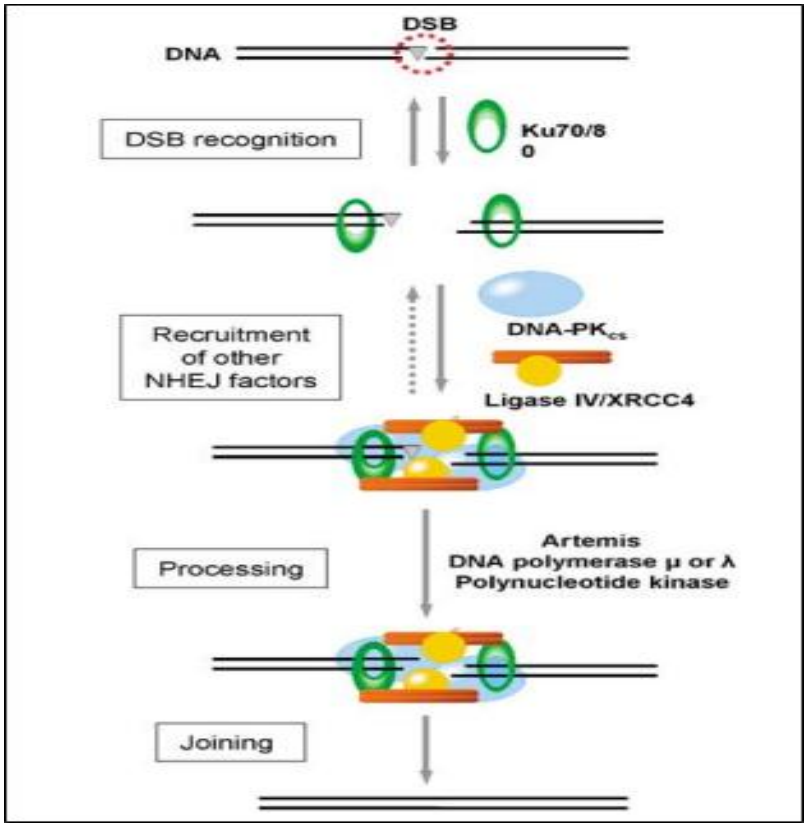

Figure 1-4: Non-homologous end-joining pathway. The main regulator of NHEJ is the Ku70/80 heterodimer, which recognises the DSB and facilitates DNA-PK_{CS} recruitment to the lesion site, followed by cleaning up of the DNA ends by RAD50-MRE11-NBS1 and ARTEMIS. Finally, DNA ligation is mediated by DNA ligase IV/ XRCC4 complex. The small triangles indicate the DNA end, which needs processing before ligation. (Adapted from: van Gent & van der Burg, 2007).

1.5.3.1.2 Homologous Recombination pathways

The dependency of Homologous Recombination (HR) on the sister chromatid restricts this pathway typically to late S and G2. It is therefore sometimes referred to as post-replication repair (PRR), which allows cells to re-start broken replication forks. (Lambert,

et.al. 2005). The HR pathway consists of three main steps as mentioned by Wyman, et.al. (2004) and illustrated in Figure (1-5). The pre-synapsis step, which mediates the DSB processing by the MRN complex to provide a 3'ssDNA end, the RPA binding substrate. Rad51 will coat this ssDNA tail in a process mediated by Rad52, Rad55 and Rad57. The synaptic stage, when the Rad51 nucleoprotein tail invades the nearest available homologous sequence with the assistance of Rad54, which was described as "the motor of homologous recombination" by Mazin, et.al. (2010), since it interacts with RPA protein at ssDNA and facilitates recruitment of RAD51 to the ssDNA site. Finally, Rad51 has to be separated from the lesion site by Srs2 DNA helicase to permit base pairing with its corresponding complimentary strand, which is followed by strand extension by a DNA polymerase. Thereafter, in mitotic cells the invading strand is moved back to its original location in the damaged chromosome to be re-annealed with its partner by DNA helicases without the generation of a holiday junction. This process is called Synthesis-dependent strand annealing (SDSA) or Non-Crossover recombination. Holliday junctions are typically common in meiosis where this cross-like DNA intermediate is resolved such that genetic information `crosses over`. Holiday junctions can also appear in mitotic cells, but they are normally resolved so that no exchange of genetic materials occurs (Wyman, et.al. 2004; Shrivastav, et.al. 2008; Mazin, et.al. 2010). This requires the activities of BLM/Rqh1 DNA helicase and the endonuclease Mus81-Eme1 (Marzon & Symington, 2013; Sarbajna, et.al. 2014).

Sonoda and others (2001a) suggested that HR is more significant in maintaining genome integrity than NHEJ pathway. Since *RAD51*-mutated, cells accumulate chromosomal breaks, which eventually lead to cell death. In contrast, NHEJ defective cells are still able to proliferate, that clarify the minor role of NHEJ in maintaining the genome integrity.

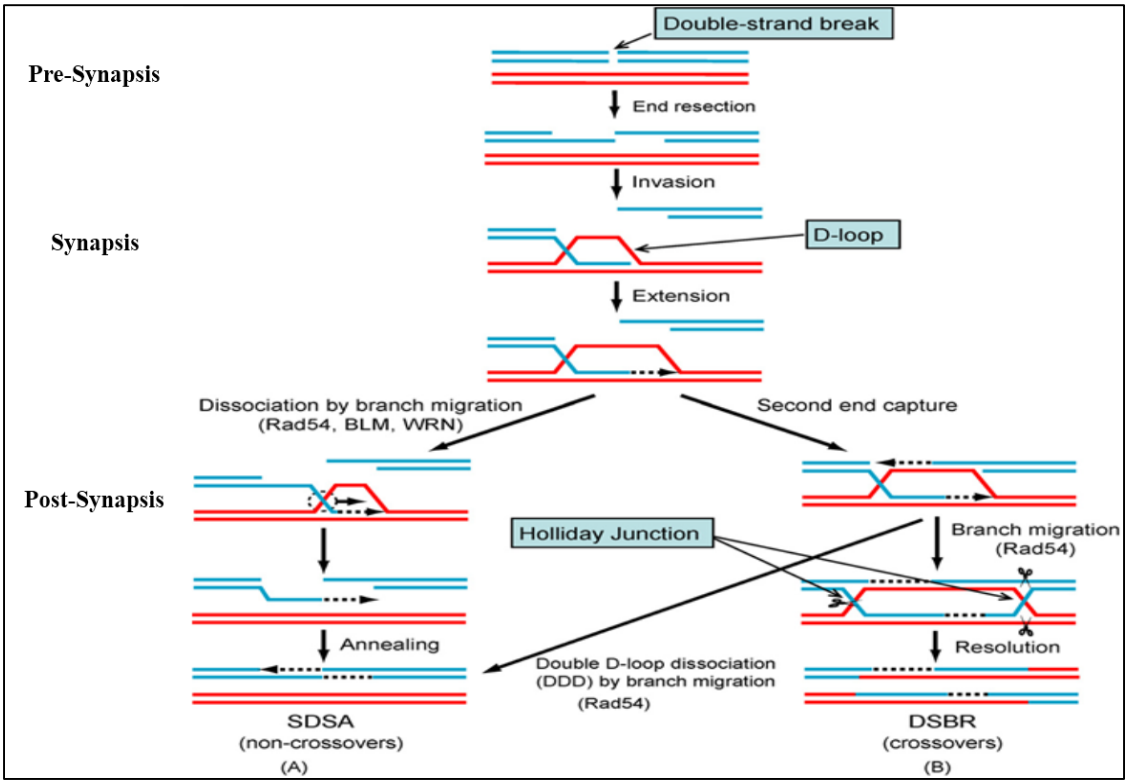

Figure (1-5): DSBs repair by HR. The resection of DSB site is followed by strand invasion, D-loop formation and DNA strands extension by DNA polymerases. Subsequently, they will be treated through two processes, SDSA & DSBR, according to the cell cycle phase. **(A):** Synthesis-dependent strand annealing (SDSA) is probably the preferred pathway in mitotic cells, whereas **(B):** Cross-over (DSBR) and formation of Holliday Junctions are specific to meiotic cells. Extension will be followed by second end capture, branch migration-mediated by *RAD54*, and Holliday junction formation. These will be resolved latterly by resolvases (Modified from Wyman, et.al. 2004; Mazin, et.al. 2010).

1.5.3.2 Replication DNA damage repair pathways

DNA replication is a major source of endogenous DNA damage. Both translesion DNA polymerases and recombination processes have evolved to limit DNA lesions accumulation in S phase. These pathways are known as Replication damage bypass systems (Sale, et.al. 2006), DNA Post Replication Repair (PRR) or DNA Damage Tolerance (DDT) (Andersen, et.al. 2008).

1.5.3.2.1 Translesion DNA synthesis pathway (TLS)

Translesion synthesis (TLS) is induced when the processive DNA polymerases stall during the replication process. This repair mechanism depends on the exchange of the processive polymerases with low-fidelity by-pass polymerases. This means, the new polymerase is able to continue the replication process over the persistent damage (i.e. bypassing the damaged base) at the cost of mutations (Friedberg, 2003). While this process can lead to genome instability because the DNA damage has not been repaired, it is advantageous because it allows cells to overcome the problem and replicate to survive (Chang & Cimprich, 2009). An alternative pathway to TLS is error-free template switching, which is homologous recombination dependent (Knobel & Marti, 2011). Cells choose between both pathways depending on the PCNA posttranslational modifications (Chang & Cimprich, 2009).

An epistasis gene group that known as the Rad6/Rad18 group controls TLS. This group includes *RAD6, RAD18, REV1, REV3* and *REV7*, which are highly conserved from yeast to vertebrates (Yamashita, et.al. 2002). TLS activation in yeast and human is mediated by PCNA monoubiquitination by the Rad6-Rad18 complex. TLS uses low fidelity of Y family DNA polymerases, which perform the replication over the damaged template (Andreassen, et. al., 2006). These Y family polymerases initiate TLS by their binding to the monoubiquitination PCNA (Knobel & Marti, 2011). After the insertion of the nucleotide opposite the lesion, cells switch back to a replicative polymerase to finalise the rest of the replication process (Figure 1-6) (Andreassen, et.al. 2006)

In comparison to TLS, the error-free bypass is achieved by using a newly synthesised sister chromatid as a replication template. Two suggested pathways of the error-free bypass were named as template switching and replication fork regression (Figure 1-6) (Andersen, et. al. 2008). Template switching is achieved by homologous sister chromatid invasion/cohesion, high fidelity DNA replication and followed by Holliday junction resolution, whereas fork regression is accomplished similarly as in bacteria, since it requires the ssDNA binding protein and RecA (Rad51) to form the chicken foot–like structure. It is thought that yeast Rad5 DNA helicase activity is responsible for the replication fork regression. In addition, it was suggested that the DNA damage checkpoints prevent the

initiation of replication fork regression while the template switching error-free DDT is taking place (Andersen, et.al. 2008; Chang & Cimprich, 2009) (Figure1-6). This was recently confirmed by the finding that *S.pombe* Cds1 kinase regulates fork regression by phosphorylating the endonuclease Dna2 (Hu, et.al. 2012).

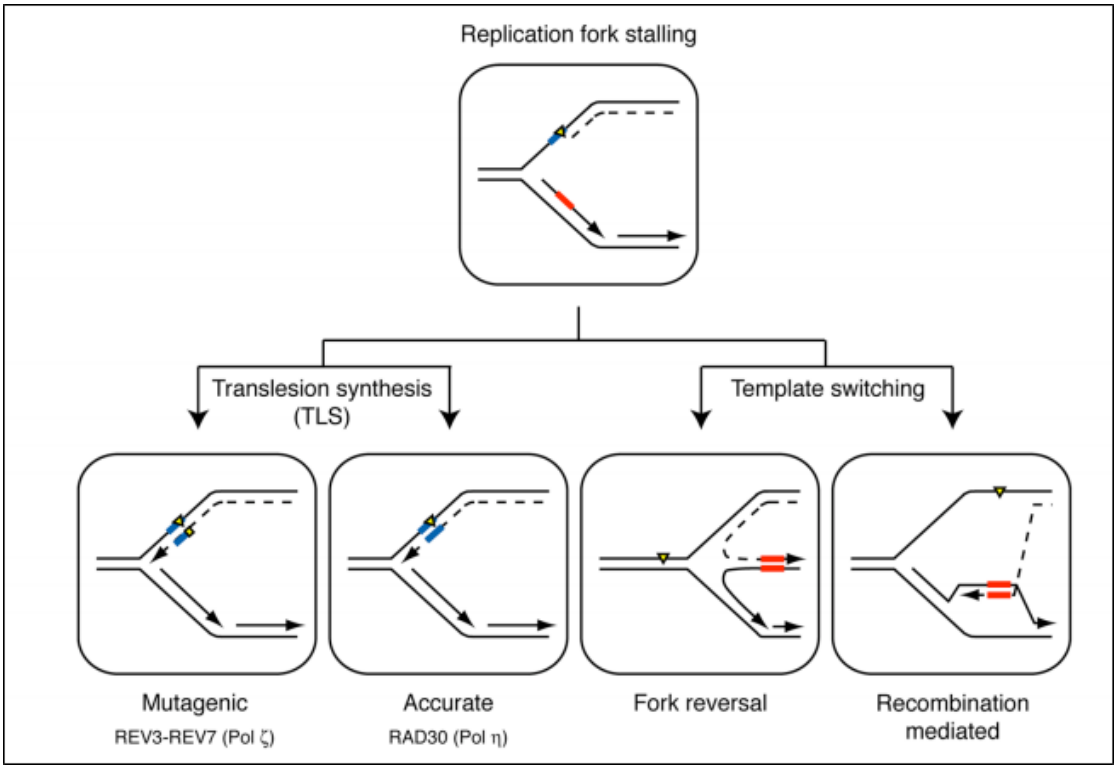

Figure 1-6: Overview of DNA damage tolerance pathways. A DNA damage lesion (yellow triangle) stalls processive DNA replication process (dashed line). Cells can choose either to bypass the damage by Translesion synthesis (left), which permits the bypass of replication block lesions by replication over the damaged lesion. On the other hand, cells can use Template switching (Right), which involves two options; either achieving Fork reversal as a four-way junction or "chicken-foot" intermediate formation (left), or establishing recombination mediated template switching by D-loop formation and strand invasion (right) (Adapted from: Chang & Cimprich, 2009).

Vertebrate cells (DT40 cells) devoid of *RAD6* and *RAD18* are highly sensitive to IR and UV radiation, DNA alkylation and DNA cross-linking agents such as mitomycin C and

cisplatin. Rad6 is an ubiquitin-conjugating enzyme (E2) forming a complex with RAD18. RAD18 exhibits DNA-binding activity and appears to recruit RAD6 to the DNA lesion. RAD18 consists of a ring –finger motif and belongs to the family of E3 ubiquitin ligases. RAD18/Smc6 is able to transfer an ubiquitin molecule from the E2 enzyme RAD6 to its target proteins (Yamashita, et.al. 2002; Ampatzidou, et al., 2006).

The DT40 *RAD6* group and TLS polymerases show structural amino acidic similarities to human *RAD6B* (100%), *PCNA* (94%), *RAD18* (47%) and *DNA-polymerase η* (51%). However, they differ from each other in two points. Firstly, chicken cells have only a single *RAD30* homologue, which is *DNA polymerase η*. Secondly; chicken cells exhibit a vertebrate photolyase homologue (an enzyme able to direct reversal of some UV-induced DNA damage). Indeed, it is not clarified yet, if this enzyme is implicated in DT40-DNA repair pathway or not (Sale, et. al., 2006).

The *REV* gene group consists of *REV1*, *REV3* and *REV7*, which contribute significantly to PRR pathways. REV1 is related to the Y-family of DNA polymerases and functions as deoxycytidyl-transferase. REV3 and REV7 are responsible for bypassing of UV-induced thymidine dimers as the catalytic subunits of DNA polymerase ζ (Pol ζ) (Okada, et.al. 2005).

The vertebrate *REV* protein group shows obvious structural and phenotypically variations to the yeast proteins. For example, REV1 and REV3 are larger in vertebrates than in yeast. REV1 can interact with REV7 or with other Y family polymerases (Polκ, Polι and Polη) in mammalian but not in yeast cells. Moreover, vertebrate Pol ζ appears to evolve in DNA damage tolerance more significantly than in budding yeast (Okada, et.al. 2005).

1.5.3.2.2 Sister Chromatid Exchange (SCE)

Sister Chromatid Exchange is an outcome of the replication damage bypass pathways. It occurs normally (1-3 per cell cycle) in vertebrate cells. This low average is elevated about five fold in response to DNA damage (Sonoda, et.al. 1999; Sonoda, et al, 2001b; Hochegger & Takeda, 2006). Wilson III and Thompson (2007) defined the SCE process, as "it is the process whereby, during DNA replication, two sister chromatids break and re-join with one another, physically exchanging regions of the parental strands in the duplicated

chromosomes" (Figure 1-7). These exchanges are represented by gene conversion correlated with crossover between the sister chromatids (Conrad, et.al. 2011; Hochegger & Takeda, 2006).

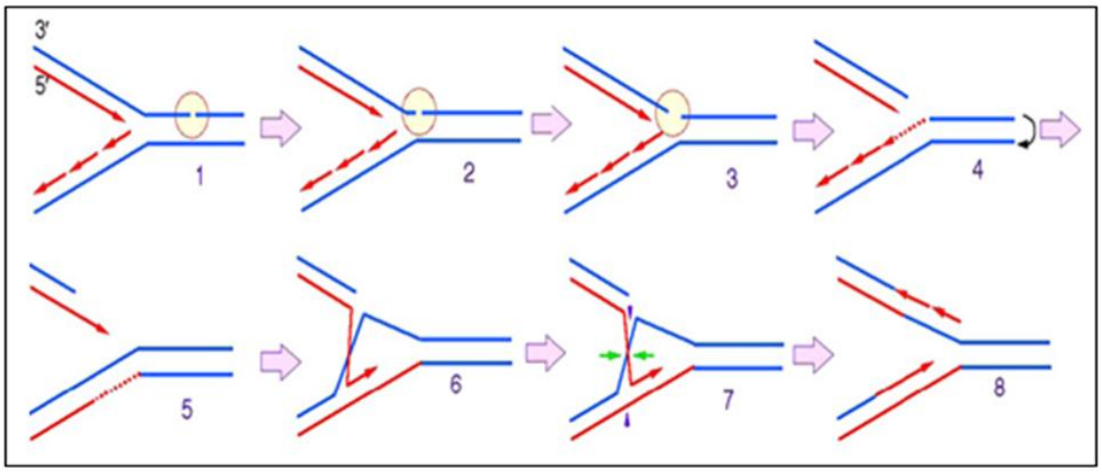

Figure (1-7): Sister Chromatid Exchange. 1-4: When replication forks encounters an ssDNA or gap (yellow circle), it will lead to a broken sister (leading strand) at the gap site. Subsequently, the broken chromatid will be resected to form its 3'-ssDNA **(5). 6:** Strand invasion is mediated by RAD51. **8:** Eventually the replication fork will re-establish. Sister chromatid exchange (SCE) can occurs when the invading 3`-ssDNA is extended by DNA polymerases and an extended stretch of DNA is copied from one sister into the other sister chromatid (Adapted from Wilson III & Thompson, 2007).

The RAD54 gene group controls SCE. This fact is supported by the findings of Sonoda, et.al. (1999), which revealed that HR-deficient (*RAD54*, *RAD51*) rather than NHEJ-deficient (*KU70*) DT40 cells show decreased levels of spontaneous and mitomycin C (MMC) induced SCE. This shows that HR but not NHEJ is the significant pathway responsible for the SCE process.

The connection between translesion synthesis and SCE is shown through the knockout of E3 ligase *RAD18* in DT40 cells (Yamashita, et.al. 2002) or by disruption of the translesion polymerases *REV1* and *Pol ζ* (*REV3* and *REV7*) (Sonoda, et.al. 2003). Those cells showed increased frequencies of the SCE process (Sonoda, et.al. 2003; Okada, et.al. 2005).

However, the triple mutants of *REV1, REV3* and *REV7* displayed only slightly increased SCE levels indicating that Y DNA polymerases are less important for this process. The reason for this phenotype is still unclear. The low SCE level may indicate that HR has repaired fewer lesions in S phase. This difference is not observed in murine ES cells devoid of REV1, which appear to have normal levels of both, spontaneous and UV- induced SCE (Yamashita, et.al. 2002; Wilson III & Thompson, 2007).

1.6 DNA damage transformation during the cell cycle

Damage repair systems represent the cellular maintenance tool kit, which maintains genome integrity. Occasionally, these systems fail leading to the conversion of primary lesions to sever secondary damage in cycling cells (Paulovich, et.al. 1997). For example, single strand breaks (SSB), which arise in G1 phase will be converted into sister chromatid breaks, DSBs, when they are not repaired before cells progress through S phase (Sonoda, et.al. 2001a & b; Yamashita, et.al. 2002). Subsequently, persistent DSBs will activate the cellular DNA damage checkpoints and they may lead to apoptosis (Yamashita, et.al. 2002). Moreover, if the DSBs are repaired incorrectly, they can produce mutations, loss of heterozygosity or translocations (Hochwagen & Amon, 2006). Paulovich, et.al. (1997) suggested that repair systems may become less efficient because of their gradually loss of repair options. For example, broken chromosomes may lose acentric fragments, if the damage persists throughout the cell cycle. Kaufmann and Paules (1996) suggested an illustrating diagram to explain how cellular DNA damage is transformed in cycling cells (Figure1-8). Intriguingly, human cells tolerate a low number of DSBs (less than 10-20) while cycling without losing viability (Löbrich & Jeggo, 2007).

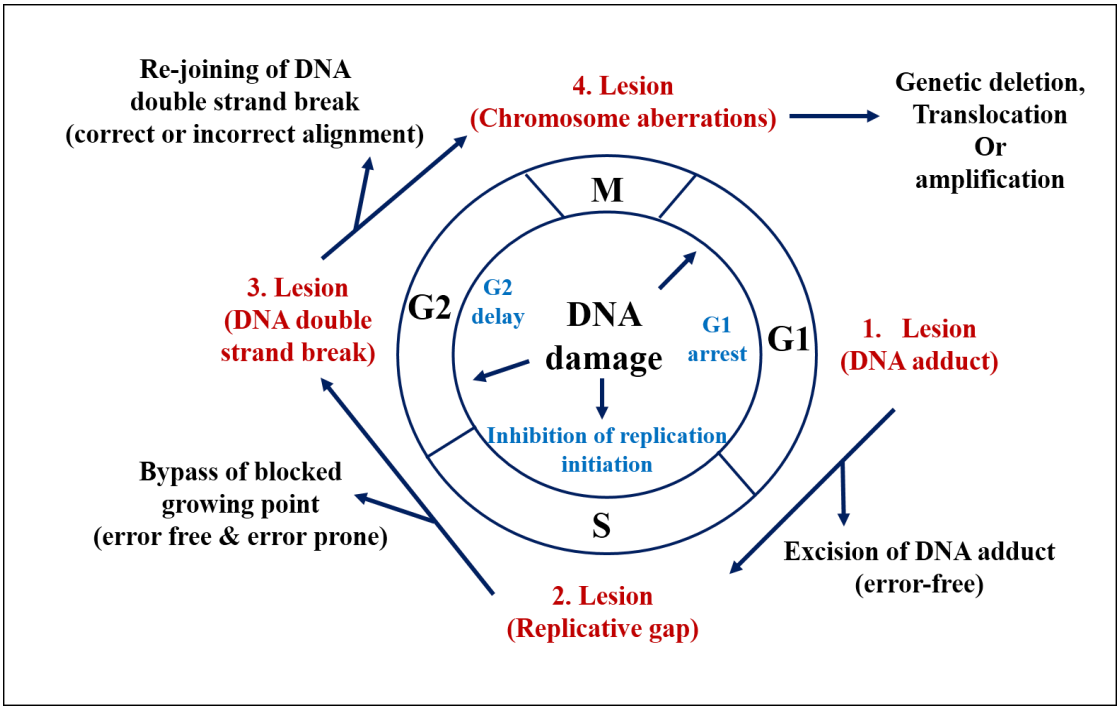

Figure 1-8: Transformation of DNA damage during the cell cycle. DNA adducts have to be repaired by the excision of adducted sites otherwise it will be converted to a replicative gap. These gaps may be bypassed during DNA replication. Untreated replicative gaps will result in DSBs, which may be treated by HR or NHEJ processes. Eventually, persistent DSBs will cause genetic deletion, translocation or amplification, which affect the genome integrity (scientific information adapted from Kaufmann & Paules, 1996).

1.7 DNA damage checkpoint signalling pathways in eukaryotes

To prevent DNA lesions development during the cell cycle, DNA damage checkpoints have evolved, which transiently arrest cell cycle progression in presence of DNA damage (Paulovich, et.al. 1997; Shackelford, et.al. 1999; Kastan & Bartek, 2004; Yamamoto, et. al. 2006; Cimprich & Cortez, 2008; Branzei & Foiani, 2009). In such pathways, the signal is initiated by the sensors and transmitted through the mediators, transducers and finally to the effectors. That eventually lead to either DNA damage repair, cell cycle arrest or apoptosis (Figure 1-9) (Chen & Sanchez, 2004; Hochwagen & Amon 2006; Niida & Nakanishi, 2006).

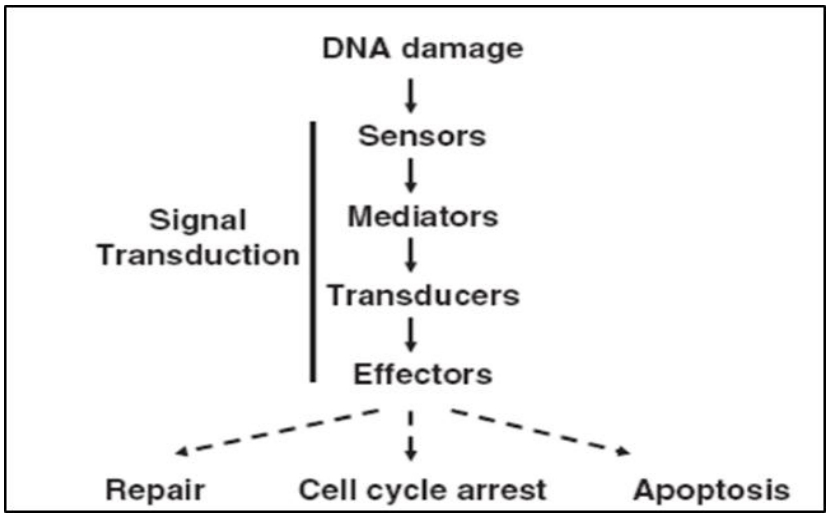

Figure 1-9: Organisation of the signal transduction of checkpoint responses. Sensor proteins detect DNA damage. The signals are transmitted to transducers (mainly kinases) and the regulated transducer molecules regulate effectors kinases, such as CDKs and Cdc7, thereby arresting the cell cycle at specific phases (Niida & Nakanishi, 2006).

These checkpoints detect DNA lesions and check the DNA repair status at the G1/S border, during S phase and at the G2/M transition point (Paulovich, et.al. 1997). Whereas both intra-S and S/M checkpoints respond to DNA replication stress, the G2/M checkpoint prevents mitotic onset in the presence of damaged chromosomes (Figure 1-10).

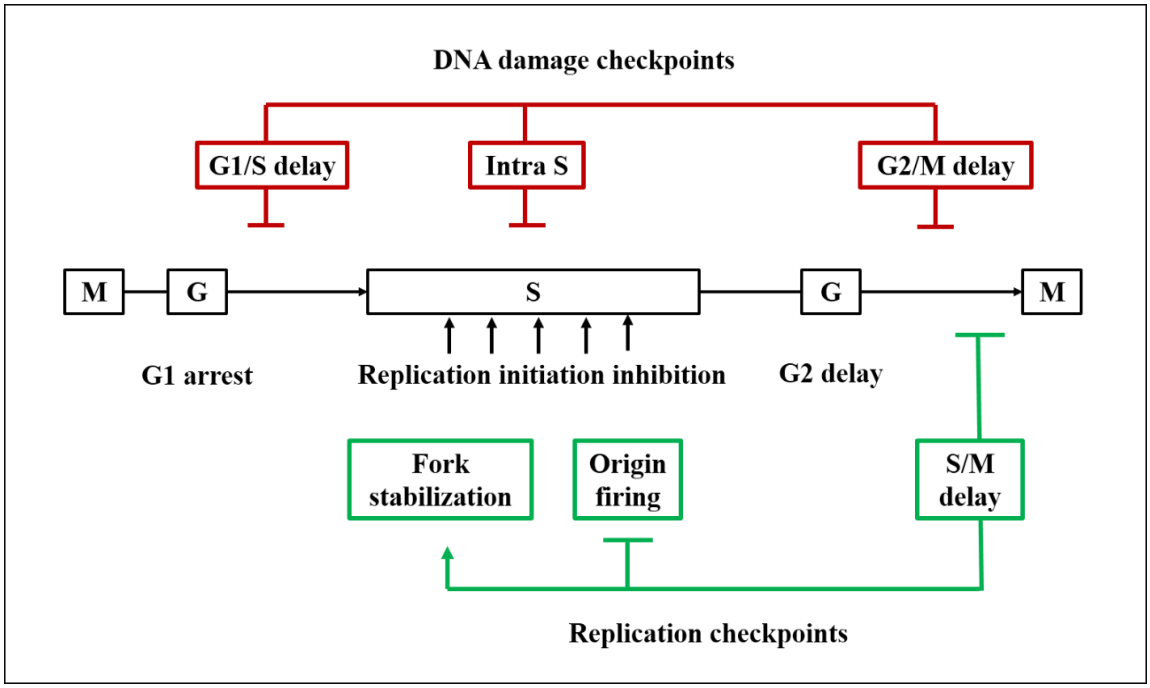

Figure 1-10: Overview of the various branches of the DNA damage (red) and replication (green) checkpoints, which exist in eukaryotic cells. G1 arrest and Intra-S phase arrests protect against DNA replication errors (e.g. Mutation and replication gaps), whereas the G2 delay protects against mitotic errors (e.g. chromosomal aberrations) (Modified from Kaufmann & Paules, 1996; Rainey et.al., 2006).

DNA damage checkpoints were discovered and first investigated in yeast (Weinert & Hartwell, 1988; Rhind & Russell, 2000; Furuya & Carr, 2003), and later in higher eukaryotes (Sancar, et.al. 2004; Niida & Nakanishi, 2006; Bartek & Lukas, 2007), which share a large number of conserved checkpoints genes. Rainey, et.al. (2006) suggested an illustrating diagram, which divided the checkpoint signalling pathways (of both yeast and vertebrate cells) into two main parts, DNA damage and replication arrest pathways (Figure 1-11). In the following paragraphs, I will discuss yeast and vertebrate checkpoints separately.

In both yeast and higher eukaryotes, cells developed different DNA damage checkpoints, which are called DNA structure checkpoints. They are divided into few checkpoints depending on the type of DNA damage. First, the G1/S checkpoint delays DNA replication as a response to damage in G1 phase. Second, the DNA replication checkpoint or intra-S

checkpoint inhibits mitosis, preserves the structure of stalled DNA replication forks and prevents the activation of late replication origines as a response to S phase problems. Third, the G2/M checkpoint inhibits mitosis in response to DNA damage in G2. The most important checkpoint in fission yeast cells is the G2/M checkpoint (Humphrey, 2000), although there is a G1/S checkpoint, which acts, however, in a different way compared to the traditional systems (Bøe, et.al. 2012). This checkpoint utilises the Gcn2 kinase, which is not involved in the traditional checkpoint pathways. Another difference is that the intra-S checkpoint in fission yeast does not block the activation of late origins (Mickle, et. al. 2007).

The choice of checkpoints is much dependent on whether the DNA lesion contains single-stranded DNA (ssDNA) or not (Figure 1-11). In the absence of ssDNA one of the first proteins recruited to the damage (e.g. a broken chromosome) are Mre11, Rad50 and Nbs1 (MRN complex). This MRN complex recruits and activates ATM/Tel1 (Ataxia Telangiectasia Mutated) kinase (Lee and Paull, 2004). Activated ATM kinase then phosphorylates the histone variant H2AX at extended regions either side of the break (Burma, et.al. 2001; Reinhardt & Yaffe, 2009). Active ATM relays the signal to Chk2 kinase, which down-regulates CDK enzymes to block cell cycle progression (Matsuoka, et.al. 2000).

In vertebrates, activation of the two related kinases ATM and ATR (Ataxia telangiectasia and Rad3 related), which belong to phosphatidylinositol 3(PI3)-kinase like kinases (PIKK) group, represents generally the first step of DNA damage detection (Sancar, et.al. 2004; Rainey, et.al. 2006; Cimprich & Cortez, 2008). While ATM is activated by DSBs without ssDNA, ATR/Rad3 works specifically, at ssDNA in S phase and outside of S phase to protect replication forks and to delay mitosis (Jeggo & Lobrich, 2006; Cimprich & Cortez, 2008). In contrast to ATM which targetes Chk2, ATR activates Chk1 (Lou & Chen, 2005; Bartek & Lukas, 2007) after its recruitment by the ATR-Interacting Protein (ATR-IP) to ssDNA covered by ssDNA binding protein RPA (Zou & Elledge, 2003) (Figure 1-11). Fission yeast cells use very similar checkpoint pathways, although there are a few key differences. ATM, which is Tel1 kinase in *S.pombe* is normally much less active compared to Rad3/ATR kinase, since DNA breaks are quickly converted into ssDNA (Limbo, et.al. 2011). Only when this end-resection is blocked, Tel1 activity becomes dominant. The ATR homologue,

Rad3 kinase activates Cds1/Chk2 mainly during S phase, whereas Chk1 acts largely in G2 with a minor role in G1 (Lindsay, et.al. 1998; Carr, et.al. 1995; Synnes, et.al. 2002). Cds1 is activated by Rad3 to protect stalled replication forks upon depletion of the nucleotide pool by the ribonucleotide inhibitor hydroxyurea (HU) or upon damage of the DNA template by UV treatment (Brondello, et.al. 1999; Xu, et.al. 2006). Rad3/ATR binds to ssDNA at stalled forks via its interaction partner Rad26 (ATRIP) (Edwards, et.al. 1999) where it phosphorylates Cds1 kinase, thereby promoting its activation (Xu, et.al. 2006). Cds1 is recruited to stalled fork by its association with the scaffold protein Mrc1 (Clasplin in human cells) (Tanaka & Russell, 2001). In the case of a broken chromosome, Rad3 kinase modifies Chk1 kinase in a process mediated by the scaffold protein Crb2 (Walworth & Bernards, 1996; Saka, et.al. 1997).

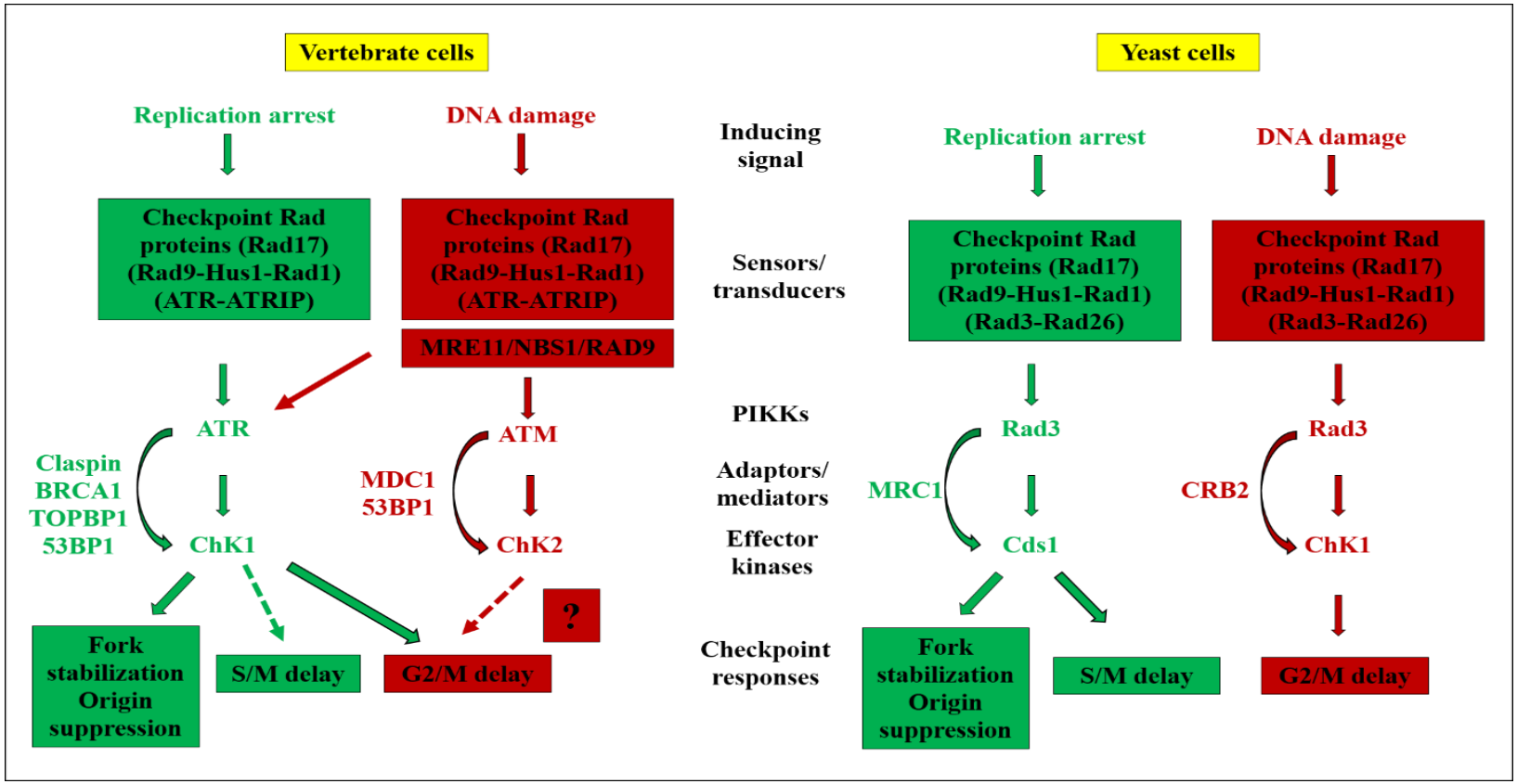

Figure 1-11: Diagram of the two checkpoint signalling pathways (ATR/Rad3 & ATM/Tel1) in vertebrate cells and fission yeasts. In vertebrate cells, ATR and ATM act separately in assistance of mediator proteins. The ATM-pathway may be linked with the ATR pathway downstream of DSBs resection. Eventually, they lead to S/M delay, fork stabilisation and inhibition of origin firing or G2/M delay. Fission yeasts have similar checkpoints pathways. However, the Rad3/ATR kinase is the dominant kinase. Whereas Tel1 is largely silent. Rad3 activates both Cds1/Chk2 and Chk1 kinase in the response to ssDNA and dsDNA breaks, which are mediated by Mrc1 and Crb2 respectively (Adapted from Rainey, et.al. 2006).

1.8 Checkpoint Kinases and their downstream substrates in cell cycle control

1.8.1 G1 and G1/S phase checkpoint responses

Most eukaryotic cells arrest in G1 prior to the commitment to S phase in the presence of DNA damage. This checkpoint is responsible for ensuring the genome integrity before the genetic material is replicated in S phase. In higher eukaryotic cells, this G1/S checkpoint is mediated by p53 and it seems that it happens on two stages. The first stage is an immediate response, which allows the damage to be repaired and can last for a few hours. The second stage, which is sometimes reversible, allows for S phase entry (Mailand, et.al, 2000; Bartek & Lukas, 2001). In the first stage, ATM kinase phosphorylates and activates Chk2, which leads to Cdc25A phosphorylation. This results in Cdc25A ubiquitination and its proteasome-dependent destruction. Consequently, replication origins do not fire and CDK2 remains phosphorylated, which disrupts the Cdk2-cyclinE complex and prevents entry into S phase (Mailand, et.al. 2000; Costanzo, et.al. 2000). Moreover, Cdc25A also regulates CDK4 activity, and its disruption leads to the prevention of S- phase entry (Terada, et.al. 1995).

The second stage of the G1 checkpoint relies on ATM-Chk2 and ATR-Chk1 pathways, which are initiated late in G1 phase. ATM-Chk2 and ATR-Chk1 activate both the p53-MDM2-p21 pathway, which results in the inactivation of the Cdk2-CyclinE complex (Ekholm & Reed, 2000) (Figure1-12). The levels of ATM and Chk2 are relatively constant throughout the cell cycle, whereas the amounts of ATR and Chk1 increase during G1/S transition. Their concentration will remain high during G2 phase to delay the mitosis onset (Kastan & Bartek, 2004; Jeggo & Lobrich, 2006; Cimprich & Cortez, 2008). This checkpoint response is found in mammalian cells, but is often absent in human tumour cells and missing in chicken DT40 cells due to a non-functional p53 gene, respectively (Rainey, et.al. 2006).

Interestingly, this G1/S checkpoint is different in lower eukaryotes. Fission yeast cells delay entry into S phase upon the treatment with UV light. This delay is neither dependent on the traditional Rad3-Chk1 nor the Rad3-Cds1 pathways but on the kinase Gcn2 (Nissen, et.al. 2003; Tvegård, et.al. 2007; Bøe, et.al. 2012). Gcn2 kinase phosphorylates the

translation initiation factor EIF2α that correlates with the G1/S delay (Krohn, et.al. 2008). Budding yeast cells do arrest in G1, which requires the resection of DNA breaks and the recruitment of Rad9 (Crb2 in *S.pombe*) (Siede, et.al. 1993; Balogun, et.al. 2013). These differences between yeast species and human cells indicates that this G1/S checkpoint evolved and driven by the specific requirements for this arrest.

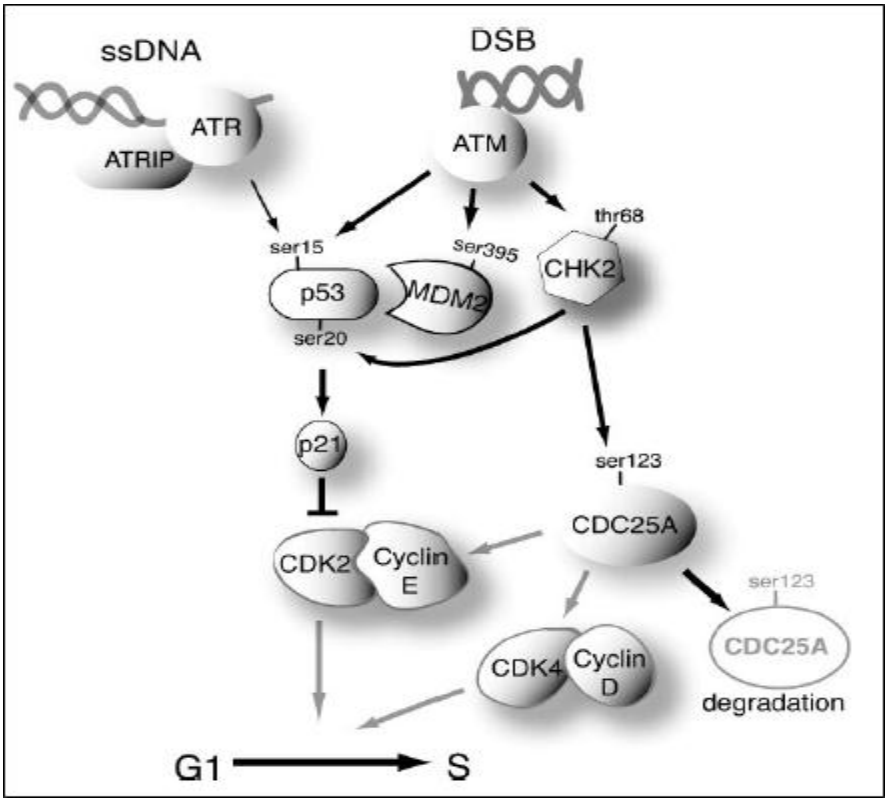

Figure 1-12: The G1 checkpoint in mammalian cells. This checkpoint functions to block the cell cycle transition from G1 to S phase as a response to DNA damage. Either ATR or ATM led to p53 phosphorylation and degradation of Cdc25A to maintain Cdk2 inactive situation to block the G1 / S transition. Gray arrows indicate to the functions that are lost as a response to the checkpoint activation. Indicated amino acids on the proteins refer to phosphorylation sites. (Adapted from Nyberg, et.al. 2002).

1.8.2 The S-phase checkpoint pathway

In vertebrates, the S-phase checkpoint pathway is divided into two branches as shown in Figure (1-10), the S/M arrest and intra-S phase responses. While the S/M arrest pathway prevents onset of mitosis in presence of incompletely replicated chromosomes, the intra-S pathway maintains integrity of stalled replisomes. The S/M pathway consists in human cells of the ATM-MDC1-MRN-SMC1-FNACD2 cascade. ATM phosphorylates SMC1 (Structural Maintenance of Chromosome) at serine 957 and 966 to maintain sister chromatid cohesion (Wei-Feng, et.al. 2006). Phosphorylation of FANCD2 (Fanconi Anaemia, Complementation group D2) protects chromosome integrity through BRCA2 (breast cancer 2) recruitment onto the chromatin (Wang & D'Andrea, 2004). Kastan & Bartek (2004) mentioned that NBS1 and SMC1 defective cells show hypersensitivity to irradiation due to prevention of ATM-mediated phosphorylation of SMC1.

In contrast, the intra S-phase pathway functions as a transient and reversible suppressor of replication origins firing and preserves the integrity of stalled forks (Wei-Feng, et.al. 2006). This occurs through an ATR-Chk1 mediated phosphorylation of the Cdc25A protein (Cell Division Cycle 25 homologue A), which leads to its ubiquitination and degradation. Subsequently, Cdc25A phosphatase cannot activate CDK2 (Cyclin Dependent Kinase 2) thereby preventing loading of Cdc45 onto pre-replication complexes at yet inactive origins of replication. Since Cdc45 is responsible for origin firing via recruitment of DNA polymerase α, origins remain inactive (Niida &Nakanishi, 2006; Bartek & Lukas, 2007).

1.8.3 G2/M delay checkpoint

The main role of the G2/M checkpoint (Figure1-13) is to prevent damaged cells (especially ones with DSBs) from entering mitosis (Nyberg, et.al. 2002; Rainey, et.al. 2006). This checkpoint function is intertwined with the replication arrest checkpoint (S/M) (Kastan & Bartek, 2004). Both fission yeast and higher eukaryotes block the G2/M transition by maintaining the Cdc2 inhibitory phosphorylation at tyrosine 15. Different pathways can mediate this (Nyberg, et.al. 2002). In mammalian cells, DNA damage triggers independently different kinase pathways that target Cdc25C, which assist in mitosis entry by de-

phosphorylating Cdc2 kinase at Y15 (Guo, et.al. 2005). First, the DNA damage that activates ATR kinase will phosphorylate Chk1, which negatively regulates Cdc25 through its Ser216 phosphorylation (Sanchez, et.al. 1997). Cdc25 modified at S216 associates with the 14-3-3 proteins. This makes Cdc25 to lose some of its activity or to re-localises from the nucleus to the cytoplasm as in the case of *S.pombe* Cdc25 (Zeng & Piwnica-Worms, 1999; Lopez-Girona et al., 1999; Graves, et.al, 2001). The second pathway that involved in human Cdc25C deactivation by the ATM-Chk2 pathway (Matsuoka, et.al. 1998). Moreover, there is a second regulator of human Cdc25C, Polo-like kinase 1 (Plk1) which phosphorylates Cdc25C at its inhibitory site Ser216 (Xie, et.al. 2001). The 14-3-3 proteins regulate Wee1 kinase in addition to Cdc25C phosphatase when Chk1 phosphorylates Wee1 at Ser549 where the 14-3-3 proteins will bind to Wee1 (Chen, et. al. 1999; Lee, et.al, 2001). Moreover, it was shown that in colorectal cell lines, p53 activates 14-3-3σ expression upon DNA damage, which is necessary for blocking entry into mitosis. 14-3-3σ binds to the Cdc2-CyclinB complex sequestering it to the cytoplasm to maintain the G2 arrest (Chen, et.al. 1999).

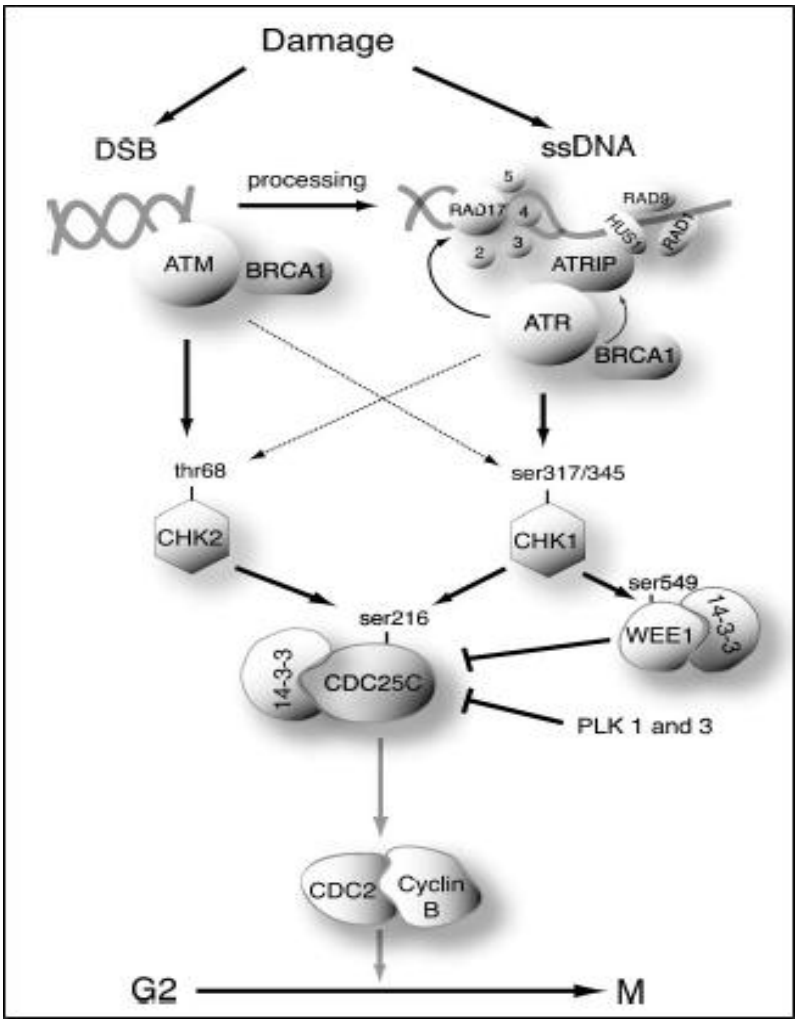

Figure 1-13: The G2/M checkpoint in mammalian cells. This checkpoint functions to block mitosis onset through blocking Cdc2-CyclinB activity. As a response to DNA damage, either ChK1 or ChK2 is activated, which leads to inhibitory Cdc25C phosphorylation. That will facilitate its binding to 14-3-3 proteins, which mediate its cytoplasmic localization and block the G2/M transition. Gray arrows indicate to the functions that are lost as a response to the checkpoint activation. Indicated amino acids on the proteins refer to phosphorylation sites. (Adapted from Nyberg, et.al. 2002).

1.9 Roles of spHus1 and hHUS1 in cell cycle and genomic stability

Hus1 is a highly conserved DNA damage checkpoint protein that assembles with Rad9 and Rad1 in the intensively studied Rad9-Rad1-Hus1 (9-1-1) ring complex. The fission yeast *hus1* gene was isolated for the first time in a screen of *S. pombe* mutants, which were treated with the ribonucleotide inhibitor hydroxyurea (HU) that stalls DNA replication forks due to the depletion of the dNTPs pool. Although the DNA replication was blocked as a response of the HU effect, *hus1* deficient cells were able to enter mitosis (Enoch, et.al. 1992; Al-Khodairy, et.al. 1994). This indicated that Hus1 is required for the S/M DNA damage checkpoint. The gene has five exons, of which one is a micro-exon that is composed of only 13 nucleotides. The gene encodes for a 33kDa protein (Kostrub, et.al, 1997). It is one of six checkpoint Rad fission yeast genes, which are called Rad (Radiation sensitive) proteins (Hus1, Rad1, Rad3, Rad9, Rad17, and Rad26). They are all required for the S-M and G2/M DNA damage checkpoints (Al-Khodairy & Carr, 1992; Enoch, et.al. 1992; Al-Khodairy, et.al. 1994). Human homologs of all of the Rad proteins (hHUS1, hRAD1, ATR/Rad3, hRAD9, ATRIP/Rad26 and hRAD17 respectively) were identified (Cimprich, et. al., 1996; Lieberman, et. al., 1996; Kostrub, et. al., 1998; Parker, et. al., 1998; Udell, et.al. 1998; Hang & Lieberman, 2000).

Hus1 associates with two additional proteins, Rad1 and Rad9, in a heterotrimeric ring complex (9-1-1 complex), which shares structural and functional similarity to PCNA (Figure 1-14) (Caspari, et.al. 2000). The 9-1-1 ring is loaded independently of Rad3 at sites of DNA damage, which possess an ssDNA region next to a dsDNA section (Wu, et.al. 2005), by the Rad17 loading complex (Rauen, et.al. 2000). Interestingly, Rad17 shares structural similaritity with the PCNA loading factor and associates with the same small subunits as RFC (Zou, et.al. 2002). Volkmer & Karnitz (1999) identified the human homologues of *S.pombe* Rad1, Hus1, and Rad9, which like the fission yeast proteins interact with each other to form a complex. Furthermore, a paralog of hHUS1, hHUS1B was identified by Hang, et.al, (2002). This second Hus1 gene has no introns and encodes a protein with 278 amino acids, which shares 48% identity and 69% similarity to hHUS1 respectively. Unlike hHUS1, hHUS1B interacts with hRAD1 but not with hRAD9 and not with hHUS1, which indicates

that it cannot replace hHUS1 in the RAD9-RAD1-HUS1 complex (Hang, et.al. 2002). In 2000, Caspari and colleagues showed that the *S. pombe hus1* gene encodes four isoforms, of which only one, the Hus1-B isoform, interacts with Rad1 and Rad9 in the 9-1-1 ring. *S.pombe* Hus1 is phosphorylated upon DNA damage by ATR/Rad3 (Kostrub, et.al. 1998; Caspari et.al. 2000). In human cells, Hus1 is an unstable protein, which is degraded by the ubiquitin-proteasome pathway in a process regulated by its interaction with Rad1 (Hirai, et.al. 2004).

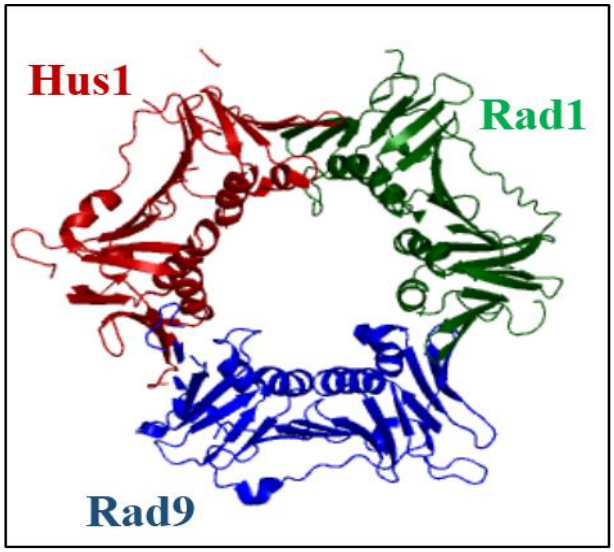

Figure 1-14: Human Rad9-Rad1-Hus1 clamp crystal structure (Sohn & Cho, 2009). The structure was created using Polyview 3D server: (http://polyview.cchmc.org/polyview3d.html). Rad9 = blue, Hus1 = red, Rad1 = green.

HUS1 plays a vital role in maintaining genome integrity especially during DNA replication. As shown in Figure 1-15, ATR activation requires the presence of ssDNA, which becomes exposed at stalled or broken replication forks. Firstly, the ATR-ATRIP (ATR-Interaction protein) complex is recruited to the ssDNA region by its subunit ATRIP where it associates with the ssDNA-binding protein RPA (Replication Protein A) (Parrilla-Castellar et.al, 2004; Wei-Feng, et.al. 2006; Niida & Nakanishi, 2006). Secondly, the Rad17-RFC complex (Replication Factor C) loads the Rad9-Rad1-Hus1 (9-1-1) complex (Morgan, 2007). The independent loading of the 9-1-1 ring and ATR is a fail-safe mechanism preventing aberrant checkpoint firing since ATR becomes only active upon binding to Rad9 within the 9-1-1 ring (Wang, et.al. 2006; Navadgi-Patil & Burgers, 2009) and to

TopBP1/Rad4 which is an essential DNA replication factor and checkpoint protein (Furuya, et. al. 2004; Qu, et.al. 2013). Finally, active ATR phosphorylates the effector kinase Chk1 at serine 345 in *S.pombe* and human cells, and S317 in human cells, in the presence of the mediator protein Claspin or Crb2 in *S.pombe* (Capasso, et.al. 2002; Wei-Feng, et.al. 2006; Cimprich and Cortez 2009). Chk1 activation by ATR phosphorylation leads eventually to checkpoint responses, which are represented by fork stabilization, suppression of late origin activation and S/M or G2/M delays (Chen & Sanchez, 2004).

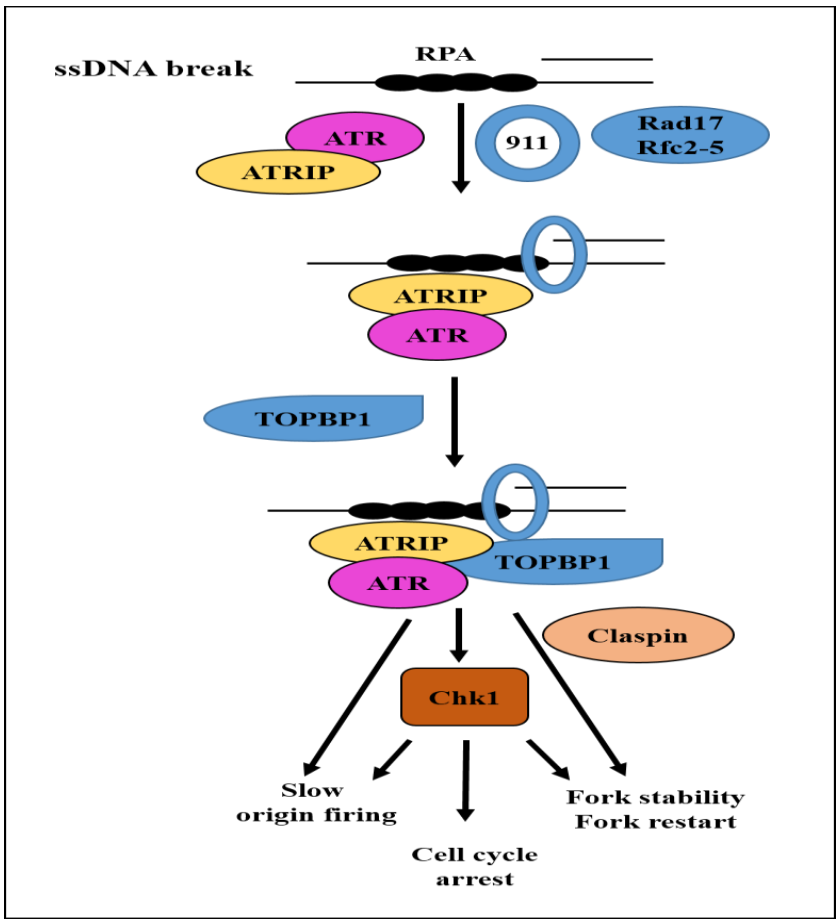

Figure 1-15: ATR pathway activation in mammalian cells. This pathway is activated especially when the ssDNA breaks ocuure as a result of stalled or broken replication fork. RPA protein covers the ssDNA and associate with the ATR-ATRIP complex, which is recruited to the ssDNA independently of the Rad9-Rad1-Hus1 complex. Loading of 9-1-1 complex to the junction of ssDNA is a Rad17 mediated procedure. This will attract TOPB1, which activates ATR in an ATRIP-mediated procedure. Eventually, Chk1 is phosphorylated leading to either origin firing suppression, fork stabilization or cell cycle arrest.

Mouse *hus1* null cells show Chk1 down-regulation after DNA replication stress, which could be reactivated by complementation with a transfected *hus1* gene (Weiss, et.al. 2003). In fission yeast, *hus1* is essential for the activation of the G2/M checkpoint in response to the treatment with either topoisomerase 1 inhibitors such as camptothecin (CPT) or DNA damaging agents such as UV or phleomycin (radiomimetic drugs) (Enoch, et.al. 1992). More evidence was obtained from mouse *hus1*$^{-/-}$ *p21*$^{-/-}$ embryonic fibroblasts (MEFs). Loss of mHus1 in these cells abolishes the reduction in replication rate when the template is modified by bulky adducts (Weiss, et.al., 2003) and it renders cells sensitive to etoposide-induced apoptosis (anticancer drug) through up-regulation of the pro-apoptotic BH3-only proteins Bim and Puma (Meyerkord, et.al. 2008). Murine Rad9 re-localizes to the cytoplasm in the absence of mHus1 where it promotes apoptosis by binding to Bcl2 (Meyerkord, et.al. 2008). Correspondingly, down regulation of human HUS1in a p53-deficiency background sensitizes cells to the DNA cross-linking agent cisplatin (Kinzel, et.al. 2002). Loss of murine Hus1 impairs chain elongation in the presence of DNA breaks that were induced by CPT treatment (Wang, et.al. 2004), and lowers the efficiency of homologous recombination at broken DNA replication forks (Wang, et.al. 2006). More support for a role of Hus1 in DNA replication comes from *in vitro* experiments with *Xenopus* oocyte extracts, which demonstrated a requirement of DNA polymerase α to load XHus1 onto chromatin at the start of S phase (You, et.al. 2002).

Further support for the role of Hus1 in DNA replication comes from its complex interactions with the human protein FHIT. FHIT is encoded at the human fragile site *FRA3B* on chromosome 3 (Ong, et. al. 1997). Chromosome fragile sites occur at specific sequences within the mammalian genome where replication forks are more likely to stall resulting in single-stranded regions, which are more prone to breakage (Ishii, et. al., 2006). It was shown that these sites are protected by checkpoint proteins such as ATR, BRCA1, SMC1 and Fanconi Aneamia proteins, in addition to Chk1 and HUS1(Zhu & Weiss, 2006). On the other hand, Ishii, et.al. (2006) showed that the FHIT protein regulates HUS1 expression upon UV treatment. The exposure of *FHIT* deficient HEK293 cells to UV light lead to a decline in HUS1 expression levels. Cells then treated with MG-132, a proteasome inhibitor, resulted in HUS1 up-regulation. Taken together, these findings are consistent with the fact that the HUS1 protein is ubiquitinated (Hirai, et.al. 2004) and confirm a role of FHIT in the

regulation of HUS1 turnover upon DNA damage treatment. Although most Hus1 functions are attributed to the 9-1-1 complex, Hus1 may act independently in the context of the tumor suppressor protein FHIT (Pichiorri, et. al., 2008). A role of HUS1 outside of the 9-1-1 ring is further supported by the recent observation that only hHUS1 levels, but neither hRAD1 nor hRAD9, are up regulated upon over-expression of the circadian clock protein Period 2 (PER2) in cancer tissues depending on cancer stage (Štorcelová, et.al. 2013). Human HUS1 also interacts with other proteins. It was shown that human Histone Deacetlyse 1 (HDAC1) associates with Hus1 and that both co-localize to the nucleus. Since hHDAC1 and HUS1 were found to form a complex with hRad9, it is very likely that this association occurs in the context of the 9-1-1 ring (Cai, et.al. 2000).

1.10 Thesis Organization

The organisation of the following dissertation chapters' will be as follow:

- **Chapter2:** reviews the materials and methods that used to achieve both yeast and human cells experiments.

- **Chapter3: Construction & Analysis of *hus1* single and double point mutations in *S. pombe* cells:** the purpose of this chapter is to construct single and double point mutation in *S.pombe hus1* gene. That is to confirm whether the Hus1 four isoforms (Caspari, et.al. 2000) are produced by Leaky Ribosome Scanning (LRS) mechanism (Kochetove, 2008). Furthermore, the resulted mutations phenotypes were analysed as treated with DNA damaging agents with variety of techniques.

- **Chapter4: Investigation of *hHUS1* and *hHUS1B* expression at mRNA Level and *hHUS1* Down-Regulation:** Following the data, which we obtained from analysis the *S. pombe* isoforms, we extended our experiments to investigate whether human cells express equivalent transcripts of *S. pombe* Hus1variants. That because it is mentioned in Ensembl data base that hHUS1 has four protein

coding alternative splice variants (hHUS1-001, hHUS1-005, hHUS1-011 and hHUS1-004). In addition, we investigated hHUS1B, since there is no much investigation were done about this gene.

- **Chapter5: Investigation of the Expression Levels of the hHUS1 Protein in Human Cell Lines:** As a result, from the previous chapter findings of hHUS1 transcripts existence confirmation on mRNA level, we tried to confirm their existence furthermore on protein level using variety of techniques. I tried to find out whether hHUS1 transcripts expression is restricted to one of the cell cycle phases, induced as a response to exposure to one of DNA damage agents, or it is restricted to senescent cells. Moreover, I used two down-regulation systems to validate the efficiency of the used antibodies.

- **Chapter6: Construction of *hHUS1B* and *hHUS1* variants stable cell lines:** This chapter explains the construction of stable cell lines of each hHUS1 transcripts in addition to hHUS1B to investigate their cellular functions.

- **Chapter7: General discussion:** This chapter includes the general discussion of yeast and human cells results.

Chapter 2: Materials and Methods

2.1 Communal materials used for yeast and human cells work

- **Media:**

  LB and LBA (Luria Bertani Agar):

  10g/l Tryptone, 5g/l yeast extract, 5g/l NaCl and 20g/l agar (for LBA).

- **Buffers:**

  EDTA (Ethylenediamine tetraacetic acid) 0.5M, pH=8:

  186.1g of $Na_2EDTA.2H_2O$ in 500ml, 10M NaOH was used to adjust pH=8 and H_2O was added up to 1 L.

  10x DNA loading dye:

  0.025g Xilene cyanol, 0.025g Bromophenol blue, 1.25ml of 10% SDS, 12.5ml glycerol and 6.25ml dH_2O.

  4x Laemmli buffer:

  40% Glycerol, 240mM Tris/HCl (pH=6.8), 8% SDS, 0.04% bromophenol blue and 5% β-mercaptoethanol.

  4% Paraformaldehyde (PFA):

  - Weigh 2g Paraformaldehyde powder in a 50ml tube.
  - Add approximately 20ml of 1xPBS and 1ml of 1M NaOH.
  - Heat in a 65^oC water bath and shake frequently for about 30min.
  - Adjust the pH= 7.0 using 1M HCl, add more 1xPBS up to 50ml.
  - Cool down to room temperature, and store as single aliquots at -20^oC.

  10x PBS (phosphate- buffered saline):

  360g NaCl, 43.6g $Na_2HPO_4.7H_2O$, 12.8g NaH_2PO_4 and dH_2O up to 4L, pH= 7.2

  10x SDS buffer:

  576g Glycine, 40g SDS, 121g Tris-HCl and dH_2O up to 4L.

  10x Transfer buffer:

  124g Tris-base and 56g Glycine and dH_2O up to 4L.

  50x TAE (Tris-Acetate-EDTA) buffer:

For routine Agarose gel electrophoresis and gel purification, 242g Tris base, 57.1ml glacial acetic acid, 37.2g $Na_2EDTA.2H_2O$ and H_2O up to 1L.

1xTE (Tris-EDTA) buffer for DNA re-suspension:

10mM Tris-HCl pH=7.5 and 1mM EDTA pH=8.

100%TCA (Trichloroacetic acid):

500g TCA in 350ml of dH_2O.

- **Antibodies:**

Table 2-1: List of Antibodies used in this study

Antibody	Company	Cat.no.	Description	Conc.
B-Actin	Sigma	A2066	Rabbit- polyclonal	Wb= 1:1000
HUS1	Abcam	AB96297	Rabbit-poly clonal	Wb= 1:1000
HUS1	Abcam	AB109371	Rabbit-monoclonal	Wb=1:10000
HUS1B	Abcam	AB115615	Rabbit-polyclonal	Wb=1:1000
HUS1B	Antibodies online	AA104-117	Rabbit-polyclonal	Wb=1:1000
RAD1	Abcam	AB5363	Mouse-monoclonal	Wb=1:1000
RAD9A	Abcam	AB96862	Rabbit-polyclonal	Wb=1:1000
ChK1S345ph	Thermo Scientific	MA5-15145	Rabbit-polyclonal	Wb=1:1000
P21WAF1/CIP1	Cell signaling	2947	Rabbit-polyclonal	Wb=1:1000
GAPDH	Abcam	AB128915	Rabbit-polyclonal	Wb=1:10000
CDC25C	Abcam	AB32444	Rabbit-polyclonal	Wb=1:5000
p16	Abcam	AB108349	Rabbit-polyclonal	Wb=1:1000
CyclinD1	Abcam	AB40754	Rabbit-polyclonal	Wb=1:1000
CyclinE	Cell signaling	4129	Mouse-polyclonal	Wb=1:1000
H3S10ph	Abcam	AB5176	Rabbit-polyclonal	Wb=1:1000
Anti-Myc tag	Santa Cruz	SC40	Mouse-polyclonal	Wb=1:2000
Histone H3	Abcam	AB1791	Rabbit-polyclonal	Wb=1:1000
GFP	Thermo Scientific	MA5-15256	Mouse-polyclonal	Wb=1:1000
Anti-mouse secondary AB-HRP anti-light chain	Jackson ImmunResearch	115-035-174		Wb=1:10000
Anti-rabbit secondary AB-HRP anti-light chain	Calbiochem	401315		Wb=1:10000

Alexa Fluor® 488 Goat Anti-Rabbit IgG (H+L) Antibody	Invitrogen	A11008		IF=1:500
Alexa Fluor® 488 Rabbit Anti-Mouse IgG (H+L)	Invitrogen	A11059		IF=1:500

2.2 General Molecular Biological Methods

The following protocols were used for both yeast and human cells. Any specification or modifications in the protocols will be mentioned as required.

2.2.1 Polymerase Chain Reaction (PCR)

Polymerase Chain Reaction (PCR) (will be termed as general PCR later on) was used to amplify entire genes or to amplify the genes of interest as two fragments. The Fusion PCR term is related to the reaction by which two or three PCR products are fused to each other to form a larger product or a gene point mutation(s).

- **General PCR Reaction:**

  The following materials were mixed in a PCR tube. All the additions were done on ice. The following additions are enough to achieve one reaction:

Component	Volumes (µl)
5x GC buffer (NEB)	10
2mM dNTPs	5
DNA template	≈100ng
10µM 5'-primer-F	2.5
10µM 3'-primer-R	2.5
Phusion polymerase (NEB)	0.5
Sterile dH_2O	Up to 50µl

PCR tubes were placed in a Thermo-cycler and the following program (usually performed with 35 cycles) was used:

Initial Denaturation	95ºC	1min
Separation	98ºC	1min
Annealing	55ºC	30sec
Extension	72ºC	1-1.30min
Final Extension	72ºC	10min

- **Fusion PCR reaction:**

  Fusion PCR was achieved in two steps. First, the initial fragments were amplified using the general PCR protocol. After their gel purification, the fusion PCR reaction was set up as follows:

  - First mixture:

Component	**Volumes (µl)**
5x GC buffer (NEB)	10
2mM dNTPs	5
Fragment 1	≈100ng
Fragment 2	≈100ng
Fragment 3	≈100ng
Phusion polymerase (NEB)	0.5
Sterile dH2O	up to 50 µl

The PCR reaction was run for 10 cycles only using the standard conditions.

The second step of the Fusion PCR is to fuse the initial fragments to each other by setting up the second mixture as follows:

- Second mixture:

  The following components were added to the previous tube:

Component	**Volumes(µl)**
5x GC buffer (NEB)	15
2mM dNTPs	10
10µM 5'-Flanking primer-F	5

10µM 3'-Flanking primer-R	5
Phusion polymerase (NEB)	1
Sterile dH2O	up to 50 µl

Samples (100µl total volume) were run in the Thermo cycler with 35 cycles of the standard PCR program.

- **PCR Products Examination by Agarose Gel:**

  An agarose gel was used to analyze the PCR products or to clean them up by gel purification. It was usually prepared as a 1% (w/v) gel in 1x TAE buffer, since it is suitable for PCR examination and gel purification. DNA samples (≈5µl) were mixed with DNA loading dye and run through the agarose gel in parallel with either 1Kb or 100bp DNA ladder (Promega, G5711 & G 2101 respectively). At the end of the electrophoresis time, the products were analyzed using the Gel Doc2000 machine with the assistance of Quantity One® software.

- **PCR Products Isolation by Gel Purification:**

  PCR product was purified from the agarose gel using GenElute™ Gel Extraction Kit (SIGMA-NA1010) according to the manufacturer's instructions.

2.2.2 Cloning into Plasmids

- **Digestion of the PCR Products and the Expression Vectors:**

  When a PCR product was required for cloning into a vector, it was first digested in parallel with the vector by specific restriction enzyme(s) to allow the ligation thereafter. I used the basic digestion protocol from New England BioLabs (NEB) (https://www.neb.com/protocols/2012/12/07/optimizing-restriction-endonuclease-reactions).

Component	25 µl Reaction	50 µl Reaction
DNA	0.5µg	1µg
10x NEB buffer	2.5µl	5µl
100xBSA(if needed)	0.25 µl	0.5 µl
Nuclease-free water	Up to 50 µl	Up to 25 µl
Restriction Enzyme 1	5 units	10 units (=1µl is used)
Restriction Enzyme 2	5 units	10 units (=1µl is used)

The digestion reaction was incubated at 37^{o}C for 1-1:30 hours. Restriction enzymes were deactivated either by loading the samples onto the agarose gel immediately at the end of incubation period followed by gel purification, or by heat inactivation according to the enzyme's features. The digestion reaction of 50µl total volume was used for cloning purpose. Whereas, the 25 µl reaction was used to validate the size and existence of an inserted DNA fragment.

- **Ligation:**

Digested vector and DNA fragment, which resulted from the previous step, can be ligated to each other using the following protocol:

Usually a 1:3 ratio of plasmid: DNA fragment was used to achieve the ligation process using T4 DNA ligase (Promega, M180A).

Ligation mixture:

Component	Volume
Plasmid	x µl
DNA insertion	x µl
1x T4 ligation buffer	2 µl
T4 ligase	1 µl
H_2O	Up to 20 µl

The ligation mixture was incubated at 16^{o}C overnight, and it was proceeded with *E.coli* transformation or kept at -20^{o}C until use.

2.2.3 *E.coli* transformation

- **DNA transformation into *E.coli* Competent Cells:**

  I performed the protocol according to NEB High Efficiency transformation protocol (https://www.neb.com/protocols/1/01/01/high-efficiency-transformation-protocol-c3019):

  1. Competent cells were thawed on ice.
  2. Plasmid DNA (1pg-100ng ≈ 1-5µl) was added to the cells, mixed gently, and kept on ice for 30min.
  3. Cells were heat shocked at 42°C for 30 seconds, and then placed on ice for 5min.
  4. Cells were mixed with 950 µl of room temperature LB medium.
  5. Cultures were shaken vigorously (250rpm) for 60min (1.30hr for low copy plasmid) at 37°C.
  6. Selection plates were warmed up to 37°C.
  7. According to the expected ligation efficiency, cells either were spun down, and re-suspended in 75-100 µl of LB medium and plated onto LBA plates with selection antibiotic, or 15-50 µl of cells were plated on the same plates.
  8. Plates were incubated overnight (up to 16hr) at 37°C until the colonies grow.

- **Plasmid DNA extraction from transformed *E.coli* cells:**

  Plasmid DNA was extracted from the transformed cells using GenElute™ Plasmid Miniprep Kit (SIGMA, PLN70) for low plasmid DNA concentration, and GenElute™ Plasmid Midiprep Kit (SIGMA, PLD35) for higher concentrations according to the Manufacturer's instructions. Plasmids carrying the desired insertion are ready for either transformation into yeast cells or transfection into human cells.

2.3 Yeast Protocols

2.3.1 Materials

2.3.1.1 Media

YEL and YEA (Yeast Extract Liquid & Yeast Extract Agar): 30g/l Glucose, 5g/l yeast extracts, 0.1g/l adenine and 20 g/l agar (for YEA).

EMM (Edinburg Minimal Media): 30g/l Glucose, supplemented with yeast nitrogen base 6.7g/l, and either 3% (w/v) adenine (30x), 6% (w/v) uracil (15x) or 3% (w/v) Leucine (30x).

ME (Malt Extract): 30g/l Malt extract, supplemented with 225mg/l of adenine/ histidine/uracil/leucine and 20g/l agar (for MEA), pH=5.5 adjusted with NaOH.

2.3.1.2 Supplements

Adenine (30x): 1.9g Adenine in 250ml of dH_2O.

Uracil (15x): 0.9g Uracil in 250ml of dH_2O.

Leucine (30x): 1.9g Leucine in 250ml of dH_2O.

2.3.1.3 *S.pombe* strains used in this study

Table 2-2: List of *S.pombe* strains used in this study

Strain	Genotype	Source
hus1wt 805	*h+ ade6-M210 leu1-32 ura4-D18*	Dr. T.Caspari
hus1wt 804	*h- ade6-M210 leu1-32 ura4-D18*	Dr. T.Caspari
hus1wt.Myc(LoxP-LoxM3)	*h+ ade6-M210 leu1-32 ura4-D18 hus1::loxP-hus1-myc13-loxM*	This study
hus1 base strain	*h+ ade6-M210 leu1-32 ura4-D18 hus1::loxP-ura4-loxM*	This study
Δhus1	*h- ade6-M210 leu1-32 ura4-D18 hus1::leu2*	Dr. T.Caspari
hus1.Myc.M1A	*h+ ade6-M210 leu1-32 ura4-D18 hus1::loxP-hus1-M1A-myc13-loxM*	This study
hus1.Myc.M32A	*h+ ade6-M210 leu1-32 ura4-D18 hus1::loxP-hus1-M32A-myc13-loxM*	This study
hus1.Myc.M46A	*h+ ade6-M210 leu1-32 ura4-D18 hus1::loxP-hus1-M46A-myc13-loxM*	This study
hus1.Myc.M176-180A	*h+ ade6-M210 leu1-32 ura4-D18 hus1::loxP-hus1-M176A-M180A-myc13-loxM*	This study
hus1.Myc.M231A	*h+ ade6-M210 leu1-32 ura4-D18 hus1::loxP-hus1-M231A-myc13-loxM*	This study
hus1.Myc.M241A	*h+ ade6-M210 leu1-32 ura4-D18 hus1::loxP-hus1-M241A-myc13-loxM*	This study
hus1.Myc.M1AM32A	*h+ ade6-M210 leu1-32 ura4-D18 hus1::loxP-hus1-M1A-M32A-myc13-loxM*	This study
hus1.Myc.M1AM46A	*h+ ade6-M210 leu1-32 ura4-D18 hus1::loxP-hus1-M1A-M46A-myc13-loxM*	This study
hus1.Myc.M32AM46A	*h+ ade6-M210 leu1-32 ura4-D18 hus1::loxP-hus1-M32A-M46A-myc13-loxM*	This study
hus1.Myc.M1AM176-180A	*h+ ade6-M210 leu1-32 ura4-D18 hus1::loxP-hus1-M1A-M176-myc13-loxM*	This study
hus1.Myc.M1AM231A	*h+ ade6-M210 leu1-32 ura4-D18 hus1::loxP-hus1-M1A-M231A-myc13-loxM*	This study
Δrad1	*h- ade6-M210 leu1-32 ura4-D18 rad1::ura4*	Dr. T.Caspari
Δrad1 hus1.Myc.M32AM46A	*h- ade6-M210 leu1-32 ura4-D18 hus1::loxP-hus1-M32A-M46A-myc13-loxM rad1::ura4*	This study
Δrad17	*h- ade6-M210 leu1-32 ura4-D18 rad17::ura4*	Dr. T.Caspari
Δrad17 hus1.Myc.M1A	*h- ade6-M210 leu1-32 ura4-D18 hus1::loxP-hus1-M1A-myc13-loxM rad17::ura4*	This study
Δrad9 hus1.Myc.M1A	*h- ade6-M210 leu1-32 ura4-D18 hus1::loxP-hus1-M1A-myc13-loxM rad9::ura4*	This study

Δcds1	*h- ade6-M210 leu1-32 ura4-D18 cds1::ura4*	Dr. T.Caspari
Δcds1 hus1.Myc.M32AM46A	*h- ade6-M210 leu1-32 ura4-D18 hus1::loxP-hus1-M32A-M46A-myc13-loxM cds1::ura4*	This study
Δchk1	*h- ade6-M210 leu1-32 ura4-D18 chk1::kanMX4*	Dr. T.Caspari
Δcds1Δchk1	*h- ade6-M210 leu1-32 ura4-D18 chk1::kanMX4 cds1::ura4*	Dr. T.Caspari
Δchk1 hus1.Myc.M32AM46A	*h- ade6-M210 leu1-32 ura4-D18 hus1::loxP-hus1-M32A-M46A-myc13-loxM chk1::kanMX4*	This study

2.3.1.4 List of Primers used for yeast work

Table 2-3: List of primers used in yeast experiments.

Primer Name	Primer Sequence (5' to 3')
Base strain construction	
Hus1-B2-F1	CATCCCGATTAGCGAGCATG
Hus1-B2-R1	TTAATTAACCCGGGGATCCGGCCAGCTAAGAAATAGCAAACTGGGC
Hus1-B2-F2	GCCCAGTTTGCTATTTCTTAGCTGGCCGGATCCCCGGGTTAATTAA
Hus1-B2-R2	GTGGCTAGTCACTCATAACGAATTCGAGCTCGTTTAAAC
Hus1-B2-F3	GTTTAAACGAGCTCGAATTCGTTATGAGTGACTAGCCAC
Hus1-B2-R3	GTATAGCGATGCCTCCAAAGTAC
***ura4*$^{+}$ Integration confirmation primers**	
Hus1-Test-1-F	GATACAACGAATAGGCTCTTGAG
Hus1-Test-2-R	CCGTTTACGTTAGTTAGGGCAATC
Hus1-Test-6-F	CTGTCAAAGCTTTCACTAATTGG
Ura4-2-R	GCTGATATGCCTTCCAAC
Mutations construction primers	
Hus1-Wt-F	CGATAGCATGCGTGGCATGCCTTAGCTGGCTTTTACGCGTTCG
Rad9-S8.1-R	GCTATCACACTAGTTAGACTAGTCAGATCTATATTACCCTGTTATCCC
Hus1-M1A-F	CAAAGACTGAAAGCAAGATTTAAAACAAG
Hus1-M1A-R	CTTGTTTTAAATCTTGCTTTCAGTCTTTG
Hus1-M32A-F	GCTGGCTTCGTCTGGCTCCTGAAACTGTAAATTTTG
Hus1-M32A-R	CAAAATTTACAGTTTCAGGAGCCAGACGAAGCCAGC
Hus1-M46A-F	GATAGTGCCAGATTTTAGGGCTACTCAAGTTTGGTCGTAAG
Hus1-M46A-R	CTTACGACCAAACTTGAGTAGCCCTAAAATCTGGCACTATC
Hus1-M176&180A-F	CAGACCGTATTATAGCTTCAGCCAACGCTTCAGGCGAATTGCAG

Hus1-M176&180A-R	CTGCAATTCGCCTGAAGCGTTGGCTGAAGCTAATAATACGGTCTG
Hus1-M231A-F	CCGAAGAATTTGTTCACGCTAGACTAGACAGCAAGGAC
Hus1-M231A-R	GTCCTTGCTGTCTAGTCTAGCGTGAACAAATTCTTCGG
Hus1-M241A-F	GCAAGGACTTAGTCAACGCTTTAAAATATCCAGTGTTGC
Hus1-M241A-R	GCAACACTGGATATTTTTAAAGCGTTGACTAAGTCCTTGC
DNA Sequencing primers	
Hus1-sequ-1-F	AGCAGAAAGTTCGTTTACTAATC
Hus1-sequ-5-R	ATCTAGCGCCTGAACAAGACC
Hus1-sequ-2-F	GTCAGTTATTAAGGAACCAACTG
Hus1-sequ-3-F	CATACCTTCAGCTAGAGTAAGCAC
Hus1-sequ-4-R	GTCCACATAGGTACTAATGTAGTATG

2.3.1.5 List of plasmids used in yeast work

Table 2-4: List of plasmids used in yeast experiments

Plasmid Name	Source
pAW8	Watson, et. al. 2008
pAW1	Watson, et. al. 2008

2.3.2 Methods

2.3.2.1 The *hus1* base strain construction

In order to construct the *hus1* base strain, I took advantage of the non-essential gene replacement protocol (Watson, et.al. 2008). This is achieved by replacing the whole *hus1* gene coding sequence with the *LoxP-ura4*$^{+}$*-LoxM3* cassette from the plasmid pAW1. The construction was performed as the following steps:

1. **Construction of the *LoxP-ura4*$^{+}$*-LoxM3* cassette:**

   To construct *LoxP-ura4*$^{+}$*-LoxM3* cassette, I amplified the flanking arms from the genomic DNA of the *S.pombe* wild type 805 strain, which represent the upstream and downstream sequences of the *hus1* gene to facilitate its replacement with the *ura4*$^{+}$ gene. The *LoxP-ura4*$^{+}$*-LoxM3* cassette was amplified from the pAW1 plasmid.

The three fragments were individually amplified by general PCR (fragments lengths and primers sequences are detailed in chapter3), prior to their fusion by Fusion PCR (section 2.2.1).

2. *LoxP-ura4*$^{+}$*-LoxM3* cassette transformation into 805 wild type cells:

To transform the *LoxP-ura4*$^{+}$*-LoxM3* cassette into the wild type strain 805, I followed the Wang et.al, (2004) protocol, which represents the general transformation protocol for either linear DNA (PCR product) or plasmid DNA into yeast cells:

1. Cells were grown in YE liquid medium at 30^{o}C up to 1x10^{7} cells/ml.
2. For each transformation, 2x10^{8} cells were washed once with equal volume of sterile dH_2O and then transferred to a new Eppendorf tube in 1ml of sterile dH_2O. Cells were centrifuged at 10,000 rpm for few seconds.
3. Pellets were washed once with 1ml of 1x LiOAc/TE solution, and then centrifuged at 3000rpm for 5min.
4. Pellets were re-suspended in 100µl of 1x LiOAc/TE solution (made from 10x filter-sterilized stocks).
5. Two microliters of boiled salmon carrier DNA (10mg/ml) and 10µl transforming DNA were added to the previous mixture, and were incubated for 10min at room temperature.
6. The previous mixture was mixed gently with 260µl of 40% PEG/LiOAc/TE solution, and incubated for 30-60min at 30^{o}C.
7. At the end of incubation time, 43µl of filter-sterilized DMSO was added and mixed gently; cells were heat shocked at 42^{o}C for 5min.
8. Cells were centrifuged at 3000rpm for 3min and washed once with sterile dH2O.
9. Cells were transferred to 10ml of YE liquid medium and incubated at 30^{o}C for 48hr in a shaker incubator.

10. Cells were plated onto selective medium as 100µl of undiluted cells, as well as of 10^{-1} and 10^{-2} dilutions and incubated for 3-5 days at 30ºC.

Stock solutions:

- **10x LiOAc:** 1M Lithium acetate, pH=7.5 (adjusted with diluted acetic acid)
- **10x TE:** 0.1M Tris-HCl and 0.01M EDTA, pH7.5
- **40% PEG/LiOAc/TE:** 8g PEG4000, 2ml of 10X LiOAc, 2ml of 10x TE and 9.75ml of dH2O. Dissolve PEG completely and filter sterilize.

Selective media:

I used EMM media supplemented with adenine and leucine but lacking of uracil to select for *ura4*$^{+}$ cells.

2.3.2.2 Yeast strains construction

2.3.2.2.1 Gene targeted integration of the *hus1* point single and double mutations

I used Fusion PCR protocol (section 2.2.1) to create single and double point mutations in the *hus1* gene. First, to create the single mutations, I used four primers: two flanking primers (5'-Flanking primer 1-F and 3'-Flanking primer 4-R), which are Hus1-Wt-F and Rad9-s8.1-R respectively. These two primers are common for all mutations and to amplify the entire *hus1* gene. I also used two primers carrying a specific mutation, which overlapped with each other in the mutation site sequence (mutation primer 2-R and mutation primer 3-F) (Table 2-3). These primers were used to amplify the gene as two individual fragments (by general PCR reaction), both of them carrying the desired mutation. Since I wanted to add the C-terminal myc13 affinity tag, I used genomic DNA from the *hus1.Myc.wt* strain (Caspari et al., 2000) as a template. After purification of the fragments from the agarose gel, they were fused to each other using the Fusion PCR reaction. In the first step of this reaction, the two overlapping fragments were fused to each other. While in the second step, the full-length fusion product was amplified with the flanking primers (5'-Flanking primer1- F and

3'-Flanking 4-R; Hus1-Wt-F and Rad9-S8.1-R respectively). All mutants fragments were sequenced to confirm the mutation and to exclude the presence of additional changes.

To create the double-point mutations, I used the genomic DNA of one of the single mutants, usually *hus1.Myc.M1A* for the double mutants with M1A in parallel with one of the other methionine mutation primers, or *hus1.Myc.M32A* for the *hus1.Myc.M32AM46A*, double mutant as a template to amplify the two initial fragments.

The mutated *hus1* cassettes of each single and double mutation were cloned using SpeI and SphI into the multiple cloning site of the plasmid pAW8, which is flanked by the *LoxP-LoxM3* sequences (following the same previously mentioned protocols of digestion, ligation and *E.coli* transformation).

To introduce our mutations into the *S.pombe* base strain, I took advantage of the Cre-Lox recombinase-mediated cassette exchange (RMCE) system (Watson, et.al. 2008) which allows the replacement of the mutated *hus1* gene (cloned onto pAW8 vector) with the *ura4*$^{+}$ cassette integrated between the *LoxP* and *LoxM3* sequences at the endogenous *hus1* locus. Transformation of mutated *hus1* plasmids achieved following the one mentioned in section 2.3.2.1, point two.

2.3.2.2.2 Yeast strains construction (mating)

This protocol was adapted from Forsburg & Rhind, (2006). I used the ability of *S.pombe* G1 cells to enter meiosis when they are starved for nitrogen supplements. This was achieved by mixing the h^{+} and h^{-} strains in a drop of water on an ME plate. This malt extract plate was then incubated for 3-4 days at 25^{o}C. During meiosis, the strains are able to exchange genes with the other as long as they are not too close to each other on the same chromosome (the closer the distance, the lower the frequency). Meiotic cells were recognized microscopically by the formation of asci structures (each ascus contains four spores). Spores were randomly selected from the whole population by cells treatment with 30% Ethanol for 30 min at room temperature. While spores survive this treatment, vegetative cells are killed. The surviving spores were plated onto YEA plates and incubated for 3-4 days at 30^{o}C. The desired strains were selected using marker genes and/or Western blot.

2.3.2.3 Yeast strains maintaining and storage

Yeast strains were kept at -80^{o}C for long-term storage. Stocks were prepared from fresh cells. A loop-full of cells was re-suspended in 50% glycerol in YE liquid medium. Working stocks were maintained on YEA plates prepared by streaking small portions of frozen cells onto the YEA plates and incubated at 30^{o}C for 3-4 days. Working stocks were kept at 4^{o}C up to one month. To prepare liquid culture, I used the following formula to inoculate determined cell number at 0-time point: $\mathbf{N_t = 2^G x N_0}$. **N_t:** represents cells number at desired time, **G:** for generation number (generation time for *S.pombe* wt cells in YEL media is 2.30 hours), and **N_0:** for initial cells number. Cells were grown at 30^{o}C in a shaker incubator (180rpm) for overnight.

2.3.2.4 Cells counting

Cells were counted using a haemocytometer (Hawksley counting champer, Thoma). 10µl of liquid cultures were loaded onto the slide and examined under the light microscope.

2.3.2.5 Genomic DNA extraction

Genomic DNA was extracted from yeast cells according to the following protocol:

1. Cells were grown up to 1x10^{7}/ml in YE liquid media at 30^{o}C shaker incubator.
2. Cells were pelleted by centrifugation at 3000rpm for 3 min, and supernatant was discarded.
3. Pellets were washed once with dH_2O volume similar to the cells initial volume, and centrifuged at 3000rpm for 3min.
4. Pellets were transferred to a fresh 2ml screw lid tube in 1ml of dH_2O and centrifuged at 10,000rpm for few seconds.
5. To the pellet, 200µl of DNA extraction buffer (2% Tritonx-100, 1% SDS, 100mM NaCl, 10mM Tris-HCl (pH=8) and 1mM EDTA) was added, in addition to 200µl of Phenol: Chloroform: Isoamyl alcohol (25:24:1, v: v) (SIGMA-P2069) mixture.
6. Six to eight spoons of silicone beads were added to the previous mixture.

7. Cells walls were broken by putting the tubes in the preparation machine for 8min.
8. Supernatant was transferred to a new Eppendorf tube using gel-loading tips and centrifuged at 10,000rpm for 5min at 4^{o}C.
9. Supernatant (represents genomic DNA) was transferred to a new Eppendorf tube, and mixed with 1ml of absolute ethanol by vortex.
10. The previous mixture was centrifuged at 10,000rpm for 5min at 4^{o}C, and supernatant was discarded.
11. Pellets were re-suspended in a 400µl of TE buffer contains 5µl of RNAse Type I A (10mg/ml) (Sigma, R4875), and incubated for 30min at 37^{o}C.
12. Ten microliters of 4M NH_4OAc, and 1ml of absolute ethanol were added and mixed by vortex.
13. Samples were centrifuged at 10,000rpm for 5min at 4^{o}C, and supernatant was discarded.
14. Pellets were re-suspended in 50µl of TE buffer.
15. Genomic DNA samples were stored at -20^{o}C.
16. To test the genomic DNA extract, 5µl were mixed with DNA loading dye and run on 1% Agarose gel.

2.3.2.6 Protein extract

2.3.2.6.1 Whole cell extract with Trichloroacetic acid (TCA)

This protocol was applied to extract whole cell protein as the following steps:

1. Cells were grown up to 1x10^{7} cell/ml in YE liquid media, at 30^{o}C in a shaking incubator.
2. Cells were counted and 4x10^{8} cell/ml only were pellet at 3000rpm for 3min to be used for protein extract.
3. Pellets were washed with the dH_2O volume similar to the cells initial volume, and centrifuged at 3000rpm for 3min.
4. Pellets were transferred in 1ml dH2O to a new 2ml screw lid tube and centrifuged as mentioned in the previous step.

5. To the pellets, 6-8 spoons of silicone beads were added, in addition to 300µl of 20% TCA.
6. Cells were broken by putting the tubes in the fast preparation machine for 8min.
7. The supernatant was transferred to a new Eppendorf tube using gel loading tips and centrifuged at 10,000rpm for 5 min. The supernatant was discarded.
8. The protein pellet was re-suspended in 150µl of 1M Tris-base (pH8.8) and 150µl of 4x Laemmeli buffer.
9. The protein sample was boiled on 95^{o}C heating block for 10min, centrifuged for few seconds to remove cells residues and stored at -20^{o}C.

2.3.2.6.2 Soluble protein extract for isoelectric focusing

Soluble protein extract was prepared from yeast cells to be used for 2D protein electrophoresis. The extraction steps were as follow:

1. Cells were grown up to 1x10^{7} cell/ml in YE liquid media, at 30^{o}C in a shaking incubator.
2. Cells were counted and 4x10^{8} cell/ml only were pellet at 3000rpm for 3min to be used for protein extract.
3. Pellets were washed with 20ml dH2O, and centrifuged at 3000rpm for 3min.
4. Pellets were transferred in 1ml dH2O to a new 2ml screw lid tube and were pelleted as mentioned in the previous step.
5. To the pellets, 6-8 silicone beads were added, in addition to 300µl of 2D lysis buffer (7.7M Urea, 10mM Tris-base (pH=8.8), 2.2M Thiourea, 0.55% Chaps and complete protease inhibitor tablet (1 tablet/7ml of the lysis buffer; Roche Applied Sciences 05892791001 EDTA-free).
6. Cells were broken by putting the tubes in the fast preparation machine for 8min.
7. Supernatant was transferred to a new Eppendorf tube and centrifuged at 10,000rpm for 5 min.
8. To the supernatant, 20mM (as a final concentration) of DL-Dithiothreitol (DDT) (1M stock solution) was added (6µl/300 µl of the extract). The mixture was incubated at room temperature for 30min.

9. N, N-Dimethyl acrylamide (99% stock solution) was added to the previous mixture as a 0.5% final concentration (1.5µl/300µl of the extract), and was incubated for 30min at room temperature.
10. Protein samples were stored at -20^{o}C until they used.
    (The protocol is adapted from Schmidt, et.al.2007).

2.3.2.6.3 Protein fractionation by Size Exclusion Chromatography

Protein extracts were prepared as described in Janes et al., (2012). Protein fractionation by Size Exclusion Chromatography (SEC) means separation of protein mixtures (for example, whole cell extracts) according to their apparent sizes. Since the chromatography column is composed of Superdex200 HR gel, large size protein complexes will not be able to enter the pores of the column media, which leads to their early release from the column. Unlike large proteins, when smaller complexes enter the gel, they are delayed, and therefore released later from the column.

The Superdex200 HR column is connected to AEKTA system and usually equilibrated in advance with the lysis buffer that is used for extracting the whole protein sample. The column was injected with 200-500µl of the whole protein extract. At the end of fractionation time, 24x of 1ml protein fractions were collected in 15ml tubes (1ml/fraction). Proteins were precipitated from each fraction using the following protocol in order to be ready for analyzing by SDS-PAGE and Western Blot.

Protein precipitation:

One volume of 100% TCA stock solution (500g of Trichloroacetic acid was dissolved in 350 ml of distilled H_2O) was added to 4 volumes of protein sample solution. The mixture was incubated on ice for 10 min, and then centrifuged at 14,000 rpm, 4^{o}C for 5 min. The supernatant was discarded and the pellet was washed in 1ml ice-cold acetone and centrifuged at 14,000 rpm at 4^{o}C for 5min. Acetone washes were repeated 2 times. Acetone was evaporated from the protein pellet by placing the tubes in a heat block (95^{o}C) for a few minutes. The protein pellet was re-suspended with 2x Lammeli buffer (4x Lammeli buffer

diluted up to 2x with Tris-HCl, pH=8.8), boiled at 95^{o}C for 5-10min and kept at -20^{o}C until used.

2.3.2.7 SDS-Polyacrylamide gel electrophoresis and Western blot

SDS-Polyacrylamide Gel Electrophoresis was used to analyze the protein extracts. It was performed either by one or by two-dimensional (2D) electrophoresis:

A. One Dimensional SDS-PAGE:

Proteins were separated according to their sizes on different Acrylamide-gel percentages. Regarding our protein samples, I used either 10% or 12.5% gels. The protocol was achieved as following:

1. Resolving gels were set at specific percentage, casted in between the Bio-Rad Wet/Tank Blotting system's glasses and were over-laid with isopropanol to remove air bubbles. Gels were left to settle down for 15min at room temperature.

- **Resolving Gel:**

Component	10% gel volumes	12.5% gel volumes
1M Tris-HCl pH=8.8	11 ml	11 ml
40% Acrylamide/bis-Acrylamide 37.5:1 solution	7.5 ml	9.4 ml
dH_2O	11.5 ml	9.6 ml
20%SDS	150 µl	150 µl
1%APS	150 µl	150 µl
TEMED	30 µl	30 µl

SDS: Sodium dodecyl Sulfate,

APS: Ammonium Persulfate,

TEMED: Tetramethylethylenediamine.

2. Isopropanol was washed off with distilled water and the stacking layer was prepared as follow:

- **Stacking Gel:**

Component	Volumes
1M Tris-HCl pH=6.8	2.5 ml
40% Acrylamide/bis-Acrylamide 37.5:1 solution	2 ml
dH_2O	15.5 ml
20%SDS	100 µl
1%APS	200 µl
TEMED	40 µl

The gel was poured immediately on top of the resolving layer, and combs were inserted. Gels were left to set for at least 10 min at room temperature.

3. Combs were removed and plates were placed in the electrophoresis tank, which contains 1xSDS running buffer (prepared from 10x SDS buffer). Samples were loaded in parallel to a standard proteins ladder (ThermoScientific PageRuler Pre-stained Protein Ladder, cat.no.26616), and were run for 1.30-2 hours on 120V.
4. Thereafter, gels were taken out of the tank and prepared for transferring to the nitrocellulose membranes.
5. Western Blot sandwiches were set up by placing the sandwich's components in a tray filled with 1x Transfere buffer (100ml of 10x Transfer buffer, 150ml Methanol and 750ml dH_2O), according to the following order: black part of the sandwich, one sponge, filter paper, the resolving gel, nitrocellulose blotting membrane (Amersham Hybond^{TM}-Ecl), filter paper, one sponge and the red color part of the sandwich.
6. Sandwiches were placed in the transfer tank filled with 1x transfer buffer, and proteins were transferred for 2hr at 70V.
7. Nitrocellulose membranes were taken off from the sandwiches and blocked with Blocking buffer (5% Milk buffer: 5g Milk powder (fat-free), 10ml of

10x PBS, 0.05% Tween-20 and dH_2O up to 100ml) for at least 30min at room temperature on rocking platform.

8. Membranes were incubated with the primary antibody (table 2-1) diluted in the blocking buffer for overnight at 4^oC on rocking platform.
9. Membranes were washed 3 times with 1x washing buffer (200ml of 10xPBS, 0.05% tween-20 and dH2O up to 2 liters); each wash was for 10min.
10. Membranes were incubated with corresponding secondary antibody (table 2-1) diluted in blocking buffer, for 1hr at room temperature on a rocking platform.
11. Membranes were washed 3 times with washing buffer, each wash for 10min at room temperature on rocking platform.
12. Membranes were developed with Western lightning® Plus-Enhanced Chemiluminescence substrate and placed in the developing cassette.
13. Membranes were exposed to the X-ray films for specific time and developed in the X-ray film processor (MI-5, JENCONS-PLS).

B. Two-Dimensional (2D) protein electrophoresis:

The protocol to run the 2D protein electrophoresis was adapted from Janes, et.al (2012):

1. Approximately 10-15µg of soluble protein extract (section 2.3.5.6.2) were loaded onto Immobiline™ DryStrip gels pH3-10L 7cm (GE Healthcare) embedded in Destreak™ rehydration solution with 2% of the corresponding IPG buffer.
2. Strips were rehydrated and focused in the Biorad PROTEAN IEF cell at 50V for 12 hr followed by the rapid focusing programme at10,000Vh (Janes et al., 2012).
3. Strips were placed in an IPG tray, and washed with 2 ml of equilibration buffer I (6M urea 0.375M Tris-HCl (pH8.8), 2% SDS, 20% glycerol, 2% (w/v) DTT) for 10 min at room temperature on a rocking platform.

4. Strips were washed as the same way with 2ml of equilibration buffer II (6M urea, 0.375M Tris-HCl (pH8.8), 2% SDS, 20% Glycerol, and 2.5% (w/v) Iodoacetamide).
5. Strips were applied to a 10% SDS-PAGE gel composed of the resolving layer only.
6. Proteins were ran normally according to the SDS-PAGE and Western blot steps that mentioned previously.

2.3.2.8 Spot assay

A single colony of each tested strains was grown in 10ml of YE liquid media up to 10^7 cells/ml at 30ºC. Cells were counted using the haemocytometer. Required volumes were prepared as 10^7 cells/ml and diluted four times 10-fold with YE liquid media. Ten microliters of each dilution were spotted on YEA plates contain a specific concentration of each drug to be tested. Plates were left to dry and incubated for 4 days at 30ºC.

2.3.2.9 Acute survival assay

A single colony of each tested strains was grown in 10ml of YE liquid media up to 10^7 cells/ml at 30ºC. Cells were counted using the haemocytometer and diluted to $5x10^4$ cells/ml in YE liquid media. To test cells survival upon UV treatment, 75 µl of cells was plated on YEA media, dried and exposed to the desired UV intensity. Regarding the treatment with DNA damaging drugs, 500µl of the tested drug (double concentration) was prepared in YE liquid media and mixed with 500µl of $5x10^4$ cells/ml, and incubated at 30ºC shaker incubator for five hours. 75 µl of treated cells were plated on YEA plates at different time intervals (0, 1, 2, 3, 4, 5hr). All plates were incubated at 30ºC for 4 days. Growing colonies were counted using colonies counter instrument. Each experiment was repeated for three times and average of cells survival percentage was estimated against each concentration or incubation time of each tested agent.

2.3.2.10 G2 phase cell cycle arrest of S.pombe cells using lactose gradient

S.pombe cells were synchronized in G2 phase using a lactose gradient, since they cannot metabolize lactose. The synchronized cell number at each time point is sufficient only for DAPI/Calcofluor staining. The following protocol was modified from Forsburg & Rhind, (2006).

- **Lactose gradient preparation:**

  To prepare the gradient, 30% and 7% lactose stock was prepared previously in YEL media. The two lactose solutions were mixed in a set of tubes as followed:

Tube number	30% lactose (ml)	7% lactose (ml)
1	10	0
2	8.75	1.25
3	7.5	2.5
4	6.25	3.75
5	5	5
6	3.75	6.25
7	2.5	7.5
8	1.25	8.75
9	0	10

  Lactose gradient was made up by layering 1ml of 30% lactose in 15ml falcon tube, followed by 1ml of 8.75/1.25 mixture and so on until layering the 7% lactose solution as the top layer of the gradient. Lactose layers were set up using a cut off blue tip by insertion of a small part of the tip in the lower layer, and then its content was emptied very slowly.

- **Yeast strains preparation:**

  Yeast strains (to be synchronized) were grown overnight at 30^{o}C until they reached mid-logarithmic phase. For each gradient 5x10^{8} cells were harvested. Cells were centrifuged at 3000 rpm for 5min, and supernatant was discarded.

Pellets were re-suspended in 1ml of YEL, and were sonicated using the Ultrasound water bath to get single cell suspension. Sonicated cells were then laid on top of the lactose gradient and spun at 750rpm for 8min using the Sorvall RT Legend bench top centrifuge with a swing-out rotor (acceleration = deceleration = 1). At the end of centrifugation, a white fussy layer of approximately 1ml of G2 synchronized cells was formed. 0.5ml of these cells were taken from the top of this layer and used for further analysis.

- **DNA damage checkpoints analysis of synchronized yeast cells:**

  Regarding my aim of this experiment to investigate the roles of hus1 variants in activating replication stress checkpoints, I released 500µl of the G2 synchronized cells in 500 µl YEL in 12 mM HU (as a final concentration) and another 500µl of such cells were released in normal YEL media. Samples were incubated at 30^{o}C in a shaker incubator up to 7 hr, during which, 40µl of cells were collected every 20 min and fixed in 200 µl of absolute methanol.

- **Cells staining:**

  Fixed cells were stained with DAPI and Calcofluor as described in Janes et al., 2012. DAPI stains the DNA while calcofluor reacts with the chitin in the new cell wall. 5 µl of fixed cells were placed onto a microscope slide, dried and stained with 15µl of DAPI/ Calcofluor white solution. Cells were then examined under Nikon ECLIPSE TE2000-U fluorescence microscope. For each time point sample, 100 cells were counted and the percentage of their G1-S phase (septated cells) was calculated.

2.3.2.11 Immune-localization of the Hus1 protein in *S. pombe*

- **Solutions preparation:**
  - **1x PEM buffer:** 0.1M PIPES pH=6.9, 1mM EGTA, 10mM MgCl2 (set up 2x PEM)

- **1x PEMS buffer:** 1.2M sorbitol dissolved in 0.5xvol of 2xPEM; and filled up with water to the final volume.
- **1xPEMBAL:** 100mM arginine hydrochloride and 1% chicken albumin dissolved in 0.5xvol of 2xPEM, and filled up with water to the final volume (store at +4°C).

➢ Protocol:

To localize Hus1 protein in yeast cells, the following protocol was applied (Dischinger et al., 2008):

1. *S.pombe* cells were grown overnight in YEL to the logarithmic phase.
2. $2x10^8$ cells of each strain were harvested (3000 rpm for 3 min).
3. Pellets were re-suspended in 1 ml of YEA and transferred to 1.5 ml Eppendorf tube.
4. Pellets were centrifuged at 3000 rpm for 3min and the supernatant was discarded.
5. Pellets were re-suspended in 1 ml of 4% Paraformaldehyde in YEA and Incubated for 20-30 min at 37°C. Then they were centrifuged and supernatant was discarded.
6. Pellets were washed twice in 1ml PEM buffer. Then once in PEMS buffer.
7. Pellets were re-suspended in 500 µl of Lyticase and incubated at 37°C for 1 hour (lyticase partly digests the cell wall).
8. The suspension was centrifuged at 5000 rpm for 1min. Then supernatant was discarded.
9. Pellets were washed twice in 1ml PEMS, 1% TritonX100, and then once in 1ml PEM buffer.
10. Pellets were washed once in 1 ml PEMBAL (blocking buffer).
11. Cells were transferred in 400 µl PEMBAL to a 500 µl PCR tube, centrifuged and supernatant was discarded.
12. Pellets were re-suspended in 400 µl PEMBAL, incubated for 30-60 min on rotating platform in cold room, centrifuged and supernatant was discarded.
13. Pellets were re-suspended in 200 µl PEMBAL contains primary antibody (1:200 of anti-Myc antibody). They were incubated overnight on rotating platform in the cold room.
14. Pellets were centrifuged and supernatant was discarded.
15. Pellets were washed twice in 1ml PEM buffer, then twice in 1ml PEMBAL buffer.

16. Pellets were re-suspended in 200 µl PEMBAL containing secondary-ALEXA Fluor 488 antibody (1:500, anti-mouse or anti-rabbit depending on the primary antibody).
17. Pellets were incubated for 4 hours on wheel at room temperature (in dark). Then they were centrifuged and supernatant was discarded.
18. Pellets were washed first twice in 1 ml of PEM, then twice in 1ml of 1xPBS contains 1:1000 diluted DAPI (stock: 10mg/ml in water).
19. Pellets were re-suspended in 200 µl 1xPBS+DAPI.
20. 10 µl of cells was loaded onto coated cover slip (64 mm long) and covered with a second cover slip.
21. Slides were examined by the Nikon ECLIPSE TE2000-U fluorescence microscope (60xobjective with oil, 488nm exaltation light for ALEXA-488 and UV for DAPI), with the assistance of HC-image software.

2.4 Human cells work

2.4.1 Materials

2.4.1.1 Buffers

DEPC treated water: prepared by adding 0.1% of Diethylpyrocarbonate (DEPC) to dH2O in RNase-free glass bottle (already autoclaved). The solution was incubated in the fume cabinet overnight at room temperature, and then autoclaved to inactivate the DEPC residues.

2.4.1.2 Human Cell Lines used in this study

Table 2-5: Human cell lines used in this study.

Cell Line	Genotype	Source
HeLa cells: Human Negroid cervix epithelial carcinoma		Purchased from Health Protection Agency (HPA) Culture Collection (cat.no. 93021013).
Flp-In Trex HEK293 cells		kind gift from Dr. Fumiko Isashi, Oxford University
Flp-In Trex HEK293 cells-HUS1-001-GFP	*FRT::HUS1-001-GFP*	This study
Flp-In Trex HEK293 cells-HUS1-005-GFP	*FRT::HUS1-005-GFP*	This study
Flp-In Trex HEK293 cells-GFP	*FRT::GFP*	This study
Flp-In Trex HEK293 cells-Flag-EGFP-HUS1-001	*FRT:: Flag-EGFP-HUS1-001*	This study
Flp-In Trex HEK293 cells-Flag-EGFP-HUS1-005	*FRT:: Flag-EGFP-HUS1-005*	This study
Flp-In Trex HEK293 cells-Flag-EGFP-HUS1-011	*FRT:: Flag-EGFP-HUS1-011*	This study
Flp-In Trex HEK293 cells-Flag-EGFP-HUS1-004	*FRT:: Flag-EGFP-HUS1-004*	This study
Flp-In Trex HEK293 cells-Flag-EGFP	*FRT:: Flag-EGFP*	This study
Flp-In Trex HEK293 cells-Flag-EGFP-HUS1B	*FRT:: Flag-EGFP-HUS1B*	This study

2.4.1.3 Plasmids used in Human cells work

Table 2-6: Plasmids used for human cells work

Plasmid	Source
pAW8NdeI-GFP	Watson et al., 2008
pcDNA5/FRT	kind gift from Dr. Fumiko Isashi, Oxford University
pcDNA5/FRT-TO-Flag-EGFP	kind gift from Dr. Fumiko Isashi, Oxford University
pOG44	kind gift from Dr. Fumiko Isashi, Oxford University
psiRNA-h7SKGFPzeo	InvivoGen
psiRNA-h7SKGFPzeo-siRNA-HUS1-ORF	This study
psiRNA-h7SKGFPzeo siRNA-HUS1-UTR	This study
pRFP-C-RS-shRNA-HUS1-001 (HT129858A)	OriGene
pRFP-C-RS-shRNA-HUS1-001 (HT129858B)	OriGene
pRFP-C-RS-shRNA-HUS1-001 (HT129858C)	OriGene
pRFP-C-RS-shRNA-HUS1-001 (HT129858D)	OriGene
pRFP-C-RS (TR30015)	OriGene

2.4.1.4 List of primers used in this study

Table 2-7: List of primers used in Human cells experiments

Primer name	Primer sequence (5'-3')
RT-PCR primers	
HUS1-I1-001-F	GAACCACTTCACACGAATCAGTAAC
HUS1-I1-005-F	CAGTGAGCGCGCGGAATCAGTAAC
HUS1-I1-011-F	TTTAGGAATCAGTAACATGATAGCC
HUS1-I1-004-F	ACGGAAGGAAGCAGAATCAGTAAC
HUS1-I-1-R	GAAATTCGTTGAAGAAGTTCTCCTG
HUS1-001-TAIL-F	CTGTCCTAGCACCCTGTCGCTGG
HUS1-001-TAIL-R	GTTAGAGAGGGACAAATAAGTAC
Amplifying *hHUS1* transcripts & *hHUS1B* full-length by RT-PCR and construction their N-terminal EGFP tagged stable cell lines	
hHUS1-001-NotI-F	ATCCGTTACATTATGCGGCCGCATGAAGTTTCGGGCCAAG ATCGTGG
hHUS1-005-NotI-F	ATCCGTTACATTATGCGGCCGCATGATAGCCAAGCTTGCCA AAACCTG
hHUS1-001-NotI-R	GTAATGTAACGGATGCGGCCGCCTAGGACAGCGCAGGGAT GAAATA
A011 (NotI)-R	GCGTAATGCGGCCGCTATGCGGCCGCCTAATGAGTTGTAA CACATACTAAT
A004 (NotI)-R	GCGTAATGCGGCCGCTATGCGGCCGCTACATAGTCTTCAA GACTGG
Confirmation of *hHUS1-001, hHUS1-005 & hHUS1-011* existence on mRNA level	
HUS1-005-II-F	AAGGAAGCAGTGAGCGCGCGG

HUS1-011-II-F	ATTCCTTATTTTAACCCCTG
HUS1-I1-001-F	GAACCACTTCACACGAATCAGTAAC
HUS1-001-II-R	TTGCTCATGTCTGTTTTGCTTTG
***hHUS1B* amplifying**	
HUS1B-F	CTTCCCTGTGGCATCATGAAGTTTCG
HUS1B-R	AGCCTGGCCTCGTGGAGGCC
HUS1B-NotI-F	CATGCTTATGCGGCCGCATGAAGTTTCGCGCCAAGATCAC C
HUS1B-XhoI-R	CGTAGTCGATTACTCGAGTTACAAGGCAGGAATGAAATAC
***B-Actin* amplifying**	
hACTB-F	ACCAACTGGGACGACATGGGAG
hACTB-R	TGCCAGTGGTTACGGCCAGAG
Amplifying of *hHUS1-005* very short transcript	
Hus1-005-Short-NotI-F	ACAAGGGTACCAGCGGCCGCATGAAGTTTCGGGCCAAGAT CG
Hus1-005-Short-XhoI-R	GAAAGCTGGGTGCTCGAGTCATGTTACTGATTCTGCTTCC
Construction of C-terminal GFP tagged hHUS1-001 & hHUS1-005 stable cell lines	
Hus1-001-F (EcoRV)	CTTACTAGATATCTCGGATATCATGAAGTTTCGGGCCAAGA TCGTGG
Hus1-001(Fusion)	CAGTATTCATCCCTGCGCTGTCCACTAGTACTGGTTCTACA GGATCAACC
Hus1-001-R(Fusion)	GGTTGATCCTGTAGAACCAGTACTAGTGGACAGCGCAGGG ATGAAATACTG

Hus1-001-F(NotI)	GCGTATGCGGCCGCATAGCGGCCGCCCATATACGAAGTTATCCCGGGAGATC
Hus1-005-F(EcoRV)	CTTACTAGATATCTCGGATATCATGATAGCCAAGCTTGCCAAAACC
GFP-F-EcoRV	GCCGCGGATATCGCAGATATCATGTCTAAAGGTGAAGAATTATTCAC
Integration confirmation of *hHUS1* transcript and *hHUS1B* in Flp-In HEK293 cells and DNA sequencing	
CMV-F	CGCAAATGGGCGGTAGGCGTG
BGH-R	TAGAAGGCACAGTCGAGG
FRT-F	CAACGGGACTTTCCAAAATGTCG

2.4.2 Methods

2.4.2.1 Human cells thawing

Cells were taken out from Liquid Nitrogen, heat shocked immediately at 37ºC in a water bath for 1-2 min and transferred quickly to the maintaining medium. Cells were left for 4hr to attach and the media was replaced with a fresh complete medium to avoid any residues of DMSO.

2.4.2.2 Human cells maintaining

All used cell lines were seeded at a determined seeding density on the plate using Dulbecco's Modified Eagle's Medium (DMEM) (SIGMA, D5546), which was supplemented with 10% Fetal Bovine Serum (FBS) (SIGMA-F2442), 1% Penicillin-Streptomycin antibiotics (SIGMA- P4333) and 200 mM L-Glutamine solution (SIGMA-G7513). Cells were incubated at 37ºC and 5% CO_2 until they reached the required cells confluence persentage. Thereafter, cells were de-attached from the plate using 1x Trypsin-EDTA solution (SIGMA, T3924). The media were supplemented with 100 µg/ml Zeocin and 15

ug/ml Blasticidine when used for HEK293 cells maintainance only. Constructed cell lines were maintained at the same conditions of HEK293 cells, but Zeocin was replaced with 100 µg/ml of Hygromycin.

2.4.2.3 Human cells freezing

Cells were de-attached from the plate and centrifuged at 1500 rpm. The pellets were re-suspended with 1 ml of freezing media (90% complete media and 10% DMSO) at $1x10^7$/ml. Cells were transferred to the Mr. Frosty equipment, incubated for 24 hr in -80^{o}C, and transferred later to Liquid Nitrogen.

2.4.2.4 Human cells counting

To obtain specific cell number, cells were trypsinized, spun down at 1500 rpm for 5min, and re-suspended with 1 ml of PBS. Ten microliters of cells suspension were mixed with 10 µl of 0.4% Trypan blue solution (SIGMA, T8154), loaded onto BIO-RAD counting slides (cat.145-0011), and cells were counted by BIO-RAD/TC10^{TM}Automated cell counter.

2.4.2.5 Genomic DNA extraction

Genomic DNA was extracted using the GenElute™ Mammalian Genomic DNA Miniprep Kit (SIGMA, G1N10), according to the manufacturer's instructions.

2.4.2.6 Total RNA extraction

Total RNA was extracted according to Abcam's protocols "RNA extraction: cells in culture" (http://www.abcam.com/ps/pdf/protocols/RNA_isolation_cell_culture.pdf). Briefly, at least 10^6/ml cells were used to achieve the protocol. Cells were washed with ice cold 1xPBS and collected in 1 ml of TRI Reagent® (SIGMA, T9424) by scraping the plate very gently. Cell lysates were transferred to an Eppendorf tube and incubated at room

temperature for 5 min, followed by the addition of 250 µl of Chloroform and vortexed for 15 sec. The mixture was left to set for 5 min at room temperature and centrifuged at 10,000 rpm for 5 min to separate the aqueous and organic contents from each other and precipitate the DNA as interphase layer. The aqueous layer was removed with a large pipette to an Eppendorf tube, and mixed gently with 500µl of Isopropanol. The mixture was left to set for 5 min at room temperature. RNA pellets were precipitated from the mixture by centrifugation at 14,000 rpm for 30 min. To purify the RNA pellet, isopropanol was aspirated and replaced with 1 ml of 75% Ethanol prepared in DEPC treated water. Pellets were centrifuged at 9500 rpm for 5min, then the ethanol was removed and the pellets were left to dry at room temperature. RNA pellets were suspended in 15-25 µl of DEPC treated water and stored at -80^{o}C.

2.4.2.7 Reverse-Transcriptase Polymerase Chain Reaction (RT-PCR)

RT-PCR was achieved after converting the human's tissues (Human Total RNA Master Panel II, Clontech Laboratories, cat. 636643) and cell lines RNAs (1µg) to their corresponding cDNA using the Tetro cDNA synthesis kit (BIOLINE-BIO-65042). Thereafter, a general PCR (section 2.2.1) was done using the produced cDNAs as a template and a pair of specific primers for each gene or isoform (primers sequences and their PCR products are shown in chapter 4). The PCR program was as follow:

Separation	98^{o}C	1min
Annealing	55^{o}C	30sec
Extension	72^{o}C	1.30min
Final Extension	72^{o}C	10min

PCR products were run on a 1% Agarose gel made with TAE buffer at 85V for 1hr. To validate the amplified genes' sequence, their PCR products were cloned onto pCR™4-

TOPO® Vector using the TOPO® TA Cloning® Kit (Invitrogen™, K4575-02) as manufacturer's instructions.

2.4.2.8 Protein extraction

2.4.2.8.1 Whole cell extract

Cells were washed once with ice-cold 1x PBS, trypsinized and counted. At least $2x10^6$ cells were used for protein extraction. Cells were pelleted at 1500 rpm for 5 min and washed with 1ml of ice cold 1xPBS, and transferred to a pre-chilled Eppendorf tube. The cells pellet was lysed in the whole cell extract buffer (50 mM Tris-HCL (pH=7.4), 200 mM NaCl, 0.5% Triton-X100 and Protease Inhibitor Cocktail III for Mammalian Cells (MELFORD-P2202**)** (1 µl/100 µl of the lysis buffer) at a ratio of 100 µl lysis buffer/$2x10^6$ cells. The buffer was supplied with 125U/ml of Benzonase and 1.5 mM $MgCl_2$, when the extract was used for 2D protein electrophoresis or Size Exclusion Chromatography. Protein samples were spun at 16,000 xg for 30 min at 4°C. Supernatant was mixed with 2x Lammeli buffer, boiled at 95°C for 5 min and kept at -20°C until it used.

2.4.2.8.2 Cell Fractionation

Cells were trypsinized and counted. At least $2x10^6$/ml cells were washed once with 1 ml of ice cold 1xPBS and pelleted at 1500 rpm for 5 min. Pellets were re-suspended into Hypotonic Buffer (50mM Tris-HCL (pH=7.4), 0.1 M Sucrose and Mammalian protease inhibitor) and Lysis Buffer C (1% Triton-X100, 10 mM $MgCl_2$ and Mammalian protease inhibitor) in a ratio of 100µl of both buffers/ $2x10^6$ cells. Lysed cells were incubated for 30 min on ice. Cells were pelleted at 6000 xg for 2 min at 4°C. The supernatant (represents cytoplasmic fraction) was transferred to another pre-chilled Eppendorf tube and mixed with a same volume of 2x Lammeli buffer, boiled at 95°C and kept at -20°C till it used. The remaining pellets (representing Nuclei) were washed once with ice-cold 1x PBS. Nuclei then were centrifuged at 6000 xg for 2 min at 4°C. Thereafter, they were lysed in Lysis Buffer N (50 mM Tris-HCL (pH=7.4), 100 mM KAc and Mammalian protease inhibitor). The buffer

was supplied with 125U/ml of Benzonase and 1.5 mM $MgCl_2$ when the extract was used for 2D protein analyzes or Size Exclusion Chromatography) as a ratio of 100 µl/2x10^6 cell, mixed with a same volume of 2x Lammeli buffer, boiled at 95^{o}C and kept at -20^{o}C until it used.

2.4.2.9 SDS-PAGE and Western blot

Protein extracts were analyzed by SDS-PAGE and Western blot as mentioned previously in section 2.3.2.7.

2.4.2.10 In situ immunofluorescence of cultured cells

- **Cells growing:**
  - Cells were seeded on Poly-D-Lysine pre-coated coverslips (Poly-D-Lysine, no.1, 12mm, VitroCam-1245-P01) placed in a 12 well plate, at 50% cells confluence (0.25x10^5-1x10^5 cells/well) for overnight.
- **Cells fixation:**
  - Coverslips were removed from the well and dipped in 37^{o}C warm 1xPBS 1mM EGTA.
  - Coverslips were placed in a well contains 2 ml of 4% PFA, and incubated for 15 min at room temperature.
  - Coverslips were washed three times (each wash for 5 min) with washing buffer 0.01% Triton x-100 in 1xPBS.
- **Cells permeabilisation:**
  - Cells were incubated in permeabilisaton buffer (0.2% Triton x-100 in 1xPBS) for 10 min at room temperature.
  - Coverslips were washed 3 times with washing buffer (each wash 5 min).
- **Cells staining:**
  - Cells were blocked in 2 ml of the blocking buffer (3%BSA and 0.01%Tritonx-100 in 1x PBS buffer) for 30 min at room temperature or overnight at 4^{o}C.

- Coverslips were incubated with primary antibody (diluted in blocking buffer) for 1 hr at room temperature or for overnight at 4^{o}C.
- Coverslips were washed 3 times with washing buffer, each wash for 5 min on rocking platform.
- Coverslips were incubated with the secondary antibody (diluted in blocking buffer) for 45-60 min at room temperature in the dark.
- Coverslips were washed 3 times with washing buffer, each wash for 5 min in the dark.
- Coverslips were mounted onto glass coverslips using <10µl of Vectashield Mounting Medium for Fluorescence with Propidium Iodide (Vector Laboratories-H-1300).
- Coverslips were incubated at room temperature to overnight (in the dark) until mounting medium is harden.
- Coverslips were sealed with nail polish.
- Slides were stored at 4^{o}C until they were examined by Zeiss LSM710 Confocal Microscope with a 63× objective. Images were analyzed by Zen2010 software and processed by Photoshop (Adobe).
    - Please note that the imaging was standarised according to the suitable laser settings for the desired engineered protein and then applied for the negative control (non-transfected HEK293 cells). That was followed by adjusting the Red, Green and Blue (RGB) signals intensitites using Photoshope (Adope).

2.4.2.11 hHUS1 Down-regulation

I tried to down-regulate hHUS1 using two systems, which are DNA based ones, as detailed in the following paragraphs.

2.4.2.11.1 psiRNA-h7SKGFPzeo (InvivoGen)

Overview:

psiRNA offers stable down-regulation of the gene of interest. That because it allows for the cloning of designed small oligonucleotides, which encode two complementary sequences of 19-21 nucleotides separated by a 5-9 nucleotides loop. These psiRNA plasmids are transfected into the cell line to target a specific sequence of the gene of interest. Post-transfection, the small oligonucleotides transcribe for the short double stranded RNA (dsRNA) with the hairpin structure are matured by Dicer and Drosha in the cell. The two arms of this structure will thereby be released as short interfering RNA molecules to target the desired gene.

- **Plasmid amplification:**

  To amplify the psiRNA vector, I used the *E. coli* GT116 competent cells, following the basic chemical transformation protocol (section 2.2.3). Since the plasmid is a low copy plasmid with a stem loop structure, I prepared Midipreps as shown in the manufacturer's instruction of the GenElute™ Plasmid Midiprep Kit (SIGMA, PLD35).

- **Plasmid preparation:**

  psiRNA-h7SKGFPzeo vector has two cloning sites, BbsI/BbsI and Acc65I/HindIII. I chose the first one to clone the oligonucleotides. The vector was digested with BbsI restriction enzyme (NEB) as the basic digestion protocol (section 2.2.2). The resulted linear plasmid fragment, 3180bp, was purified from the agarose gel using GenElute™ Gel Extraction Kit (SIGMA, NA1111).

➢ siRNA sequence design:

I selected two siRNA sequences that target either *hHUS1* ORF or its UTR region with the assistance of siRNAWizard (http://www.sirnawizard.com/). I designed two complementary oligonucleotides (Forward and Reverse, each one is 19-21 nucleotides), which were compatible with BbsI/BbsI restriction enzyme. These oligonucleotides were separated from each other with a sequence represents the spacer, which forms the hairpin structure post-transfection. See figure 4-18 for the siRNA sequences that target *hHUS1* ORF or UTR regions with their scrambled sequences that act as a negative control.

➢ Cloning into psiRNA:

1. Annealing of siRNA insert:

The forward and reverse oligonucleotides were annealed with each other as the following steps:

Annealing mixture:

25 µM Forward oligonucleotide	2 µl
25 µM Reverse oligonucleotide	2 µl
0.5 M NaCl	6 µl
H_2O	to a final volume of 30 µl

Annealing reaction:

The previous mixture was incubated for 2 min at 80°C on a heating block, then the heating was stopped and the mixture was kept in the heating block until the temperature reaches 35°C. The annealed siRNA was used immediately or stored at -20°C until they are used.

2. Ligation of siRNA insert to psiRNA

Ligation solution was prepared by mixing the following components:

Digested psiRNA	1 µl (100 ng)
Annealed siRNA insert	1 µl
T4 DNA Ligase	1 µl (1 unit)
10X ligation buffer	2 µl
H2O	to a final volume of 20 µl

The mixture was incubated at 16ºC overnight.

3. Transformation of LyoComp *E.coli* GT116:

I used LyoComp *E.coli* GT116 as manufacture's recommendation for plasmid amplification. That because they are *sbcCD*$^{-}$ mutant, rather than the standard laboratory competent cells, which are *sbcCD*$^{+}$ to prevent hairpin remodeling post transformation.

The LyoComp *E.coli* GT116 cells were provided as lyophilized cells, I produced more cells following the Modified RbCl method provided by Promega Company to prepare ES1301 *mut*S and JM109 Competent Cells.
(http://www.promega.com.cn/techserv/tbs/TM001-310/tm001.pdf).

The transformation was done as previously explained (section 2.2.3), with the exception of the plasmid amplification time. I used 1.30 hr rather than 1hr since it is a low copy plasmid. Transformed cells were plated onto LB media plates containing Zeocin (25 µg/ml), X-Gal (100 µg/ml) and IPTG (100µg/ml) antibiotics to take advantage of the blue / white colonies selection.

4. DNA extraction and integration confirmation of the siRNA insert:

Plasmid DNA was extracted from white *E.coli* colonies (transformed cells) using GenElute™ Plasmid Miniprep Kit (SIGMA, PLN70). The presence of the siRNA insert was confirmed by plasmids DNA digestion with SpeI restriction enzyme.

The positive plasmids show three bands (1644bp, 1206bp and 741bp), when their digested DNA is run on 1% Agarose gel.

- **Transfection into Human cells:**

Plasmids containing the siRNA insertion were transfected into HeLa cells using LyoVec™ (InvivoGen, lyec-1,) transfection reagent (as recommended by the company, since it is optimized for psiRNA transfection). Twenty-four hours post-transfection, the Zeocin antibiotic (250 µg/ml) was added to the transfected cells as a selection marker. I dealed with the transfection as a transient and permanent transfection. For the first one, I extracted protein as a time course at 24, 48 and 72 hr post-transfection. Whereas, for the second one, I maintained the transfected cells for a long period, two weeks, under selection conditions to remove un-transfected cells and to allow the transfected cells to form distinct clones. Green- fluorescent positive and Zeocin resistant clones were isolated and their whole cell protein extract was prepared. hHUS1 siRNA-induced down-regulation was analyzed by SDS-PAGE and Western blot.

2.4.2.11.2 HuSH shRNA Plasmid (29-MER) system (OriGene)

- **Overview:**

This system is similar to the previous one as it is a DNA based down-regulation one. Furthermore, the shRNAs that target the gene of interest were designed by the company as sequence of oligonucleotides and were cloned into BamHI / HindIII cloning sites of the pRS vector. Each gene-specific shRNA was inserted immediately after U6 RNA promoter and consisted of 29 nucleotides, which are homologous to a sequence of the gene of interest, and their reverse complement ones, which form the shRNA stem loop structure. These arms are separated by seven nucleotides forming the hairpin loop. As a result, all shRNA insertions have the following cassette sequence:

U6 promoter-GATCG-29nt_sense-TCAAGAG – 29nt_reverse_complement - TTTTTT (termination) – GAAGCT

➢ pshRNA vector features:

This system performs the gene silencing via a range of pRS expression vectors contain gene-specific shRNA insertions, which can be used for shRNA transient and stable expression using Puromycin selection upon the transfection into chosen mammalian cell line. Specifically, I used the pRFP-C-RS Vector contains hHUS1-specific silencing shRNA insertions as well as a pCMV promoter that controls the constitutive expression of the tRFP gene (Red Fluorescence Protein) and a Chloramphenicol bacterial selectable marker. The system provides a pRFP-C-RS plasmid containing a non-effective shRNA cassette as a gene silencing negative control (Table 2-8).

Table 2-8: pRFP-C-RS Plasmids, which purchased from OriGene that carrying shRNA oligonucleotides targets hHUS1 mRNA

Plasmid name	shRNA sequence
HT129858A:492	GCCACTGCCTTGGTTACTCAGAGCACTGT
HT129858B:716	TTCCACAGTGTATCGGATCTGTCGTTCTG
HT129858C:1017	GCAGTGCCACAATCATGGCTACCGCATT
HT129858D:1526	AAGTTCAAGCGATTCTCCTGCCTCAGCCT
TR30015	Scrambled negative control non-effective shRNA cassette in pRFP-C-RS vector

➢ Plasmid amplification:

I used *E.coli* Top10 competent cells to amplify hHUS1-shRNA plasmids under Chloramphenicol selection (34 µg/ml as a final concentration prepared in ethanol) and follow the previously mentioned transformation protocol (section 2.2.3).

➢ Transfection into Human cell line:

hHUS1- pshRNA vectors were transfected into HEK293 cells using Lipofectamine® 2000 Transfection Reagent (Invitrogen™, 11668-019). The transfection reaction was

mediated by Opti-MEM®I Reduced Serum Media (Invitrogen™, 11058021), according to manufacturer's instructions.

hHUS1- pshRNA transfection into chosen cell line was achieved firstly as transient single plasmids transfection and protein extraction was done after 72 hr under Puromycin selection (3 µg/ml) according to the manufacturer's instructions. Moreover, a small population of these transfected cells was maintained furthermore (for ten days) to create stable cell lines of each single shRNA plasmid under 3 µg/ml Puromycin selection as well.

To enhance *hHUS1* down-regulation, I achieved a transfection of *hHUS1*-pshRNA mixture, the protein extraction was done 72 hr (transient transfection), as well as, 10 days post transfection (stable transfection) under the same selection conditions.

2.4.2.12 Human cells synchronization

2.4.2.12.1 Synchronization procedures

HeLa cells were arrested in one of cell cycle phases by using different treatments as explained in the following procedures:

A. Serum starvation

Cells were plated as 40% seeding density in a 15 cm plate containing a complete media and were incubated at 37^{o}C for few hours until the cells attached to the plate. Cells were washed twice with 1xPBS to remove all the FBS residues from the plate. Thereafter, cells were incubated at 37^{o}C for 24 hr in starving media (FBS-free DMEM media) followed by releasing cells in a complete media to enter the cell cycle as normal. Protein samples were taken as cells fractionation at 0 and 6hr post-release. (The protocol is adapted from Banflavi, 2011).

B. Thymidine block

Cells were synchronized at the G1-S phase transition point using a double Thymidine block (Ma & Poon, 2011). Briefly, cells were seeded as mentioned previously in serum starved cells, then they were incubated for 18hr in a complete

media containing 2 mM final concentration of Thymidine (100 mM stock solution was prepared in DMEM media). Cells were released for 5 hr in a complete media supplemented with 24 µM final concentration of Deoxycytidine. Cells were washed twice with 1xPBS to remove the effect of Deoxycytidine, followed by a second Thymidine block for 19 hr and protein samples were taken immediately at the end of this treatment.

C. Nocodazole treatment

To arrest cells in G2-M phase border, cells were plated in T150 flasks at 40% seeding density and were incubated at 37^{o}C till they attached to the flasks, then they were treated with 2mM of Thymidine for 24hr, released in a complete media supplemented with 24uM Deoxycytidine for 2hr, followed by 17hr treatment with 100ng/ml Nocodazole. At the end of that treatment, most cells were rounded up and loosely attached to the flasks, which indicated that they were arrested in G2-M phase transition point. Mitotic cells only were collected using mitotic shaking off at 0hr time point after Nocodazole treatment. Protein samples were extracted as cells fractionation. This protocol was modified from Ma & Poon (2011).

2.4.2.12.2 Preparation of the cells for Fluorescence Activated Cell Sorting (FACS)

Cells were collected after each treatment, centrifuged at 1,500rpm for 5min and washed once with 1xPBS. Cells were re-suspended with approximately 100µl of 1xPBS. Cells were fixed by drop wising of -20^{o}C cold 100% Methanol while vortex. Fixed cells were kept at -20^{o}C until they were analyzed by Flow Cytometry.

2.4.2.12.3 Cell cycle analysis by Flow Cytometry

The cell cycle was analyzed by Flow Cytometry using Partec PASIII machine. To achieve that fixed cells were spun at 1,500 rpm for 5min, then pellet were re-suspended in 1ml of 1xPBS supplemented with 100 µg/ml RNAse Type I A (SIGMA, R4875) and

incubated at 37ºC for 3 hr. Cells were stained with 50 µg/ml Propidium Iodide and were run on Flow Cytometer and analyzed using Partec-FloMax software.

2.4.2.13 Premature cells senescence induction

Cells senescence was induced in HeLa cells by oxidative stress. Cells were seeded at 40% seeding density as mentioned previously. Cells were treated with 200 µM H_2O_2 in FBS-free media for 1 hr. Cells were washed twice with 1xPBS and once with complete media, then they were incubated in a complete media up to 72 hr at 37ºC and images were taken using EVOSx1 core/AMG microscope. Protein samples (as whole cell extract) were taken at 0, 48 and 72 hr post- H_2O_2 treatment (Burova, et.al, 2013).

2.4.2.14 DNA damage treatment

To induce DNA damage, HeLa and HEK293 cells were treated with different DNA damaging agents as shown in Table 2-9.

Table 2-9: DNA damage treatments and their conditions. This table shows the DNA damage treatments conditions, which were applied onto HeLa and HEK293 cells. (*) cells were treated with H_2O_2 in FBS-free media. H_2O_2, UV, Cpt and Phl DNA damage agents' treatments were adapted from Chen, et.al. (2013).

Agent	Abbreviation	Dose	Treatment time	Protein extraction time
*Hydrogen peroxide	H_2O_2	500 µM	1 hr	0, 2 and 4 hr post treatment
Heat Shock	HS	42ºC	1 hr	0, 3 and 5 hr post treatment
Hydroxyurea	HU	5 mM	2 and 4 hr	End of each treatment time point
Methyl methanesulfonate	MMS	50 µg/ml	2 and 4 hr	End of each treatment time point
Ultraviolet radiation	UV	40 or 50 J/m^2	2 and 4 hr	End of each treatment time point
Camptothecin	CPT	1 µM	2,4 and 24 hr	End of each treatment time point

Phleomycin	Phl	60 µg/ml	2, 4 and 24 hr	End of each treatment time point
Aphidicolin	Aph	200 µM	2, 4 and 24 hr	End of each treatment time point

2.4.2.15 Construction of *hHUS1* and its isoforms and *hHUS1B* stable cell lines

Flp-In™ T-Rex™-293 cells with the assistance of Flp-In™ System were used to construct all stable cell lines, which are mentioned in this section.

2.4.2.15.1 Construction of the C-terminally *GFP* tagged *hHUS1-001* and *hHUS1-005*

To study hHUS1-001 and hHUS1-005 overexpression phenotype, stable cell lines were constructed as C-terminally *GFP* tagged *hHUS1-001* and *hHUS1-005* genes.

1. Construction of the cassettes:

hHUS1-001-GFP, *hHUS1-005-GFP* and *GFP* cassettes were constructed as follows:

A. *hHUS1-001 and hHUS1-005* genes were amplified from HEK293 cells cDNA using the primers set: Hus1-001-F (EcoRV) and Hus1-001-R (Fusion) for *hHUS1-001*, and Hus1-005-F (EcoRV) and Hus1-001-R (Fusion) for *hHUS1-005*. The linker-GFP cassette was amplified from pAW8NdeI-GFP plasmid using the primers set: Hus1-001-F (Fusion) and Hus1-001-R (NotI).

B. GFP (only) cassette was amplified from pAW8NdeI-GFP plasmid using the primers set: GFP-F (EcoRV) and Hus1-001-R (NotI).

All cassettes were amplified by general PCR reaction and program as mentioned in section (2.2.1).

C. The two cassettes (*hHUS1-001* or *hHUS1-005*, and linker-GFP) were fused to each other using Fusion PCR as mentioned previously (section 2.2.1).

All primers sequences and their priming sites are elucidated in chapter 6, section 6.2.1.

2. Cassettes cloning into pcDNA5/FRT:

hHUS1-001-GFP and *hHUS1-005-GFP* cassettes were cloned onto pcDNA5/FRT vector (a kind gift from Dr. Fumiko Isashi, Oxford University) according to the previously mentioned cloning protocols (Sections2.2.2 and 2.2.3). The inserted genes are expressed constitutively. Plasmids that contain the *hHUS1-001-GFP*, *hHUS1-005-GFP* and *GFP* were sent for DNA sequencing to validate their sequence.

3. Transfection into Flp-In- ™T-Rex™-293 cells:

A. Overview:

Flp-In™ T-Rex™-293 cells are stably express lacZ-Zeocin fusion protein and Tetracyclin (Tet) repressor, and contain single integrated Flp Recombination Target (FRT) site as demonstrated in Figure (2-1). As a result, these cells are Zeocin and Blasticidin resistant cells.

Flp-In ™T-Rex™-293-cell line was used to create stable cell lines expressing either hHUS1-001-GFP, hHUS1-005-GFP or GFP proteins. That was achieved by cells transfection with pcDNA5/FRT, which contains one insertion of the mentioned cassettes, in parallel with pOG44, which mediates homologous recombination at FRT site.

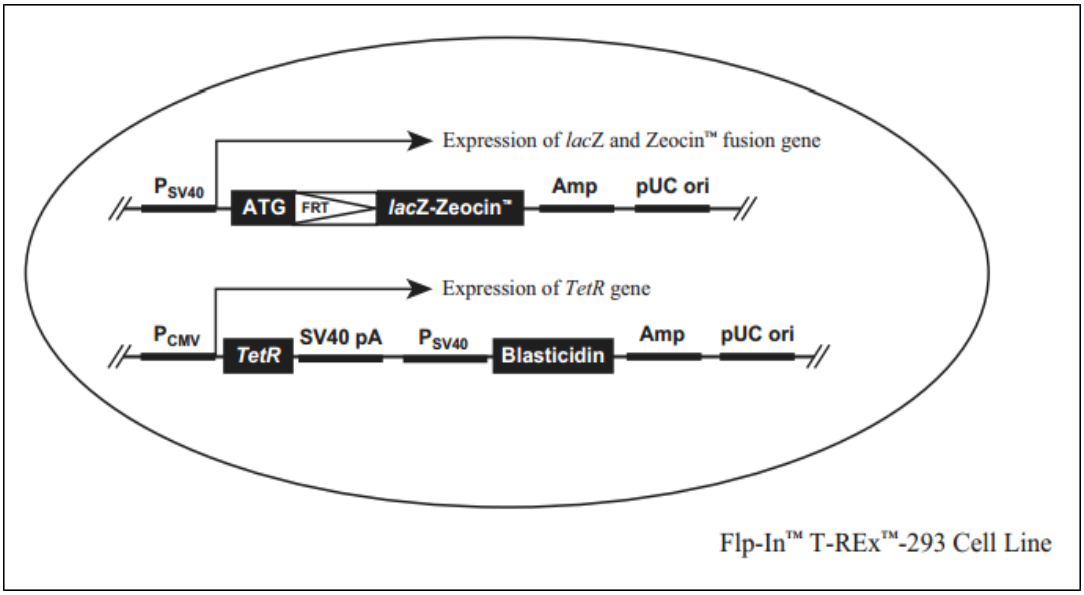

Figure 2-1: Flp-In™ T-Rex™-293 Cell Line genotype. Flp-In ™T-Rex™-293 cell line stably express lacZ-Zeocin fusion protein and Tet repressor from pcDNA6/TR, and contain single integrated Flp Recombination Target (FRT) site from pFRT/lacZeo. (Adapted from Growth and Maintenance of the Flp- In™ T-Rex™ Cell Line, (http://tools.lifetechnologies.com/content/sfs/manuals/flpintrexcells_man.pdf).

B. Transfection protocol:

The cells were transfected with pcDNA5/FRT containing either *hHUS1-001-GFP, hHUS1-005-GFP or GFP* itself as a negative control, in parallel with pOG44 in a ratio of 1:9 respectively. The transfection was carried out using LyoVec™ (InvivoGen, lyec-1) transfection reagent. Cells were incubated overnight in complete medium lacking antibiotic. On the second day, the medium was changed and replaced with a complete mediuma contain Hygromycin (200 µg/ml) as a selection marker. Cells were maintained under these conditions for approximately two weeks until single clones were formed with changing the growth media every four days. Single Hygromycin resistant clones were isolated using cloning rings and transferred to individual plates. Post-transfection cells will be Zeocin sensitive, Hygromycin resistant and lacking of β-galactosidase activity. Clones were tested later for gene of interest expression by whole cell extract, which was analyzed by SDS-PAGE and Western blot. In addition to immune-localization of transfected genes.

C. Integration confirmation:

To confirm the transfected genes' integration in HEK293 cells genome, their genomic DNA was extracted as mentioned in section 2.4.2.5. The investigated genes were then amplified from their corresponding genomic DNA by general PCR reaction using the primers set: FRT-F (binds in CMV promoter and HUS1-001-R (NotI), which was used previously to amplify the genes.

2.4.2.15.2 Construction of the N-terminally *Flag-EGFP* tagged *hHUS1-B* and *hHUS1-001* and its alternative splice variants stable cell lines

N-terminally *Flag-EGFP* tagged *hHUS1* (and its isoforms) and *hHUS1B* stable cell lines were constructed to improve the GFP fluorescent signal, since the previously constructed ones (C-terminally tagged *GFP* cell lines) were not fluorescent enough under the fluorescence microscope.

1. Cassettes amplifying:

hHUS1-001 and its alternative splice variants (*hHUS1-005, hHUS1-011 and hHUS1-004*), in addition to *hHUS1B* genes were amplified from HEK293 cDNA as the previously mentioned protocol using the following primers sets respectively:
hHUS1-001-NotI-F and hHUS1-001-NotI-R, hHUS1-005-NotI-F and hHUS1-001-NotI-R, hHUS1-005-NotI-F and A011-(NotI)-R, hHUS1-05-NotI-F and A004-(NotI)-R and HUS1B-NotI-F and HUS1B-XhoI-R.

2. Cloning onto the pcDNA5/FRT/TO-Flag-EGFP vector:

This plasmid contains the Tetracycline repressor, in addition to the N-terminal *Flag-EGFP* tag, which was already inserted in the KpnI cloning site of the plasmid by Dr. Fumiko Isashi research group. In order to achieve the cloning, each cassette of *hHUS1* and its isoforms was digested with the NotI restriction enzyme and inserted into the NotI cloning site. Conversely, the plasmid DNA that was used to achieve the cloning was digested with the NotI restriction enzyme and was dephosphorylated by Antarctic

Phosphatase (NEB, M0289S) following the manufacturer's instruction. The *hHUS1B* cassette was inserted between NotI and XhoI restriction enzymes sites.

The gene cassettes were ligated to their corresponding linear plasmid DNA and transformed into *E.coli* Top10 competent cells as mentioned previously (section 2.2.3). For sequence verifications, the constructed plasmids were sent for DNA sequencing.

3. Transfection into Flp-In™ T-Rex™-293 Cell Line:

hHUS1 and its splice variants and *hHUS1B,* which were cloned into pcDNA5/FRT/TO-*Flag-EGFP* plasmids, were transfected (as mentioned previously) into the Flp-In™ T-Rex™-Hek293 cells, since these cells already contain the Tetracycline Repressor. As a result, to express the recombinant proteins, cells should be treated with Doxycycline (1 µg/ml) for at least 2-4 hours to induce protein expression.

4. N-terminally *Flag-EGFP* tagged genes integration confirmation:

Genomic integration of the genes integrated into HEK293 cells was confirmed by extraction of the stable cell lines genomic DNA according to the previously mentioned protocol in section 2.4.2.5. General PCR was carried out using the following primers sets: CMV-F or FRT-F in a combination with gene's specific-R primer, which was used to amplify the corresponding gene from HEK293 cDNA. Primers sequences and their priming sites are mentioned in Chapter6, section 6.2.2, Figure 6-11.

2.4.2.16 Time course Induction of the N-terminally Flag-EGFP hHUS1 and hHUS1B proteins

Recombinant proteins of hHUS1 and its alternative splice variants, in addition to hHUS1B and EGFP, were tested for their optimal induction period by using 1µg/ml of Doxycycline. This was achieved by plating the engineered stable cell lines in 10 cm petri dishes at 70% cells confluence for overnight. Then, the medium was supplemented with freshly prepared 1µg/ml of Doxycycline (prepared in H_2O) and one plate was left without

Doxycycline treatment as a negative control. Whole cell protein extracts were done at 4, 8, 12, 16, 20, 24 and 48 hours post-treatment. Protein extracts were analyzed using SDS-PAGE and Western Blot. Nitrocellulose membranes were probed either with anti-hHUS1 or anti-GFP antibodies for hHUS1 and EGFP cell lines. Whereas, hHUS1B protein was probed with anti-GFP antibody, since we could not find a proper commercial hHUS1B antibody.

2.4.2.17 Induced recombinant proteins stability post-Doxycycline removal

Recombinant proteins stability post doxycycline removal was studied by inducing cells for 16hr in a media containing Doxycycline and then this media were washed off twice with 1xPBS to remove the antibiotic residues and to switch the promoter off. Protein samples were taken at 0, 4, 8, 24 and 53 hours post the inducer removal, and they were analyzed by SDS-PAGE and Western Blot at the same way mentioned in section 2.3.6.7.

2.4.2.18 N-terminally Flag-EGFP hHUS1 and hHUS1B proteins cell localization

Cell localization of the recombinant proteins was investigated by achieving immune-staining protocol as mentioned in section 2.4.2.10 using anti-hHUS1, anti-GFP and anti-hHUS1B antibodies as primary antibodies in a combination with either Alexa-Fluoro488 or Alexa-Fluoro633 antibodies, and cells were examined by Zeiss LSM710 Confocal Microscope. Images were analyzed by Zen2010 software.

2.4.2.19 Size Exclusion chromatography on Superdex-200 HR gel filtration column

This experiment was done to get a preliminary information about whether the recombinant proteins (hHUS1 and its isoforms and hHUS1B) interact with other proteins to form larger complexes. The experiment was done by extracting whole cell proteins followed by treatment for 1 hr on ice with Benzonase (125U/ml) in lysis buffer, which was

supplemented with 1.5 mM of $MgCl_2$ as a final concentration (section 2.4.2.8.1). Protein samples were centrifuged at 16.000 xg for 30 min at 4^{o}C, supernatant was kept at -20^{o}C until it used and the pellet were discarded. Proteins were eluted through the Superdex-200 HR gel filtration column as mentioned in section 2.3.6.6.3. Protein fractions were concentrated later by protein precipitation procedure, and analyzed in parallel with their whole extract sample by SDS-PAGE and Western Blot.

Chapter 3: Construction & Analysis of *hus1* single and double point mutations in *S. pombe* cells

3.1 Introduction

Informed by the preliminary findings of Caspari, et.al. (2000), who showed that the *hus1* gene in *S.pombe* produces four protein isoforms, of which only Hus1-B can contribute to Rad9-Hus1-Rad1 complex, I decided to investigate how *S.pombe* cells can produce them. Although the *hus1* gene contains 4 introns and alternative splicing has been reported in *S.pombe*, results obtained by Janes et al (2012) showed that the *S.pombe* Rad9 variant is produced from a cryptic AUG start codon when ribosomes initiate translation down-stream of the first AUG codon. Kochetov, 2008 clarified that eukaryotic genes can use one of three ways to produce different protein variants from a single gene. These ways are the usage of alternative promoters or alternative splicing, which are well investigated and have the priority in consideration in the field of gene expression studies. The third way, which allows single genes to produce a protein variant, is alternative translation. In this mechanism, ribosomes can scan the mRNA down-stream of the first methionine codon and initiate translation at an internal site, which will result in the expression of an N-terminally truncated variant of the full-length protein. This mechanism is called "Ribosome leaky scanning" (Fig.3-1), and could happen by more than one way (reviewed by Kochetov (2008). If this mechanism was to apply to the *hus1* mRNA, the usage of the internal AUG codons seems to be continuous rather than induced as in the case of the *rad9* mRNA (Janes et. al., 2012).

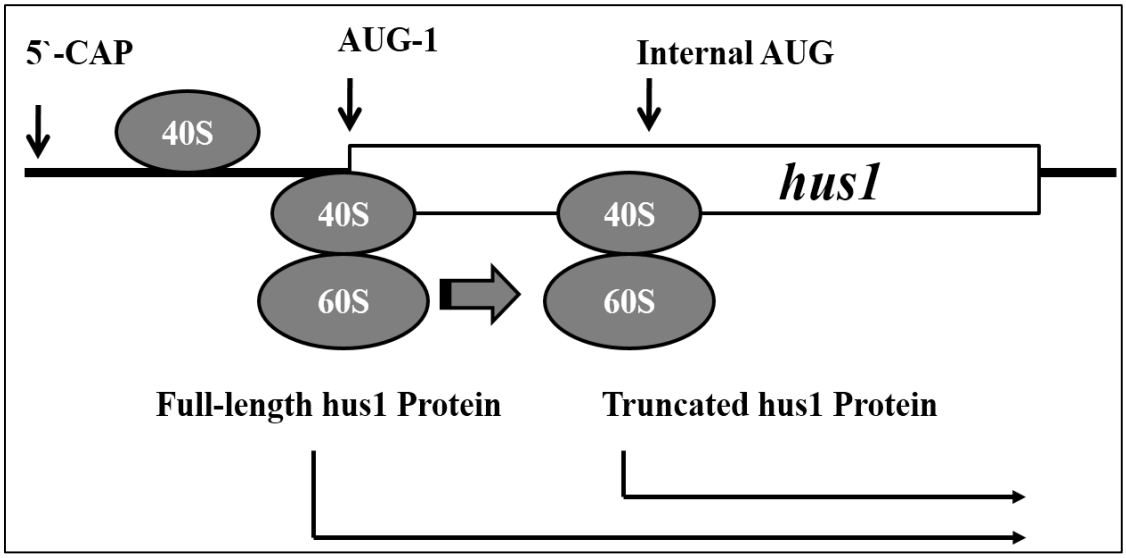

Figure 3-1: Ribosome leaky scanning mechanism. As reported by Kochetov (2008), ribosomes can either initiate mRNA translation at the first methionine codon or from an internal AUG codon, which is located furthered down the mRNA, to produce either full-length or truncated proteins, respectively.

The *hus1* gene in *S. pombe* has five exons encoding a protein with the size of 32.71kDa and consisting of 287 amino acids, which contain seven methionines (Figure 3-2). To test whether any of the six internal AUG codons could act as an internal translational codon, which could contribute to expressing a Hus1 isoform, I mutated either each methionine codon, including the first one, to an alanine codon, separately or two of them simultaneously (M1 in parallel with another AUG codon, or M32 and M46 together). The following chapter summarises the construction and analysis of these strains.

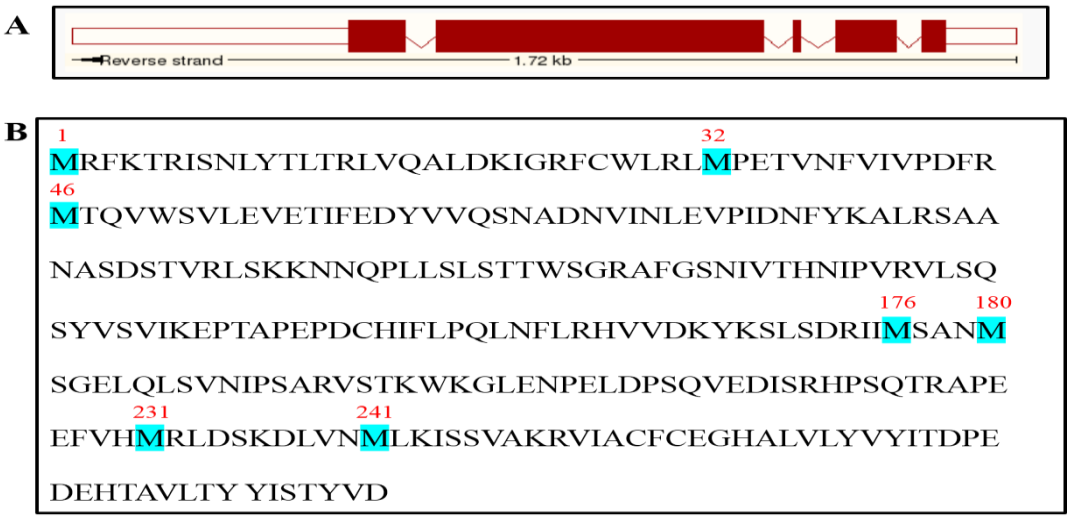

Figure 3-2: *S. pombe hus1* gene structure and its protein sequence. A: The *hus1* gene structure consists of five exons that are separated by four introns. **B:** The Hus1 protein sequence with highlighted methionines. (Adapted from PomBase the scientific resource for fission yeast, http://www.pombase.org/spombe/result/SPAC20G4.04c, accessed on April 2014).

3.2 Results

3.2.1 Construction of the *hus1* Base strain

In order to integrate the different *hus1* mutant alleles, I adopted the base strain system developed by Adam Watson in Tony Carr`s group (Watson et al, 2008). This system uses site-directed recombination to integrate genes at a selected chromosomal locus. The selected locus, in this case the *hus1* gene on chromosome 1, is replaced with a *ura4*$^{+}$ marker flanked by the recombination sequences *LoxP* and *LoxM3*. To this end, the *hus1* base strain was constructed by *hus1* gene replacement with *ura4*$^{+}$ according to the protocol described by Watson and his colleagues (2008) (Figure 3-3 & 3-4, A). This was achieved by PCR amplifying of the *LoxP-ura4*$^{+}$*-LoxM3* cassette (from pAW1 plasmid), flanked by two arms of *hus1* upstream and downstream sequences (from *hus1-Wt.* strain) at the 5' and 3' ends respectively. To avoid any interference with the context of the start codon (AUG-1) the *LoxP* sequence was inserted 121nt up-stream of this site (Figure 3-5). 117nt of this sequence between *LoxP* and the start codon was later restored when the *hus1* alleles were cloned into the integration plasmid pAW8 (Figure 3-5). The three fragments were amplified from their

templates by the general PCR protocol and fused to each other by a triple Fusion-PCR. Thereafter, the constructed cassette was transformed into the *S.pombe* wild type strain 804 (*ade*$^{-}$ *leu*$^{-}$ *ura*$^{-}$ *hus1*$^{+}$*)* and transformants were selected on EMM plates that were supplemented with adenine and leucine but not with uracil (EMM, Ura^{-}). To confirm the *hus1* base strain construction, a few examinations were done. First, PCR reactions were carried out using four primers sets (Figure 3-4, B & C). The PCR products showed that the *hus1* base strain was constructed correctly, as the *ura4*$^{+}$ marker gene replaced the endogenous *hus1* gene. In addition, the *hus1* base strain construction was confirmed by conducting spot assays and acute survival assays with DNA damage treatments (HU, CPT, MMS and UV) as the *hus1* base strain equals a *hus1* gene deletion rendering the base strain DNA damage sensitivity. Both assays showed a very high sensitivity of the base strain to the mentioned treatments, which is due to the absence of the *hus1* gene and consequently the Rad9-Hus1-Rad1 complex as shown in Figures 3-7, 3-8 & 3-9.

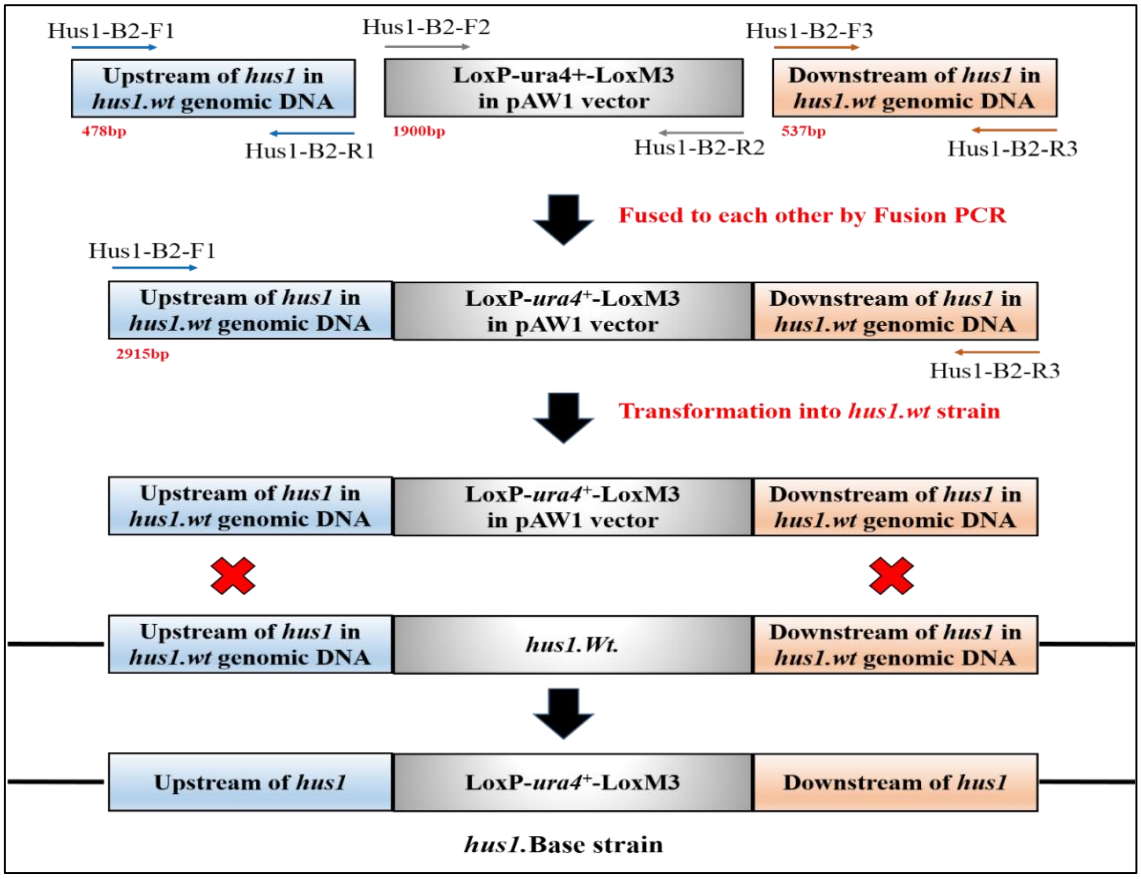

Figure 3-3: Illustrative diagram of *hus1* base strain construction. The diagram shows the construction of the *LoxP-ura4*$^{+}$*-LoxM3* cassette, which replaced the endogenous *hus1* gene in the *hus1-Wt*. strain. The cassette was amplified from the pAW1 vector and the flanking arms were amplified from genomic DNA isolated from the *S.pombe* wild type strain 804 (*hus1-Wt*.strain) to provide the homologous sequences, which mediates the gene replacement. All fragments were amplified separately by PCR, and fused to each other by a triple Fusion-PCR. The cassette was then transformed into the *hus1-Wt*. strain to construct the *hus1* base strain.

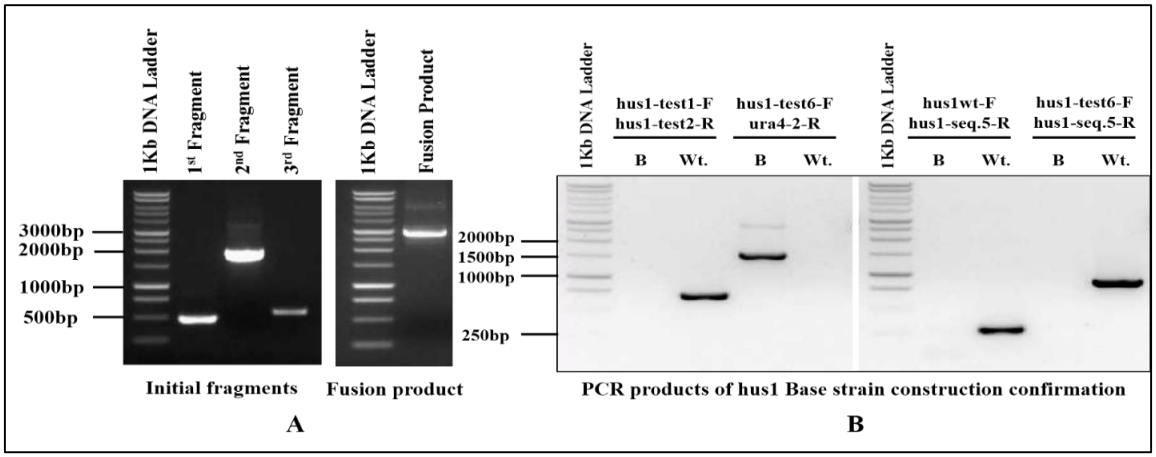

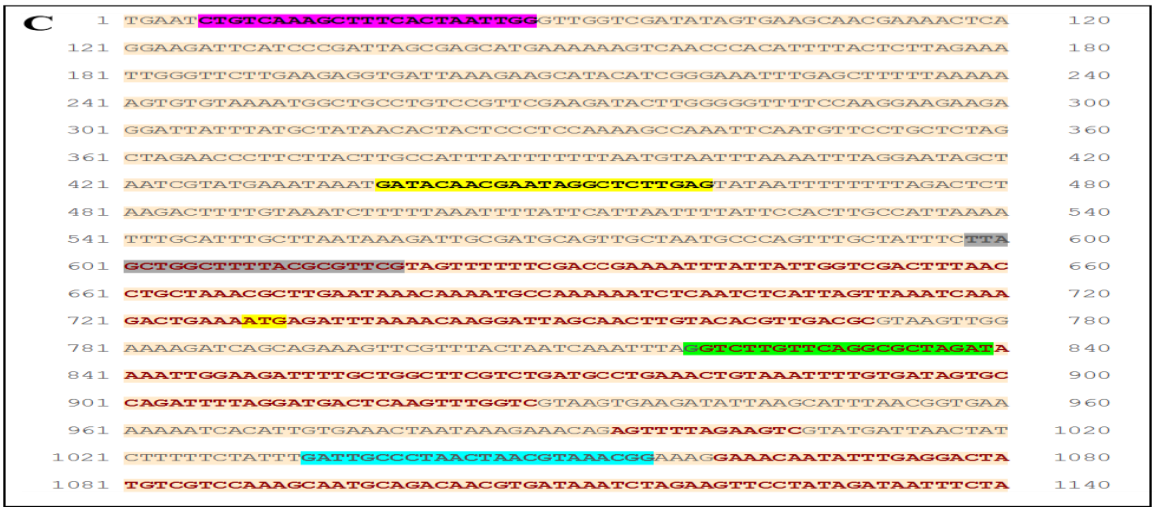

Figure 3-4: PCR products of the *hus1* base strain construction. A: PCR products of the amplified fragments of *LoxP-ura4*$^{+}$*-LoxM3* cassette (fragment 2) and the flanking genomic arms (fragments 1 and 3), in addition to the triple fusion PCR product. **B:** PCR product of *hus1* base strain construction test. **C:** Locations of the primers (in *hus1* gene sequence) that used to confirm the *hus1* base strain construction. (*hus1* gene sequence obtained from Ensembl Fungi database, *hus1* gene, accessed on June 2014)

(http://fungi.ensembl.org/Schizosaccharomyces_pombe/Gene/Sequence?db=core;g=SPAC20G4.04c;r=I:4820987-4822706;t=SPAC20G4.04c.1). The color code and the PCR product of each primers sets are as follow: please note that Ura4-2-R binds at the end of *Ura4*$^{+}$ gene sequence when it replaces *hus1* gene.

Hus1-Test-1-F + Hus1-Test-2-R = 619bp

Hus1-Wt-F + Hus1-sequ-5-R= 254 bp

Hus1-Test-6-F + Hus1-sequ-5-R= 774bp

Hus1-Test-6-F + Ura4-2-R= 1472bp

```
   1 TGCTGCAAAATTGATGCAAGCATGTATTTGTCTAAACCCGAATAATGAAAGAGTTAGAAA   60
  61 TGAATCTGTCAAAGCTTTCACTAATTGGGTTGGTCGATATAGTGAAGCAACGAAAACTCA  120
 121 GGAAGATTCATCCCGATTAGCGAGCATGAAAAAAGTCAACCCACATTTTACTCTTAGAAA  180
 181 TTGGGTTCTTGAAGAGGTGATTAAAGAAGCATACATCGGGAAATTTGAGCTTTTTAAAAA  240
 241 AGTGTGTAAAATGGCTGCCTGTCCGTTCGAAGATACTTGGGGGTTTTCCAAGGAAGAAGA  300
 301 GGATTATTTATGCTATAACACTACTCCCTCCAAAAGCCAAATTCAATGTTCCTGCTCTAG  360
 361 CTAGAACCCTTCTTACTTGCCATTTATTTTTTTAATGTAATTTAAAATTTAGGAATAGCT  420
 421 AATCGTATGAAATAAATGATACAACGAATAGGCTCTTGAGTATAATTTTTTTTAGACTCT  480
 481 AAGACTTTTGTAAATCTTTTTAAATTTTATTCATTAATTTTATTCCACTTGCCATTAAAA  540
 541 TTTGCATTTGCTTAATAAAGATTGCGATGCAGTTGCTAATGCCCAGTTTGCTATTTCTTA  600
 601 GCTGGCXTTTACGCGTTCGTAGTTTTTTCGACCGAAAATTTATTATTGGTCGACTTTAAC  660
 661 CTGCTAAACGCTTGAATAAACAAAATGCCAAAAAATCTCAATCTCATTAGTTAAATCAAA  720
 721 GACTGAAAATGAGATTTAAAACAAGGATTAGCAACTTGTACACGTTGACGCGTAAGTTGG  780
 781 AAAAGATCAGCAGAAAGTTCGTTTACTAATCAAATTTAGGTCTTGTTCAGGCGCTAGATA  840
 841 AAATTGGAAGATTTTGCTGGCTTCGTCTGATGCCTGAAACTGTAAATTTTGTGATAGTGC  900
 901 CAGATTTTAGGATGACTCAAGTTTGGTCGTAAGTGAAGATATTAAGCATTTAACGGTGAA  960
 961 AAAAATCACATTGTGAAACTAATAAAGAAACAGAGTTTTAGAAGTCGTATGATTAACTAT 1020
1021 CTTTTTCTATTTGATTGCCCTAACTAACGTAAACGGAAAGGAAACAATATTTGAGGACTA 1080
1081 TGTCGTCCAAAGCAATGCAGACAACGTGATAAATCTAGAAGTTCCTATAGATAATTTCTA 1140
1141 TAAAGCCTTACGATCAGCGGCCAACGCTAGTGATTCTACTGTTCGTCTATCCAAGAAGAA 1200
1201 TAACCAGCCATTACTTTCGTTGTCTACCACTTGGAGTGGAAGGGCGTTTGGTTCGAATAT 1260
1261 TGTGACTCATAATATACCTGTTCGAGTACTATCACAATCATACGTGTCAGTTATTAAGGA 1320
1321 ACCAACTGCTCCTGAACCAGACTGTCATATATTCCTTCCACAACTGAATTTTCTAAGACA 1380
1381 CGTCGTGGACAAATACAAGAGTCTTTCAGACCGTATTATAATGTCAGCCAACATGTCAGG 1440
1441 CGAATTGCAGTTATCGGTAAACATACCTTCAGCTAGAGTAAGCACAAAATGGAAAGGATT 1500
1501 AGAGAATCCAGAGTTAGATCCTAGTCAAGTCGAAGACATCAGTCGACATCCCTCTCAAAC 1560
1561 AAGGGCACCCGAAGAATTTGTTCACATGAGACTAGACAGCAAGGACTTAGTCAACATGTT 1620
1621 AAAAATATCCAGTGTTGCAAAGCGTGTAATAGCGTGTATGTACTATGAGAGAATCCTTTT 1680
1681 TATGACCACGAACTAACCTTTTTACATTACAGGTTTCTGTGAAGGACATGCGCTAGTACT 1740
```

1741 TTATGTTTATATAACAGATCCAGAAGATGAACATACGGCTGTTTTAACATACTACATTAG 1800

1801 TACCTATGTGGACTAAGGTTACTTCAATTTGTTTATGATTTGATTTAATTAACGAATAAT 1860

1861 TGTTATGAGTGACTAGCCACATTTTTAATGTACATTAAAATGAAAAGAGATTAATCAACA 1920

1921 TCTACCATGCTTATACTTATTTTCTCTCTCTTCCTTTATCGATCTTACCGTTCTTTTTTA 1980

1981 TTTATTTTATACAGTTGTXGTAATCTCGGCAACTCAGTGTTTTACTATTCCGTTGATATC 2040

2041 TCTTAAAAGGATAACACCAAAAAGAAATATAATGTTCAAGTCACAGAAAATCTGTTGATA 2100

2101 AAATCCATATGTTTTCACGTTTTCAATGAGAGATACATACGATTAAACACAAACGTATGT 2160

2161 TTTCAAGCAATTAACTTGAATATGAATAAACCTTGGTTCATCTTTCTTTAATCTTTTAGA 2220

2221 CAAGCAACTGTTCAGAAATCTATAAAGTCTCAATTGAACATTTAAGTGCTCAATGGGAAA 2280

2281 TATATACTTAATAAAAATTGAATATTTTAATCGTTTTTTTTGAGAAGATATATGCCATTGA 2340

2341 CTGTAGCTTCTATTAATTTCCGCCTATTCTTTCTTGTACTTTGGAGGCATCGCTATACAT 2400

2401 TTTACGTAGAAGTGATGAAAATGGCGAGTTCCTCTTTAAAAGTGCGAAAATTTCAGGCTG 2460

2461 TCTGTCATCGGAATTGACTATGTTCGATAGTTATTCCTCCTCCGATGCAGTCGGCTACAC 2520

2521 ATGTAAACTGTACCAACATTCAGTACGAAAGGGGCTGAACGTTGTTACCTAGAAAAGTTG 2580

2581 GTATCGCAATAGAGGTAACGATAGTGAAAATCCCACAATAACTTAAATATGGAGAGGTAT 2640

Hus1-B2-F1/ CATCCCGATTAGCGAGCATG

Hus1-B2-R1/ TTAATTAACCCGGGGATCCGGCCAGCTAAGAAATAGCAAACTGGGC

Hus1-B2-F2/ GCCCAGTTTGCTATTTCTTAGCTGGCCGGATCCCCGGGTTAATTAA

Hus1-B2-R2/ **GTGGCTAGTCACTCATAAC**GAATTCGAGCTCGTTTAAAC

Hus1-B2-F3/ GTTTAAACGAGCTCGAATTC**GTTATGAGTGACTAGCCAC**

Hus1-B2-R3/ GTATAGCGATGCCTCCAAAGTAC

Yellow: upstream and downstream of Hus1 arms

Brown: overlapped sequence between Hus1 ubstream arm and pAW1 (LoxP)

X**:** site of *LoxP* and *LoxM3* intigration.

ATG and TAA: start and stop codon respectively.

GCCCAGTTTGCTATTTCTTAGCTGGC: overlapped part between *hus1* upstream sequence and pAW1.

GTTATGAGTGACTAGCCAC: overlapped part between *hus1* downstream sequence and pAW1.

CTTAGCTGGC**X*****TTTACGCGTTCG***: represents part of the Hus1-WT-F primer (5'-CGATAGCATGCGTGGCATGCCTTAGCTGGCTTTTACGCGTTCG-3').

Figure 3-5: Genomic *hus1* sequence and location of *LoxP and LoxM* sites. The open reading frame (includes introns) of the *S.pombe hus1* gene is shown in grey with ATG-1 and the stop codon highlighted. The two red X symbols mark the sites were the *LoxP* (upstream) and *LoxM3* (down-stream) sites were integrated. The yellow sequences overlap with the upstream and down-stream genomic arms, which start at the pink and light blue sequences respictively. The underlined brown and green sequences show the overlapped sequence between upstream and downstream (respectively) of *hus1* gene arms and pAW1 vector. The underlined italic sequence (brown and pink colors) represents part of the Hus1-WT-F primer sequence, which was used to introduce the SphI cloning site for the insertion of the *hus1* genes into the integration plasmid pAW8. The reverse primer introducing the SpeI cloning site binds down-stream of the myc-affinity tag sequences (Caspari, et.al. 2000), which is not shown.

3.2.2 Construction of *LoxP-hus1.Wt.Myc-LoxM3* strain

To re-integrate the C-terminally Myc-tagged wild type *hus1*gene, *LoxP-hus1.Wt.Myc-LoxM3*, the base strain was transformed with the plasmid pAW8 containing the affinity-tagged *hus1* wild type gene containing the 117nt of up-stream sequence (Figure 3-5). This strain was constructed for two reasons. First, to obtain a control for the single and double point mutations of the *hus1* gene, which will be detailed later in this chapter. Second, the construction of such strain can be used to investigate whether the *LoxP-LoxM3* sequences or the 13 copies of the Myc tag have any impact on the cellular functions of Hus1 protein.

The mentioned strain was constructed by Cre-Lox recombinase-mediated cassette exchange (RMCE) according to the non-essential gene replacement protocol (Watson, et.al. 2008). This was achieved by amplifying the *hus1-Wt.Myc* cassette from *hus1-Wt.Myc* strain, which expresses a *hus1* gene with 13 in-frame myc epitopes from the endogenous locus (Caspari, et. al., 2000). The PCR fragments were cloned using SphI and SpeI sites into the Cre-expression plasmid pAW8 and transformed into the previously constructed *hus1* base strain (Figure 3-3 & 3-4). The transformed cells were selected on YEA plates supplemented with 5-Fluoroorotic acid (5-FOA), which kills all base strain cells that did not exchange the

ura4^{+} marker gene with the *hus1-Myc* gene as the *ura4*$^{+}$ gene product converts 5-FOA into a toxic substance.

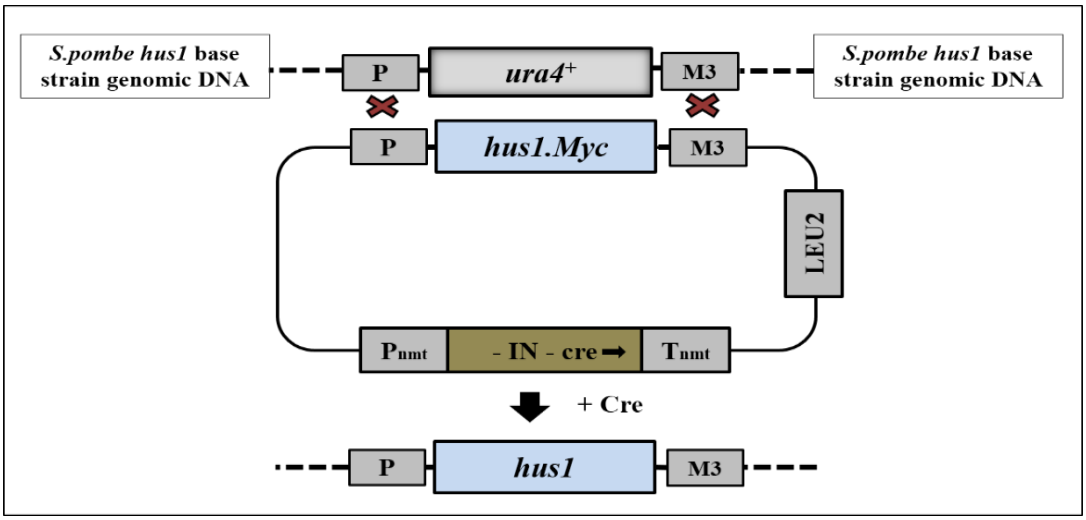

Figure 3-6: Illustrative diagram of the *LoxP-hus1.Wt.Myc-LoxM3* strain construction by Cre-Lox recombinase-mediated cassette exchange (RMCE). The cassette of *LoxP-hus1.Wt.Myc-LoxM3* was PCR amplified from genomic DNA obtained from the *hus1.Wt.Myc* strain, cloned onto the plasmid pAW8 using SphI and SpeI cloning sites and transformed into the *hus1* base strain. Transformed cells were counter-selected for the loss of the *ura4*$^{+}$ marker gene using YEA media supplemented with 5-FOA (selection for *ura4*$^{+}$ loss). (Adapted from: Watson, et.al. 2008).

The phenotypes of the resulting *LoxP-hus1.Wt.Myc-LoxM3* strain were examined in parallel with the *hus1-Wt.* and *hus1* base strain by Western blot, in addition to the spot and acute survival assays in the presence of a variety of DNA damaging agents (UV, HU, MMS and CPT) (Figure 3-7 ,3-8 & 3-9). The *LoxP-hus1.Wt.Myc-LoxM3* strain showed a slightly higher sensitivity to UV light and the topoisomerase 1 inhibitor camptothecin (CPT) than the normal wild type cells (*hus1-Wt*). However, the difference in sensitivity was very low, which could be attributed to the addition of the C-terminal myc tag or an effect of the *LoxP* and *LoxM* sequences in the genome, although the latter is less likely. The *LoxP-hus1.Wt.Myc-LoxM3* strain is fully resistant to the used doses of the replication inhibitor Hydroxyurea (HU) and the DNA alkylation agent methyl methanesulfonate (MMS) (Figures 3-7, 3-8 & 3-9).

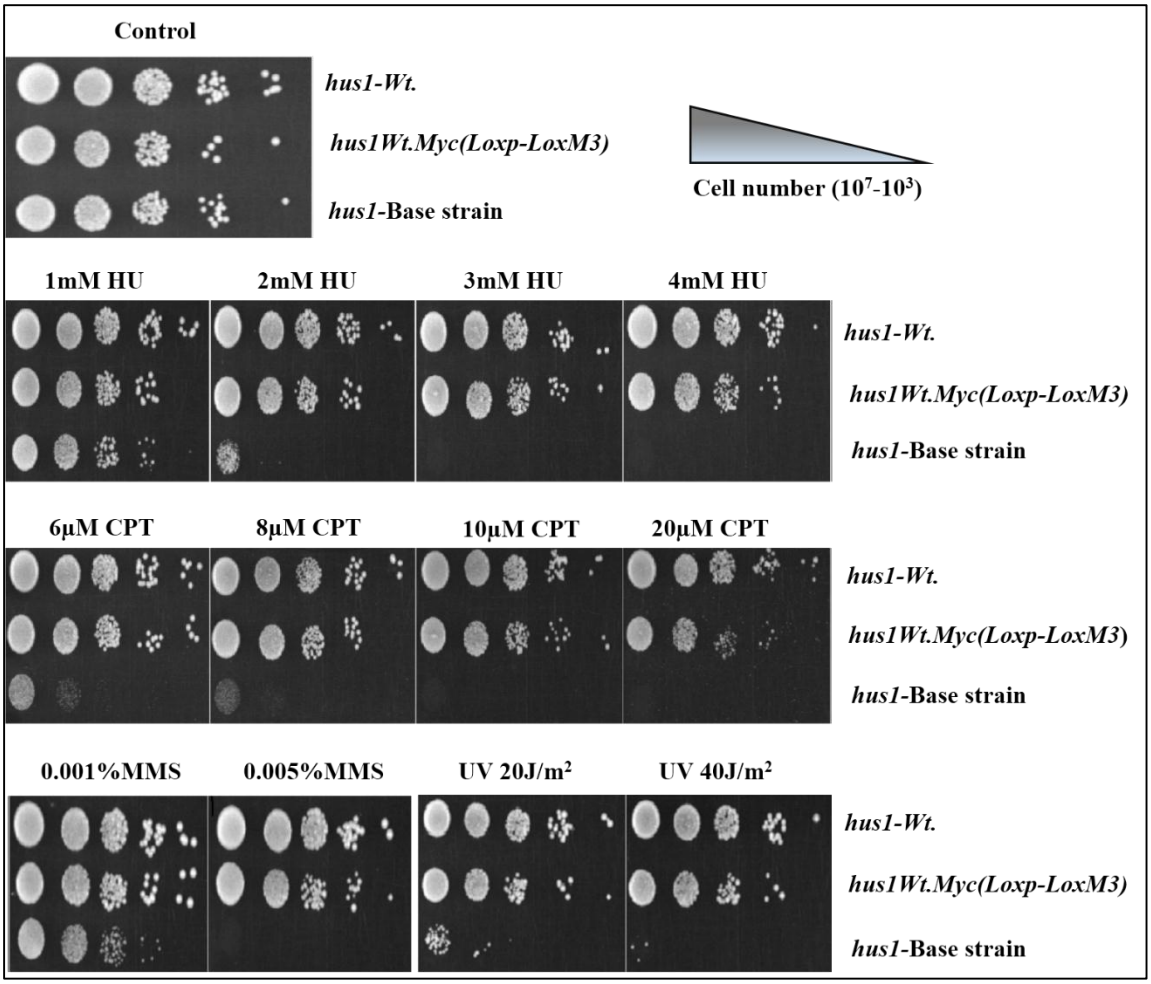

Figure 3-7: Spot assay test to confirm the base strain construction and successful re-integration of the *hus1-Myc* wild type gene. Cell suspensions diluted 10-fold starting from 10^7 cells/ml was spotted onto YEA plates. Control plates were left without a drug or UV treatment. For the DNA damage treatments, cells were plated onto YEA plates supplemented with the indicated drugs or exposed to the indicated doses of UV light. Plates were incubated for 3-4 days at 30°C until the results were analyzed. As expected, the *hus1* base strain was highly sensitive and this sensitivity was abolished upon the re-integration of the C-terminally Myc-tagged *hus1* wild type gene (*LoxP-hus1.Wt.Myc-LoxM3*). In comparison to the normal wild type strain (*hus1-Wt.*), the strain expressing the *hus1-myc* wild type gene from the manipulated locus (*LoxP-hus1.Wt.Myc-LoxM3*) were slightly sensitive to the topoisomerase inhibitor camptothecin (CPT) and higher doses of UV light. That could be attributed to the addition of the C-terminal myc tag.

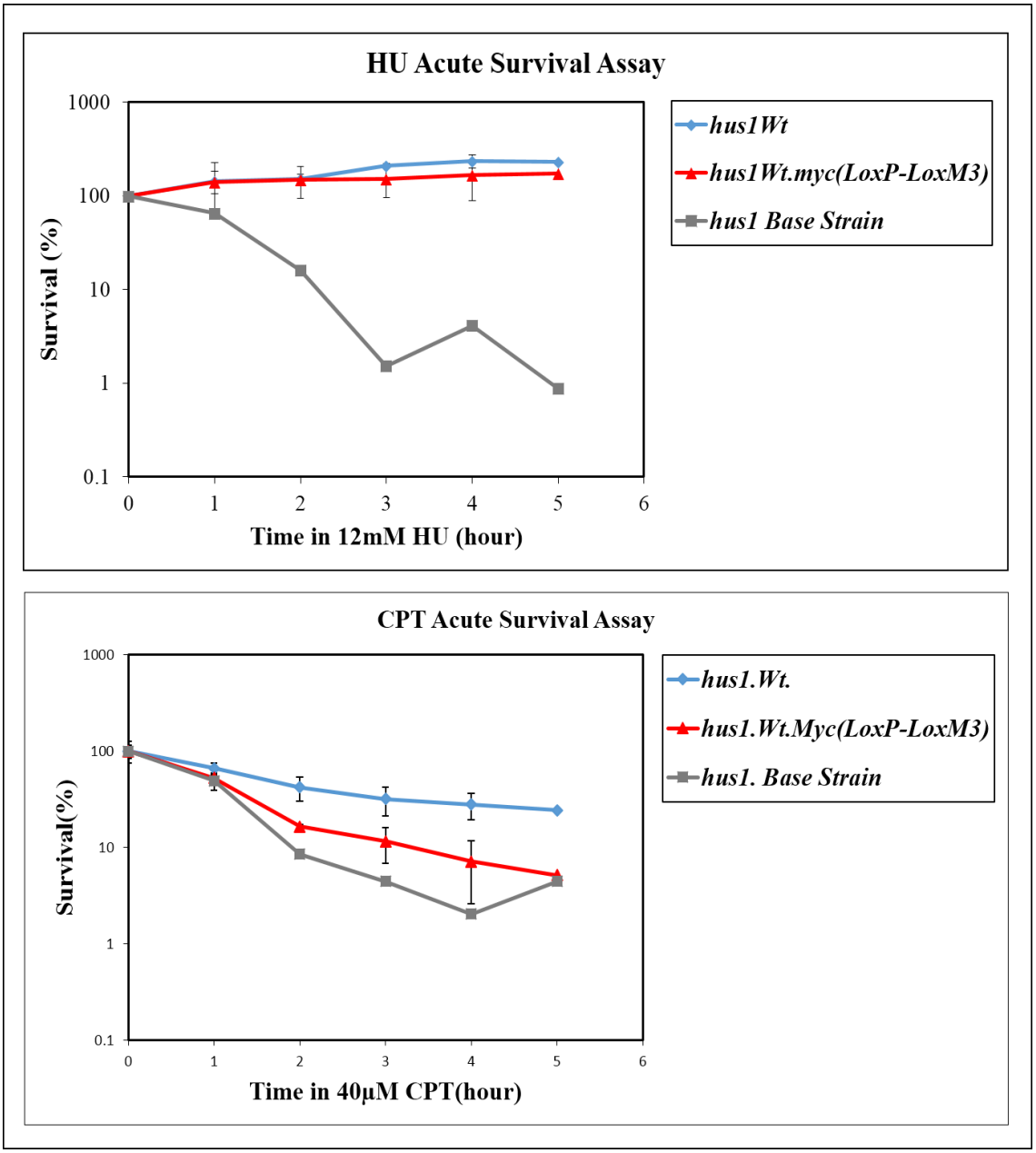

Figure 3-8: HU and CPT Acute Survival Assay Charts of *hus1.Wt, hus1.Wt.Myc.* (*LoxP-LoxM3*) and the *hus1* base strain. Cells were exposed to the indicated drugs for 5 hours, samples were taken at the indicated times and plated onto YEA plates. Colonies were counted 3 days post-incubation at 30°C. *hus1.Wt and hus1.Wt.Myc. (LoxP-LoxM3)* strains were resistant to the effect of HU, but they were slightly sensitive to the topoisomeraseI inhibitor camptothecin (CPT). However, the second was slightly more sensitive. In comparison, the *hus1* base strain was very sensitive to both HU and CPT treatments. Error bars (standard deviation) were calculated from three independent experiments.

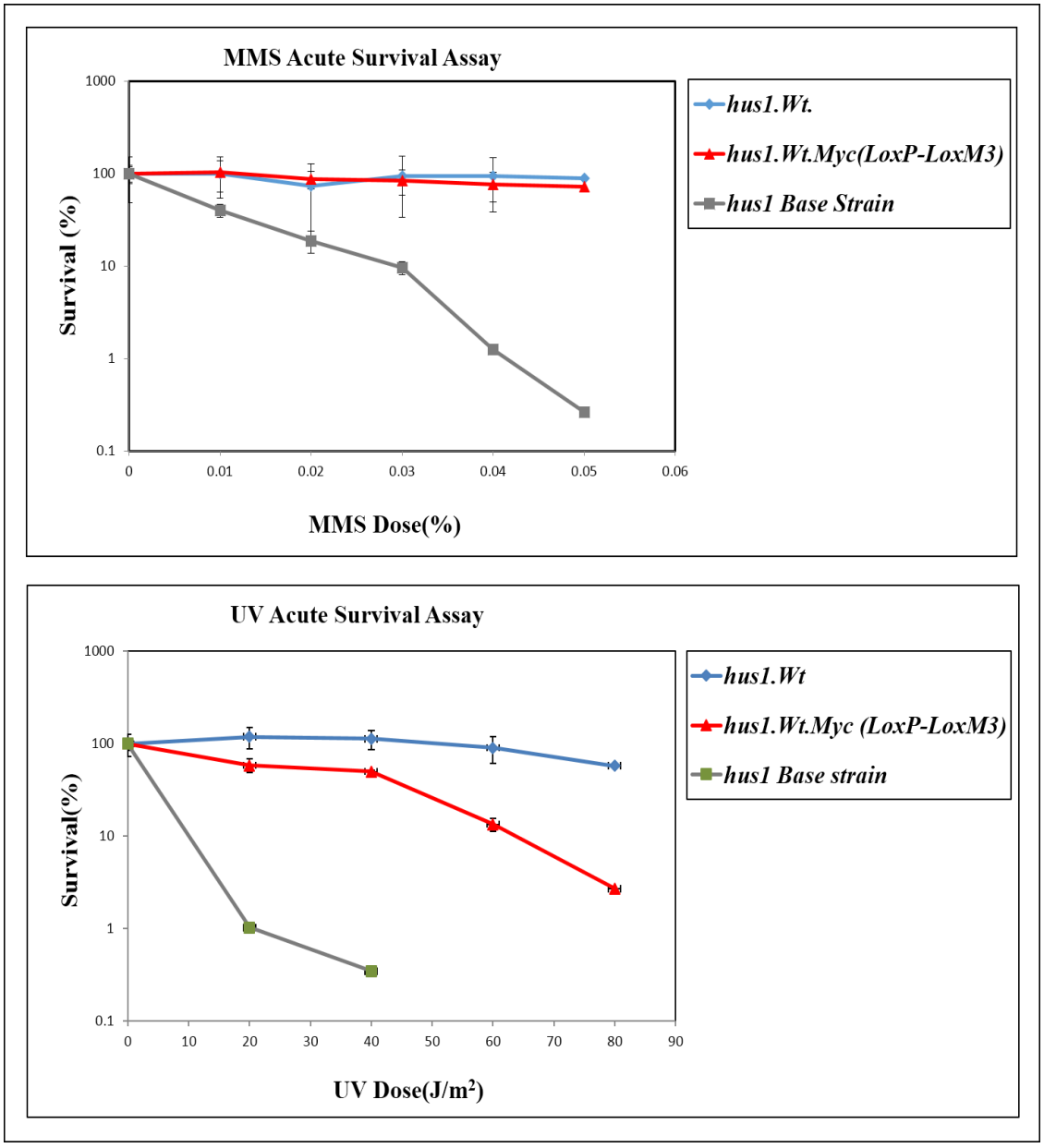

Figure 3-9: MMS and UV Acute Survival Assay Charts of *hus1.Wt, hus1.Wt.Myc.* (*LoxP-LoxM3*) and the *hus1* base strain. Cells were treated with the indicated doses of MMS or plated onto YEA plates and exposed to the indicated UV doses (20-80 J/m^2). Colonies were counted after 3 days incubation period at 30^{o}C. Both *hus1.Wt* and *hus1.Wt.Myc.* (*LoxP-LoxM3*) were resistant to the alkylation agent methane-methylsulfonate (MMS). However, *hus1.Wt.Myc.* (*LoxP-LoxM3*) strain was less resistant to the higher doses of UV light. In contrast, the *hus1* base strain was very sensitive for both treatments. Error bars (standard deviation) were calculated from three independent experiments.

3.2.3 The construction of *hus1* gene single and double point mutations revealed a variety of effects on the expression of the Hus1 variants

In order to apply the hypothesis of Hus1 isoforms production by a Ribosome Leaky Scanning mechanism, I mutated each methionine codon in the *hus1* gene individually to an alanine codon. I also created double mutant alleles in which each one of the internal methionine codons was simultaneously replaced jointly with the first AUG codon, and I also made a double mutant in which AUG-32 and AUG-46 were simultaneously mutated to alanine.

As shown in Figure 3-10, all single mutations were constructed by Fusion-PCR. First, the *hus1* gene was amplified in two fragments, which overlapped at the point mutation, which was encoded in the mutant primer pair by the general PCR protocol from genomic DNA obtained from the *hus1-myc* strain (Caspari et al., 2000). Each fragment contained the same single mutation in the overlapping region, since they were amplified by mutation primers (Mutation primer 2-R or Mutation primer 3-F) in combination with flanking primers (5'-Flanking primer 1-F or 3'- Flanking primer 4-R) respectively. The two fragments were then fused to each other by Fusion-PCR, and the mutated gene was amplified using the flanking primers (Figure 3-10, B). Double mutations of M1A simultaneously with another methionine mutation were constructed by using genomic DNA prepared from the *hus1.Myc-M1A* strain as a template for the Fusion-PCR. In the case of the *hus1-M32AM46A* double mutant, genomic DNA from the *hus1.Myc-M32* strain was used as a template. All mutant alleles were confirmed by sequencing.

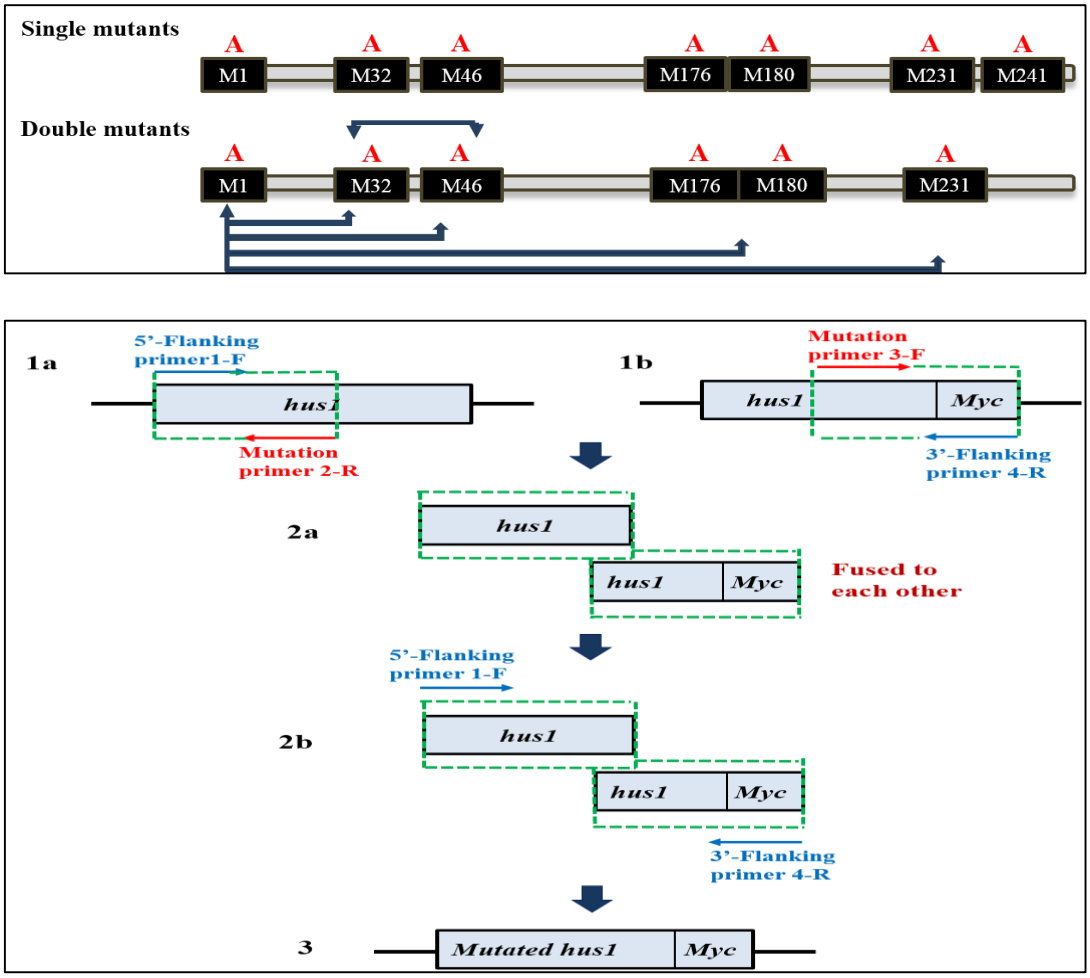

Figure (3-10): Illustrative diagram of *hus1* single and double mutations construction. Top panel: shows the single and double mutations that were created within the *hus1* gene. Single mutations were obtained by mutating each methionine codon individually to alanine. Double mutations were obtained by mutating the first methionine (M1) to Alanine (M1A) simultaneously with another methionine within the *hus1* sequence. Moreover, a double mutation was constructed by mutating M32 in parallel with M46. **Lower panel:** explains the steps of single and double mutations construction by Fusion-PCR protocol. First, the *hus1* gene was amplified in two initial fragments by sets of primers, a flanking primer (5'- Flanking primer1-F and 3'- Flanking primer2-R) with a corresponding primer that carries the desired single mutation (Mutation primer 2-R and Mutation primer3-F respectively). In a second step, the initial fragments were fused to each other by Fusion-PCR and the entire mutated gene was amplified using the two flanking primers. All mutant alleles were sequenced.

To analyze the expression pattern of Hus1, whole cell extracts of all *hus1* single and double mutants, in addition to *hus1.Wt.Myc (LoxP-LoxM3)*, were prepared and analyzed by 10% SDS-PAGE and Western blot (Fig. 3-11). As reported previously by Caspari, et.al. (2000), the non-mutated Hus1 protein of *S.pombe* appears as four bands, Hus1A (seemed as a Hus1 modified protein), Hus1B (the main band), which represents the full-length protein that weighs approximately 65kDa, in addition to the smaller variants Hus1C and Hus1D. Moreover, we detected another band, which was named Hus1E, which did run between Hus1C and Hus1D at approximately 55kDa. This band was largely restricted to cells expressing the Hus1-myc wild type protein. In contrast to the other bands, this Hus1E band was not always observed implying that its expression may depend on the physiological growth conditions.

In summary, the construction of the *hus1* single and double point mutations revealed the following interesting results (Figure 3-11). As expected, loss of the first ATG in *hus1.Myc.M1A* abolished expression of the full-length Hus1 protein (Hus1B) and rendered cells highly DNA damage sensitive (Figure 3-13). This is consistent with the previous finding that Hus1B is the full-length protein associating with Rad9 and Rad1 in the 9-1-1 ring (Caspari, et.al. 2000). Loss of Hus1B led also to the disappearance of the modified band Hus1A and the smaller variant Hus1E, whereas expression of the smallest band Hus1D was not affected (Figure 3-11). This could indicate that Hus1E is a breakdown product of the full-length protein or that the expression of this band is dependent on the full-length protein. Interestingly, the expression of Hus1C and Hus1D is restricted to dividing cells as stationary cells only expressed the full-length protein, the modified band and probably Hus1E (Figure 3-11, lower panel). As reported previously (Janes et al., 2012), Hus1 is the only one of the three 9-1-1 subunits expressed in non-growing cells. This intriguing observation also indicates that expression of the other variant Hus1C is limited to dividing cells. Consistent with this conclusion, Hus1C levels strongly decreased in stationary cells.

To obtain a more detailed picture of the different Hus1 protein variants, I subjected a protein extract from untreated Hus1-Myc wild type cells to isoelectric focusing. The mentioned technique was achieved by using a ready gel strip with a linear pH gradient (Biorad, pH3-10) prior to 10% SDS-PAGE electrophoresis. As shown in Figure 3-12A, this

more sensitive technique revealed that Hus1C is a double band consisting of two slightly different variants. My further work showed that these two bands originate at AUG-32 and AUG-46, respectively. Expression of both variants is abolished in the *hus1.Myc-M32A-M46A* double mutant (Figure 3-11; 3-12B). Expression of full-length Hus1B and the smallest variant Hus1D was unaffected. This shows that the variants H32 and H46, which jointly form Hus1C, are expressed independently of the 9-1-1 ring in dividing cells. Loss of both variants in the *hus1.Myc-M32A-M46A* double mutant had an interesting impact on the DNA damage sensitivity of the cells. Unlike cells without Hus1B (full-length Hus1), which were highly sensitive to all tested treatments, cells without the two variants were mainly MMS sensitive and displayed a slight sensitivity to higher doses of HU and CPT (Figure 3-13, 3-14).

Another interesting observation was the covalent modification in the Hus1 mutant protein in which the two neighboring methionine residues 176 and 180 were simultaneously replaced by an alanine. This modification band was approximately 35-40kDa larger than the full-length Hus1B protein (Figure 3-11). As this band was also present in non-dividing cells, which do not express the variants H32 and H46, it is possible that this modified band is linked with either the full-length protein or the Hus1E variant. The nature of this modification is not yet known.

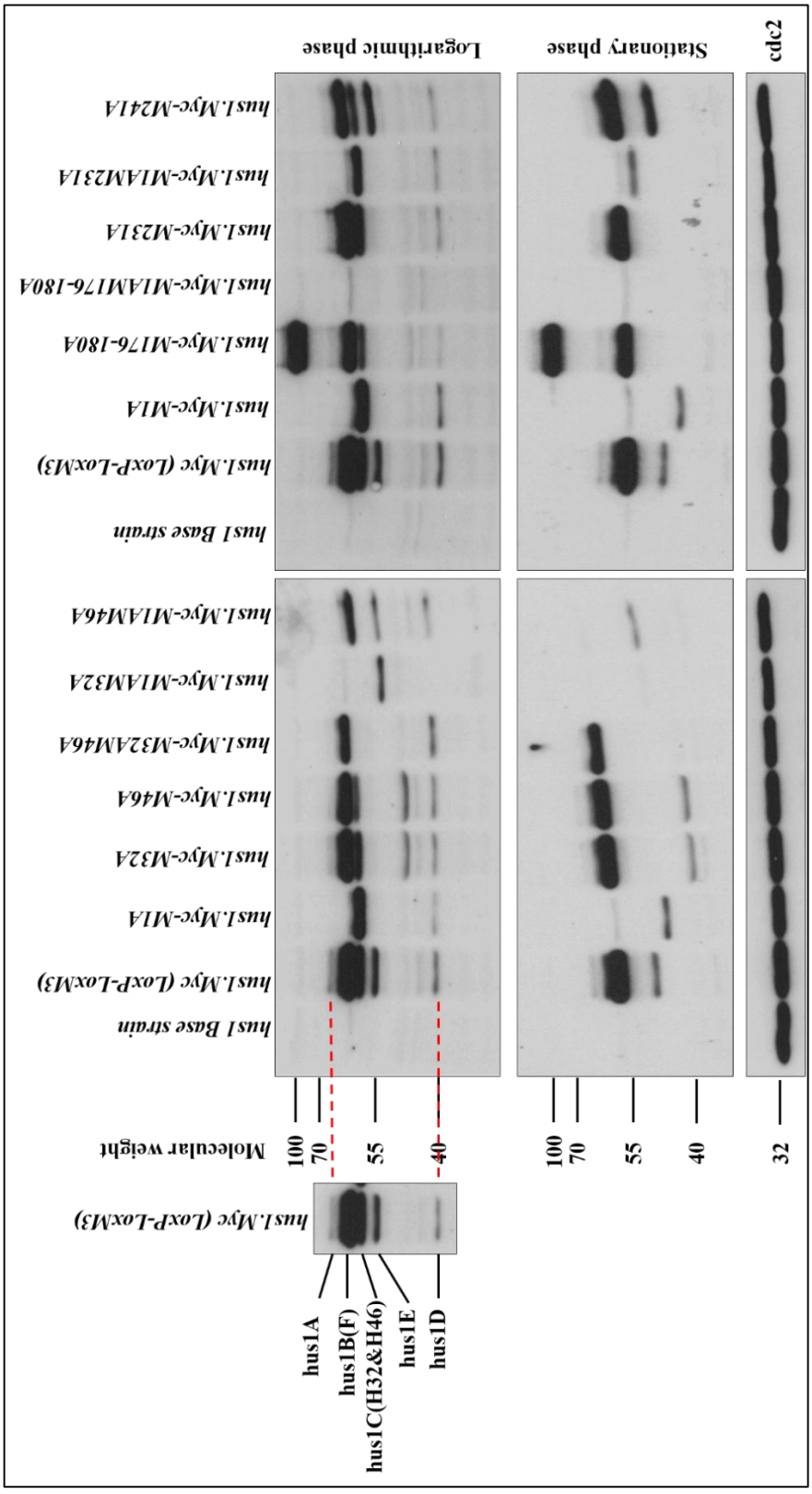

Figure 3-11: Expression pattern of single and double mutation versions of Hus1 during logarithmic and stationary phase. The Hus1-Myc wild type protein has four isoforms, Hus1A, B, C and D (Caspari, et.al. 2000). The band Hus1E was previously not reported and its expression seem to vary with the physiological growth conditions. The Hus1 expression patterns of the indicated strains are shown during logarithmic growth and in stationary phase. Please note that the expression of Hus1C, the double band of Hus1-32 and Hus1-46, is limited to the logarithmic growth phase and not detected in stationary cells. Cdc2 protein was used as a loading control.

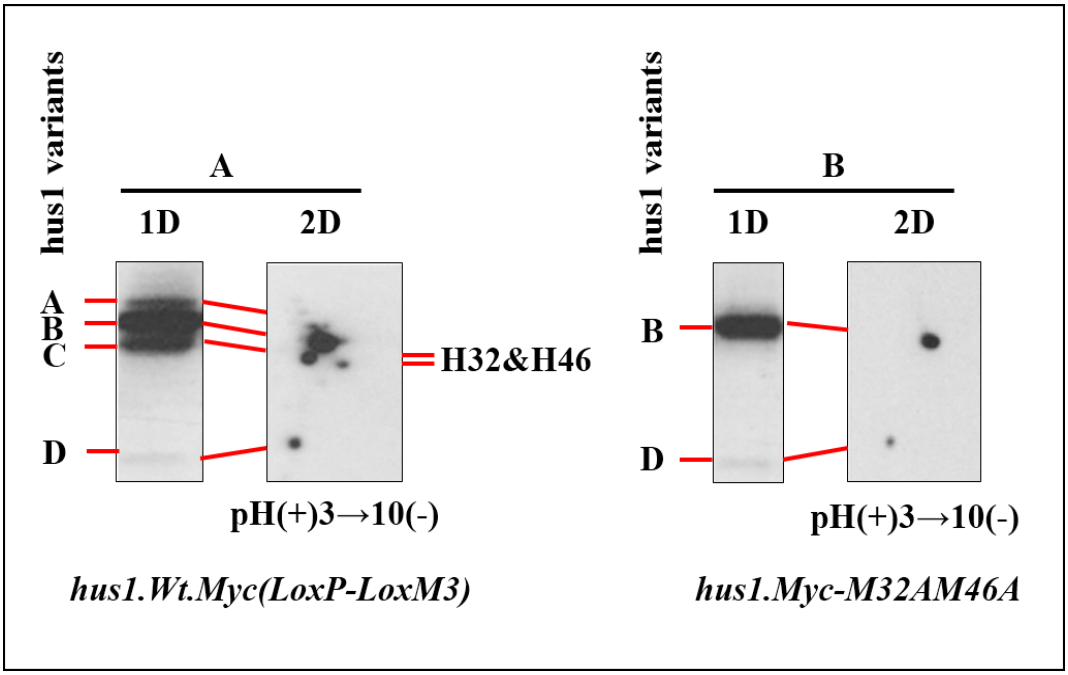

Figure 3-12: The Hus1C band is formed by two variants, H32 and H46. A: One and two-dimensional (1D, 2D) protein electrophoresis of a protein extract obtained from untreated *hus1.Wt.Myc. (LoxP-LoxM3) cells*. **Left panel:** shows the four bands, which represents the previously reported variants Hus1A (A), full-length Hus1B (B), Hus1C (C) and Hus1D (D). **Right panel:** 2D protein electrophoresis of Hus1.Wt.Myc. (LoxP-LoxM3) revealed that the band Hus1C is composed of two bands (H32 & H46), which are deleted from the proteins that produced by *hus1.Myc.M32A* and *hus1.Myc.M46A*. **B:** 1D & 2D protein electrophoresis of a protein extract prepared from untreated *hus1.Wt.Myc.M32AM46A cells*. **Left panel:** 1D protein electrophoresis shows that the *hus1.Wt.Myc.M32AM46A* strain expresses full-length Hus1B and Hus1D, but not the variants Hus1-32 and Hus1-46. That was confirmed by the 2D protein electrophoresis (Right panel) of the same protein extract.

3.2.4 Construction of the *hus1* gene single and double point mutations affected the response to DNA damage differently

Concerning with the previously mentioned effects of *hus1* single and double mutations on the biochemistry of the Hus1 protein, I decided to characterize the effect of the mutations on the cellular behaviour to different types of genotoxic treatments. As expected, the deletion of the full-length Hus1B protein and the subsequent abolishment of Rad9-Hus1-Rad1 complex rendered cells highly sensitivity to all tested DNA damaging treatments (Figure 3-13, 3-14). Thus, *hus1.M1A* and all double mutations with M1A rendered cells highly sensitivity to of UV, MMS, HU and CPT treatment. The single mutations of M32A, M46A, M176 &180A, M231A and M241A had no impact on the DNA damage sensitivity. Only the simultaneous mutation of M32 and M46 rendered cells sensitivity to high doses of MMS and to a lesser degree to HU and CPT (Figure 3-13, 3-14). This suggests that the two mutations act in parallel pathways and only loss of both has an impact on the DNA damage response.

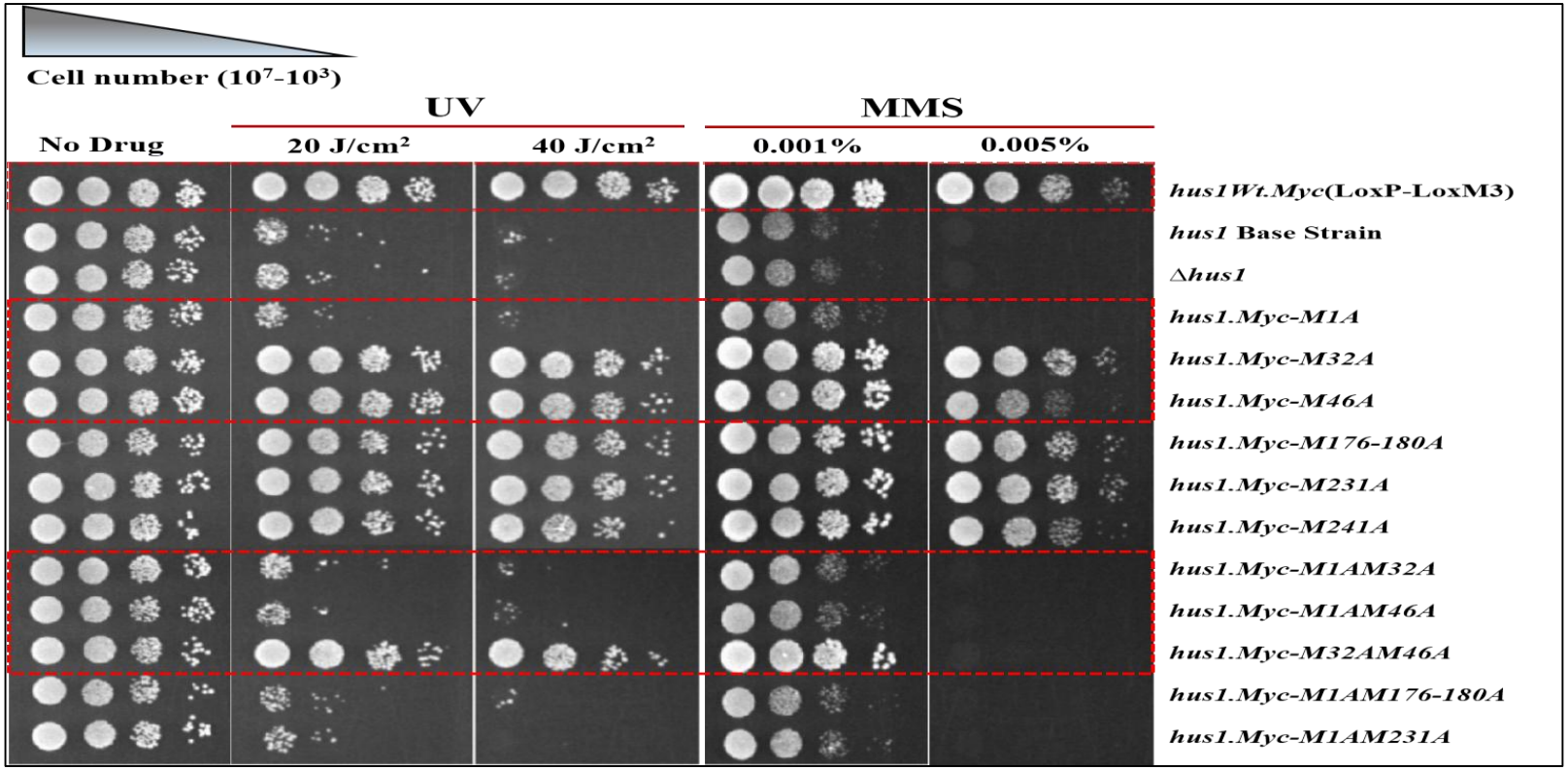

Figure 3-13: Loss of the first AUG in the *hus1* mRNA renders cells highly sensitive to UV and MMS treatments. Cells as 10x fold diluted starting from 10^7 cells/ml and 5µl were spotted onto YEA plates with the indicated MMS concentrations. Control plates were left without a drug. Whereas for the UV exposure, cells were spotted on YEA plates and exposed to the indicated UV doses. All plates were incubated for 3-4 days at 30°C until the results were analyzed. Inactivation of the first Methionine renders cells highly sensitive to both UV and MMS treatment, which is due to the loss of the full-length hus1 protein and the subsequent loss of the 9-1-1 DNA damage sensor. Mutation of M32 and M46 (*hus1.Myc.M32AM46A*) rendered cells sensitive to higher doses of MMS (0.005%).

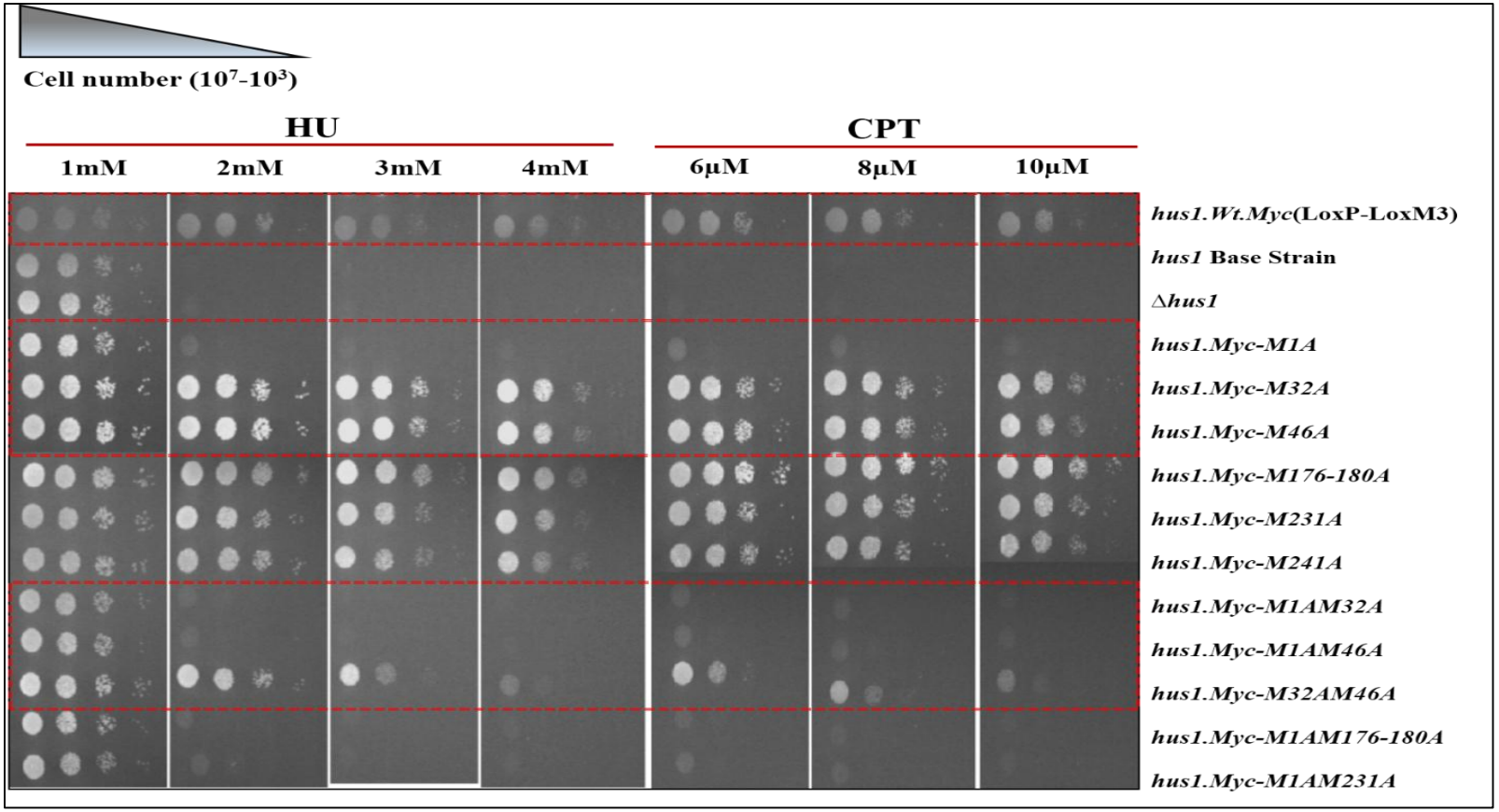

Figure 3-14: Loss of AUG-1 in the *hus1* mRNA renders cells highly sensitive to HU and CPT treatments. Serial dilutions starting from 10^7 cells/ml were spotted onto YEA plates, which were supplemented with either HU or CPT at the indicated doses. All plates were incubated for 3-4 days at 30ºC until the results were analyzed. Inactivation of the first Methionine renders cells highly sensitive to both HU and CPT treatment, which is due to the loss of functional Hus1 protein and subsequent loss of the 9-1-1 DNA damage sensor. Mutation of M32 and M46 (*hus1.Myc.M32AM46A*) had only a mild effect at high doses of HU and CPT.

3.2.5 Phenotypic characterization of the Hus1 variants H32 and H46

Informed by the interesting finding that loss of Hus1-H32 and Hus1-H46 from dividing cells interferes with the DNA damage response, I decided to analyze the *hus1.Myc.M32AM46A* mutant strain in detail.

Figure 3-15/A shows an illustrative diagram explaining the differences between the full-length Hus1 protein and the two variants. Initiation of translation at AUG-32 would delete the first 31 amino acids, which form one alpha helix and one beta-sheet in the inner section of the Hus1 protein (Figure 3-15, B). Although this has no direct impact on the interaction surfaces of Hus1 with Rad1 and Rad9, it may change their folding and it would shorten the protein. Initiation of translation at AUG-46 would delete another 14 amino acids, deleting a second beta-sheet from the protein. The variant H46 is particularly interesting since it is missing a similar section as the previously reported *S.pombe* Rad9-M50 variant (Janes, et.al. 2012). Given the structural similarity between Rad9 and Hus1 (Sohn & Cho, 2009), this observation implies that loss of this section can be tolerated in both proteins possibly resulting in similar changes in the N-terminally truncated variants.

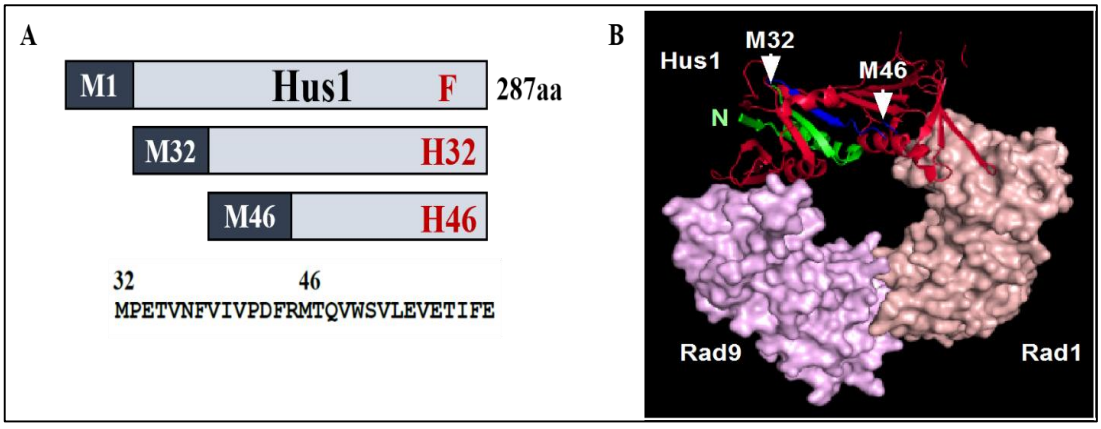

Figure 3-15: Illustrative diagram of full-length Hus1 and its variants H32 and H46. A: shows the truncated parts of the H32 and H46 proteins in comparison with the full-length protein. **B:** Structure of the human 9-1-1 protein complex (Dore, et. al., 2009). The protein map was created using the Polyview 3D server (http://polyview.cchmc.org/polyview3d.html). The green section is missing from variant H32, while the green and blue sections are missing from the H46 variant.

3.2.5.1 Loss of H32 and H46 in *hus1.Myc-M32AM46A* affects the acute survival to DNA damage

Given the moderate MMS sensitivity and slight sensitivity to HU and CPT in the chronic exposure tests (Figures 3-13, 3-14), acute survival assay were applied to the strains using different treatments as HU, CPT, UV or MMS respectively (Figures 3-16 & 3-17). Loss of both variants, H32 and H46, in *hus1.Myc-M32AM46A* cells rendered cells mildly sensitivity to CPT, HU and UV treatment but not to MMS. While all drugs should interfere with DNA replication, Camptothecin (CPT) causes DNA breaks by trapping topoisomerase 1 in front of replication forks, hydroxyurea (HU) stalls forks by depleting the dNTPs pool and UV slows down replication by inducing the formation of thymidine dimers in the template. Combined with the expression of the variants only in growing cells (Figure 3-11), this suggests a role of H32 and H46 in the response to DNA replication stress. The fact that the mutant is not sensitive to MMS when exposed to 0.005% for 1 hour (Figure 3-17), but dies when cells have to grow in the presence of the DNA alkylating drug (Figure 3-13) could indicate that the variants are only required when extensive DNA methylation occurs.

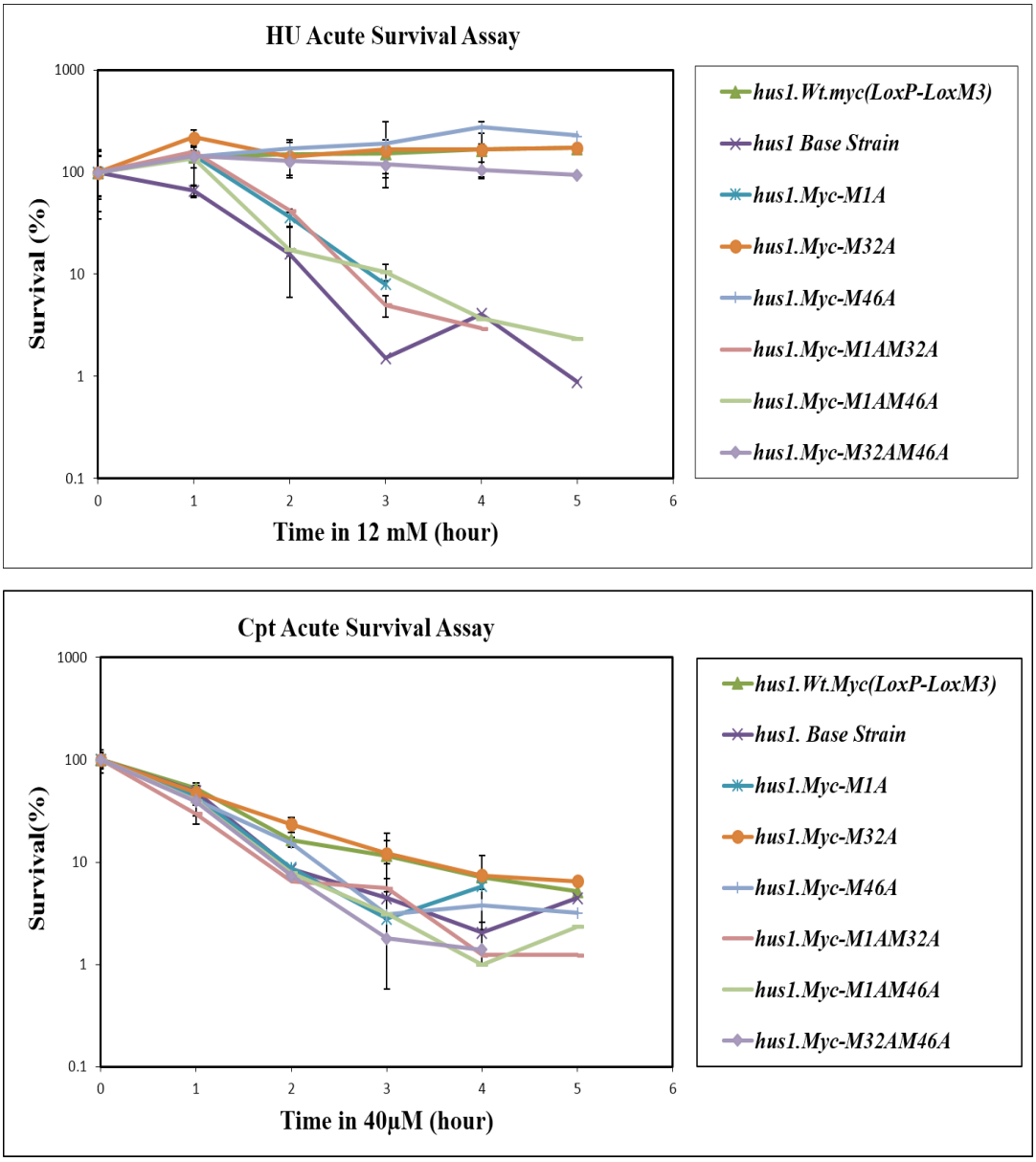

Figure 3-16: Loss of both H32 and H46 variants renders cells slightly HU and CPT sensitive. Cells ($5x10^4$ cell/ml) were exposed to either 12mM HU or 40µM CPT for up to 5 hours. Cells samples were collected at the indicated time points, plated onto YEA plates and incubated for 4 days at 30°C until the resistant colonies were grown. Surviving colony number was drawn against their corresponding time points. The top panel shows that cells lacking both variants (*hus1.Myc-M32AM46A*) are slightly sensitive to the depletion of the nucleotide pool by hydroxyurea (HU). The lower panel shows a robust sensitivity of the mutant strain to replication breakage when camptothecin (CPT) immobilizes Topoisomerase 1. Error bars (standard deviation) were calculated from three independent experiments.

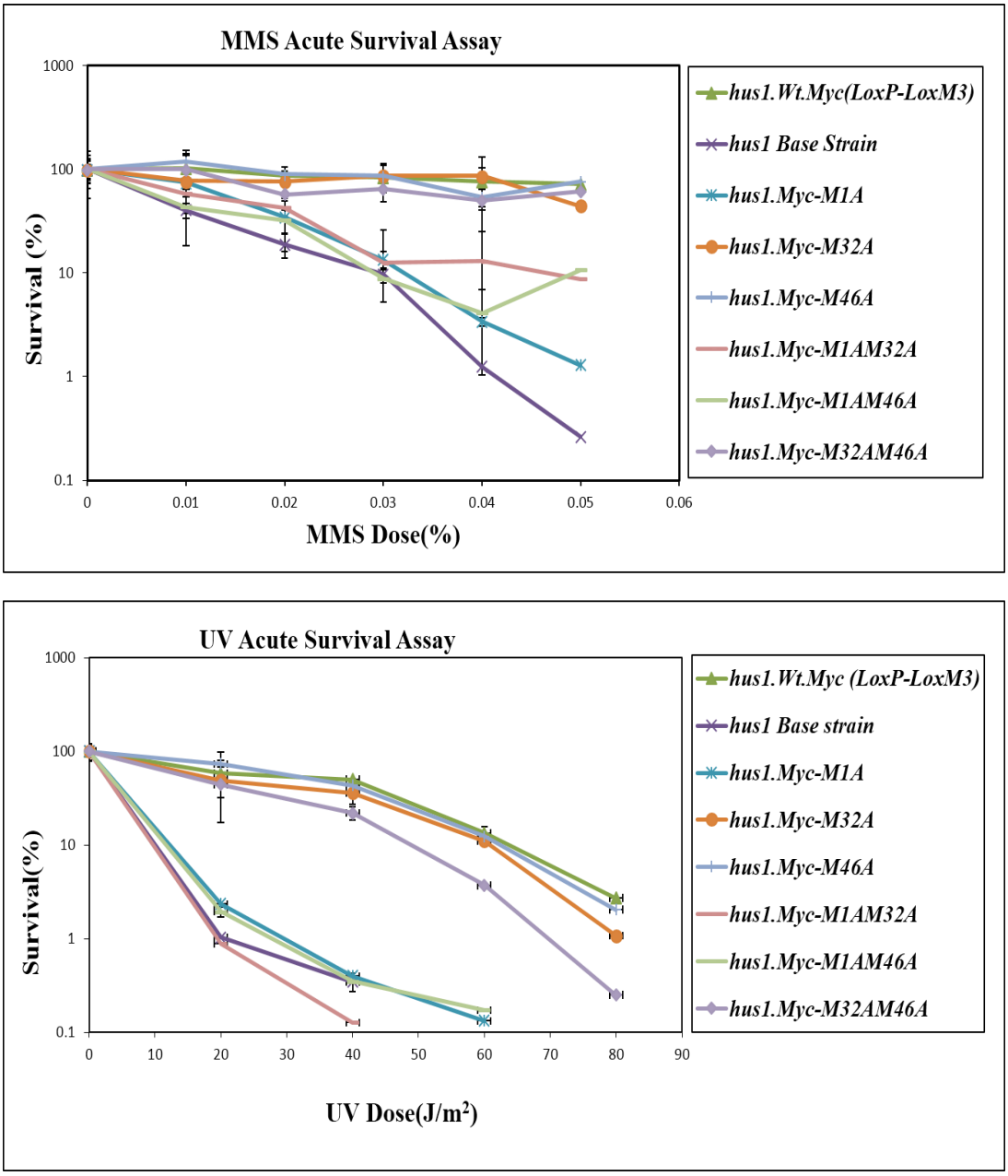

Figure 3-17: Loss of both H32 and H46 variants renders cells UV sensitive. Cells ($5x10^4$ cell/ml) were exposed to different doses of MMS (0-0.05%) for 1 hour or to a range of UV doses (0-80 J/m^2). Cells samples were plated onto YEA plates and incubated for 4 days at 30^{o}C until the resistant colonies grow. Surviving colonies number was drawn against their corresponding time points. The top panel shows that loss of H32 and H46 did not affect the cells resistance to the DNA methylating agent MMS when cells are only exposed for 1 hour. In contrast, cells showed a slight sensitivity to UV light. Error bars (standard deviation) were calculated from three independent experiments.

3.2.5.2 Hus1-H32 and H46 form a high molecular weight complex independently of the Rad9-Hus1-Rad1 complex

As the variants H32 and H46 are expressed continuously by the *hus1* gene in dividing cells, I tried to find out whether they biochemically associate with the 9-1-1 complex. To achieve this, I fractionated the soluble protein extract of the strains *hus1.Wt.Myc (LoxP-LoxM3), hus1.Myc-M1A* and *hus1.Myc-M32AM46A* on a Superdex-200 column that separates protein complexes between 50kDa and 700kDa. As shown in Figure 3-18, the full-length Hus1 had a broad elution profile across all fractions with a peak at fractions 12-14 (500-200kDa) as reported previously (Caspari, et.al. 2000; Janes, et.al. 2012). The elution profile of the 9-1-1 complex in fractions 11-14 was more obvious in the *hus1.Myc-M32AM46A* strain, which only expresses the full-length protein and the smallest variant (Hus1D) (Figure 3-18). This shows that the 9-1-1 complex has an approximate molecular weight of 500 kDa to 200 kDa, probably depending on its association with other proteins. Interestingly, the small variant Hus1D co-eluted with the 9-1-1 complex suggesting that it might associat with the ring. The elution profile of the two larger Hus1 variants H32 and H46 was, however, distinct from the 9-1-1 ring as both proteins were enriched in the fractions 9 and 10 (Figure 3-18) (700-500 kDa). This difference indicates that Hus1-H32 and H46 form a separate complex. It should however be noted that some full-length Hus1 is also present in these fractions in wild type cells. Hence, both variants could associate with the full-length protein. To test whether the absence of the 9-1-1 loader Rad17 influences the elution profile of the variants, I fractionated a protein extract obtained from a *Δrad17-hus1.Myc-M1A strain*. Consistent with the idea that the variants form a complex independently of the canonical 9-1-1 ring, the elution profile was not affected (Figure 3-18). The fourth variant, Hus1E, which has a size between H32 & H46 and Hus1D, co-eluted with the 9-1-1 ring suggesting that it associates with it like Hus1D.

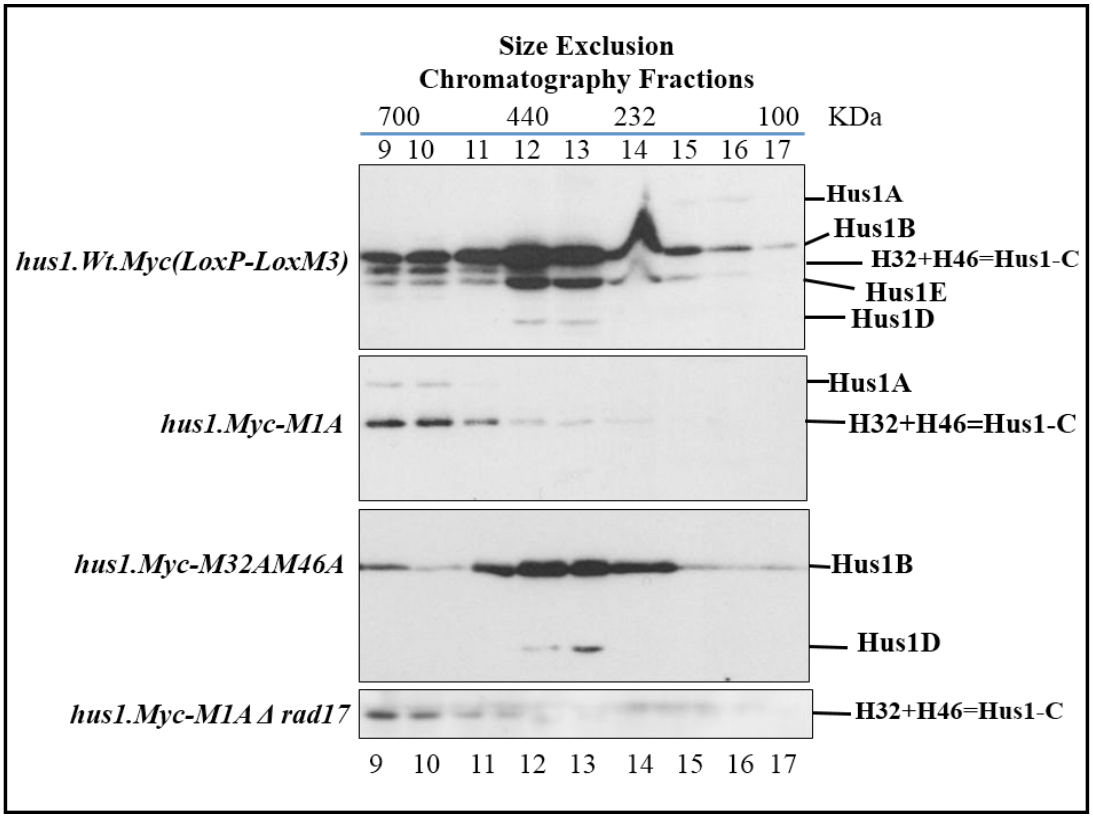

Figure 3-18: Hus1-H32 and H46 associate in a high molecular weight complex independently of 9-1-1 complex. Separation of soluble protein extracts by Size Exclusion chromatography revealed that Hus1-H32 and H46 are not incorporated within the canonical 9-1-1 ring since the elution profile of the protein variants is different from the 9-1-1 complex. While the complex eluted in fractions 11-14, which can be seen in the *hus1.Myc-M32AM46A* strain that only produces the full-length protein, both variants co-eluted in fractions 9-11 with a tail in the lower molecular weight fractions. The latter is most obvious in the *hus1.Myc.M1A* strain, which only produces the variants but not the full-length protein (H32 and H46=hus1C variant). The elution profile of the variants was not affected upon deletion of the 9-1-1 loader Rad17.

3.2.5.3 Hus1-H32 and H46 variants work in the same DNA checkpoint pathway as the Rad9-Hus1-Rad1 complex

According to the Size Exclusion Chromatography results, it seemed that H32 and H46 variants are associated with a larger complex than the 9-1-1 ring. To verify whether they are genetically located in the same pathway (epistasis) as the 9-1-1 ring, I proceeded to construct the strains *Δrad1-hus1.Myc-M32AM46A* and *Δrad17-hus1.Myc-M32AM46A* to be tested for HU (12mM) sensitivity in parallel with their single mutants *Δrad1, Δrad17 and hus1.Myc-M32AM46A* in addition to *hus1.Wt.Myc (LoxP-LoxM3).*

Although the Hus1 variants H32 and H46 seemed to be independent of 9-1-1 complex (Figure 3-18), they appeared to be genetically located within the same pathway as the double mutants of *Δrad1-hus1.Myc-M32AM46A* and *Δrad17-hus1.Myc-M32AM46A* were as HU sensitive as the single mutants of *Δrad1 and Δrad17* respectively (Figure 3-19).

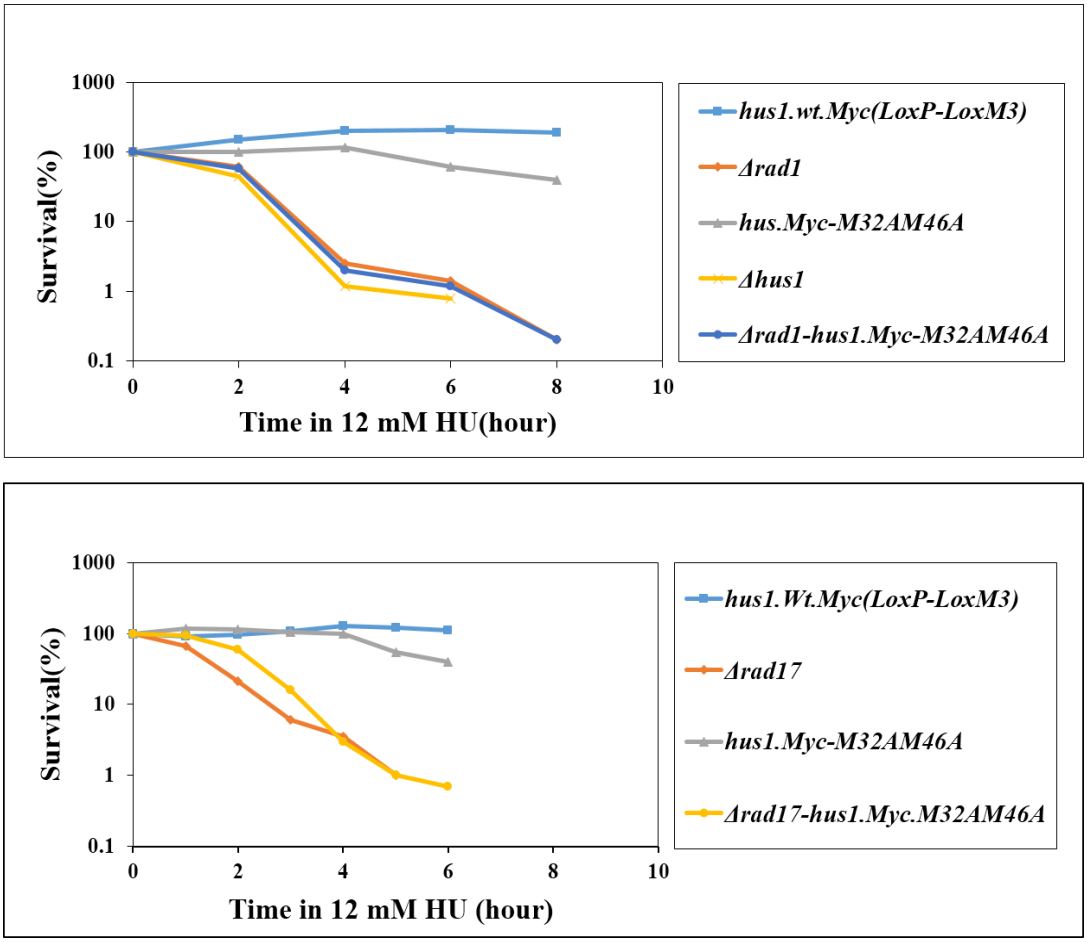

Figure 3-19: The Hus1 variants H32 and H46 are genetically in the same pathway as the 9-1-1 complex. Cells ($5x10^4$ cell/ml) were incubated with 12mM HU for 6 hours at 30°C. Cells samples were collected every hour and plated onto YEA media, and incubated up to 4 days at 30°C until the survived colonies were formed. Their survival percentages were blotted against the collection time points. The double mutants of *Δrad1-hus1.Myc-M32AM46A* and *Δrad17-hus1.Myc-M32AM46A* have the same sensitivity as the single mutants of *Δrad1*and *Δrad17* respectively, which indicates that both variants are genetically located in the same pathway. The experiment was done only one time.

The difference between the genetic and biochemical findings could be explained by a functional collaboration of the Hus1 variants H32 and H46 with the 9-1-1 ring when replication forks stall in HU medium.

3.2.5.4 Cells without H32 and H46 variants are partly replication checkpoint deficient

The slight HU sensitivity of the *hus1.Myc-M32AM46A* strain, which sets once cells are exposed for at least 4 hours, indicates a role of both variants in the response to stalled replication forks. I therefore tried to investigate whether loss of both variants affects the cell cycle response. I incubated the *hus1* wild type strain in addition to *hus1.Myc-M1A* and *hus1.Myc-M32AM46A*, either without or with 12mM HU for 5 hours at 30^{o}C. Cells were withdrawn, fixed in 4% para-formaldehyde (PFA) and stained with the anti-Myc antibody for Hus1 and DAPI for the DNA staining. As shown in Figure 3-20, wild type cells arrested in G2 as elongated cells with a strong nuclear Hus1 signal, whereas cells without the full-length protein (*hus1.Myc-M1A*) failed to arrest and died as small cells. This complete checkpoint deficiency is consistent with the absence of nuclear Hus1 staining and shows that the variants, which accumulate in the cytoplasm in *hus1-M1A* cells, are unable to enter the nucleus. Cells without H32 and H46 (*hus1.Myc-M32AM46A*) arrested in G2 as elongated cells but some cells showed signs of premature cells division and chromosomal fragmentation.

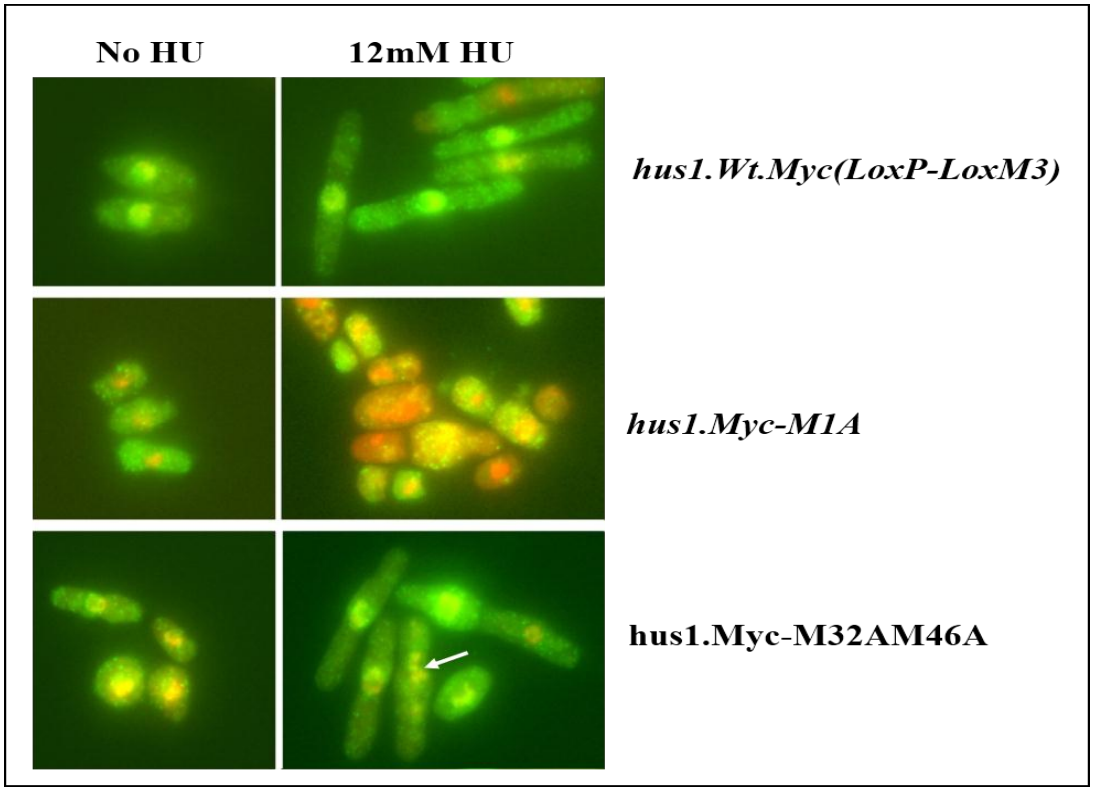

Figure 3-20: Cells without H32 and H46 variants undergo premature cells division and chromosomal fragmentation when forks arrest. Cells were incubated either without or with 12mM HU for 5hr at 30ºC. Cells were collected and fixed with 4% PFA and stained with the anti-Myc antibody (green) and DAPI (DNA = red). *Hus1.Wt.Myc* cells arrested in G2 phase, as they appeared elongated in the presence of HU. Whereas, cells that lack the full-length Hus1 protein (*hus1.Myc-M1A*) were checkpoint deficient and die as short cells. Conversely, most *hus1.Myc-M32AM46A* cells arrested in G2 but with a partial checkpoint defect since they had signs of chromosomal fragmentation. The images were taken by Nikon ECLIPSE TE2000-U fluorescence microscope (60xobjective with oil, 488nm exaltation light for ALEXA-488 and UV for DAPI), with the assistance of HC-image software.

This observation indicates that the variants are not required for the initiation of the G2 arrest, but for its maintenance. Informed by the previous results, I proceeded with measuring the G2 delay by synchronizing the cells in early G2 phase using a lactose gradient (Forsburg & Rhind, 2006) and released them for 6 hours at 30°C into a medium supplemented with 12mM HU. Consistent with the previous findings (Caspari, et.al. 2000), wild type cells progressed into the first S phase (first peak of septation) where forks stall in the presence of HU. Since cell division is not delayed, cells progressed with arrested forks further into G2 where they arrested until replication was completed (Figure

3-21). In contrast, cells devoid of the *hus1* gene (*Δhus1*) and cells without the full-length Hus1 protein (*hus1.Myc-M1A*) were checkpoint deficients since the 9-1-1 complex acts upstream of the point at which the replication checkpoint branches into the MRC1-Cds1 and Crb2-Chk1 pathways (Kostrub, et.al. 1997; Lindsay, et.al. 1998). However, cells with full-length Hus1 but without the H32 and H46 variants (*hus1.Myc-M32AM46A*) were partially checkpoint deficient cells. They initiated the G2 delay but re-enter the cell cycle approximately 2 hours earlier than wild type cells (Figure 3-21). This partial checkpoint defect is in line with the earlier observation that *hus1.Myc-M32AM46A* cells elongate but show signs of chromosomal damage (Figure 3-20).

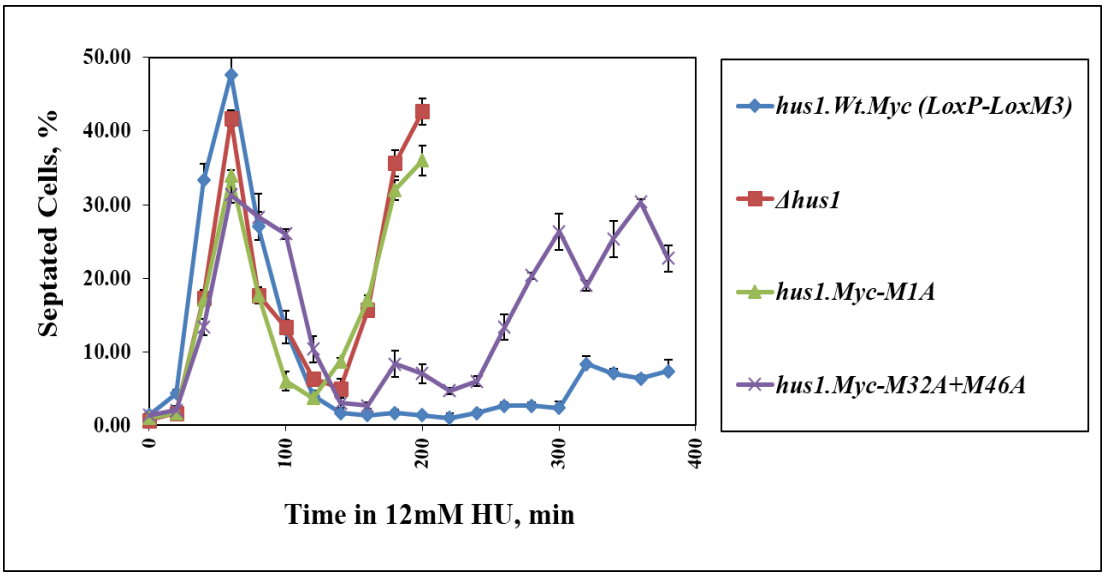

Figure 3-21: Cells without the variants H32 and H46 are partly replication checkpoint deficient. Cells were synchronized in early G2 phase by lactose gradient and released in YEA medium supplemented with 12mM HU. Samples were collected every 20min. Hus1 wild type cells were elongated as they entered an extended G2 delay upon HU treatment. In contrast, cells lacking either the *hus1* gene or the full-length Hus1 protein (*Δhus1* and *hus1.Myc-M1A* respectively) were completely checkpoints deficient and died as short cells. Interestingly, *hus1.Myc-M32AM46A* cells that express full-length Hus1 protein but not the variants H32 and H46 were partially checkpoint deficient since they entered a shorter G2 delay and re-enter the cells cycle earlier than the wild type cells. Error bars (standard deviation) were calculated from three independent experiments.

3.2.5.5 The Hus1 variants H32 and H46 activate Chk1 when forks stalled

Following the previous results, I tried to find out the exact checkpoint pathway in which H32 and H46 are active. To do this, I constructed *Δcds1-hus1.Myc-M32AM46A*, *Δchk1-hus1.Myc-M32AM46A* and *Δcds1- Δchk1* strains. As reported previously (Lindsay, et. al., 1998), cells without both down-stream kinases Cds1 and Chk1 are completely checkpoint deficient in the presence of HU. Consistent with the previous report, *Δcds1- Δchk1* cells failed to arrest in G2, whereas both single deletion strains entered a normal arrest (Figure 3-22). The reason for this is that cells arrest using either Cds1 or Chk1 (Lindsay, et.al. 1998). Interestingly, *Δcds1-hus1.Myc-M32AM46A*, which lacks the Cds1 checkpoint pathway in addition to the variants H32 and H46 were as checkpoint deficient as the *Δcds1- Δchk1* strain. This implies that the loss of H32 and H46 variants impairs the activation of the Chk1 pathway. These findings were confirmed further by the partial checkpoints deficiency of the *Δchk1-hus1.Myc-M32AM46A* strain, which is very similar to the *hus1.Myc-M32AM46A* strain (Figure 3-22). This implies that Chk1 and the variants act in the same pathway when replication forks stall in HU medium.

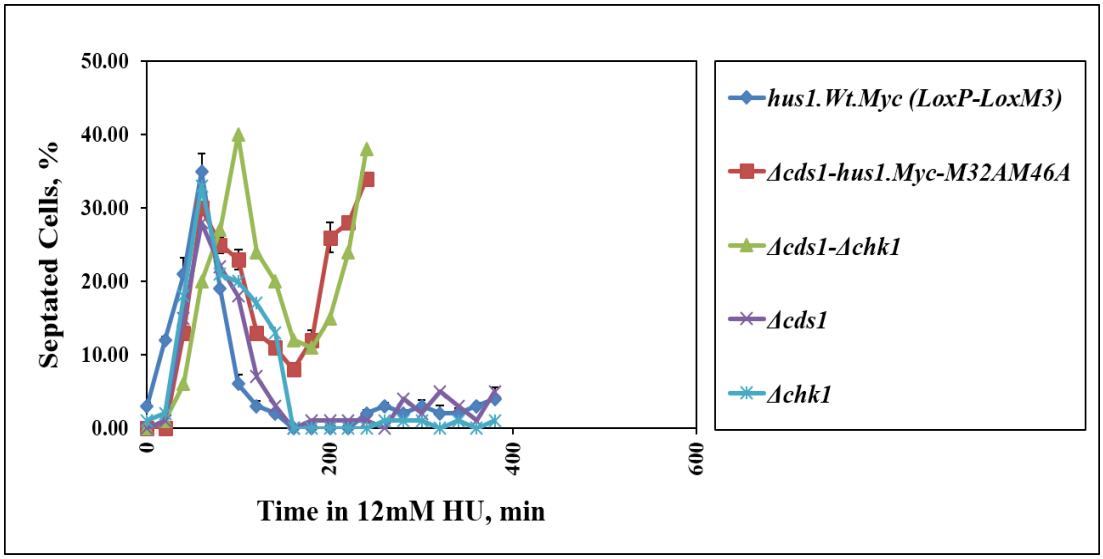

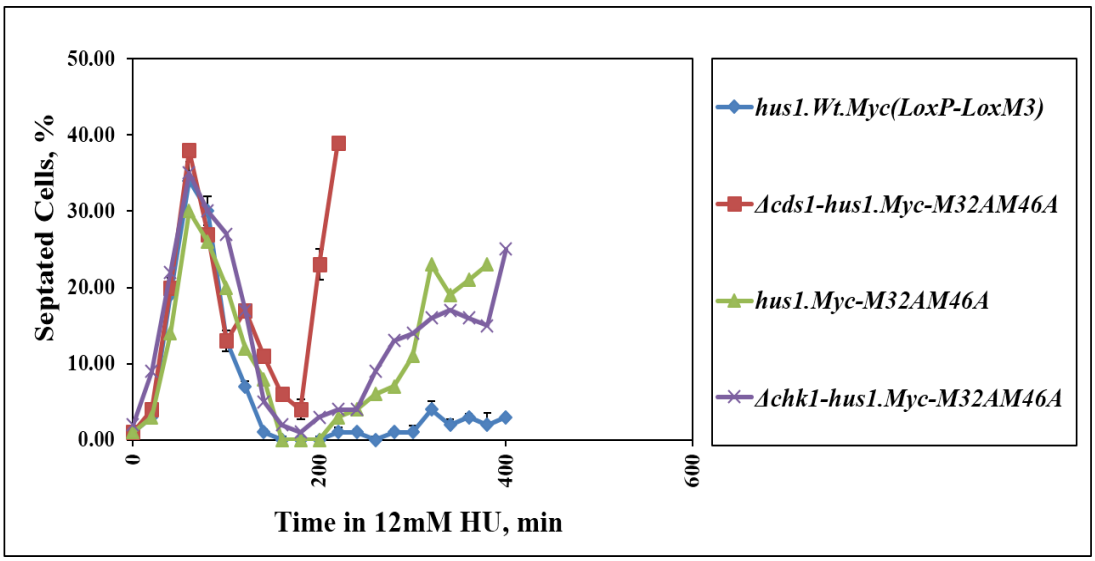

Figure 3-22: The Hus1 variants H32 and H46 activate Chk1 when forks collapse. A: Cells with the intact *hus1* gene *hus1.Wt.Myc (LoxP-LoxM3*), *Δcds1* and *Δchk1* delay in G2. Whereas, loss of both Cds1 and Chk1 or loss of Cds1 and both Hus1 variants (H32 and H46) renders cells completely checkpoint deficient. B: Since the *Δchk1-hus1.Myc-M32AM46A* and *hus1.Myc-M32AM46A* strains show a similar premature entry into the cell cycle, both variants act in the Chk1-dependent G2 arrest pathway. Error bars (standard deviation) were calculated from three independent experiments.

3.3 Discussion

The main findings reported in this chapter are: **(1)** the methionine codons AUG-32 and AUG-46 act as internal translation start sites in the Hus1 mRNA to produce two N-terminally truncated variants, which lack alpha-helical and beta-sheet sections from the middle part of the Hus1 protein. **(2)** Only loss of both variants renders cells slightly HU, CPT and MMS sensitive suggesting that they might act in two parallel pathways. **(3)** Only loss of both variants results in the premature entry into mitosis when cells arrest in G2 as a response to stalled replication forks, and **(4)** only loss of both variants interferes with the activation of the Chk1 checkpoint pathway when replication forks collapse in the absence of Cds1.

As reported recently for the Rad9 variant, Rad9-M50 (Janes, et.al. 2012), ribosomes can detect internal AUG codons in the *hus1* mRNA to initiate translation. However, in contrast to *rad9* where the internal AUG codon at position 50 has to be activated by heat stress, usage of the internal codons in *hus1* is independent of stress but restricted to replicating cells. The other striking difference between Rad9 and Hus1 is that the expression of the full-length Rad9 protein and its variant both stops when cells enter stationary phase (Janes, et.al. 2012), whereas this expression blockage applies only to the Hus1 variants but not to the full-length protein (Figure 3-11). Taken together, this indicates that the Rad9 and Hus1 variants act in dividing cells, whereas the full-length Hus1 protein has a yet unknown role in non-growing cells.

A role of the Hus1 variants H32 and H46 in dividing cells is consistent with their requirement for the activation of the Chk1 kinase arm of the DNA damage checkpoint when replication forks break in the absence of Cds1 kinase. Normally, Cds1 kinase protects HU-arrested forks from DNA damage, which makes Chk1 redundant (Lindsay, et.al. 1998). Chk1 kinase is however activated when forks are damaged either in the absence of Cds1 or under chronic HU exposure conditions. This may explain why the *hus1.Myc-M32AM46A* strain is only mildly sensitive to HU when cells are exposed for at least 4 hours (Figures 3-14 & 3-16). Interestingly, this double mutant is not very CPT sensitive (Figures 3-14 & 3-16) although camptothecin causes replication fork breakage (Pommier, et.al. 2010). This implies that the type of replication fork collapse is different under both conditions (i.e. when forks break in the absence of Cds1 or when forks break upon inhibition of topoisomerase 1).

Why only loss of both Hus1 variants renders cells sensitive and partly checkpoint deficient (Figure 3-21) is not yet known, but it indicates that both variants act in two redundant, parallel pathways, which activate Chk1 when forks experience damage in HU medium without Cds1 (Figure 3-22).

As reported previously, Cds1 is responsible for the protection of the replication fork (Lindsay, et.al. 1998), and Chk1 is only recruited to the broken forks at early G2 phase (Chen & Sanchez, 2004). That because it depends on the S phase specific modification of Rad9 within the 9-1-1 complex (Furuya, et.al. 2004), it is very likely that both variants act in this Chk1 activation pathway. This idea is consistent with the similar defect in Chk1 activation when the Rad9 subunit of the 9-1-1 ring cannot be modified during S phase (Furuya, et.al. 2004). This implies that Hus1 variants are acting in the 9-1-1 pathway, which is primed by the Rad3 and Tel1-dependent modifications of Rad9 at its C-terminal domain in S phase. Such a model would explain why the variants act genetically in the 9-1-1 pathway (Figure 3-19). One possibility is that they form probably two complexes as that seem to act in redundant pathways, which collaborate, with the 9-1-1 ring in the activation of Chk1 under these conditions. A second possibility, that the full-length Hus1 protein requires both variants to be assembled to the Rad9-Rad1-Hus1 complex (Figure 3-23). The third possibility is that the creation of alanine mutations at the ATG-32 and ATG-46 partiallyl modified the full-length Hus1 protein, which rendered cells partial deficiency in the cell cycle checkpoints. Although alanine residues are typically used to replace most amino acids in a process known as alanine scanning mutagenesis (Cunningham & Wells), however there is a possibility that the mutated amino acids have an impact on the full-length protein.

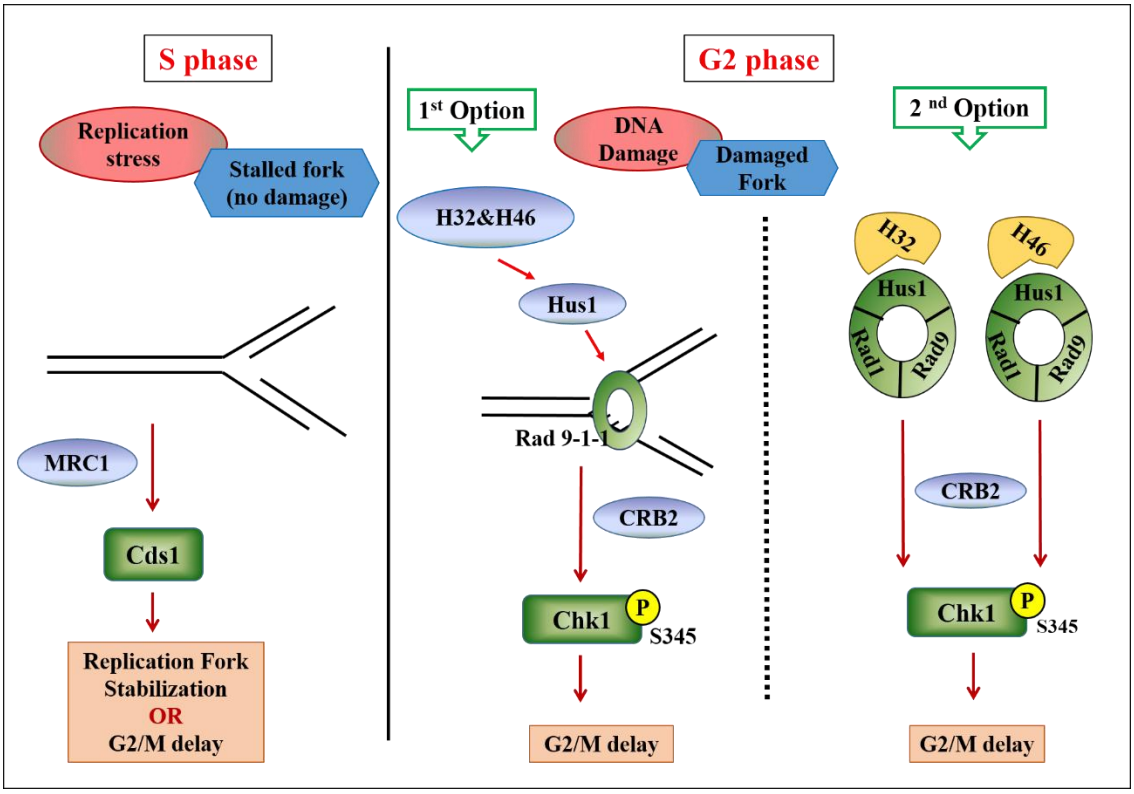

Figure 3-23: Model of how the Hus1 variants H32 and H46 activate the Chk1 pathway when forks collapse in the absence of Cds1. The diagram explains that H32 and H46 variants contribute to the assembly of one or more complexes, which may contain full-length Hus1, which collaborate with the 9-1-1 ring after its S phase priming by Rad3 and Tel1 to activate Chk1 kinase. Another possibility, that they are required for Hus1 assembly to the Rad9-Rad1-Hus1 complex. This is supposed to happen in G2 phase when the replication forks are collapsed upon HU treatment in the absence of Cds1 or under chronic exposure conditions.

Chapter 4: Investigation of *hHUS1* and *hHUS1B* expression at mRNA Level and *hHUS1* Down-Regulation

4.1 Introduction

Pre-mRNA in eukaryotes undergoes a process called alternative splicing in which one gene can produce more than one mRNA transcript. This process takes place in multi-exonic genes like *hHUS1*, which are composed of more than one exon interrupted by non-coding sequences called introns, and it is clear that this process is absent from intron-less genes like the *hHUS1B* gene. Alternative splicing can happened in different ways:

1. Exon skipping: in which one or more complete exons are omitted from the mature mRNA.
2. Alternative exon size: since some exons have more than one splice site at both ends, they could be spliced into mRNA with different sizes according to the splice site that is utilized.

   The first and second types of alternative splicing are most common in metazoans.
3. Intron retention: some eukaryotic genes retain an intron in the mature mRNA. This type is more common in yeast and plants (Elliott & Ladomery, 2011).

As a result, eukaryotic cells benefit from this mechanism by producing a wide diversity of proteins from a smaller number of genes.

hHUS1 (HUS1 checkpoint homolog (*S. pombe*)) and *hHUS1B* (HUS1 checkpoint homolog B (*S. pombe*) are located on different chromosomes in the human genome (chromosome 7 and 6 respectively) and represent an example of genes which contain introns (*hHUS1*) or the intron-less (*hHUS1B*). Therefore, all genome databases agree that *hHUS1B* has only one protein-coding transcript while they are discrepant regarding how many transcripts are produced from the *hHUS1*.

The National Center for Biotechnology Information database (NCBI) lists two transcripts, variant 1 and variant 2, which is a non-coding RNA for *hHUS1*. On the other hand, the Human-Transcriptome Database for Alternative Splicing (H-DBAS) curates

two alternative splice variants (RASV) for the *hHUS1* gene. The first one was found in fetal brain tissue (HIT000423256) and is referred to as the "Checkpoint protein HUS1 (hHUS1)". The second one is HIT000488741, which was found in the cortex of Alzheimer patients and it is nominated as "similar to Checkpoint protein HUS1 (hHUS1)". The database mentions a third transcript, which was found in a bladder carcinoma (Figure 4-1).These transcripts show some similarity to the four variants mentioned in the Ensembl Genome Browser (Figure 4-2).

Locus and transcript information

AS locus

Hyperlink management	Corresponding other species locus
HIX0006675	11-0000242 (mouse_flcdna)

RASV

Hyperlink management	HUGO OMIM	Cell type	Tissue type	Development stage	Sex Definition
HIT000423256	HUS1 603760		brain	fetal	Checkpoint protein HUS1 (hHUS1).
HIT000488741	HUS1 603760		alzheimer cortex		Similar to Checkpoint protein HUS1 (hHUS1).

Other ASV

Hyperlink management	HUGO OMIM	Cell type	Tissue type	Development stage	Sex Definition
HIT000032986	HUS1 603760		Bladder, carcinoma		Checkpoint protein HUS1 (hHUS1).

H-DBAS - Human-transcriptome DataBase for Alternative Splicing
(http://h-invitational.jp/h-dbas/index.jsp)
H-InvDB_8.3 released on March 26, 2013.

Figure 4-1: *hHUS1* transcripts according to the H-DBAS database. This table is derived from the H-DBAS website, which shows the *hHUS1* locus and its transcript information. (RASV: Representative Alternative Splice Variant). (H-DBAS accessed January 2014).

The Ensembl database revealed nine transcripts related to the *hHUS1* gene. One of them is a non-protein coding transcript, which retained an intron, four are nonsense-mediated decay and four are protein coding as shown in Figure 4-2. The four protein coding isoforms represent my focus in this study.

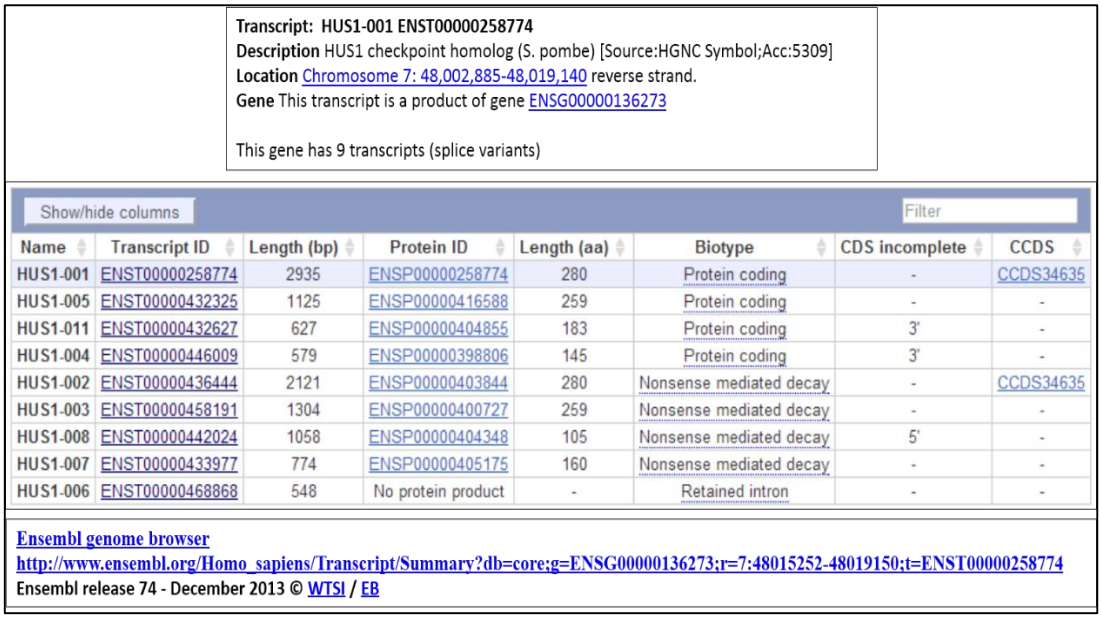

Transcript: HUS1-001 ENST00000258774
Description HUS1 checkpoint homolog (S. pombe) [Source:HGNC Symbol;Acc:5309]
Location Chromosome 7: 48,002,885-48,019,140 reverse strand.
Gene This transcript is a product of gene ENSG00000136273

This gene has 9 transcripts (splice variants)

Show/hide columns | Filter

Name	Transcript ID	Length (bp)	Protein ID	Length (aa)	Biotype	CDS incomplete	CCDS
HUS1-001	ENST00000258774	2935	ENSP00000258774	280	Protein coding	-	CCDS34635
HUS1-005	ENST00000432325	1125	ENSP00000416588	259	Protein coding	-	-
HUS1-011	ENST00000432627	627	ENSP00000404855	183	Protein coding	3'	-
HUS1-004	ENST00000446009	579	ENSP00000398806	145	Protein coding	3'	-
HUS1-002	ENST00000436444	2121	ENSP00000403844	280	Nonsense mediated decay	-	CCDS34635
HUS1-003	ENST00000458191	1304	ENSP00000400727	259	Nonsense mediated decay	-	-
HUS1-008	ENST00000442024	1058	ENSP00000404348	105	Nonsense mediated decay	5'	-
HUS1-007	ENST00000433977	774	ENSP00000405175	160	Nonsense mediated decay	-	-
HUS1-006	ENST00000468868	548	No protein product	-	Retained intron	-	-

Ensembl genome browser
http://www.ensembl.org/Homo_sapiens/Transcript/Summary?db=core;g=ENSG00000136273;r=7:48015252-48019150;t=ENST00000258774
Ensembl release 74 - December 2013 © WTSI / EB

Figure 4-2: *hHUS1* transcripts in the Ensembl database. The table is adapted from Ensembl Genome Browser. It shows the *hHUS1* variants information, the transcript IDs and their length in base pairs, in addition to their proteins details. (Ensembl genome browser, accessed January 2014).

The full-length *hHUS1-001* transcript differs from the other three protein coding mRNAs (*hHUS1-005*, *hHUS1-011* and *hHUS1-004*) in a few important points as shown in Figure 4-2. Firstly, it represents the full-length transcript with all eight exons coding for the hHUS1 protein of 280aa, which is part of the Rad9-Rad1-Hus1 DNA damage checkpoint ring (Dean, et. al. 1998). Secondly, the cDNA contains an unusually long 3' untranslated region (UTR) of 2068bp, which contains several potential open reading frames. This region will be later referred as the hHUS1-001-tail. The first N-terminal 21 amino acids encoded by exon 1 are missing from the other three transcript sequences. The *hHUS1-011* (5 coding exons) and *hHUS1-004* (4 coding exons) transcripts encode proteins, which lacking 76 and 114aa respectively from the C terminal end in addition to the N-terminal 21 amino acids (Figure 4-3).

Although it is shown in the Ensembl genome browser that *hHUS1-001* is the only transcript which has a Consensus Coding Sequence (CCDS) (Figure 4-2), I decided to investigate whether the other *hHUS1* transcripts exist at mRNA level (in current chapter) and at protein level (in the forthcoming chapter 5). To analyze their existence at mRNA level, the total RNA of two human cell lines (HeLa: cervical cancer cells and HEK293:

non-cancer embryonic cells), and five human tissues (heart, fetal brain, kidney, fetal liver and uterus), were reverse transcripted to their corresponding cDNAs. Their cDNAs were used as a template in the RT-PCR amplification tests using specific primers for each transcript.

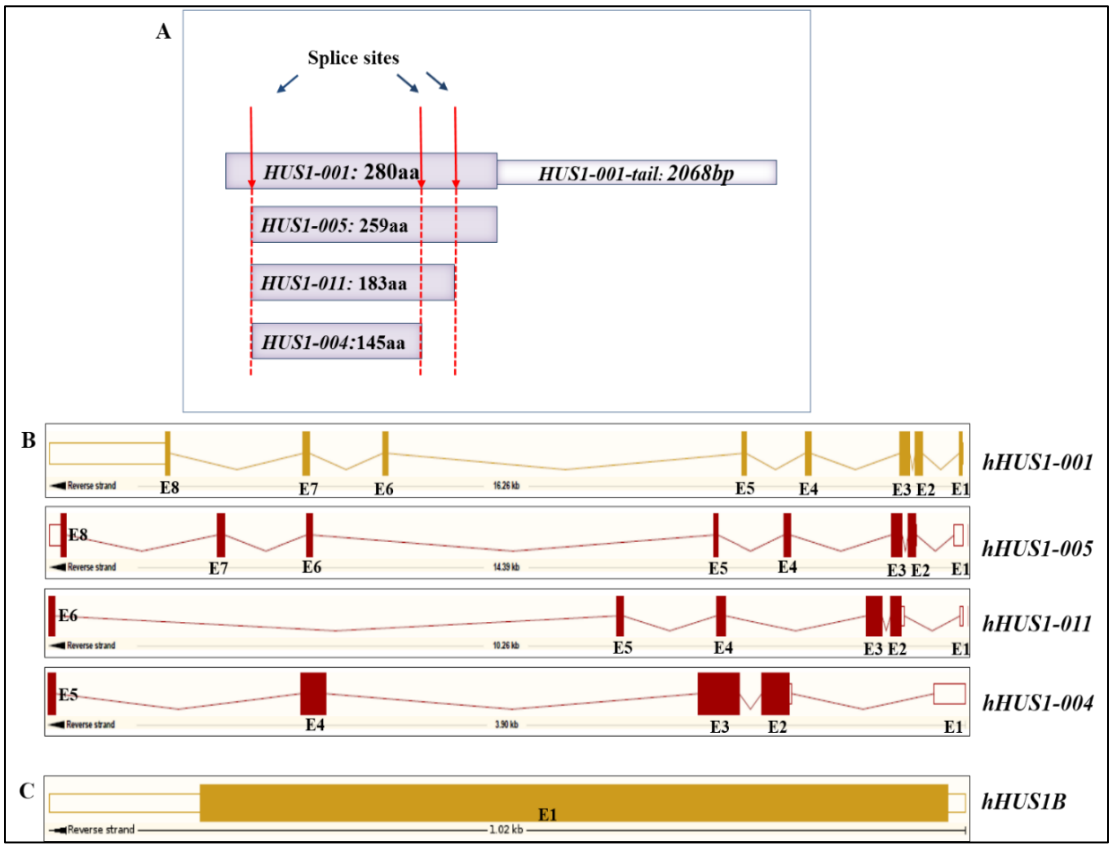

Figure 4-3*: hHUS1* and its alternative splice variants *and hHUS1B.* A: The protein coding regions of full- length *hHUS1* and its alternative splice variants. Their alternative splice sites are indicated. The hHUS1-001 full-length cDNA contains an unusual long 3`-non-translated region (UTR). **B:** The total number of exons in each transcript. The empty boxes related to non-coding exons while the filled boxes are the protein coding exons. The lines that link the exons represent the introns. **C:** The *hHUS1B* gene has only one exon. (Obtained from Ensembl genome browser; accessed January 2014).

As mentioned previously, *hHUS1B* is an intron-less gene and it is reported as well in the Human Intronless Gene Database (IGD), therefore it has one transcript only. This gene was identified for the first time by Hang, et.al. (2002). It encodes for 278aa protein and it is expressed in many of human tissues similar to *hHUS1* gene. Since the mentioned study is the only one about *hHUS1B*, it has excited my curiosity to find out more about this gene.

4.2 Results:

4.2.1 *hHUS1* transcripts and *hHus1B* exist on mRNA level of used cell lines and tissues

Two sets of primers were designed to amplify the *hHUS1* and *hHUS1B* transcripts. The first set was used to amplify a short fragment of each transcript to confirm their existence at mRNA level, while the other set of primers was used to amplify the corresponding full-length sequence to be used later in the construction of the stable cell lines (chapter 6).

To amplify a short fragment of each transcript of the *hHUS1*, I designed a specific forward primer, while the same reverse primer was used with the exception of *hHus1-001-tail* and *hHUS1B*, which had their specific sets of primers. Figure 4-4 shows the priming sites of all *hHUS1* splice variants, in addition to *hHUS1B* primers. For more details, please refer to Appendix (2), which explains the *hHUS1* and *hHUS1B* primers locations within their corresponding cDNAs sequences that obtained from Ensembl database.

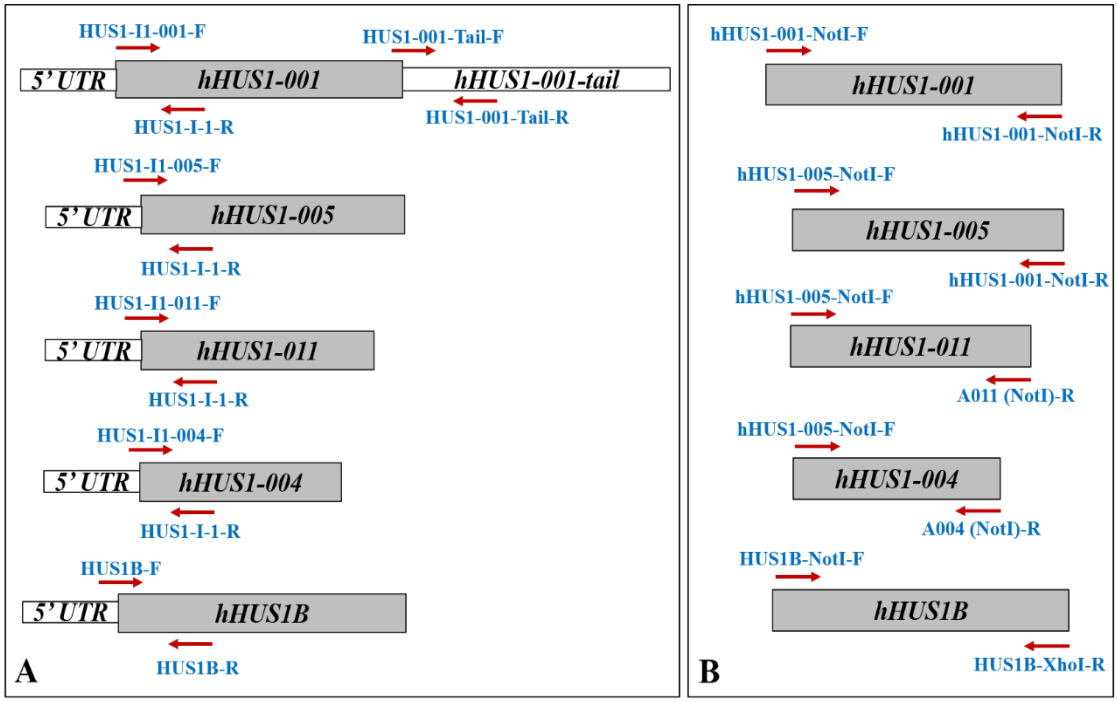

Figure 4-4: Illustrative diagram of the priming sites of *hHUS1* transcripts and *hHUS1B* amplifying primers. Two set of primers were designed to amplify *hHUS1* transcripts and *hHUS1B* from their corresponding cDNAs. **A:** Primers set that used to amplify a short fragment of each transcript of the *hHUS1* and *hHUS1B* to prove their existence on mRNA level. **B:** Primers set that used to amplify full-length fragments of the mentioned genes to be used later for stable cell lines construction (chapter 6).

The results of the RT-PCR experiments proved the existence of all *hHUS1* transcripts as well as of *hHUS1B* at the mRNA level (short and full lengths) in all cell lines and tested tissues with the B-Actin gene as a control (Figure 4-5). In order to confirm the identity of the amplified short PCR products all fragments obtained from fetal brain tissue were cloned onto the plasmid pCR4-TOPO using the TOPO TA Cloning Kit (Invitrogen) and sent for DNA sequencing. All cloned variants were identical to their corresponding sequences from the Ensembl genome database, thus confirming the existence of the variants at RNA level. All primers amplify across an exon-intron boundary thereby preventing the contamination from genomic DNA. The only example is the *hHUS1B* gene since this gene has no introns. All full-length PCR products obtained from fetal brain tissue were cloned onto the integration plasmid pcDNA^{TM} 5/FRT/TO to construct stable cell lines, which will be discussed in detail later in chapter 6. Their DNA sequences were also correct. Only the cloned *hHUS1-011* variant had a 19 amino acid in frame

deletion when compared to the curated Ensemble sequence (Figure 6-10). Whether this deletion is a brain-specific splice variation is currently not clear.

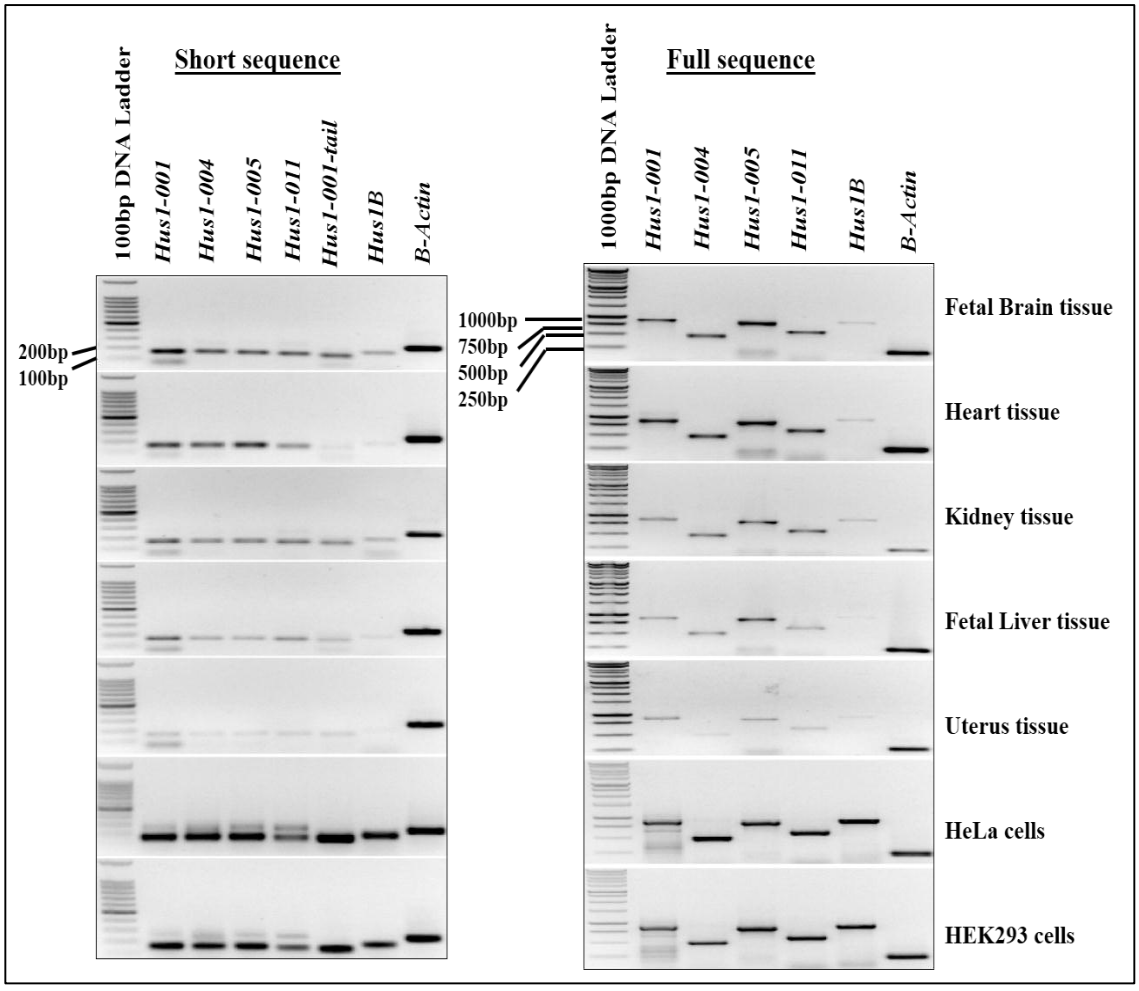

Figure 4-5: The RT-PCR results of amplified short and full-length fragments of *hHUS1B, hHUS1* and its shorter isoforms. The RT-PCR was performed using cDNA produced from each human tissue and indicated cell lines. The cDNA was produced from total RNA obtained from the cell lines or purchased for the different human tissues (Human Total RNA Master Panel II, Clontech Laboratories, cat. 636643) using Tetro cDNA synthesis kit (BIOLINE). **A & B:** The genes exsistence was investigated either as short or full-length sequences using the general PCR protocol and B-Actin primers as a positive control. **C:** PCR products were run on 1% agarose gel and images were taken by the Bio-Rad gel documentation system. RT-PCR results were positive for all *hHUS1* transcripts, the *hHUS1-001-tail* and *hHUS1B* in all tested cell lines and tissues. The sequence identity was confirmed for all fragments amplified from fetal fetal brain tissue.

4.2.2 Confirmation of *hHUS1-001, hHUS1-005* and *hHUS1-011* existence in human cells using primers that are more specific

Given the high sequence identity between the *hHUS1* variants at DNA level (Appendix 2), I designed more forward primers for *hHUS1-005* and *hHUS1-011* (Figure 4-6) as both variants showed the largest degree of dissimilarity. The same was not possible for *hHUS1-001 and hHUS1-004* because the previous forward primers utilised the only unique DNA sequences across the splice site. The new forward primers were used in parallel with the previous reverse primer, which was used to amplify the short fragment of each isoform (Figure 4-4). Neither the *hHUS1-004* nor the *hHUS1-011* cDNAs have a 3'UTR according to the Ensembl database (Figure 4-2 & Appendix3). Since *hHUS1-001 and hHUS1-005* share an identical 3`-UTR with the only difference that the 3`-UTR of *hHUS1-001* is significantly longer (Figure 4-6), I designed an alternative reverse primer, which is specific for the longer, unique section of the 3'-UTR of *hHUS1-001*. This one was used in parallel with the previous forward primer of the isoform (Figure 4-4). See Figure (4-6) and the cDNA sequence alignment for the new primers locations, the PCR primers combination and product size (Appendix 3).

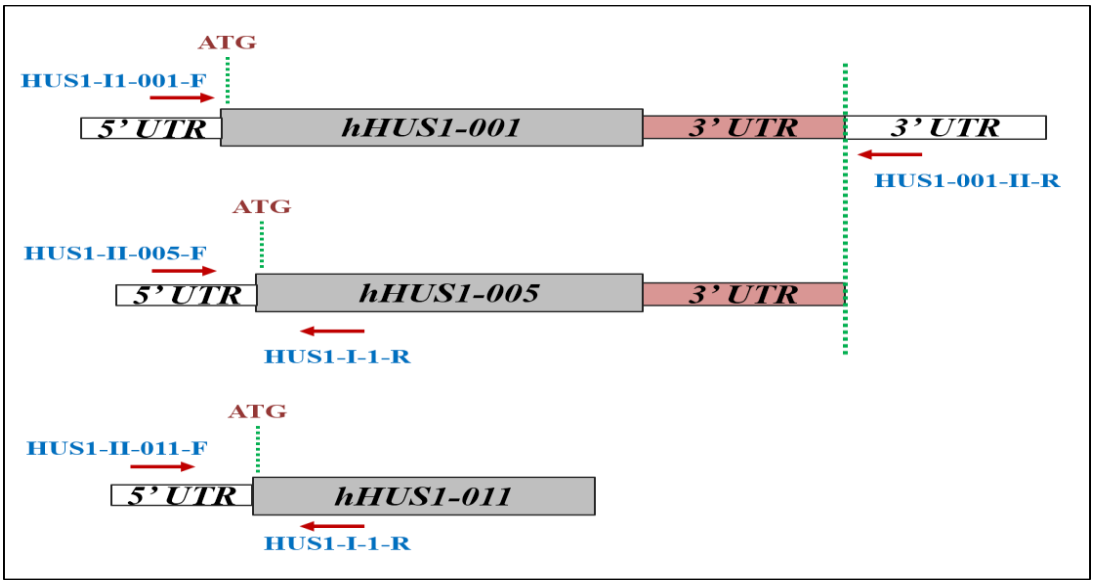

Figure 4-6: Priming sites of the more specific primers of *hHUS1-001, hHUS1-005* and *hHUS1-011*. New forward primers were designed to confirm the existence of *hHUS1-005* and *hHUS1-011*, which were used in parallel with the previous reverse primer as shown in figure (4-4). As *hHUS1-001*and *hHUS1-005* have some similarities of the 3'UTR sequence (shown in pink colour), a specific reverse primer was designed downstream of this region to amplify *hHUS1-001*.

Using the new primer combination for *hHUS1-001*, I obtained the expected RT-PCR fragment of 1018bp from all tested tissues. This confirms the existence of the *hHUS1-001* transcript including the long 3`-UTR (Figure 4- 7). The sequence identity of this band was confirmed. In the case of the shorter variants *hHUS1-005* and *hHUS1-011*, the new primer combination amplified more than one band. All fragments obtained from the fetal brain tissue were cloned onto the plasmid pCR4-TOPO. The ~170bp bands of *hHUS1-005* and of *hHUS1-011* had both the correct sequence. The upper *hHUS1-011* band was identical in its N-terminal sequence but was longer due to an unspecific prime event. The two top bands of *hHUS1-005* showed unrelated sequences. These results are consistent with the previous conclusion that all tested human tissues express the shorter *hHUS1* variants 005 and 011 at mRNA level (Figure 4-7).

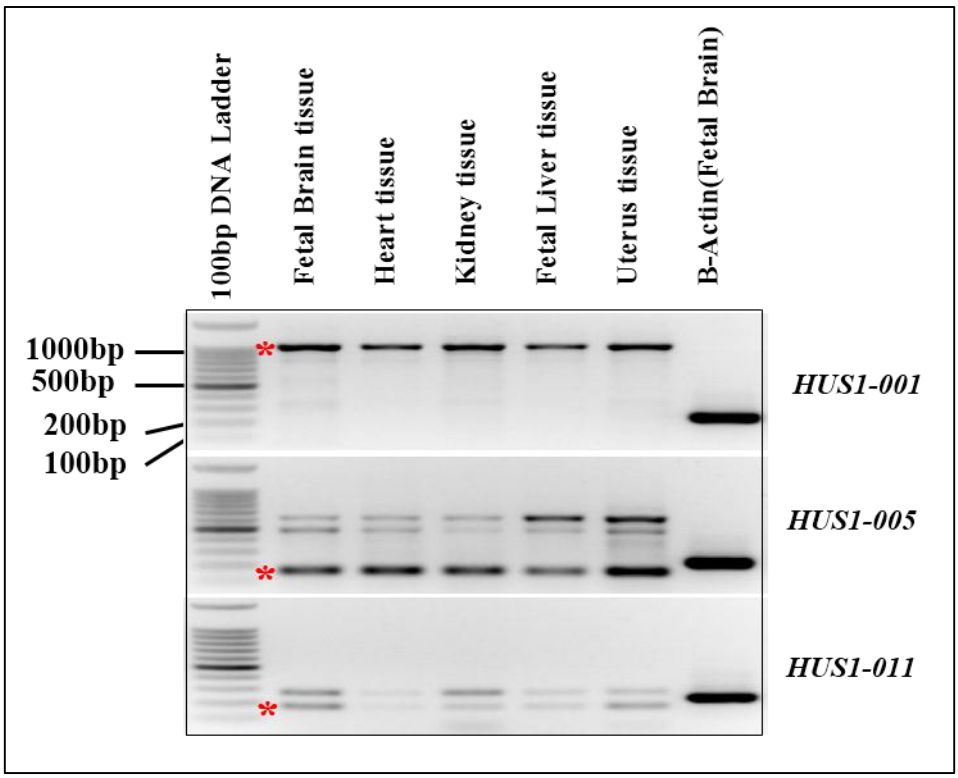

Figure 4-7: RT-PCR results for *hHUS1-001, hHUS1-005* and *hHUS1-011* using the new primers combination. * indicates the bands of the correct size and sequence. Both bands of *hHUS1-011* are identical in their N-terminal sequence but the upper band was longer due to an unspecific primer site. The top two bands of *hHUS1-005* showed unrelated sequences.

4.2.3 Investigation of a possible N-terminal variant of *hHus1-005*

The careful analysis of the 5`-UTR of the *hHUS1-005* and *004* cDNAs revealed the existence of a very short potential open reading frame in both cDNAs (Figure 4-8). Both ORFs could encode short proteins of 39 aa and 35 aa respectively. Interestingly, all three cDNAs contain an ATG close to their 5`-UTR region, but in the case of *hHUS1-005* and *004*, an in-frame stop codon just before the active ATG, which would terminate translation from the up-stream start sites. This stop codon is absent in the full-length *hHUS1-001* cDNA due to a splice event.

```
hHUS1-001      ----------GCCGCGGCTGCGCCATCCGCGGCCATGAAGTTTCGGGCCAAGATCGTGGA    50
hHUS1-005      ACAGAGGCCCGCCGCGGCTGCGCCATCCGCGGCCATGAAGTTTCGGGCCAAGATCGTGGA    60
hHUS1-004      ACAGAGGCCCGCCGCGGCTGCGCCATCCGCGGCCATGAAGTTTCGGGCCAAGATCGTGGA    60
                          **************************************************

                                  Splice site
hHUS1-001      CGGGGCCTGTCTGAACCAC----------------------------------------    69
hHUS1-005      CGGGGCCTGTCTGAACCACTTCACACGTGAGCAGGGAGGCCGGAGAGGAGCGAGGGAGGA    120
hHUS1-004      CGGGGCCTGTCTGAACCACTTCACACGTGAGCAGGGAGGCCGGAGAGGAGCGAGGGAGGA    120
               ******************
hHUS1-001      -----------------TTCACACGAATCAGTAACATGATAGCCAAGCTTGCCAAAACCT    112
hHUS1-005      ACGGAAGGAAGCAGTGAGCGCGCGGAATCAGTAACATGATAGCCAAGCTTGCCAAAACCT    180
hHUS1-004      ACGGAAGGAA-----------GCAGAATCAGTAACATGATAGCCAAGCTTGCCAAAACCT    169
                                   . **********************************
hHUS1-001      GCACCCTCCGCATCAGCCCTGATAAGCTTAACTTCATCCTTTGTGACAAGCTGGCTAATG    172
hHUS1-005      GCACCCTCCGCATCAGCCCTGATAAGCTTAACTTCATCCTTTGTGACAAGCTGGCTAATG    240
hHUS1-004      GCACCCTCCGCATCAGCCCTGATAAGCTTAACTTCATCCTTTGTGACAAGCTGGCTAATG    229
               ************************************************************
```

ATG active ATG **ATG inactive ATG** **TAA stop codon**

Splice site splice site, which is found in *hHUS1-001* but not in the others.

ATGAAGTTTCGGGCCAAGATCGT represents the location of Hus1-005-Short-NotI-F primer

GAATCAGTAACATG represents the location of Hus1-005-Short-XhoI-R primer

Figure 4-8: Alignment of the 5`-UTR of *hHUS1-001, 005* and *004* as curated in the Ensembl database. The first active translational start site (ATG) is shown in green. Interestingly, both cDNAs of the shorter variants have the ATG used in the full-length cDNA HUS1-001 as the first ATG codon (shown in yellow). Translation from these ATG codons would however be terminated by two in frame stop codons (TAA, shown in red) located just upstream of the active ATG. Due to a splice event, this stop codon is not present in the full-length cDNA 001 (blue). (The alignement was produced by Clustal Omega: (http://www.ebi.ac.uk/Tools/msa/clustalo/).

To test whether such short mRNAs exist in human tissues, I tried to amplify the very short, N-terminal cDNA of *hHUS1-005* using a specific set of primers (Hus1-005-Short-NotI-F & Hus1-005-Short-XhoI (Figure 4-9, 4-10). The resulting RT-PCR products (Figure 4-10) were cloned into the plasmid pCR4-TOPO to confirm their identity by DNA sequencing. Only fetal brain and HEK293 samples showed an RT-PCR band with the expected size and correct DNA sequence, while the other tissues and HeLa cells did not reveal this band (Figure 4-10). This strongly implies that the very short *hHUS1-005* polypeptide is expressed in brain tissue and HEK293 cells. The predicted polypeptide sequence is MKFRAKIVDGACLNHFTREQGGRRGAREERKEAVSARNQ* (Program: transeq, Version: 6.6.0). X

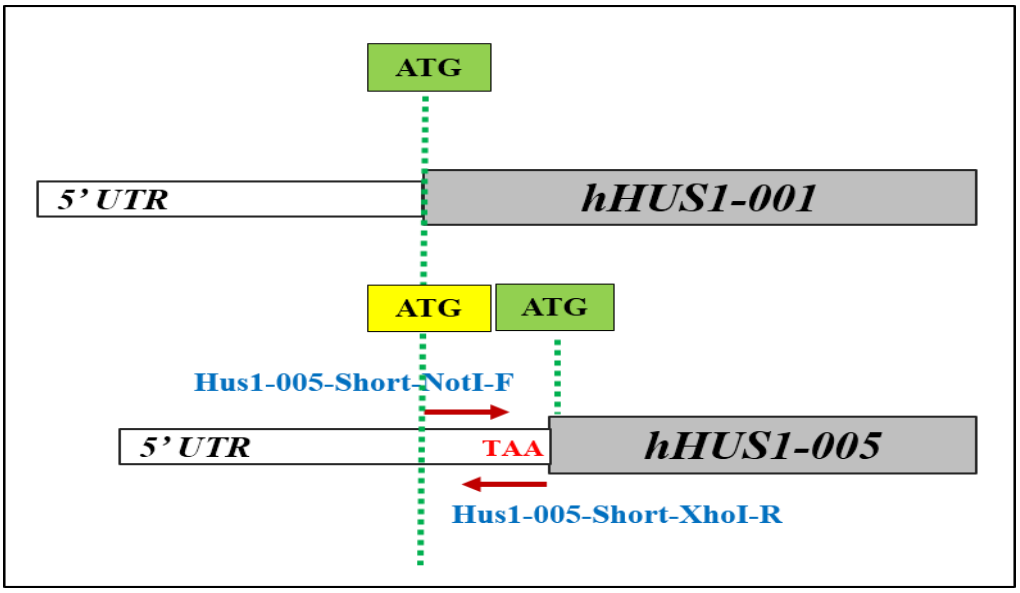

Figure 4-9: Illustrative diagram of the primers locations, which used to amplify the N-terminal very short hHUS1-005 transcript. The predicted N-terminal short variant of *hHUS1-005* ORF starts at the ATG (yellow) and terminated by the stope codon TAA (red) which is missed from the hHUS1-001 sequence due to a splice event. (Please refer to Figure 4-8 and Appendix (4) for the primers sequences and PCR product size).

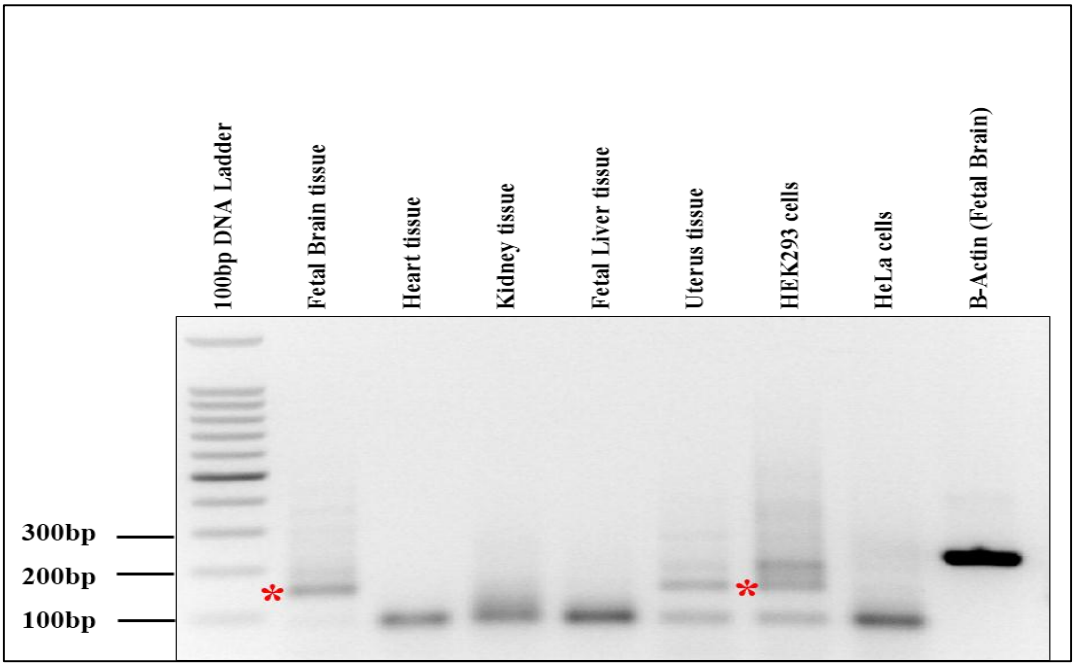

Figure 4-10: RT-PCR results of the very short N-terminal *hHUS1-005* version amplified from the indicated human tissues and cell lines. *represents the bands with the correct sequence. The other bands had unrelated sequences. Short length *B-Actin* gene was used as a positive control.

Taken together, these findings imply the existence of all *hHUS1* variants as well as *hHUS1B* at their mRNA level in the tested human tissues and cell lines.

4.2.4 *hHUS1* cell localization

Although much is known about the Rad9 subunit of the RAD9-RAD1-HUS1 complex (Parrilla-Castellar, et.al. 2004; Ishikawa, et.al 2006; Lieberman, 2006), the biology of the remaining two subunits is much less well researched. It was reported that the 9-1-1 ring shuttles between the nucleus and cytoplasm. . In the response to DNA damage Rad9 forms discrete foci in the nucleus (Cai, et.al, 2000; Hopkins, et.al. 2003; Madabushi, et.al. 2010).

I investigated the localisation of hHUS1 by protein fractionation and immune-localization. For protein fractionation, untreated HEK293 cells were lysed and the resulting extract was treated with different buffers to separate the cytoplasmic from the nuclear components. To stain hHUS1 in the cells (immune-localization), HEK293 cells

were grown on glass cover slips coated with poly-D-Lysine and then fixed by 4% paraformaldehyde (PFA).

The protein fractions were tested by Western blot with a polyclonal and a monoclonal anti-Hus1 antibody as well as antibodies, which recognise the cytoplasmic marker GAPDH (glyceralaldehydephosphate-dehydrogenase) or the nuclear marker histone H3, in addition to B- actin antibody.

The polyclonal anti-hHUS1 antibody recognized one main band with three smaller fainter bands. Whereas the monoclonal antibody recognized only one band, (Figure 4-11, B). Whether these smaller bands are the N-terminally truncated hHUS1 isoforms is not yet clear. That since the monoclonal antibody, which did not recognise them, binds to one epitope that is present in all hHUS1 variants (personal communication with Abcam customer service, while the polyclonal antibody recognition sites were undeclared for commercial reasons), and recognises therefore all four engineered hHUS1 variants when fused to EGFP (Figure 6-13). According to the protein fractionation results, the hHUS1 protein resides mainly in the cytoplasm or it is released from the DNA during the fractionation process, and to a lesser extent in the nucleus. The marker antibodies confirmed the identity of the two different protein fractions (Figure 4-11, B).

The Immune-localization results were consistent with the fractionation data as the strongest hHUS1 staining was in the cytoplasm (blue) and to a much lesser extent in the nucleus (pink). The control cells were stained for beta-Actin to validate the immune-staining protocol (Figure 4-11, A).

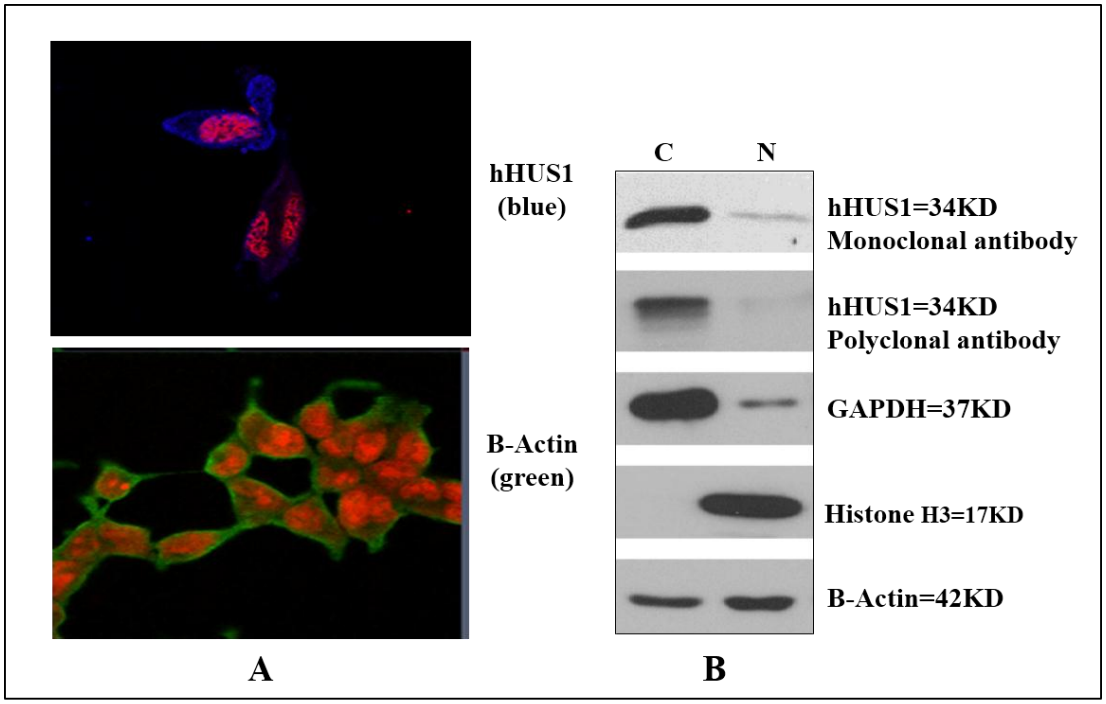

Figure 4-11: hHUS1 cell localization. A: Untreated HEK293 cells were stained either for hHUS1 using the monoclonal anti-hHUS1 antibody with Alexa fluro-633 (Blue) as the secondary antibody, or for beta-Actin using an anti-beta-Actin antibody with Alexa flouro-488 (Green) as secondary antibody. Chromatin and the more compact nucleoli were stained with Propedium Iodide (Red), which changes to a pink colour when it overlaps with the blue HUS1 signal. The images show that hHUS1 resides mainly in the cytoplasm, and to a lesser extent, in the nucleus. **B:** Western blot confirmed the cell localisation results. The polyclonal anti-hHUS1 antibody recognized one main band with three smaller fainter bands, whereas the monoclonal antibody recognized only one band.

4.2.5 hHUS1 down-regulation

The down-regulation experiment was conducted to check whether the used anti-HUS1 antibodies identify the hHUS1 specific bands. Moreover, that would help to study the activities of recombinant HUS1 fusion proteins in the engineered cell lines (Details in chapter6).

Two different down-regulation systems were used to reduce the endogenous levels of hHUS1. Both are DNA based systems. The first system is based on the psiRNA-h7SKGFPzeo Kit (InvivoGen), while the second system based on the HuSH shRNA Plasmids (29-MER) from Origene.

4.2.5.1 The psiRNA-h7SKGFPzeo system

The psiRNA-h7SKGFPzeo Kit (InvivoGen) (Figure 4-12) is based on the transfection of psiRNA plasmids, which carry small synthetic oligonucleotides that encode for the precursor of the small interfering RNAs (siRNA). To this end, long primers are annealed and cloned into the BbsI digested plasmid (Figure 4-12, B). The long primers encode two complementary 21nt long arms separated by an 8nt loop sequence. Both arms align to a stem loop structure, which is recognised by the Dicer-Drosha nuclease system in cells as a siRNA precursor. The two complementary sequences of 21 nucleotides are homologous to a sequence in the target gene of interest. After transfection, the DNA primer insert will be transcribed into a short double strand RNA (dsRNA) with a hairpin structure, which will be cleaved by the Dicer-Drosha system (Brummelkamp, et.al 2002). To achieve the down-regulation of hHUS1 using this system, two sequences of 17 nucleotides were chosen from the ORF and UTR region of *hHUS1* gene, as well as two scrambled sequences, which were used as a negative control (Figure 4-13). The complementary oligonucleotides were designed to be compatible with BbsI/BbsI restriction site of the psiRNA plasmid with the help of the siRNA Wizard software (www.sirnawizard.com). After cloning of the annealed oligonucleotides into the plasmid, it was transfected into HeLa cells using the LyoVec transfection reagent. hHUS1 down-regulation was assessed at protein level in two steps. First, I considered the transfection as transient transfection and protein samples were extracted in a time course manner at 24, 48 and 72 hours post-transfection. Secondly, transfected cells were maintained under the Zeocin selection for several days. Few days later, positive green florescent and Zeocin resistant clones were isolated as stable cell lines supposedly expressing the *hHUS1* siRNA. Protein samples were extracted following the whole cell extract protocol and loaded onto a 10% SDS-PAGE to be analysed by western blot.

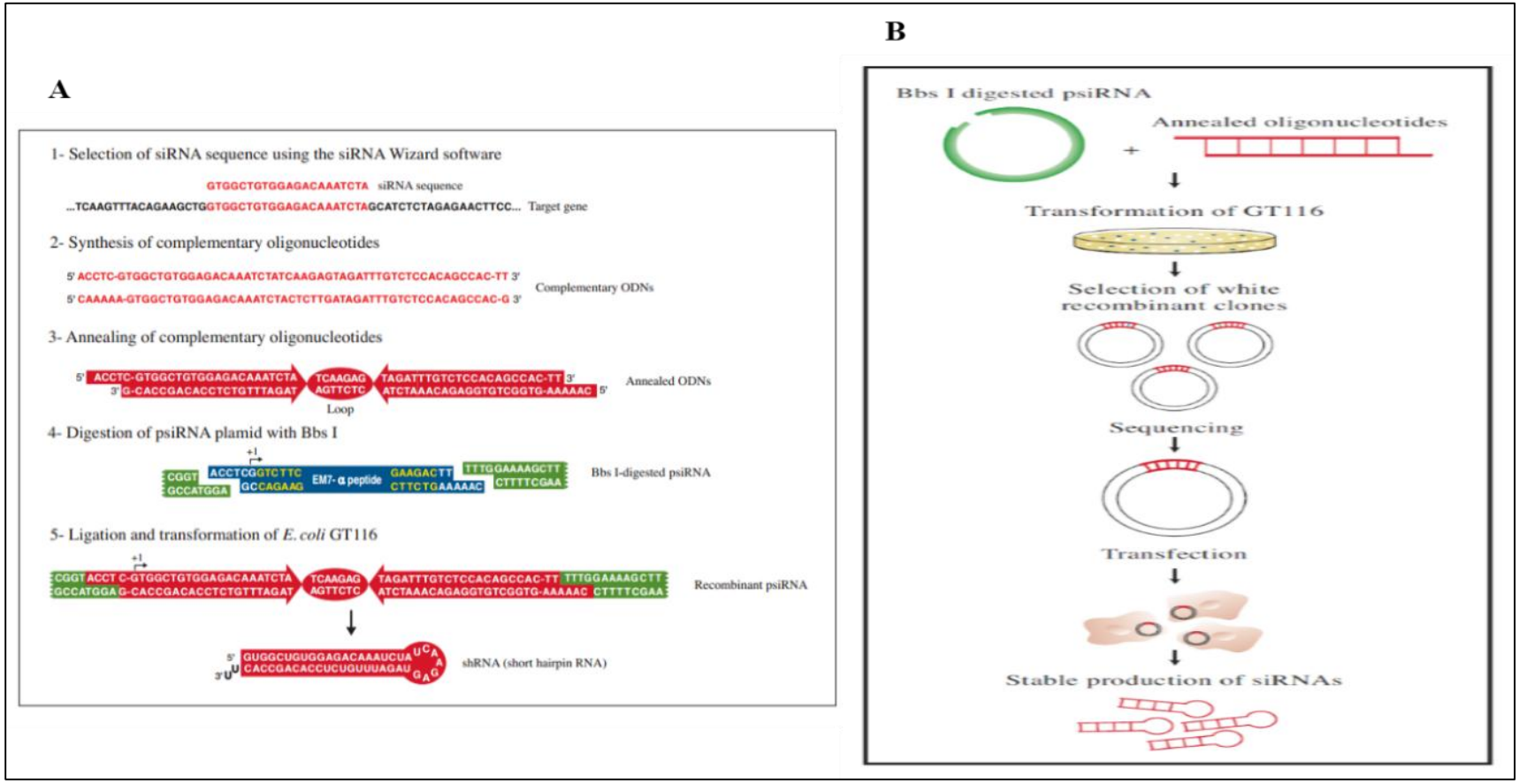

Figure 4-12: Schematic diagrams elucidating the psiRNA-h7SKGFPzeo down-regulation system. A: Cloning steps: **1.** Selection of the siRNA oligonucleotides **2.** Synthesis of the complementary oligonucleotides **3.** Annealing of the complementary oligonucleotides after heat treatment. **4.** Ligation of the sticky ends with the BbsI cut plasmid psiRNA-h7SKGFPzeo. **5.** Ligation and transformation into *E.coli* GT116, which tolerates plasmids with hairpin structures. **B:** Flow chart of the steps leading to the transfection of human cells (Obtained from psiRNA-h7SKGFPzeo kit manual, http://www.invivogen.com/PDF/psiRNA4-7SKGFPzeo_TDS.pdf)

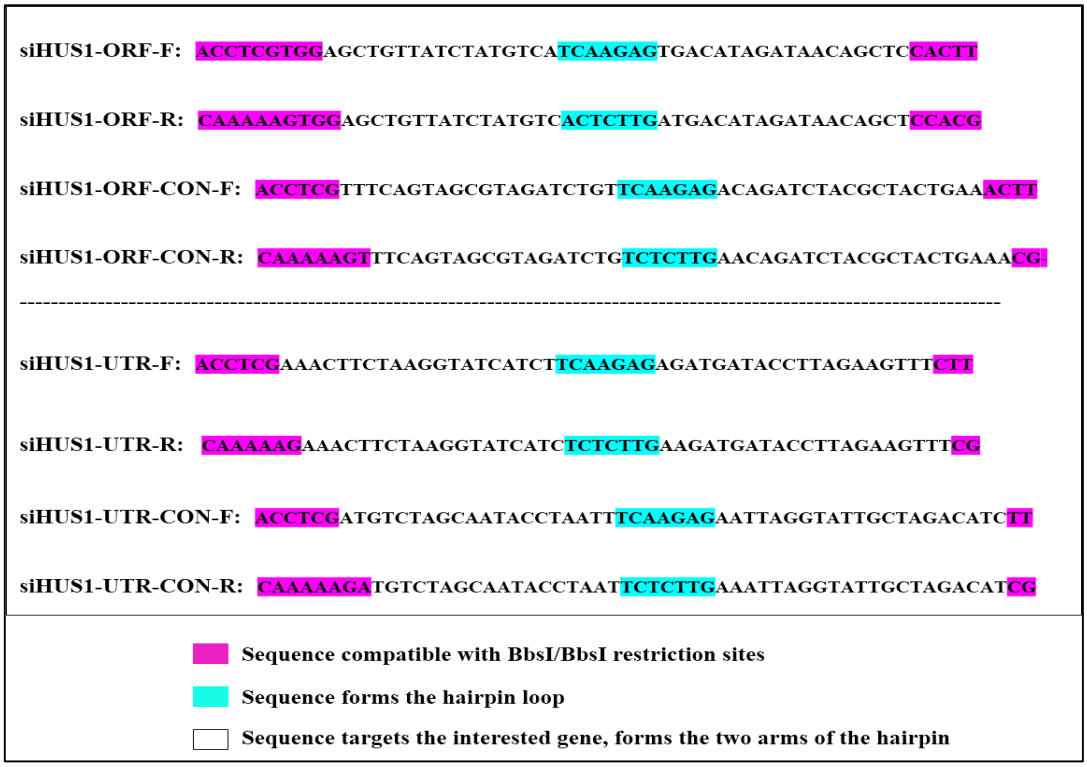

Figure 4-13: Oligonucleotides sequence to target the ORF and UTR segments of the *hHUS1* transcript. The figure shows the siRNA sequence, which target the ORF and UTR regions in the *hHUS1* gene. Purple sequences represent the sequence, which are compatible with the BbsI/BbsI restriction site in the cloning plasmid. Light blue sequences represent the sequence, which will form the hairpin loop. Unlabelled sequences represent the siRNA sequence, which target the hHUS1 transcript.

As shown in Figure 4-14, the system was not successful in the down-regulation of the hHUS1 protein independently of whether cells were transiently transfected or after a Zeocin selection for around two weeks. The cells were green and the presence of the transfection marker GFP was present. Thus confirming that the cells contained the down-regulation plasmid. hHUS1 was detected with the monoclonal antibody.

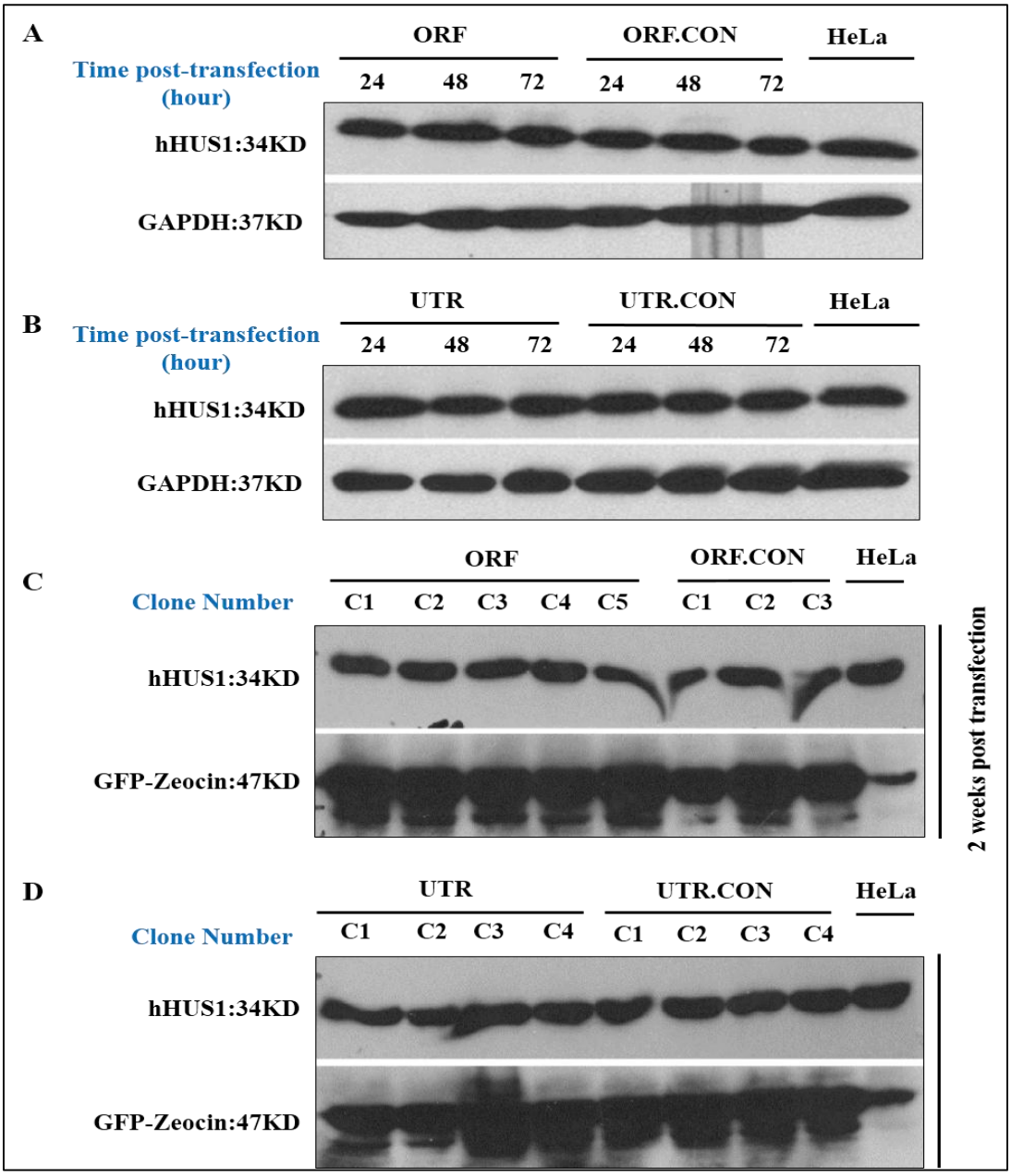

Figure 4-14: Down-regulation of hHUS1 using the psiRNA-h7SKGFPzeo Kit (InvivoGen). **A & B:** HeLa cells were transiently transfected with the psiRNA-h7SKGFPzeo plasmids carrying the oligonucleotides targeting the hHUS1 open reading frame (ORF) or 3`-UTR (UTR). The ORF.CON and UTR.CON sequences were scrambled and should not down-regulate hHUS1. No down-regulation of the hHUS1 protein was noticed at the indicated times after transfection. **C & D:** Stable HeLa cell lines. Transfected cells were selected with the Zeocin antibiotic for two weeks. Unfortunately, there was no down-regulation even after the Zeocin selection. (GAPDH = Glycerolaldehyde-Dehydrogenase, loading control, GFP-Zeocin = GFP-Zeocin Resistance protein fusion was detected with the anti-GFP antibody).

4.2.5.2 The HuSH shRNA Plasmid (29-MER) system (OriGene)

This system is similar to the previous one as both are DNA based. It works by transfection of the pRFP-C-RS plasmid into human cells, which offers both transient and stable shRNA down-regulation. The plasmid carries the shRNA expression cassette, which is formed by 29 nucleotides that are designed to disrupt expression of the gene of interest, followed by a seven nucleotide long loop and the reverse complementary sequence of the 29 nucleotides. Expression of the shRNA precursor is controlled by the U6 RNA promoter and terminated by an oligo-TTTTTT sequence, which terminates the transcription by RNA Pol III. Four oligonucleotide sequences were designed by the company (OriGene) against the *hHUS1* gene, and used in parallel with a negative control sequence. The company already cloned all oligonucleotides onto pRFP-C-RS Vector.

Single plasmid transfection in parallel with transfection of a mixture of all 4 plasmids and transfection of the negative control was achieved using Lipofectamine® 2000 Transfection Reagent (Invitrogen™) in HEK293 cells. Protein samples were taken at two time points 72 hours and 10 days post-transfection. Transfected cells were red due to expression of the red fluorescence protein from the plasmid and puromycin resistant. Cell maintenances and selection of stable cell lines was performed according to the manufacturer's instructions.

This system was more successful than the previous one as the protein levels of hHUS1 were clearly down regulated when all four plasmids were transfected simultaneously (Figure 4-15). Interestingly, the down-regulation was only transient since the hHUS1 protein levels recovered when cells were kept for 10 days in culture although the cells were still puromycin resistant and expressed the red fluorescence protein. Moderate down-regulation was observed for plasmid B and to a lesser extent for plasmid C. This indicates that the efficient inhibition of the translation of the *hHUS1* mRNA requires more than one shRNA and that cells may induce a rescue pathway to overcome the reduction in hHUS1 protein levels since the protein plays an important role in the DNA Damage response machinery. Importantly, this experiment validates the monoclonal anti-Hus1 antibody, which has been used throughout this study.

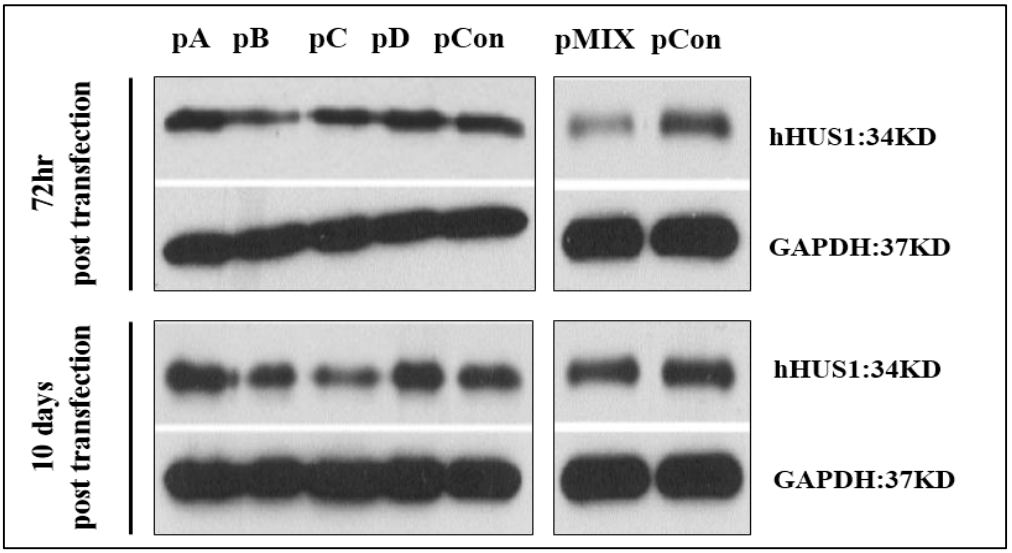

Figure 4-15: Down-regulation of hHUS1 by the HuSH shRNA system. HEK293 cells were transfected with the four indicated plasmids (A-D) separately. Each plasmid contains a different shRNA expression cassette. Cells were also transfected with a mixture of all four plasmids simultaneously (pMIX) or with a control plasmid (pCON). Protein extracts were prepared 72 hours and 10 days post-transfection. Western blot results showed a moderate down-regulation in the cells transfected with plasmids B and to a lesser extent with plasmid C. the most efficient down-regulation was achieved when all four plasmids were transfected simultaneously and when protein samples were prepared 72 hours post-transfection. The down-regulation effect was only transient as the hHUS1 protein levels recovered 10 days post-transfection.

4.3 Discussion

The key findings of this chapter are: **(1)** that all four *hHUS1* variants and *hHUS1B* are expressed at the mRNA level in HEK293 embryonic kidney cells, HeLa cervical cancer cells and different selected human fetal and adult tissues (Figure 4-5). **(2)** The N-terminal region of the mRNA of the *hHUS1* variants *005* and *004* may encode a mini open reading frame in addition to the longer N-terminally truncated ORF (Figures 4-8, 4-9 & 4-10). This N-terminal short ORF is absent from the full-length *hHUS1-001* mRNA, since alternative splicing removed the in-frame stop codon. **(3)** Down-regulation of hHUS1 requires more than one shRNA and is only transient and not complete. This indicates that human cells need hHUS1 for survival. Since the transfected shRNA cells are still positive for the down-regulation markers, but fail to show low levels of hHUS1 after prolonged growth periods, cells may neutralise the anti-HUS1 shRNA molecules; and **(4)** hHUS1 resides mainly in the cytoplasm in untreated HEK293 cells (Figure 4-11).

All four *hHUS1* variants and *hHUS1B* are expressed at mRNA level in an array of human tissues and cell lines. Although all tissues and cell lines were positive and the amounts of the template and primers were fixed, the expression levels varied between the cells ones, which showed higher expression levels, compared to the human tissues. This was especially true for hHUS1B, which was only expressed at low levels in some human tissues (fetal liver and uterus) (Figure 4-5). Our results are consistent with the data of Hang, et al. (2002) since they reported that hHUS1 and hHUS1B have variations in their expression in different human tissues and cell lines (Spleen, thymus, prostate, testis (highly expression), uterus (very low expression), small intestine, colon and leukocytes). Moreover, it was found that the hHUS1 protein is expressed in epithelial ovarian tumours and in human colorectal carcinoma in a correlation with the apoptotic biomarkers such as p53 and BAX (de la Torre, et.al, 2008), and the human circadian clock protein PER2 (Storcelova, et.al. 2013) respectively.

More recently, large number of human short open reading frames (sORF) that encoded polypeptides have been discovered (Ma, et.al. 2014), some of which, have already an identified role in cellular signalling pathways (Slavoff, et.al, 2014). The very short N-terminal *hHUS1-005* mRNA, which originates from a short ORF located just up-stream of the main ORF (Figure 4-8, 4-9) was only expressed in fetal brain tissue and

embryonic kidney cells HEK293 cells (Figure 4-10). That may indicates that this very short hHUS1 related peptide plays a role in the early developmental stages. The expression of this variant in fetal brain tissue is consistent to some extent with the data in the H-DBAS data base where it is mentioned that one of the hHUS1 alternative splice variants, HIT000488741, was found in the cortex of Alzheimer patients (Figure 4-1).

Down-regulation of hHUS1 was reported previously using antisense oligonucleotides in human H1299 non-small lung carcinoma cells (Kinzel, et.al. 2002) but the efficiency was only tested at RNA level using quantitative PCR technique. The down regulation efficiency varied between 30%-80%. Why only the combination of more than one shRNA yielded the strongest down-regulation of hHUS1 (Figure 4-15) is not yet clear. However, the observation that the down-regulation is transient although the transfected cells maintain the puromycin and red fluorescence marker suggests that cells need certain levels of hHUS1 for survival since the plasmids provide a continuous source of shRNAs over a prolonged time (Brummelkamp, 2002; psiRNA-h7SKGFPzeo kit manual; HUSH shRNA Plasmids (29-MER) Application Guide). This idea is supported by the importance of HUS1 protein for the cellular response to DNA damaging agents (Kinzel, et.al. 2002; Meyerkord, et.al. 2008) and its important role in maintaining the intra-S phase DNA damage checkpoint in murine cells (Weiss, et.al. 2003).

Researchers were negotiated about hHUS1 cell localization. Cai and his colleagues (2000) found hHUS1 protein co-localized with HDAC1 in the H1299 cells nuclei. In addition to Hopkins, et.al (2003) study, where they showed that hRAD9B protein is a nucleoprotein and it can interact with hRAD9, hRAD1, hHUS1 and hHUS1B. It was reported by Madabushi, et.al. (2010) and Gene Cards website (http://www.genecards.org/cgi-bin/carddisp.pl?gene=HUS1), (accessed on January 2014) that hHUS1protein is found in the cytoplasm and/or nucleus. All of these facts confirm our finding about hHUS1 localization in the cytoplasm mainly and to some extent in the nucleus.

Chapter 5: Investigation of the Expression Levels of the hHUS1 Protein in Human Cell Lines

5.1 Introduction

My previous findings confirmed the expression of *hHUS1-001*, *hHUS1-005*, *hHUS1-011*, *hHUS1-004* and *hHUS1B* at mRNA level (Figure 4-9). In this chapter, I summarize my work to find out under which conditions the *hHUS1* splice variants are expressed in normal human cell lines. As reported for other proteins, alternative splicing could be induced by cells at different cell cycle phases or as a response to the exposure to DNA damaging agents or environmental stress (Chandler, et.al., 2006; Filippov, et.al, 2007; Shkreta, et.al., 2011; Janes, et.al., 2012). In some cases, splice variants are specifically induced when cells become senescent at the end of their life span (Blanco, et.al. 2008). Taken together, I speculated that the variants could be restricted to a specific cell cycle phase, to senescent cells or expressed as a response to DNA damage. Since the cell cycle phases and DNA damaging checkpoints were detailed in the first chapter, I will review here the principles used to synchronize cells, induce premature senescent or inflict DNA damage.

Cell synchronization techniques provide a unique way to collect a cell population in a specific cell cycle phase or at the transition border between two stages. This allows studying the molecular and structural phenomena throughout cell cycle progression, the regulation of gene expression and possible protein post-transcriptional modifications. This can be achieved by different procedures varying between physical fractionation using centrifugal elutriation or cell sorting by Flow Cytometry, and chemical treatments (Banflavi, 2011), which I applied to my experiments.

Chemical blockade methods use a range of drugs, which block cell cycle progression like nocodazol, which arrests cells in mitosis. Other techniques interfere with cells biological events like the G1/S transition, or target the genes, which are responsible for cell cycle progression to block cells at a defined cell cycle phase or at one transition

point. Nutrition deprivation blocks cells in G1 phase as serum starvation, the nucleoside analogue Thymidine arrests cells at the G1-S border as it blocks DNA synthesis. A similar early S phase arrest can be achieved by Hydroxyurea (HU), which blocks the enzyme ribonucleotide reductase responsible for the synthesis of dNTPs, or Aphidicolin (APH), which interferes with DNA polymerase-alpha. Drugs like Nocodazole and Colchicine arrest cells in mitosis as they interfere with the mitotic spindle. (Fox, 2004; Harper, 2005; Banflavi, 2011; Ma & Poon, 2011).

Another type of cell cycle arrest, which I used to search for the hHUS1 variants, is the "senescence". However, not all cell cycle arrests are classified as senescence. There is a big difference between quiescent and senescent cells. Quiescent cells are arrested in G0-G1 due to nutrition deprivation (i.e. serum starvation). These cells have normal size and cellular activities but low metabolic processes. On the other hand, senescent cells are permanently arrested in the G1 phase, which means that they cannot re-proliferate while serum starved cells can re-enter the cell cycle. They are characterized by defined phenotypes such as enlarged and flat cell morphology and β-galactosidase expression. Moreover, they highly express cell cycle inhibitor proteins such as p16INK4B, p21 WAF1/CIP1 and p53 (Blagosklonny, 2011; Kuliman, et.al. 2013). There are two types of senescence, replicative and premature cell arrest.

Replicative senescence, known also as the Hayflick's limit occurs due to telomeric DNA shortening during cells proliferation (Ju, et.al, 2006; Zdanov, et.al. 2006). Telomeres are the specialized nucleoprotein structures at the end of each chromosome of eukaryotic cells, which are synthesized by the RNA-dependent DNA polymerase, Telomerase. They protect chromosomes and replicate late in S phase (Morgan, 2007). Since the length of the telomeres is reduced with each round of S phase, cycling cells without expression of telomerase suffer from continuous telomere shortening. Once telomeres have reached their minimal length, the DNA damage checkpoints are activated, which is characterized by gamma-H2AX foci in addition to the accumulation of DNA damage response proteins such as 53BP1, NBS1 and MDC1 at the end of the chromosomes. The resulting checkpoint signal will lead to Chk1 and Chk2 kinase activation and phosphorylation of their downstream targets CDC25 and p53. This will arrest cells in G1 and induce apoptosis or senescence (D'Adda di Fagagna, et.al. 2003; D'Adda di Fagagna, 2008).

Premature senescence can be triggered by oxidative stress (Burova, et.al. 2013), DNA damaging agents (ionizing radiation) or overexpression of oncogenes apart from telomeres shortening. Oxidative stress can be triggered as a treatment with sub-lethal doses of hydrogen peroxide (H_2O_2), ethanol or UVB radiation. Premature senescent cells have the same morphology and phenotypes as replicative senescent cells (Zdanov, et.al. 2006, D'Adda di Fagagna, 2008).

Both replicative and premature senescence activate the DNA damage response through the ATM pathway. As the replicative senescence results from telomere erosion, premature senescence can be initiated by DNA double strand breaks (DSBs) during the DNA replication process (Rufini, et.al, 2013). On the other hand, oxidative stress, which produces Reactive Oxygen Species (ROS), causes different types of DNA damage as clarified in Figure 5-1. Especially the accumulation of single-stranded (ssDNA) breaks because of incomplete base excision repair can lead to DSBs (Lieber & Karanjawala, 2004). Thereafter, p53 is activated by ATM-mediated phosphorylation, which in turn triggers cell cycle arrest in G1 phase through p21 WAF1/ CIP1 or block of mitosis through the E2F7 pathways (Figure 5-2) (Rufini, et.al, 2013).

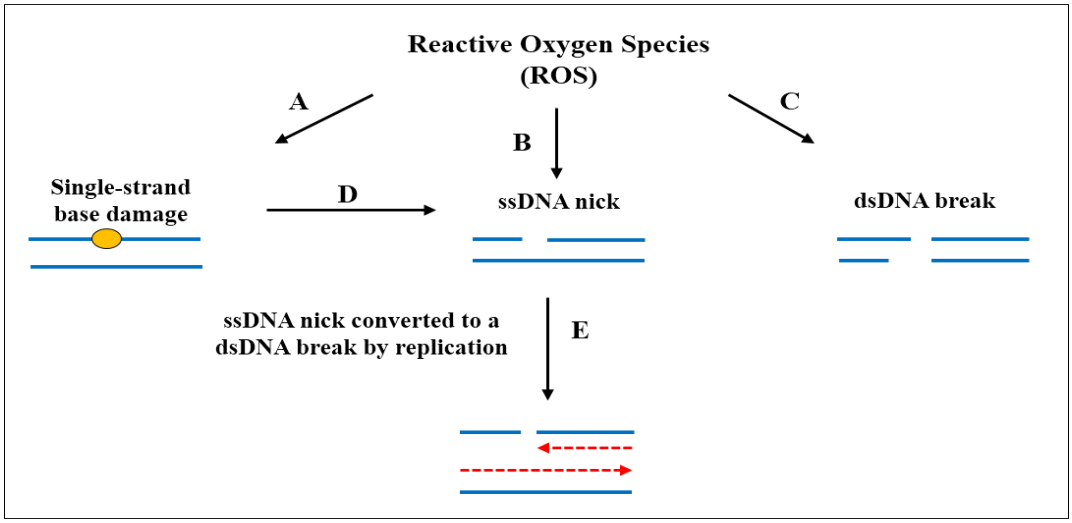

Figure 5-1: DNA damage types caused by Reactive Oxygen Species (ROS). A, B, &C: ROS modify nucleotides, which are recognized by the base excision repair pathway. If this pathway is overloaded single-stranded breaks (ssDNA), which are a repair intermediate, accumulate **(D).** Especially during DNA replication ssDNA nicks can be converted to DNA double-strand breaks (dsDNA breaks) **(E).** In some cases, ROS can cause dsDNA directly **(C).** (Adapted from Lieber & Karanjawala, 2004).

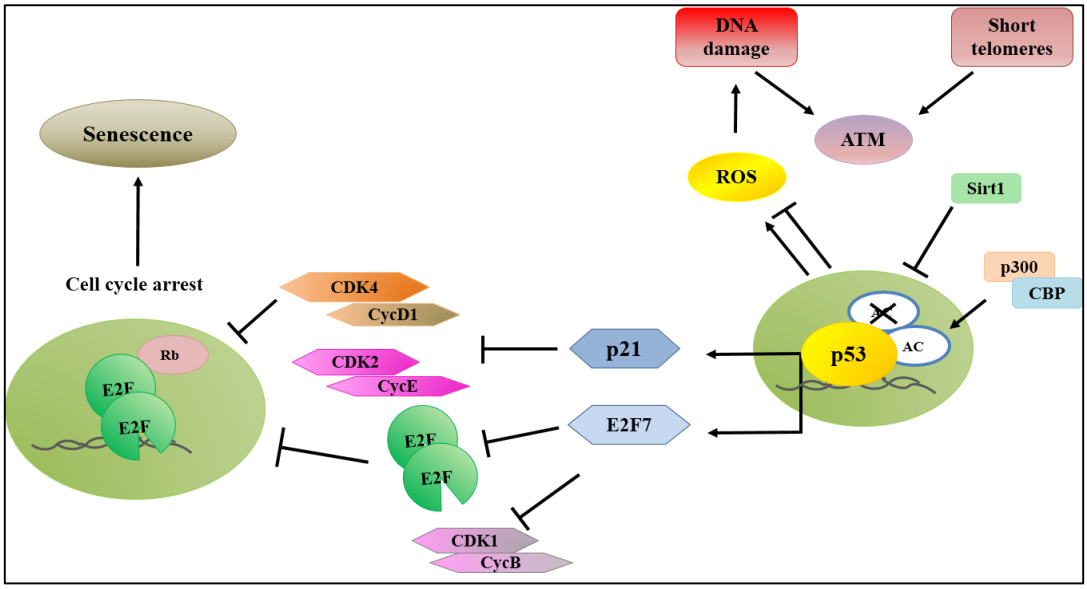

Figure 5-2: Senescence regulation by p53. p53 is activated through ATM-mediated phosphorylation as a result of DNA damages or short telomeres. p53 activates a G1 or M phase arrest through p21 or E2F7 phosphorylation respectively. That will end with cells in senescence. p53 has a positive and negative effects on ROS, which are still unclear. p53 controls several pathways related to cell aging, which are not shown in this diagram (Modified from Rufini, et.al, 2013).

Over-expression of oncogenic proteins and ionizing radiation can initiate a G1 cell cycle arrest through a p53-independent pathway. This occurs when these stimuli activate the p38 Mitogen-Activated Protein Kinase (MAPK) pathway after the production of reactive oxygen species. p38 kinase leads to the activation of the tumor suppressor protein p16/INK4A, which inhibits CyclinD-CDK4/6 kinase activity. As a result, the Retinoblastoma protein (Rb) remains attached to the transcription factor E2F thereby preventing S phase progression, which eventually leads to entry into senescence (Figure 5-3) (Chen & Goligorsky, 2006; Karnoub & Weinberg, 2008).

Taken together, p21 WAF1/CIP1 & p16INK4A are the main initiators of senescence through two separate pathways. However, it seems that p21 WAF1/CIP1 is responsible to maintain the cell cycle arrest only for a short period. Thereafter, its expression decreases to a level, which is slightly higher than in normal non-senescent cells. Then, the responsibility in maintaining the cell cycle arrest lies with p16INK4A (Huschtscha & Reddel, 1999; Chen & Goligorsky, 2006; C´mielova´ & Rezacova´, 2011; Burova, et.al. 2013).

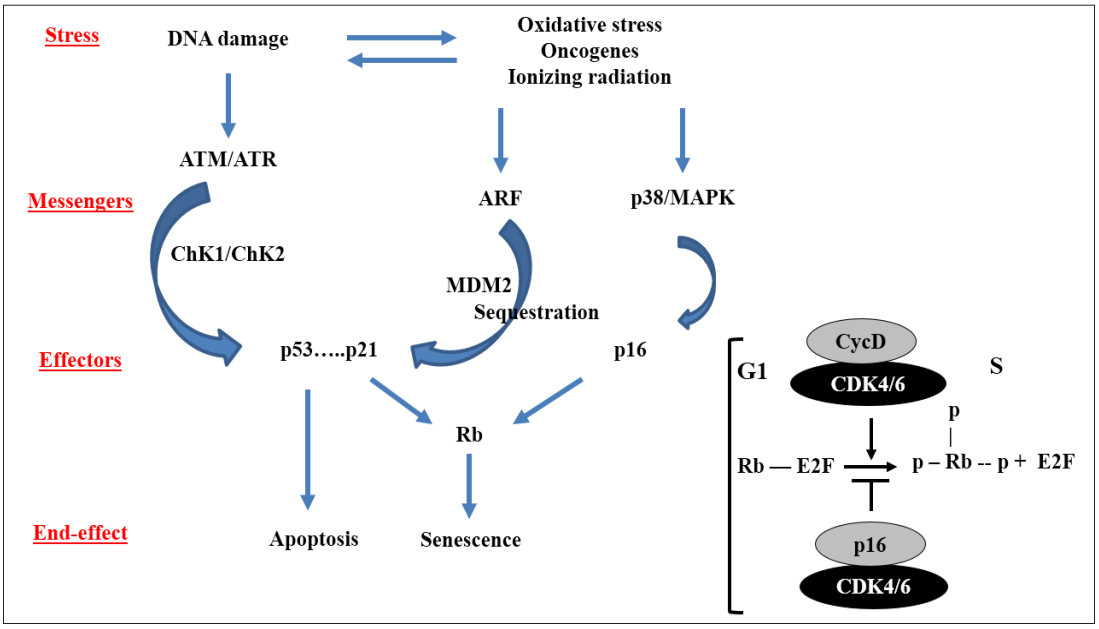

Figure 5-3: Pathways regulating apoptosis and cell senescence. Senescence is initiated by two independent regulatory pathways, p53-p21 and p16-pRb (retinoblasoma). The p53-p21 pathway is triggered by DNA damage such as telomere shortening. p53 is activated through its ATM-mediated phosphorylation, which leads to p21 up-regulation. Oxidative stress, oncogenic proteins and ionizing radiation trigger the p38-p16-pRb pathway. Up-regulation of ARF adds another signal to the p53-p21 pathway by the inhibition of MDM2, the inhibitor of p53 activity. The other branch of the p38-p16-pRb pathway is induced by p16 activation by the MAP kinase p38. Active p16 maintains the hypo-phosphorylated (active) form of pRb by blocking Cyclin D-CDK4/6 kinase activity, which inhibits RB thereby preventing the E2F transcription activity. This leads to a G1 cell cycle arrest and senescence. (Modified from the references: Huschtscha & Reddel, 1999; Chen & Goligorsky, 2006).

The last condition, which I would like to investigate the *hHUS1* variants are different types of DNA damaging agents. I used agents inducing either DNA single, double strand breaks or replication stress, which are represented by oxidative stress (H_2O_2), DNA synthesis inhibition (Aphidicoline), replication fork stabilization (HU and Camptothecin), DNA methylation (MMS), DNA pyrimidine dimers (UV) and DNA degradation (Phleomycin). DNA damage types and cells response were detailed in Chapter 1.

5.2 Results:

5.2.1 Expression of the hHUS1 splice variants is not cell cycle specific

In order to study the protein expression of the hHUS1 splice variants throughout the cell cycle, I used HeLa cells as a model system since they are used widely in biomedical research, especially in cell cycle studies (Ma & Poon, 2011). Moreover, I found them to be synchronized successfully using serum starvation, 2x thymidine block and nocodazole treatment rather than HEK293 cells, which did not synchronize by our serum starvation protocol.

Cell synchronization was achieved successfully at three time points throughout the cell cycle. At the G0-G1, G1-S and G2-M transition points using serum starvation, 2x thymidine block and nocodazole treatment respectively. The DNA content at each time point was measured with propidium iodide using flow cytometry. The protein expression levels were elucidated by Western Blot (Figures 5-4 & 5-5). Protocols are detailed in the Materials and Methods chapter.

Flow Cytometry histograms showed the successful cell synchronization after serum starvation as most cells had a G1 DNA content, which was shifted to the left compared with asynchronous control cells (Figure 5-4, A). This shift could be caused by the loss of S phase cells, which have a DNA content between G1 and G2, upon serum starvation. This result was consistent with the confirmative cell cycle protein markers. Starved HeLa cells accumulated at the G1 phase at 0 time point as indicated by the presence of the G1 cyclin, cyclin D1, and the low nuclear concentration of the S phase cyclin E1 (Figure 5-4, B). Consistent with the re-entry of the cells into the cell cycle, the nuclear levels of cyclin E1 increased 6 hours post-release. While the cytoplasmic levels of Cdc25 phosphatase remained constant, the rate of phosphorylation of histone H3 at serine 10 strongly increased in G1 arrested cells and upon release of the cells (Figure 5-4, B). This was unexpected as this modification is a marker for the G2-M transition and linked with chromosome condensation (Van Hooster, et. al., 1998). Since the DNA content of the arrested cells was inconsistent with mitosis, this histone modification may also be triggered by serum starvation. This may be a novel observation as no related finding has yet been reported. Neither the expression pattern nor the fractionation of hHUS1 changed under these conditions.

To test whether hHUS1 expression changes in S phase or mitosis, HeLa cells were arrested early in S phase by a double-thymidine block and in mitosis by nocodazol (Figure 5-5). Although flow cytometry confirmed the accumulation of cells in S phase and mitosis (Figure 5-5, A), the levels and cellular distribution of hHUS1 remained unaffected and no shorter variants were detectable with the monoclonal antibody. As reported previously (Van Hooster, et. al., 1998), serine-10 phosphorylated histone H3 accumulated in mitotic cells, which showed also the hyper-modification and chromatin association of Cdc25C (Figure 5-5, C).

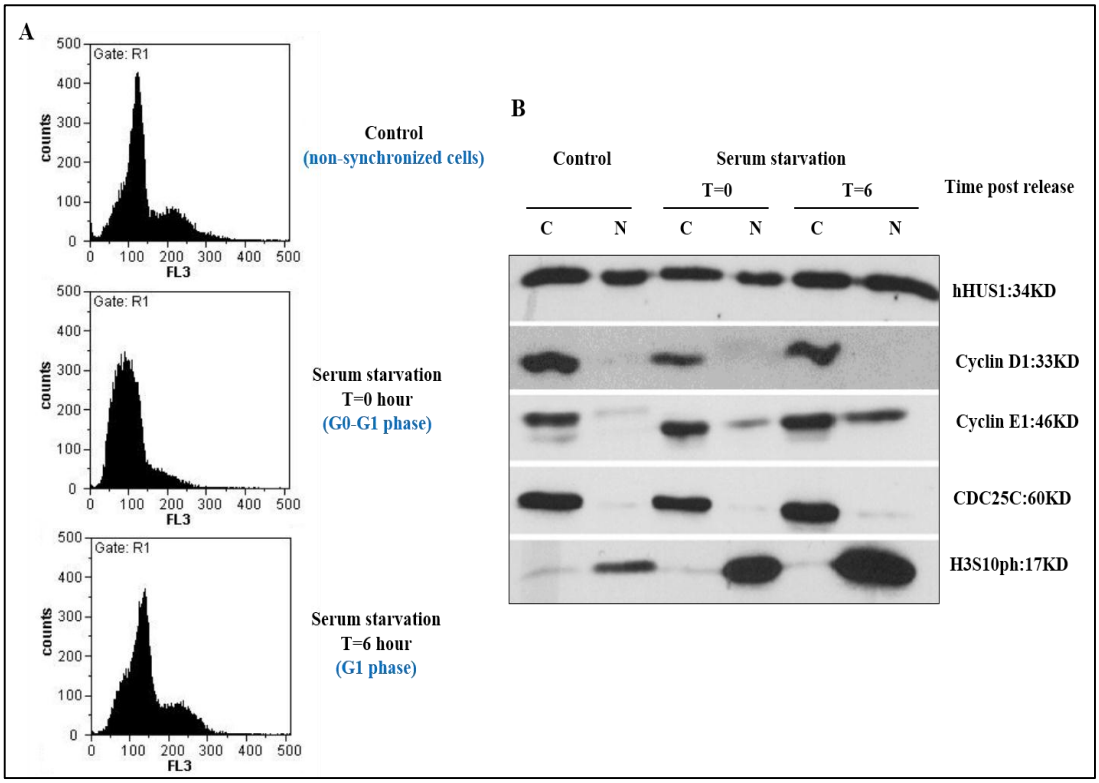

Figure 5-4: HeLa cell synchronized at the G0-G1 border. Cells were synchronized by serum withdrawal at the G0-G1 transition point. **A:** Flow Cytrometry histograms showing that the starved cells arrested at the G1 stage at the 0-hour time point. Arrested cells were released by the addition of rich medium and analyzed 6 hours after the release when they had re-entered the cell cycle (peak at 100 FL3 [DNA content] = G1, peak at 220 FL3 = G2). **B:** Western Blot analysis of cell synchronization through the expression patterns of marker proteins. Cyclin D1 & E1 proteins concentrations elevated while cells traverse to G1 phase. CDC25C resided the cytoplasm outside of G2 phase, and histone H3-Serine-10 phosphorylation is significant in quiescent cells. The expression and cellular fractionation of hHUS1 did not change at the G0-G1 arrest; no smaller variants were detected using the monoclonal antibody. (C: cytoplasmic fraction, N: nuclear fraction).

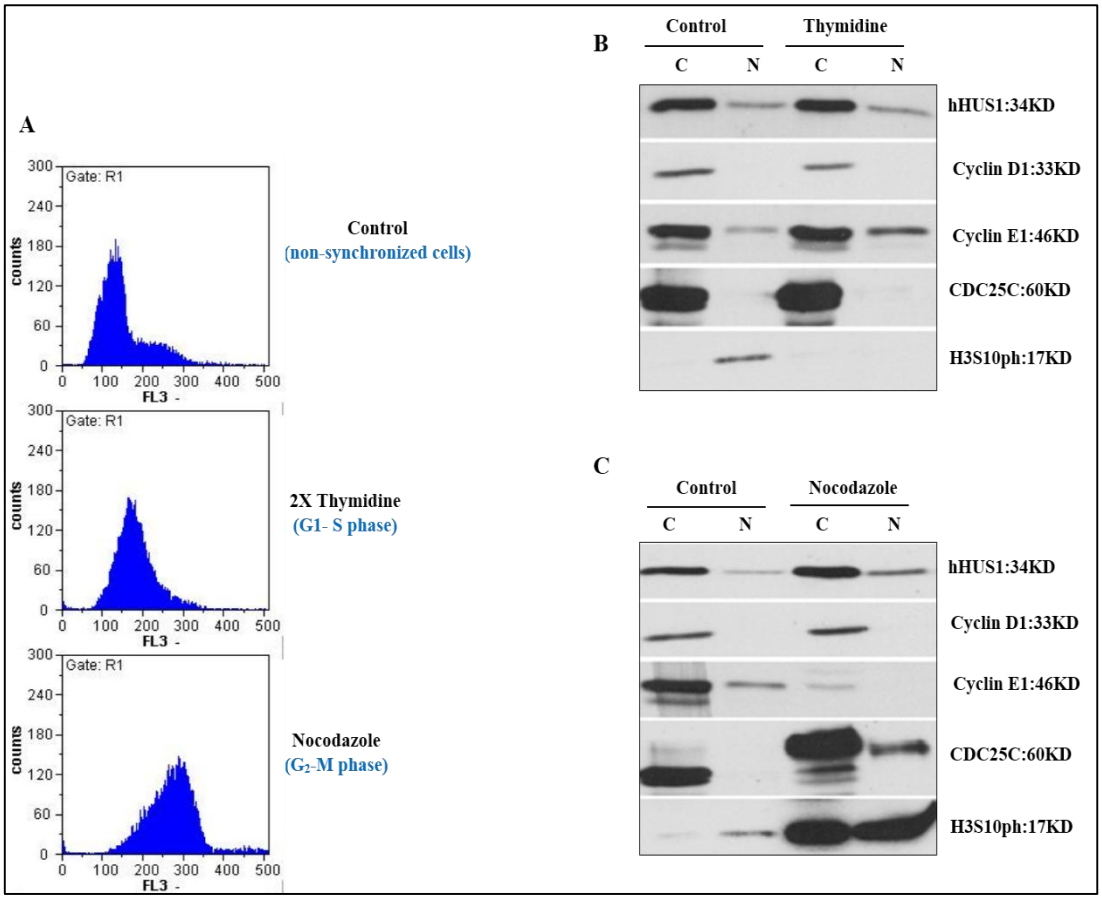

Figure 5-5: HeLa cell synchronized early in S phase and in mitosis. Cells were synchronized by 2x Thymidine block early in S phase and by nocodazole treatment in mitosis. **A:** Flow Cytrometry histograms showing the DNA content of asynchronous cells (control), cells arrested early in S phase by a 2x Thymidine block and in mitosis by nocodazole treatment. The DNA content of S phase cells is between the G1 (dominant left peak at 130 FL3) and G2 peak (lower peak at 220 FL3) observed in the control population. Mitotic cells arrest with a G2 peak shifted from 220 to 300 FL3. **B & C:** Western Blot results of the cell synchronization experiment. Cyclin D1 & E1 proteins concentrations remain constant while cells are arrested early in S phase, whereas the levels of cyclin E1 drop in mitotic cells. The mitotic marker, phosphorylation of histone H3 at serine-10 is absent in S phase cells but sharply accumulates in mitosis. The electrophoretic mobility of Cdc25 phosphatase changes and some of the phosphatase relocates to the nuclear fraction. Neither the levels nor the fractionation pattern of hHUS1 was affected under these conditions. (C: cytoplasmic fraction, N: nuclear fraction).

5.2.2 Senescent cells do not express the *hHUS1* splice variants

I triggered senescence in HeLa cells by oxidative stress using sub-lethal doses of H_2O_2 (200µM) with a 1 hour exposure time in FBS free media (the high protein content in the fetal serum quenches hydrogen peroxide). H_2O_2 was washed out and cells were

maintained for up to 72 hours in normal complete media. Treated cells had a senescent cells morphology, non-proliferating flat enlarged cells 72 hours post H_2O_2 treatment (Figure 5-6, A). Protein samples, which were taken at 0, 24, 48 and 72 hours' time points, were analyzed by Western Blot. They showed an elevated expression and modification of senescence regulatory proteins p21 WAF1/CIP1 at the 48 and 72 hour time points (Figure 5-6, B). The protein levels of p16INK4A also increased in the response to H_2O_2 treatment. No signal for the DNA damage marker, the serine-345 phosphorylation on Chk1 kinase (ChK1-S345ph) was detected. Taken together, these findings indicate that the cells entered into the senescent stage. hHUS1 expression levels were constant at all-time points showing that senescence and H_2O_2 treatment have no impact on this protein and its variants (Figure 5-6, B).

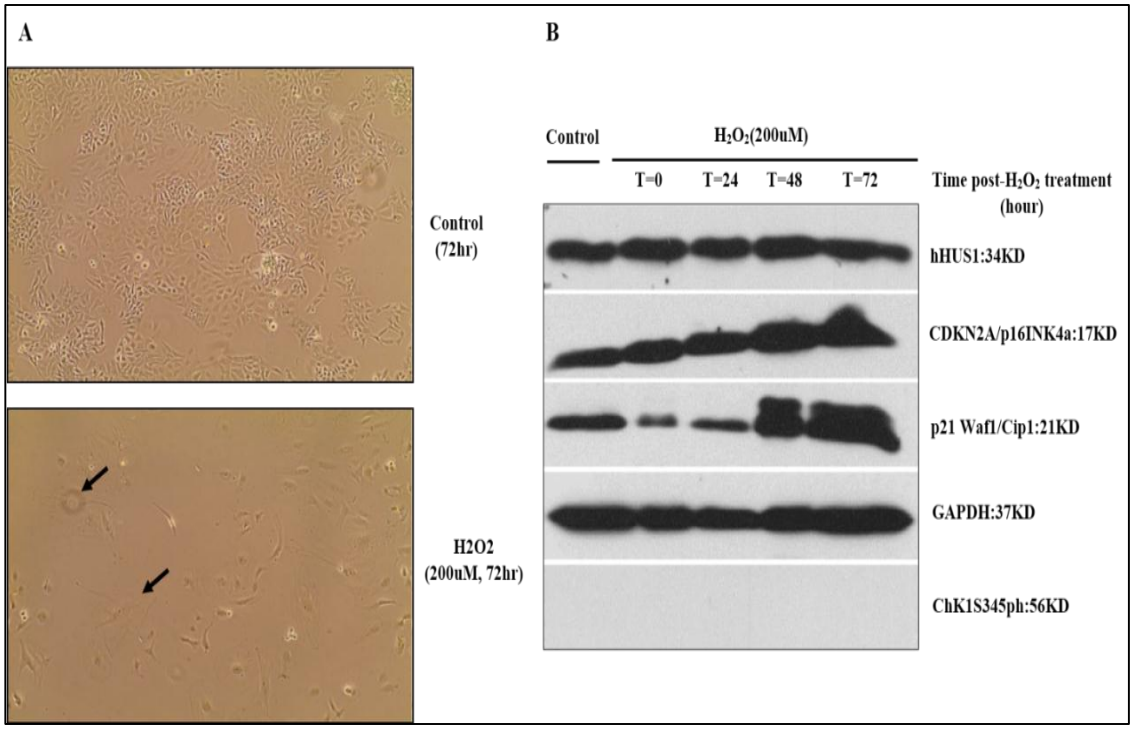

Figure 5-6: Induction of cell senescence in HeLa cells. Cell senescence was induced in HeLa cells by oxidative stress using 200µM of H_2O_2 for 1 hour. **A:** control cells were proliferated normally and reached about 80% confluence after 72 hour. H_2O_2 treated cells entered senescence after 72 hours post H_2O_2 treatment (Arrows indicate to enlarged flattened senescent cells which have less contrast in the microscope comparing with control cells) (images were taken by EVOSx1/AMG Microscope, on x10 magnification). **B:** senescent cells showed up-regulation of senescence regulatory proteins p21 WAF1/CIP1 and p16INK4A, with no signal for ChK1S345ph. hHUS1 protein expression levels remained constant in senescent cells with no expression of its alternative splice variants.

5.2.3 hHUS1 expression as a response to different DNA damaging agents

5.2.3.1 Oxidative stress

Cells were treated with 500µM H_2O_2 for 30 minutes in FBS-free medium. Samples were taken at the indicated time points after cells were released in H_2O_2 free, complete media. The response to the higher concentration of H_2O_2 was immediate, since the Chk1 kinase became phosphorylated at serine-345 shortly after the treatment (Figure 5-7). The expression levels of p21WAF1/CIP1 increased slightly during the experiment. In contrast to the senescence experiment with a sub-lethal dose of 200µM H_2O_2 for 60 minutes (Figure 5-6, B), no modification of p21 was evident after 4 hours. This implies that this post-translational modification is a late response linked with senescence rather than an early DNA damage response. No changes to the expression pattern of hHUS1 were observed using the monoclonal antibody.

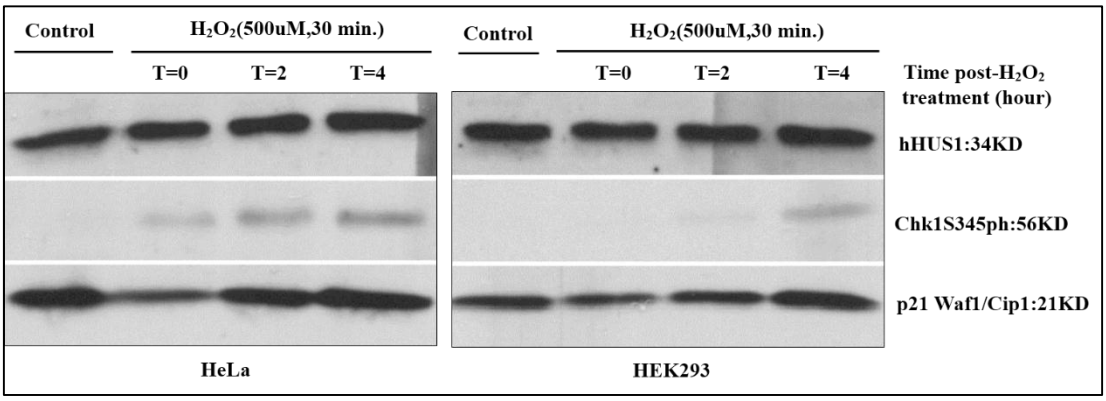

Figure 5-7: Induction of oxidative stress in HeLa and HEK293 cells. Cells were treated with 500µM H_2O_2 for 30 min in FBS free media. Protein extracts were taken at the indicated time points after the release in H_2O_2 free-complete media. HeLa cells showed an immediate response to the treatment as detected by the phosphorylation of Chk1 at S345 and a gradual up-regulation of p21WAF1/CIP1. The levels and expression pattern of hHUS1 did not change.

5.2.3.2 Heat stress

To test whether heat stress affects hHUS1, both HeLa and HEK293 cells were exposed for 1 hour to 42ºC. Although there was a moderate up-regulation of p21WAF1/CIP during the five-hour recovery period (Figure 5-8), no signal for

ChK1S345 phosphorylation was detected. This was unexpected since human Chk1 is modified by ATR kinase under similar heat stress conditions (Furusawa et al., 2012). As a result, I could not judge if the *hHUS1* alternative splice variants are affected by the heat shock as Chk1 phosphorylation was not observed (Figure 5-8).

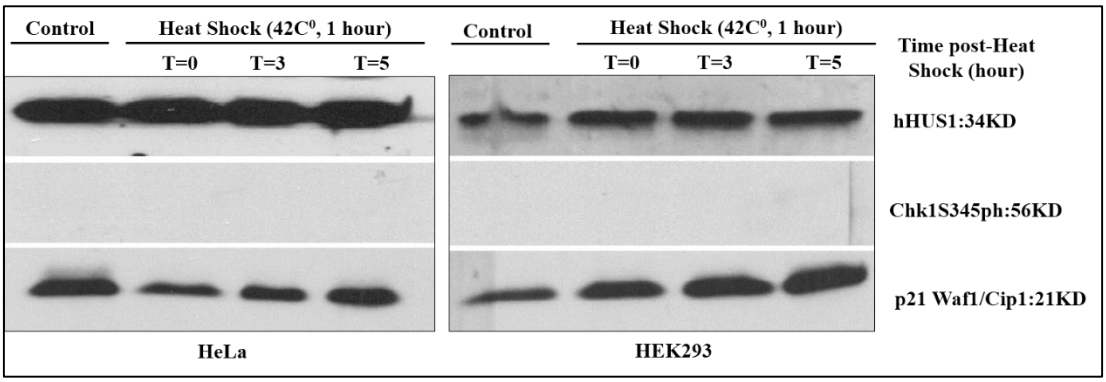

Figure 5-8: Heat shock treatment of HeLa and HEK293 cells. Cells were heat shocked at 42ºC for 1 hour in complete medium. Protein samples were taken at the indicated time points after cells were returned to 37ºC. hHUS1 did not show any changes under these conditions. There was no signal for ChK1S345ph, but there were very slightly elevated expression levels of p21WAF1/CIP1.

5.2.3.3 Replication fork stress by Hydroxyurea (HU) treatment may induce the hHUS1 variant 005 that missing the first 21 amino acids

HU is a well-known agent used widely to stall replication forks by inhibition of ribonucleotide reductase, which produces deoxy-nucleotides. Cells were treated with 5mM HU for 2 and 4 hours to induce replication fork arrest. Both cell lines were affected by HU treatment, since Chk1 was phosphorylated as reported previously (Zhao & Piwnica-Worms, 2001). However, the cell cycle arrest signal started earlier in HEK293 cells compared to HeLa cells, which is also obvious from the decline in p21WAF1/CIP1 protein levels upon HU treatment. hHUS1 was expressed differently in the cell lines. In HEK293 cells, there was a slower migrating band visible, which migrated just below the main band. The latter was most obvious when cells were treated for 2 hours with HU (Figure 5-9). Since the hHUS1-005 variant is, only 21 amino acids (~2kDa) shorter than the full-length protein (hHUS1-001), the smaller band would be consistent with this N-

terminally truncated protein. Given the higher expression levels of hHUS1 in HeLa cells, the presence of this variant could be masked. At this stage, I cannot exclude the possibility that the slower migrating band is a modified form of the full-length protein.

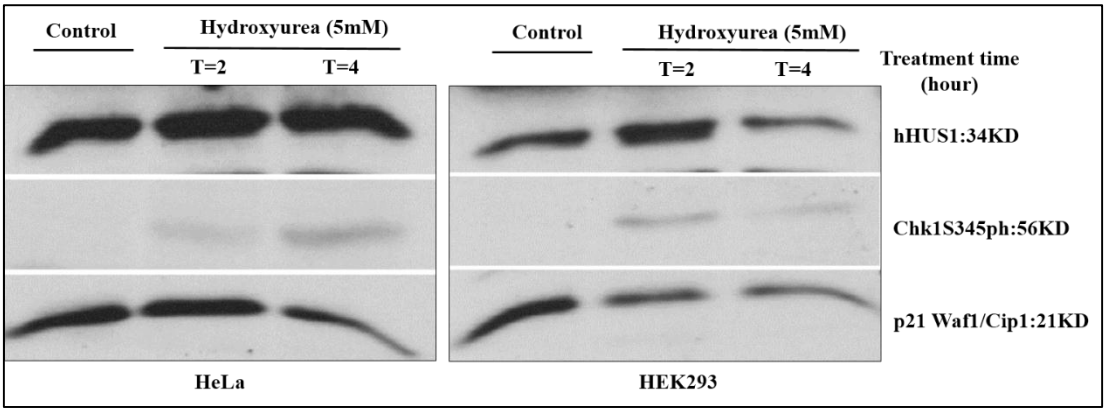

Figure 5-9: Replication fork stress induced by Hydroxyurea (HU) treatment. Replication fork stress was induced with 5mM HU treatment for 2 and 4 hours in complete medium. This triggered the checkpoint-dependent phosphorylation of Chk1 kinase at serine-345. This was accompanied with a decline in p21WAF1/CIP1 protein levels. Noteworthy; a smaller slower migrating hHUS1 band became visible in HEK293 cells especially at the 2-hour time point. Given the small difference between the full-length hHUS1-001 protein and its N-terminally truncated variant hHUS1-005, which misses only the first 21 amino acids (~2kDa), the smaller band could be this splice product of the *hHUS1* gene.

5.2.3.4 DNA replication inhibition by Aphidicolin (APH) treatment

To search for the hHUS1 splice variants, I treated cells with 200µm of aphidicolin (Aph), which inhibits DNA synthesis by deactivating DNA polymerase alpha and delta (Morita, et.al., 1982). As in the case of a replication arrest triggered by HU, a double-band of hHUS1 was evident in HEK293 cells, which appeared to increase in intensity upon treatment with aphidicolin (Figure 5-10). However, unlike the case of HU, the protein levels of p21 WAF1/CIP1 did not drop upon the inhibition of the DNA polymerases. On the contrary, in HEK293 cells the levels seemed to increase at the later time points. There was, however, no evidence of Chk1 phosphorylation at S345 under these conditions, although Chk1 was reported to be modified in chicken DT40 cells in the response to aphidicolin (Zachos, et. al. 2005).

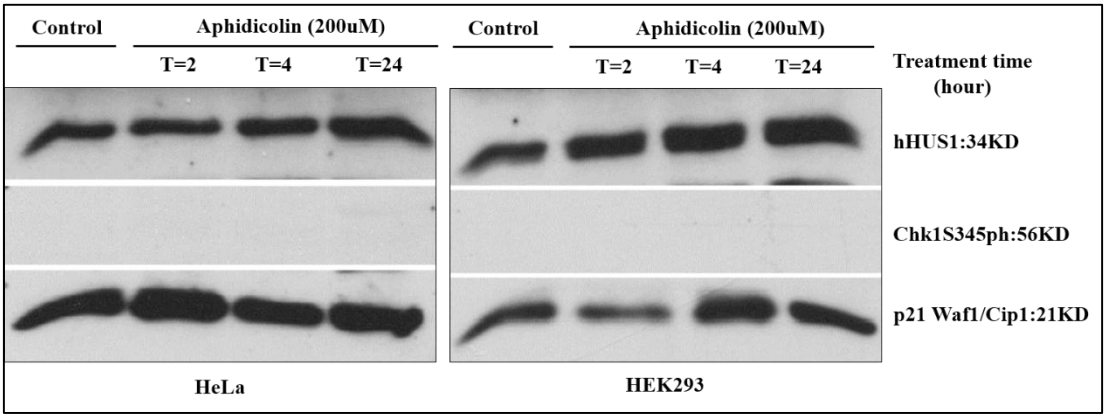

Figure 5-10: Aphidicolin treatment of HeLa and HEK293 cells. DNA synthesis was inhibited in both cell lines using 200µm final concentration of Aphidicolin. HeLa cells showed a lately treatment response, at 24 hours, while HEK293 cells were affected at 2 hours' time point. That was obvious from the slightly up-regulation of p21WAF1/CIP1, with no signal for Chk1S345 in both cell lines.

5.2.3.5 DNA methylation by Methyl methanesulfonate (MMS) may also trigger expression of the hHUS1-005 variant

DNA methylation was induced in both cell lines using 50µg/ml of methyl methanesulfonate (MMS) for 2 or 4 hours respectively (Figure 5-11). This dose seems to be apoptotic for both cell lines with HEK293 cells being more sensitive to this dose. As in the case of HU, MMS triggered the phosphorylation of Chk1 at S345 and the decline in p21 WAF1/CIP1 protein levels. Importantly, a slower migrating hHUS1 band was detected in HEK293 cells upon a 2-hour exposure. The band was also weakly detectable in untreated cells (Figure 5-11).

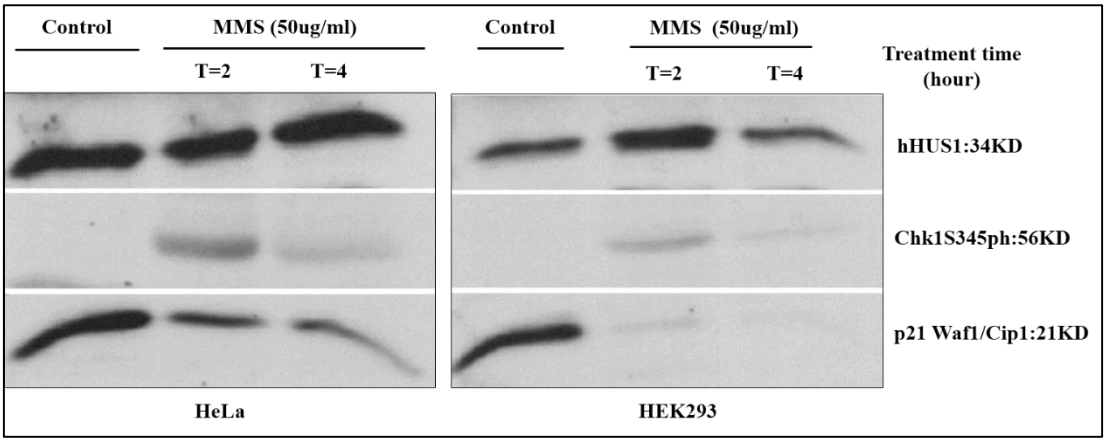

Figure 5-11: DNA methylation in HeLa and HEK293 cells by MMS treatment. Cells were treated with 50µg/ml of methyl-methanesulfonate (MMS) for the indicated time points. The dose triggered Chk1 phosphorylation at S345 and the degradation of the p21 WAF1/CIP1 protein in both cell lines. Importantly, hHUS1 showed the two bands again especially at the 2 hour time point.

5.2.3.6 Pyrimidine dimer formation through exposure to ultraviolet light (UV)

UV light induces pyrimidine dimer in the DNA structure, which interfere with transcription and DNA replication. Here two doses, 40 and 50 J/m^2 were used. Both doses were very effective on both cell lines as they triggered checkpoint-dependent phosphorylation of Chk1 at S345 and the rapid degradation of p21 WAF1/CIP1 (Figure 5-12). hHUS1 showed, as previously mentioned in the case of HU and MMS treatment, two bands, which were detected at all-time points in the 50 J/m^2 experiment with HEK293 cells. The smaller band may also be present in HeLa cells, but due to the stronger expression level of the full-length hHUS1 protein, it is more difficult to see.

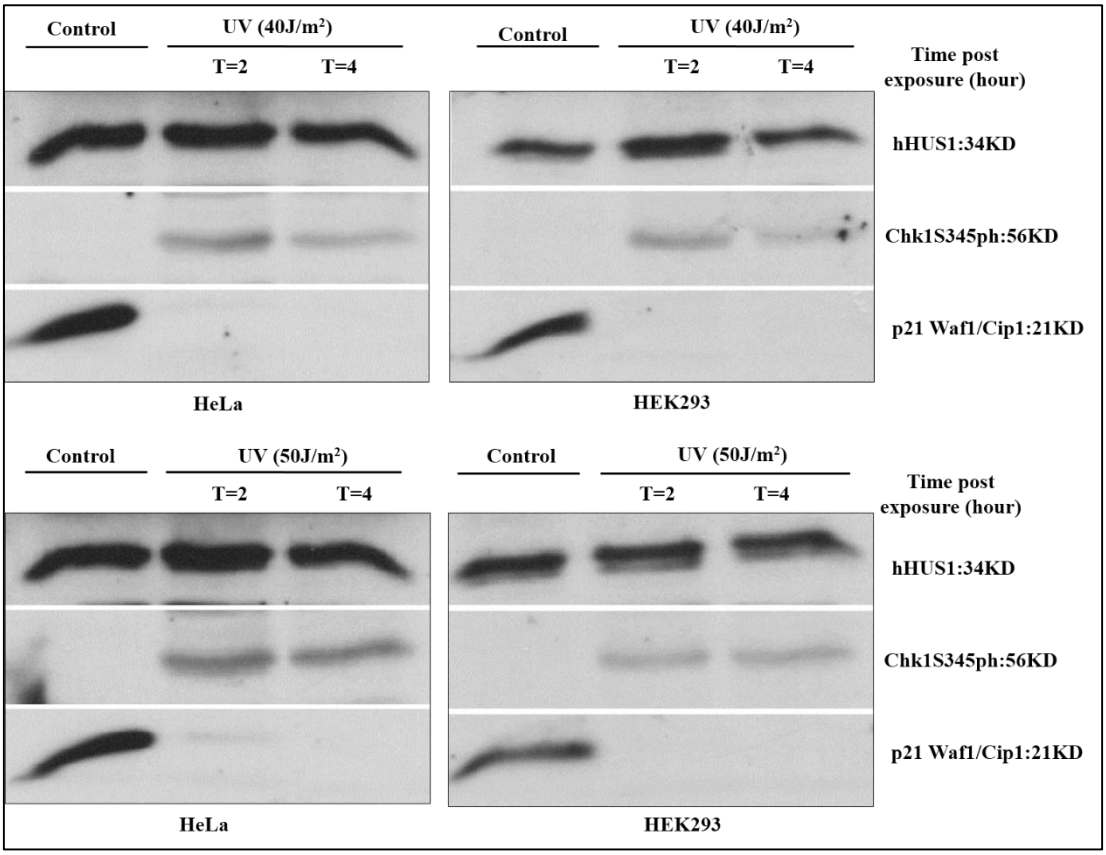

Figure 5-12: Pyrimidine dimer formation in HeLa and HEK293 cells. Cells were exposed to either 40 or 50 J/m^2 of UV light. The DNA damage signal was very strong upon the exposure, which is clearly shown by the signal of Chk1S345 phosphorylation and the degradation of the p21 WAF1/CIP1 protein. hHUS1 showed the same two bands that appeared upon HU and MMS treatment although they may be present at all stages without an up-regulation by UV light.

5.2.3.7 Replication fork damage by Camptothecin (CPT) treatment

It is well known that the topoisomerase1 poison, camptothecin (CPT) arrests cells in S-phase when replication forks break upon their collision with the immobilized Topoisomerase1 enzyme (Ryan, et. al., 1991). While HeLa cells were more resistant to the exposure to 1µM CPT for up to 24 hours, the DNA damage checkpoint response was much stronger and earlier in HEK293 cells as indicated by the S345 modification of Chk1 (Figure 5-13). Interestingly, the levels of p21 WAF1/CIP1 remained high throughout the experiment unlike in the cases were cells were treated with HU, MMS or UV light (Figures 5-9, 5-11 & 5-12). This interesting observation implies that the decline in p21

protein levels is a p21 related to arrest or slow-down the replication forks rather than collapsed forks. Whether the slower migrating of hHUS1 band was present in CPT-treated cells was difficult to judge, but it appeared that the hHUS1 band turned into a double-band in the presence of CPT.

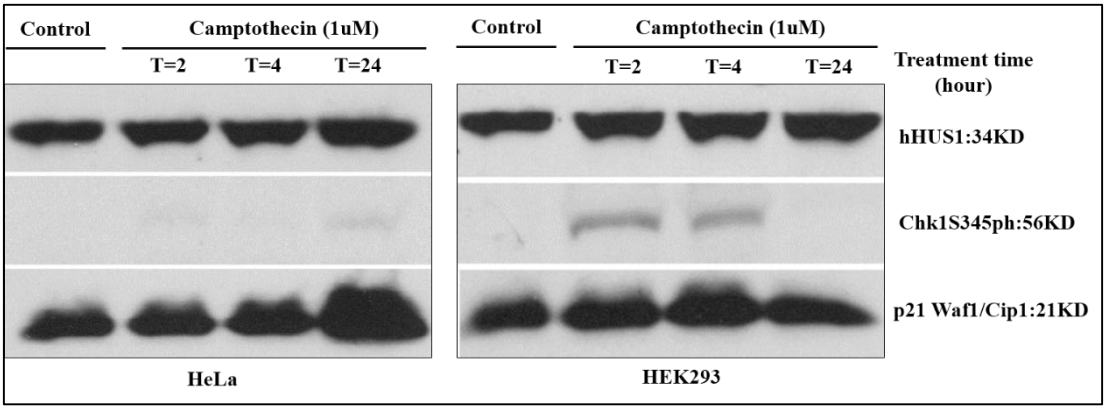

Figure 5-13: Camptothecin treatment of HeLa and HEK293 cells. Cells were treated with 1μM of CPT up to 24 hours. HeLa cells were more resistant to the CPT effect, since they showed only a weak signal for Chk1S345 phosphorylation after being exposed for 24hr. On the other hand, HEK293 cells showed a much stronger signal for Chk1S345ph even after a 2-hour exposure. Interestingly, the levels of p21 WAF1/CIP1 did not decline throughout the CPT exposure unlike in the case of HU, MMS and UV treatments. Regarding the hHUS1 protein, I noticed a slightly up-regulation of the protein in both cell lines upon the CPT treatment. The smaller band may be present, as the hHus1 band appeared to turn into a double-band in the presence of CPT.

5.2.3.8 DNA breaks induction by Phleomycin

Phleomycin triggers single and double strand breaks in the cell genome (Moore, 1988). Incubation of cells with 60 μg/ml for up to 24 hours triggered only a moderate effect in HeLa cells as indicated by a weak signal for Chk1S345 phosphorylation (Figure 5-14). HEK293 cells showed no response to this treatment. Hence, it is difficult to judge whether the dose was sufficiently high to induce a full DNA damage response.

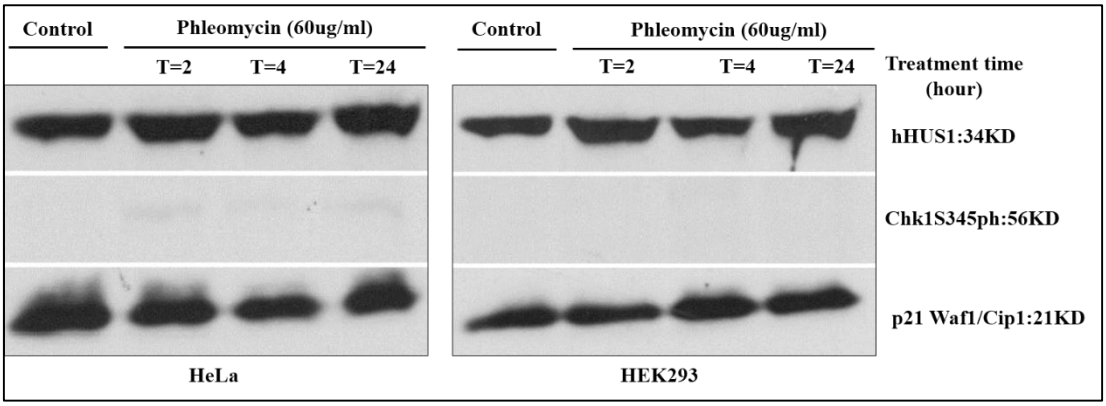

Figure 5-14: Treatment of HeLa and HEK293 cells with Phleomycin. HeLa and HEK293 cells were exposed for the indicated time points in complete medium with 60μg/ml phleomycin. While HeLa cells showed a weak signal for Chk1S345 phosphorylation, HEK293 cells failed to respond.

5.3 Discussion:

5.3.1 Key Findings

The key findings of this chapter are as following. **(1)** Exposure of HEK293 cells, and to a lesser extent HeLa cells, to treatments with either arrest (hydroxyurea) or reduce replication movement (MMS & UV light) either up-regulate a smaller band of hHUS1, which migrates close to the full-length protein or modified (phosphorylated) the full-length hHUS1 protein. **(2)** Arresting HeLa cells in G1, S or mitosis does not result in a similar double band. In addition, **(3)** Replication arrests or reduced replication speed induces the fast degradation of the CDK inhibitor p21WAF1/CIP1, which is not observed when replication forks break in the presence of camptothecin (CPT).

5.3.2 Cells synchronization

Serum starvation, double thymidine block and nocodazole treatment were chosen to arrest cells in G1, S and mitosis phases, respectively. When cells suffer from nutrient depletion, they enter the G0 phase where they are called "quiescent cells". This exit from the cell cycle is reversible since the cells start cycling again once the nutrients are available (Banflavi, 2011). Interestingly, in my experiment (Figure 5-4), serum starved cells arrest was confirmed by the cyclin D1 expression and the lower nuclear concentration of cyclin E1, which indicates that the arrest was at the G1 phase rather than in G0. Both cyclins act at distinct stages in G1. It was shown that Cyclin D1 acts at the stage in G1 where cells can enter or exit the quiescent phase G0 (Baldin, et.al., 1993). When cells progress in S phase, Cyclin D1 remains at a low concentration to permit the efficient DNA synthesis which is driven by Cyclin E1 (Guo, et.al. 2005; Yang, et.al. 2006). Although Baldin, et.al. (2006) clarified the nuclear localization of cyclin D1, Alao and co-workers (2006) reported that the protein is predominantly in the cytoplasm. My observation that the levels of Cyclin E1 increase at the later time points of 6-8 hours (Figure 5-4B) are in line with the observation that the Cyclin E1-CDK2 complex is inactive until cells have reached the second part of G1 phase when they are committed to enter S phase. The other interesting observation is the high levels of histone H3 phosphorylated at serine-10, which is normally a marker for the G2-M transition (Van Hooser, et.al., 1998; Johansen & Johansen, 2006). The DNA content of the serum starved cells clearly shows that cells are arrested in G1 and not in mitosis (please compare the DNA content profiles in Figures (5-4, A and 5-5, A). This implies that this histone variant

becomes modified in the response to serum starvation. To my knowledge, this has not yet been reported. However, it was reported by previous studies that histone H3 phosphorylation at Ser10 can happened in interphase but at a much smaller extent than in mitosis (reviewed in Johansen & Johansen, 2006).

The double thymidine block, which arrests cells early in S phase (Figure 5-5, A) works through the inhibition of DNA replication by the disruption of deoxynucleotide synthesis (Harper, 2005; Ma & Poon, 2011). Nocodazole arrests cells in mitosis (Figure 5-5, A) because it interferes with microtubule assembly (Harper, 2005). None of these arrest treatment changed the expression pattern of hHUS1 and I could not observe the same double-band as in the response to HU, MMS or UV treatment. This implies that the *hHUS1* splice variants are not cell cycle regulated. Nevertheless, the situation could be that their expression is peaked up in the middle of one of the cell cycle phases. I could not follow the cells progression as a time course post each release point. That because cells lose their synchrony after a while from the release time (Darzynkiewicz, et.al. 2011).

5.3.3 hHUS1 expression in senescent cells and after heat shock

I induced senescence in HeLa cells by a sub-lethal dose of oxidative stress, since immortal cells in culture do not undergo replicative senescence (Kuilman, et.al. 2013). Judging by the change in cell shape (Figure 5-6, A), cells became senescent, which was accompanied by the post-translational modification of the CDK inhibitor p21 after 24 and 72 hours, but not by the checkpoint-induced phosphorylation of Chk1 kinase (Figure 5-6, B).

As shown in Figure 5-3, oxidative stress is detected by the ARF-p53 and p38 MAP kinase pathways that regulate the CDK inhibitors p21 and p16 independently of ATM-Chk1 activation. (Lieber & Karanjawala, 2004; Chen & Goligorsky, 2006; Rufini, et.al, 2013; Pospelova, et.al. 2009). The observation that p21 becomes modified at the later time points of 24 and 72 hours is consistent with the switch from the initial p21-dependent cell cycle arrest to a later p16 dependent arrest (C´mielova´ & Rezacova´, 2011). This might explain why there was no signal for the phosphorylation of Chk1 at serine-345. The modification of Chk1 at the higher dose of 500μM H_2O_2. (Figure 5-7) is consistent with the ability of high doses of hydrogen peroxide to inflict DNA damage,

which would trigger the ATM-dependent modification of Chk1 at S345 (Pero, et. al., 1990; Bartek & Lukas, 2007). The hHUS1expression pattern was affected neither at the sub-lethal nor at the DNA damaging dose of hydrogen peroxide. Heat treatment for 1 hour at 42°C (Figure 5-8) did also not inflict any changes on the hHUS1 expression pattern.

5.3.4 hHUS1 expression pattern was affected by treatments which either arrested or slowed down replication forks

The most interesting observation of this set of experiments was the appearance of a double-band of the hHUS1 protein, which was particularly obvious when HEK293 were treated with first, hydroxyurea (HU, Figure 5-9), which arrests replication forks. Second, with methyl methanesulfonate (MMS, Figure 5-11), which interferes with DNA replication by DNA alkylation. Third, with UV light (Figure 5-12), which also interferes with DNA replication. The slower migrating hHUS1 band was detectable in untreated HEK293, and to a smaller extent, in HeLa cells (Figure 5-12), and appeared to increase in intensity with the full-length protein at the early time point of 2 hours in most experiments. Since this double band was not obvious when replication forks broke upon the treatment with the topoisomerase1 inhibitor camptothecin (CPT, Figure 5-13), although hHUS1 may also run as a double-band under these conditions, the smaller band seems to correlate with DNA replication problems. Without further experiments, like isoelectric focusing (Janes, at.el. 2012), it is difficult to decide whether the slower migrating hHUS1 band is a modified form of the full-length protein (hHus1-001) or it is related to the N-terminally truncated variant hHUS1-005 which lacks the first 21 amino acids (Figure 5-2). Expression of this variant 005, which shares similarities to the *S.pombe* Hus1 variant Hus1-H32 (Figure 6-1), in the response to DNA replication stress would be in line with the requirements of the yeast variant for the response to HU (Figures 3-14, 3-16, 3-21) and the activation of Chk1 kinase when replication forks break in the absence of Cds1 kinase (Figure 3-22). The reason why the double band is less obvious in HeLa protein extract could be that the higher expression levels of the full-length protein may mask the smaller band.

5.3.5 The CDK inhibitor p21WAF1/CIP1 is rapidly degraded in the response to DNA replication stress but not when replication forks break

p21WAF1/CIP1 is a p53 target gene that is induced by ionizing radiation (IR) and binds to CDK4/cyclinD and CDK6/cyclinD complexes to block the G1–S transition in mammalian cells (Deng et al., 1995). Contrary to the general view that p21 is up-regulated in the response to DNA damage, my data showed that this CDK inhibitor is rapidly degraded in the response to HU (Figure 5-9), MMS (Figure 5-11) and UV light (Figure 5-12). Nevertheless, that is not occur when replication forks break in the presence of CPT (Figure 5-13), or when DNA polymerase alpha is blocked by aphidicolin (Figure 5-10). This implies that CDK4/cyclinD and/or CDK6/cylinD activity may be important for the response to replication stress caused by HU, MMS and UV. It is known that p21 is degraded upon the treatment with high doses of HU and UV. HU treatment is known to inhibit *p21* mRNA transcription rather than affecting its stability (Mattia, et.al. 2007), whereas its degradation upon UV exposure helps to prevent replication defects by facilitating the tolerance to UV-induced DNA lesions (Mansilla, et.al. 2013).

Chapter 6: Construction of *hHUS1* variants and *hHUS1B* stable cell lines

6.1 Introduction

As a summery from Chapters 3 and 4, the *hus1* gene in yeast cells encodes two N-terminally truncated variants Hus1-H32 and Hus1-H46 by a process known as Leaky Ribosome Scanning. Interestingly, the human *hus1* gene, *hHUS1*, has nine transcripts, of which only four are protein coding. I successfully found them at mRNA level together with the transcript of the *hHUS1B* gene (Chapter4), but up to now, I could not detect them at protein level (Chapter5). In the case of hHUS1B, I could not find an efficient commercial antibody against its protein, which made it difficult to investigate its endogenous expression conditions. Thus, to compare the yeast and human variants of *HUS1*gene, I decided to construct the corresponding stable cell line for each human isoform, in parallel with *hHUS1B*, using site-directed Flp-In gene integration system in human cells (embryonic kidney HEK293, Invitrogen). I became very interested in the human variants especially hHUS1-005 variant, since it resembles the *S.pombe* Hus1-M32 protein (Figure 6-1). Although they are produced by different mechanisms (alternative splicing in human cells and leaky ribosome scanning in yeast cells), both of them are N-terminally truncated proteins missing a similar section of Hus1. Moreover, they resemble each other to some extent in their protein sequence.

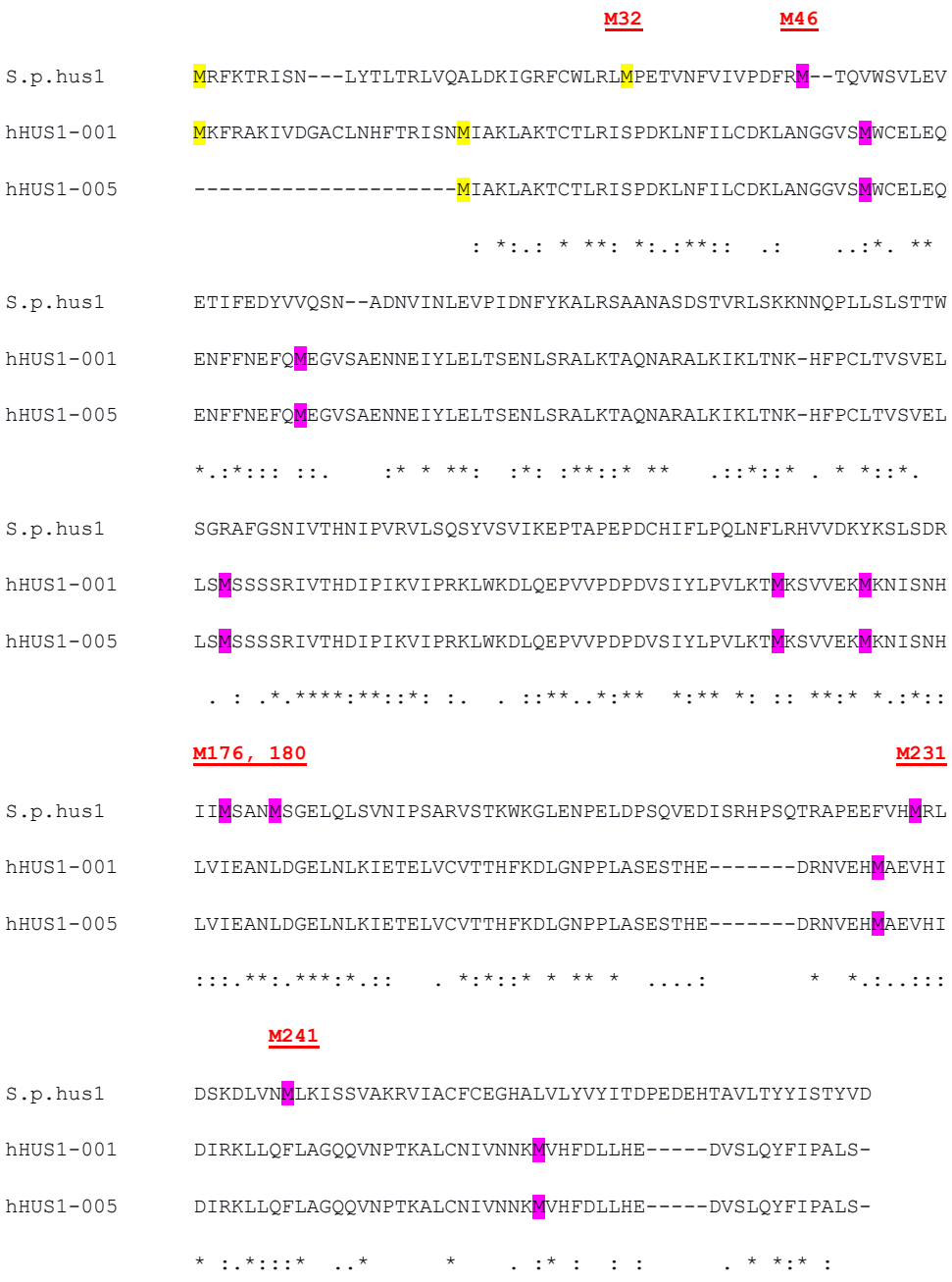

Figure 6-1: Alignment of human full-length HUS1 (hHUS1-001), the human splice variant HUS1-005 and the *S.pombe* full-length Hus1 protein. Internal methionine codons are highlight. The two internal translation start sites AUG-32 and AUG-46 in *S.pombe* Hus1 are shown. (Proteins alignment was produced with Clustal Omega: (http://www.ebi.ac.uk/Tools/msa/clustalo/).

I proceeded to establish stable cell lines of EGFP-tagged hHUS1 proteins as this would allow me to perform biochemical experiments with the full-length protein, its splice variants and hHUS1B. The human *HUS1B* gene is unusual as it does not contain any introns and should therefore have no splice variants unlike *hHUS1* (Hang, et.al. 2002). I chose the Flp-In™ T-Rex™-293 cells from Invitrogen to establish the stable cell lines for two correlated reasons. First, HEK293 embryonic kidney cells have a simple cell cycle and maintenance requirements; they are easy to transfect by different methods with faithful cellular mechanisms of translation and protein expression (Thomas & Smart, 2005). Second, the cells have one integrated copy of the Flp-In™ T-Rex™ cassette, which allows for targeted gene integration. The integration is mediated by Flp recombinase-mediated DNA recombination at the single FRT site. As shown in Figure 6-2, co-transfection of the HEK293 cell line with the plasmid pOG44, which expresses the FLP recombinase, and the plasmid pcDNA5/FRT/TO, which carries the EGFP fusion gene of interest, results in the stable integration of the EGFP fusion gene at the single FRT site. Positive clones can be selected based on the change in antibiotic resistance from zeocin (no integration) to Hygromycin (integration). For more information, please refer to the Flp-In™ T-REx™ Core Kit for Generating Stable, Inducible Mammalian Expression Cell Lines by Flp Recombinase-Mediated Integration, Invetrogen,

(http://tools.lifetechnologies.com/content/sfs/manuals/flpintrex_man.pdf .)

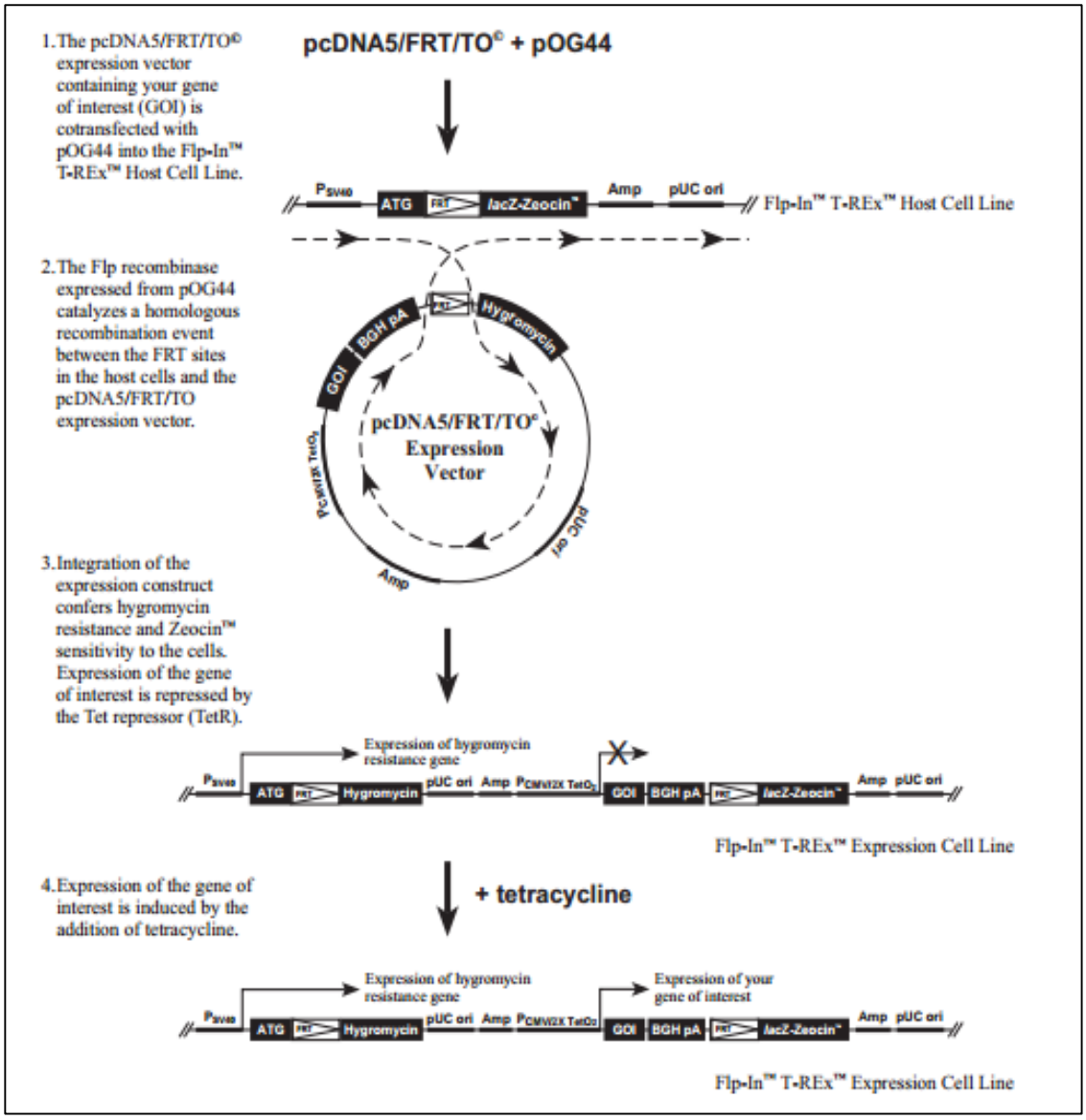

Figure 6-2: Illustrative diagram of the Flp-In™ T-REx™ System. The steps of transfection and the expression of gene of interest are explained in details. (Adapted from Flp-In™ T-REx™ Core Kit for Generating Stable, Inducible Mammalian Expression Cell Lines by Flp Recombinase-Mediated Integration, Invetrogen,

(http://tools.lifetechnologies.com/content/sfs/manuals/flpintrex_man.pdf).

This chapter summarizes the construction of the stable cell lines expressing full-length hHUS1 (hHUS1-001) as well as the shorter protein variants hHUS1-005, hHUS1-011 and hHUS1-004 in addition to hHUS1B with a C-terminal GFP tag, N-terminal EGFP tag and EGFP as a negative control. Figure 6-3 shows an alignment of all three known hHUS1A variants with the full-length protein.

```
Hus1-001_H.s    MKFRAKIVDGACLNHFTRISNMIAKLAKTCTLRISPDKLNFILCDKLANGGVSMWCELEQ
Hus1-004_H.s    ----------------------MIAKLAKTCTLRISPDKLNFILCDKLANGGVSMWCELEQ
Hus1-011_H.s    ----------------------MIAKLAKTCTLRISPDKLNFILCDKLANGGVSMWCELEQ
Hus1-005_H.s    ----------------------MIAKLAKTCTLRISPDKLNFILCDKLANGGVSMWCELEQ
                                      ************************************

Hus1-001_H.s    ENFFNEFQMEGVSAENNEIYLELTSENLSRALKTAQNARALKIKLTNKHFPCLTVSVELL
Hus1-004_H.s    ENFFNEFQMEGVSAENNEIYLELTSENLSRALKTAQNARALKIKLTNKHFPCLTVSVELL
Hus1-011_H.s    ENFFNEFQMEGVSAENNEIYLELTSENLSRALKTAQNARALKIKLTNKHFPCLTVSVELL
Hus1-005_H.s    ENFFNEFQMEGVSAENNEIYLELTSENLSRALKTAQNARALKIKLTNKHFPCLTVSVELL
                ************************************************************

Hus1-001_H.s    SMSSSSRIVTHDIPIKVIPRKLWKDLQEPVVPDPDVSIYLPVLKTMKSVVEKMKNISNHL
Hus1-004_H.s    SMSSSSRIVTHDIPIKVIPRKLWKDLQEPVVPDPDVSIYLPVLKTM--------------
Hus1-011_H.s    SMSSSSRIVTHDIPIKVIPRKLWKDLQEPVVPDPDVSIYLPVLKTMKSVVEKMKNISNHL
Hus1-005_H.s    SMSSSSRIVTHDIPIKVIPRKLWKDLQEPVVPDPDVSIYLPVLKTMKSVVEKMKNISNHL
                *******************************************

Hus1-001_H.s    VIEANLDGELNLKIETELVCVTTHFKDLGNPPLASESTHEDRNVEHMAEVHIDIRKLLQF
Hus1-004_H.s    ------------------------------------------------------------
Hus1-011_H.s    VIEANLDGELNLKIETELVCVTTH-----------------------------------
Hus1-005_H.s    VIEANLDGELNLKIETELVCVTTHFKDLGNPPLASESTHEDRNVEHMAEVHIDIRKLLQF

Hus1-001_H.s    LAGQQVNPTKALCNIVNNKMVHFDLLHEDVSLQYFIPALS
Hus1-004_H.s    ----------------------------------------
Hus1-011_H.s    ----------------------------------------
Hus1-005_H.s    LAGQQVNPTKALCNIVNNKMVHFDLLHEDVSLQYFIPALS
```

Figure 6-3: Alignment of human full-length hHUS1 (hHUS1-001) with its three splice variants 005, 011 and 004, which are curated in the human Ensembl database. (The alignment was produced with Clustal Omega:

(http://www.ebi.ac.uk/Tools/msa/clustalo/).

As shown in Figures 6-3 and 6-4, all three hHUS1 variants lack the first 21 amino acids and variants 004 & 011 miss large sections of their C-terminal domains. The resulting proteins may therefore adopt a different structure from the full-length hHUS1 protein.

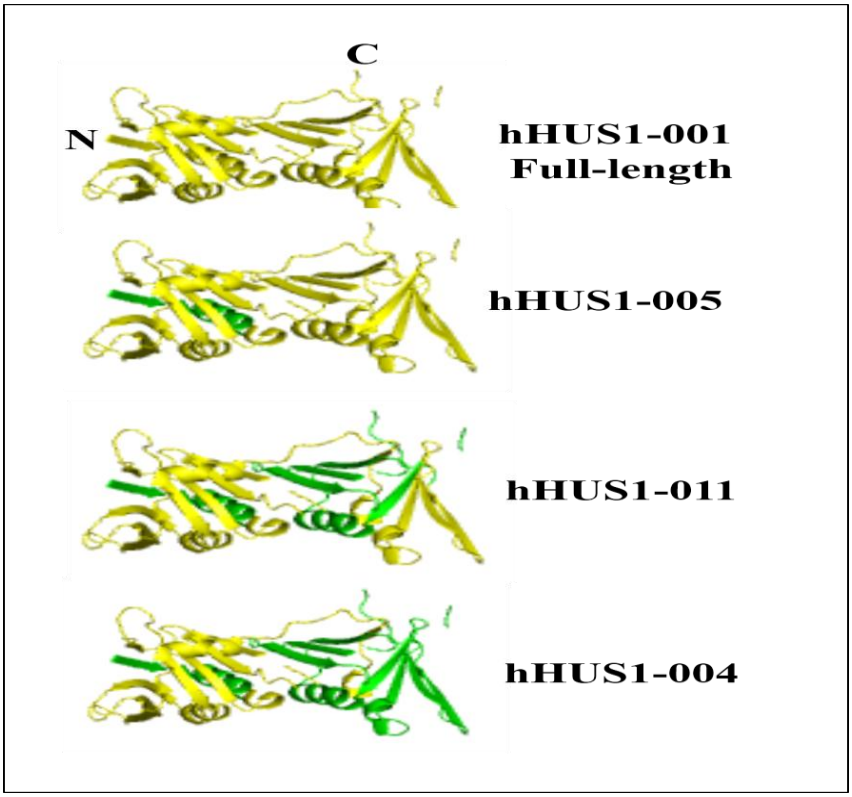

Figure 6-4: Structural alignment of hHUS1 full-length and its protein coding alternative splice variants. All hHUS1 variants (hHUS1-005, hHUS1-011 and hHUS1-004) are lacking the first 21 N-terminal amino acids. In addition, hHUS1-011 and hHUS1-004 are lacking 76 and 114 amino acids respectively from their C-terminal end. The missing sequence is shown in green color. The protein map was created using the Polyview 3D server (http://polyview.cchmc.org/polyview3d.html).

6.2 Results

6.2.1 Construction of C-terminally *GFP*-tagged *hHUS1-001* and *hHUS1-005* stable cell lines

In order, to construct *hHUS1-001-GFP*, *hHUS1-005-GFP* cell lines, I amplified the genes from HEK293 cDNA and fused them with the amplified *GFP* tag from the plasmid pAW8NdeI-GFP using the Fusion PCR protocol (section 2.2.1) mediated by the primers sets that are shown in Figure 6-5.

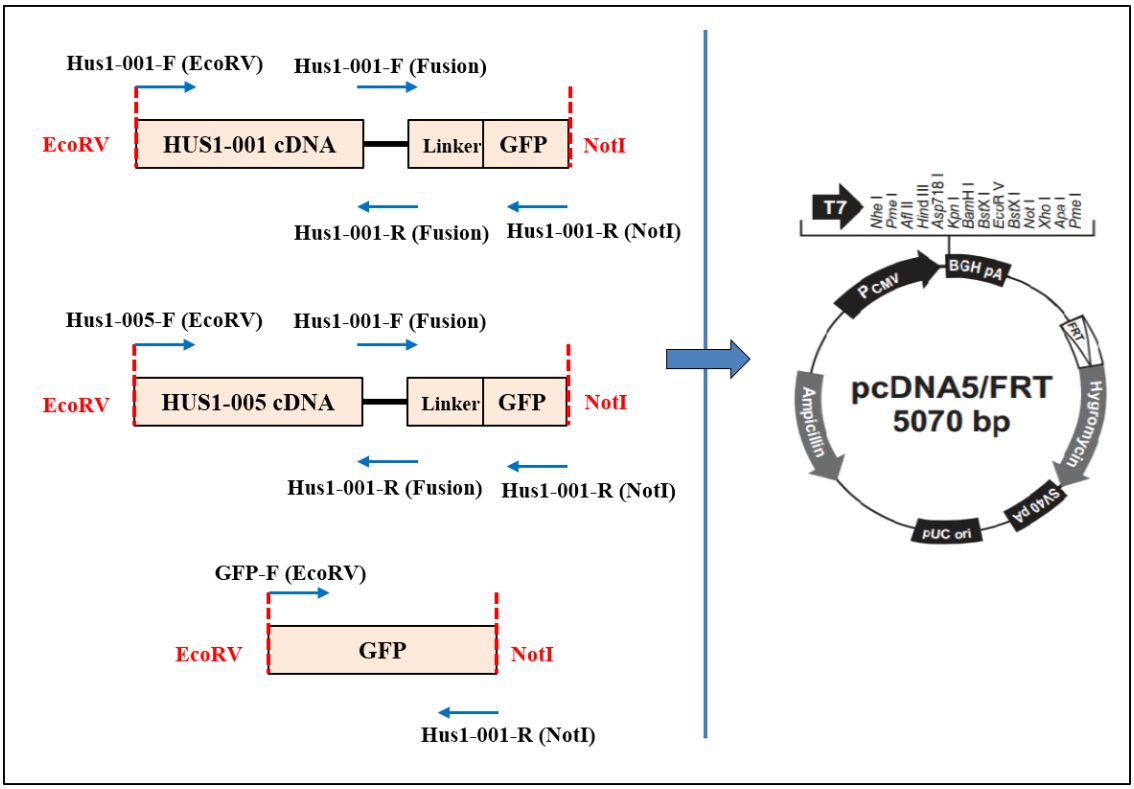

Figure 6-5: Schematic diagram of *hHUS1-001*, *hHUS1-005* and *GFP* cassette construction. The mentioned genes were amplified from HEK293 cDNA by the indicated primers and fused with the amplified *GFP* cassette using the Fusion PCR protocol. Then, the three cassettes were cloned onto pcDNA5/FRT vector using EcoRV and NotI.

Figure 6-6 shows the PCR products of the amplified cassettes from HEK293 cDNA and the amplified *GFP* fragment from pAW8NdeI-GFP and their fusion products. The three cassettes were cloned into the pcDNA5/FRT plasmid and then transfected into HEK293 cells. Stable cell lines of each transfection were isolated and the gene's integration was confirmed by amplifying the corresponding genes from the cells genomic

DNA. The primers, which were used to confirm the integration, were FRT-F, which binds in the CMV promoter region, and HUS1-001 (NotI)-R that used previously to amplify the gene.

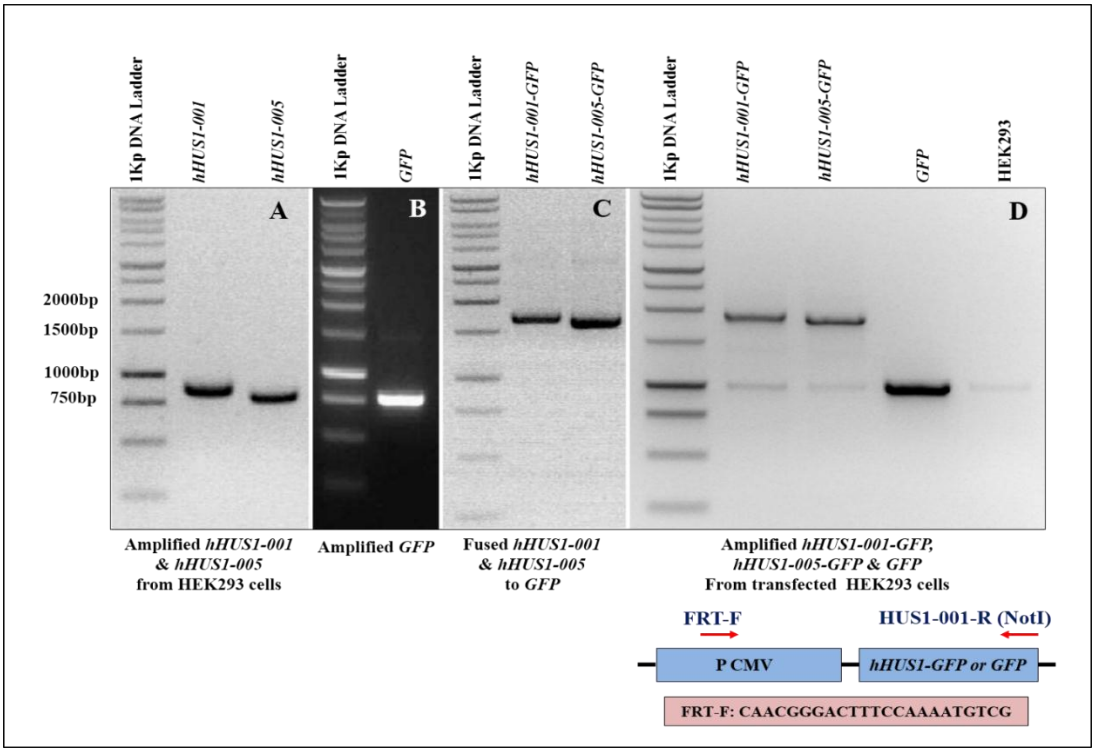

Figure 6-6: PCR products of the constructed *hHUS1-001, hHUS1-005* and *GFP* cassettes and their integration confirmation by PCR. (A) *hHUS1-001* and *hHUS1-005* genes were amplified from HEK293 cells, whereas **(B)** the *GFP* cassette was amplified from pAW8NdeI-GFP. **(C)** The two *hHUS1* gene fragments were fused to the *GFP* tag by fusion PCR, and cloned into the pcDNA5/FRT vector. Thereafter, the three cassettes *hHUS1-001-GFP, hHUS1-005-GFP* and *GFP* itself were transfected into HEK293 cells. Stable cell lines of each transfection were selected using hygromycin. **(D)** The genes' integration was confirmed by genomic PCR using the primers FRT-F (binds in the CMV promoter and HUS1-001-R (NotI), which was previously used to amplify the genes.

The integration of *hHUS1-001-GFP, hHUS1-005-GFP* and *GFP* into HEK293 cells was followed by the extraction of the whole cell proteins (Figure 6-7, A). The extracts were analyzed by 10% SDS-PAGE and Western Blot. The nitrocellulose membranes were probed with either anti-GFP or the monoclonal anti-HUS1 antibody. The extracts, which were probed with the anti-GFP antibody, showed a new band specific for either

hHUS1-001-GFP or hHUS1-005-GFP. For reasons, which remained unresolved, there was no signal for the GFP protein despite of its confirmed integration by PCR. Un-transfected HEK293 cells were negative for the GFP signal. When the membranes were probed with anti-HUS1 antibody, I noticed bands for both the recombinant proteins and the endogenous hHUS1 protein in both *hHUS1-001-GFP* and *hHUS1-005-GFP* cells. Whereas only endogenous hHUS1 was recognized in *GFP* and HEK293 cells. The western blot (Figure 6-7) revealed extra bands located in between the recombinant and endogenous HUS1 proteins. These might represent breakdown products of the hHUS1-GFP recombinant proteins. Another possibility, that the endogenous hHUS1 protein underwent significant post-translational modifications when the hHUS1-001-GFP or the hHUS1-005-GFP protein was overexpressed. Interestingly, the extent of these modifications was much less in the *hHUS1-005-GFP* cells. These slower migrating protein bands could be produced by phosphorylation or the addition one-10kDa ubiquitin moiety in the case of HUS1-001-GFP (Figure 6-7, A). Since the expression levels of the endogenous hHUS1 protein were much more strongly reduced in *hHUS1-001-GFP* cells than in *hHUS1-005-GFP* cells, the engineered hHUS1-GFP fusion protein may replace hHUS1 in the RAD9-RAD1-HUS1 complex, which could lead to the modification and degradation of the endogenous protein. Since this modification was strongly reduced upon expression of hHUS1-005-GFP (Figure 6-7, A), the N-terminally truncated protein may not interfere with the assembly of the ring to the same extent as the full-length protein.

Cell fractionation of *hHUS1-001-GFP, hHUS1-005-GFP, GFP* and HEK293 cells (Figure 6-7, B) showed that the majority of hHUS1 and hHUS1-001-GFP are in the nuclear fraction with a lower concentration in the cytoplasmic fraction. While the recombinant hHUS1-001-GFP protein mirrored the distribution of the endogenous protein, hHUS1-005-GFP resided mainly in the cytoplasm. Interestingly, modification of the endogenous hHUS1 took place in both the cytoplasm and the nucleus.

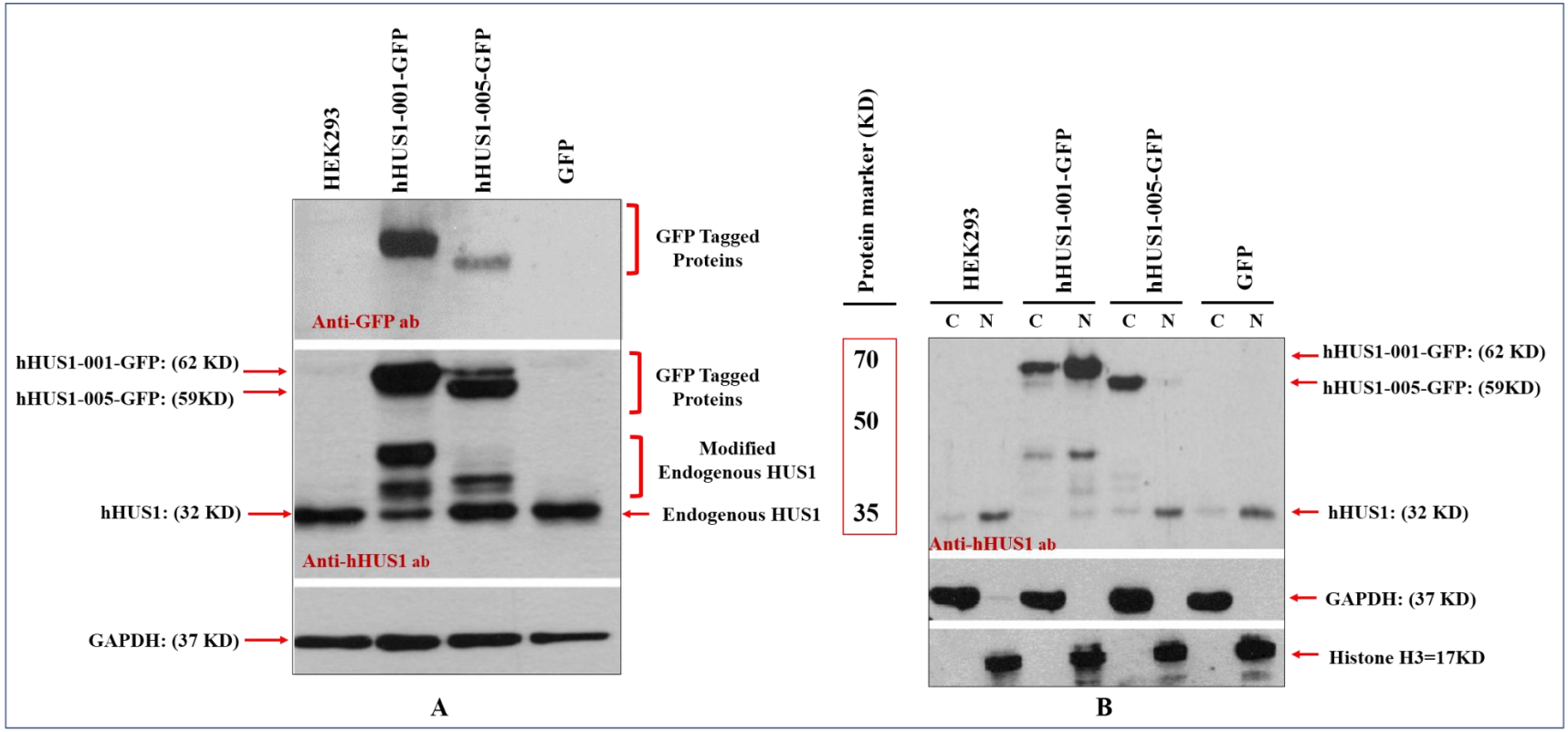

Figure 6-7: Western Blots of hHUS1-001-GFP, hHUS1-005-GFP and GFP proteins. A: whole cell extracts of the three stable cell lines and HEK293 cells as a negative control. The top panel shows the engineered proteins probed with the anti-GFP antibody. There was no signal for the GFP protein itself. The middle panel shows the same extracts probed with the monoclonal anti-HUS1 antibody. Both recombinant and endogenous hHUS1 in all cell lines and HEK293 cells were recognized by the antibody. *hHUS1-001-GFP* cells showed intensive modification of the endogenous hHUS1 protein and to a lesser extent in *hHUS1-005* cells comparing to *GFP* and HEK293 cells. **B:** Cells fractionation shows the accumulation of hHUS1-001-GFP and the endogenous protein in the nuclear fraction with a lower concentration in the cytoplasmic fraction. In contrast, the hHUS1-005-GFP protein was mainly in the cytoplasm and a very low amount was in the nucleus. (The predicted protein sizes are mentioned between two brackets, please refere to the protein marker for the observed protein size).

Immune-localization of the mentioned proteins was investigated using the GFP signal in cells fixed with 4% para-formaldehyde. While the hHUS1-001-GFP green signal was strong in the cytoplasm, expression of hHUS1-005-GFP resulted in no signal for GFP protein when compared to the low background signal in HEK293 cells (Figure 6-8). For yet unknown reasons, the immunolocalisation experiments were not consistent with the mainly nuclear fractionation of HUS1-001-GFP (Figure 6-7, B). Since I could not recognize the GFP signal in *hHUS1-005-GFP* cells properly without using more anti-GFP antibody, I did not use these cell lines for further experiments and decided to construct N-terminally *EGFP* tagged *hHUS1* cell lines.

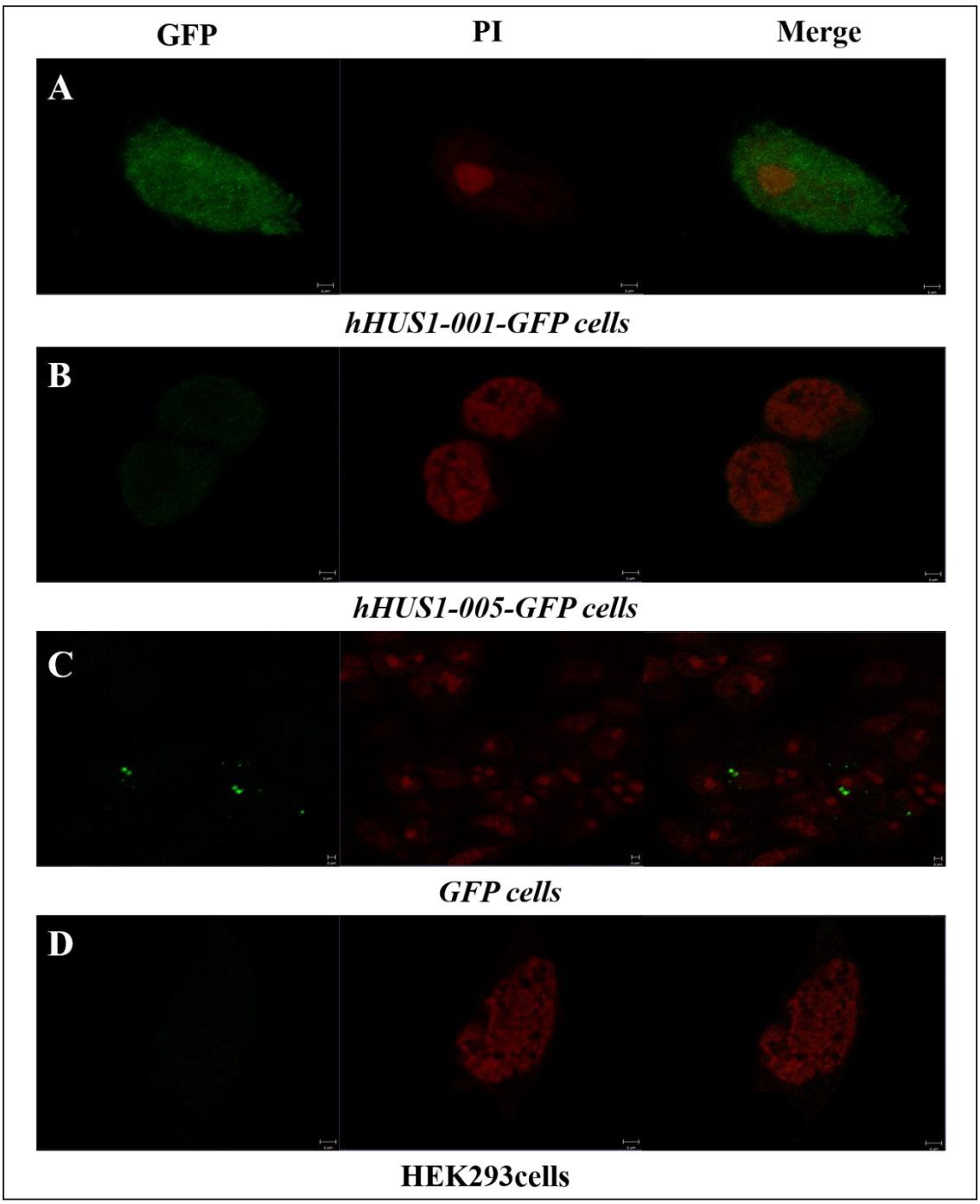

Figure 6-8: Immune-localization of hHUS1-GFP, hHUS1-005-GFP and GFP proteins. A: hHUS1-001-GFP cells show an intensive signal for the hHUS1-GFP tagged protein (Green) after fixation with para-formaldehyde, which is distributed all over the cells with a strong accumulation in the cytoplasm. **B:** hHUS1-005-GFP cells show a very weak cytoplasmic signal for the GFP tagged protein, which was as low as in the negative control (HEK 293 cells), **C & D:** GFP and HEK293 cells respectively. Cells DNA was stained with Propidium Iodide (Red) only (Scale bar= 2µm).

6.2.2 Construction of stable cell lines expressing N-terminally EGFP-tagged full-length hHUS1, its splice variants and hHUS1B

To overcome the lack of a GFP signal in the constructed cell lines expressing the C-terminally tagged proteins, I decided to re-construct N-terminally EGFP fusion proteins with full-length hHUS1, all its shorter splice variants and hHus1B. To achieve this, I amplified the mentioned genes from the HEK293 cDNA using the primers sets, which were used to amplify the full-length genes by RT-PCR in chapter 4 (Figure 6-9). This time the cassettes were cloned onto pcDNA5/FRT/TO, since HEK293 cells express Tetracycline repressor and LacZ-Zeocin fusion gene. Plasmids containing each gene were sent for sequencing and the sequence of the EGFP-HUS1 proteins was confirmed. Interestingly, the *hHUS1-011* gene showed the same sequence as curated in the Ensembl database but missed in frame 19 amino acids in the middle of the gene (Figure 6-10). This might indicate the existence of another, yet unknown splice variant within the collection of hHUS1 proteins. One of the sequenced plasmids had the *hHUS1-011* sequence with a stop codon placed a few amino acids downstream of the EGFP protein. This plasmid would express EGFP with the linker sequence and a few N-terminal hHUS1-011 amino acids. I considered this plasmid as a negative control for the *hHUS1* gene and a positive control for EGFP.

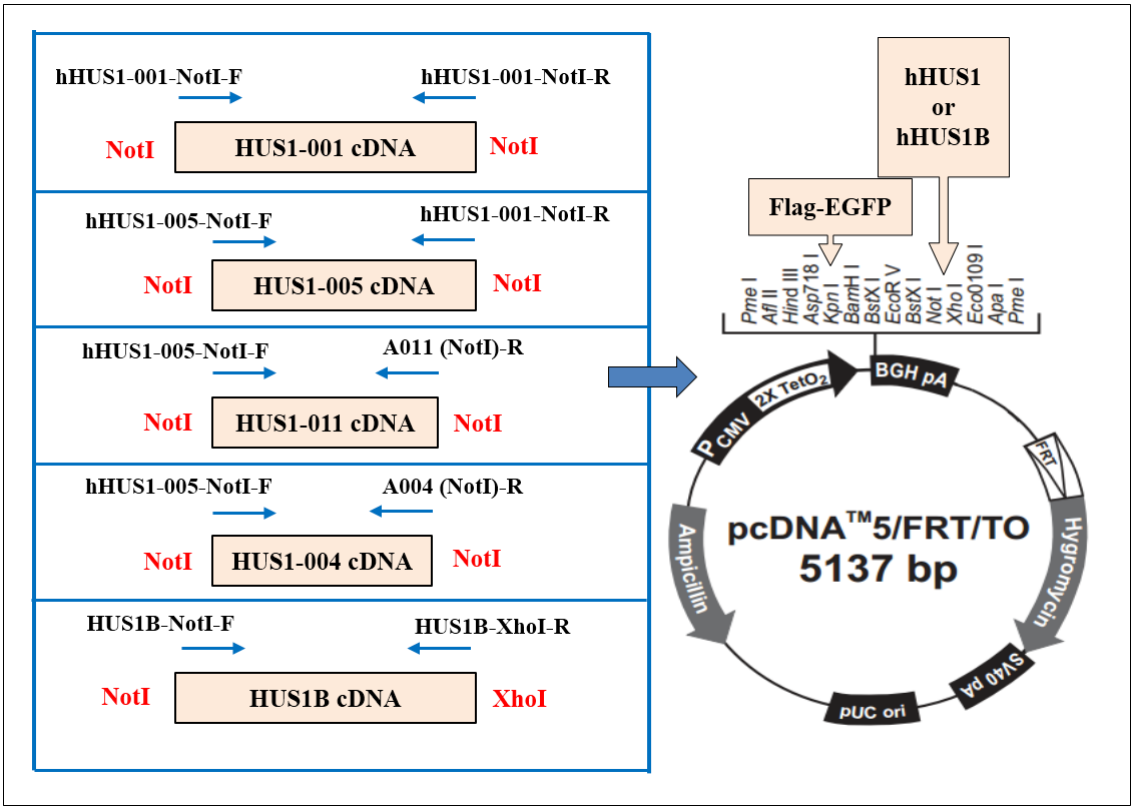

Figure 6-9: Schematic diagram of *hHUS1B, hHUS1* full length and its splice variants 005, 011 and 004. The mentioned genes were amplified from HEK293 cDNA by the indicated primers and were cloned using NotI cloning site into the pcDNA5/FRT/TO plasmid in frame with the N-terminal Flag-EGFP tag, which was cloned into the KpnI site.

```
Hus1-011_No_4_Protein MIAKLAKTCTLRISPDKLNFILCDKLANGGVSMWCELEQENFFNEFQMEG 50
Hus1-011_Protein      MIAKLAKTCTLRISPDKLNFILCDKLANGGVSMWCELEQENFFNEFQMEG 50
Hus1-011_Protein_No5  MIAKLAKTCTLRISPDKLNFILCDKLANGGVSMWCELEQENFFNEFQMEG 50
                      **************************************************

Hus1-011_No_4_Protein VSAENNEIYLELTSENLSRALKTAQNARALKIKLTNKHFPCLTVSVELLS 100
Hus1-011_Protein      VSAENNEIYLELTSENLSRALKTAQNARALKIKLTNKHFPCLTVSVELLS 100
Hus1-011_Protein_No5  VSAENNEIYLELTSENLSRALKTAQNARALKIKLTNKHFPCLTVSVELLS 100
                      **************************************************

Hus1-011_No_4_Protein MSSSSRIVTHDIPIK------------------VSIYLPVLKTMKSVVE 131
Hus1-011_Protein      MSSSSRIVTHDIPIKVIPRKLWKDLQEPVVPDPDVSIYLPVLKTMKSVVE 150
Hus1-011_Protein_No5  MSSSSRIVNHDIPIK------------------VSIYLPVLKTMKSVVE 131
                      ********.******                  ***************

Hus1-011_No_4_Protein KMKNISNHLVIEANLDGELNLKIETELVCVTTH 164
Hus1-011_Protein      KMKNISNHLVIEANLDGELNLKIETELVCVTTH 183
Hus1-011_Protein_No5  KMKNISNHLVIEANLDGELNLKIETELVCVTTH 164
                       *********************************
```

Figure 6-10: Alignment of the DNA sequences of human *hHUS1-011* as curated in the Ensembl database and two plasmids (no 4 & 5) which contain the *hHUS1-011* sequence amplified from HEK293 cDNA with the 19aa in frame deletion. The splice sites VEL/LSM and DPD/VSI are indicated. The alignment was produced with Clustal Omega: (http://www.ebi.ac.uk/Tools/msa/clustalo/).

The pcDNA5/FRT/TO plasmids that carried the constructed genes were then transfected into the Flp-In™ T-Rex™-293 cells to establish the stable cell lines. The integration of the fusion genes was confirmed by amplifying the corresponding cassettes from genomic DNA using a forward primer, which primes in the CMV promoter and a gene-specific reverse primers (Figure 6-11).

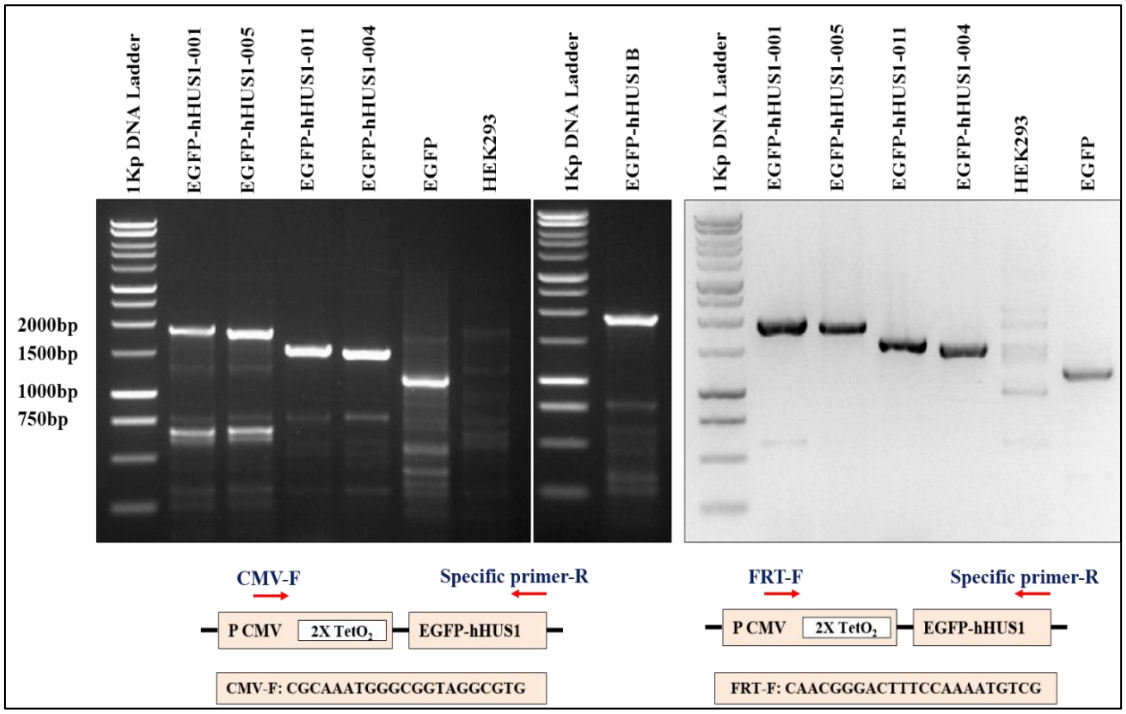

Figure 6-11: Confirmation of the integration of *EGFP-hHUS1, EGFP-HUS1-005, EGFP-HUS1-011, EGFP-HUS1-004* and *EGFP-hHUS1B*. The confirmation was carried out using genomic PCR and the indicated primers.

6.2.3 Features of the N-terminally EGFP-tagged hHUS1 protein, its splice variants and hHUS1B

To study the recombinant proteins, I started with a time course of Doxycycline induction, to define the time when each protein expression would peak (Figure 6-12). In my experiments, it seemed that the protein expression is fully induced at the 4hr time point. However, it is mentioned in the Flp-In system manual that expression of the recombinant proteins starts at 2hr post-induction.

As observed in the earlier experiments using the C-terminal GFP fusion constructs (Figure 6-7), overexpression of full-length EGFP-hHUS1 in the transfected cells seemed to interfere with the endogenous hHUS1 protein expression as its levels declined upon induction of the recombinant protein (Figure 6-12). That since none of the other fusion proteins resulted in a similar decline of the endogenous protein; the recombinant protein may substitute for the endogenous hHUS1 in the RAD9-RAD1-HUS1 complex. Interestingly, the endogenous hHUS1 protein is modified differently in both N and C-

terminally tagged hHUS1 cell lines. While expression of the C-terminally tagged protein produced higher molecular weight bands (Figure 6-7), these bands were not observed upon expression of the N-terminally tagged protein (Figure 6-12). Since I could not find an efficient anti-hHUS1B antibody for western blot use, I used the anti-GFP antibody to detect the recombinant protein (Figure 6-12). Figure 6-13 shows the actual sizes of all recombinant proteins, which were probed with the anti-HUS1 antibody or the anti-GFP antibody. The smaller bands detected by the anti-HUS1 antibody, may be C-terminal degradation products of the over-expressed fusion proteins since they were not detected with the anti-GFP antibody. The EGFP tagged proteins showed two bands running very closely to each other (Figure 6-13). They are most likely caused by phosphorylation of the EGFP moiety of the fusion protein. Isoelectric focusing revealed that EGFP is phosphorylated in the transfected human cells (Saad Aljohani, personal communication).

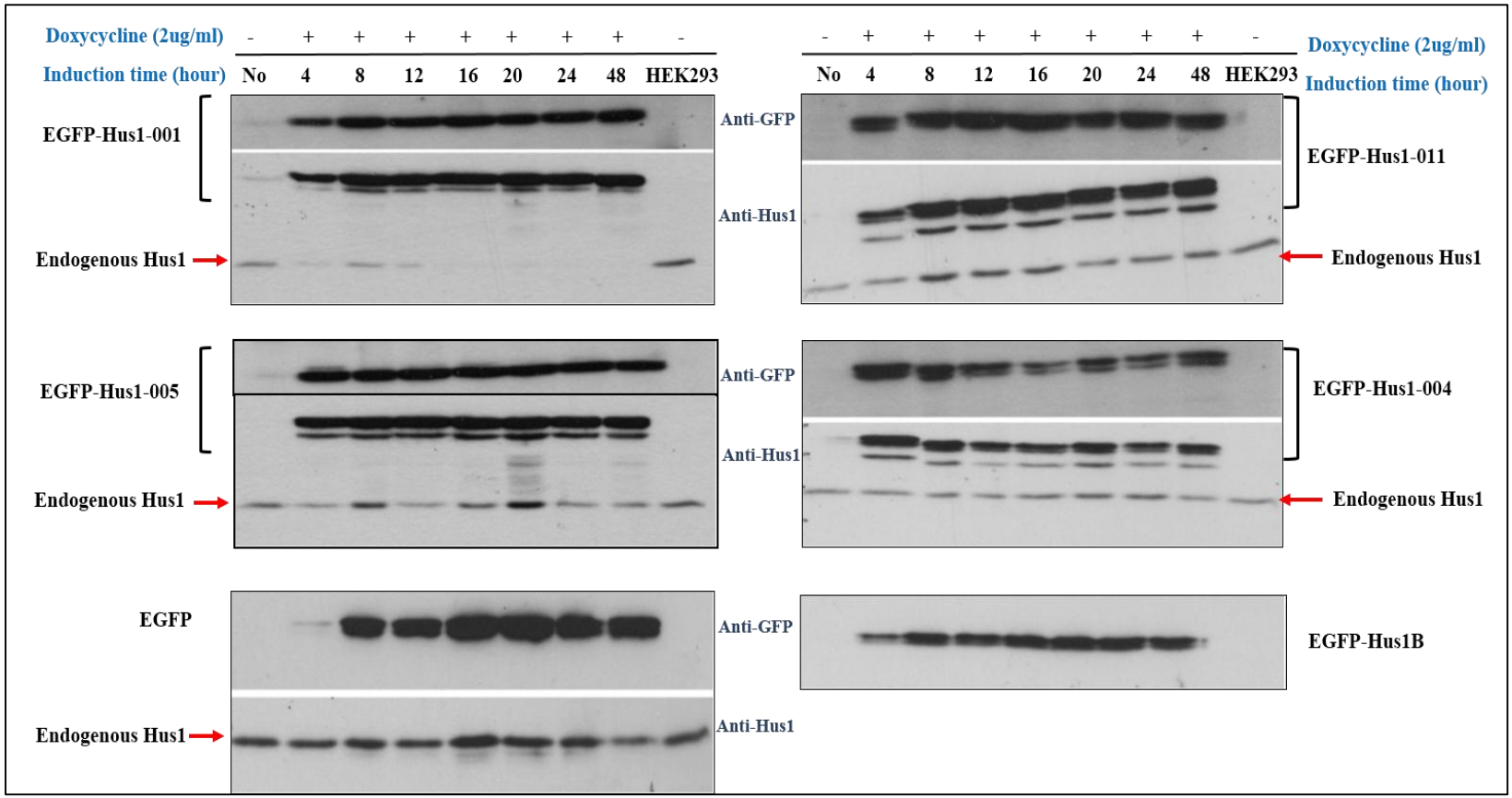

Figure 6-12: Doxycycline time course induction of hHUS1B and full-length hHUS1 and its shorter isoforms. The time course induction showed that the protein expression induction started at the 4hrs time point or may be earlier as stated in the manual instructions. At twelve hours post-induction expression peeked for most of fusion proteins. Only expression of EGFP-hHUS1 full-length interfered with the expression of the endogenous hHUS1 protein. (Please refere to Figure 6-13 for the predicted & observed proteins sizes).

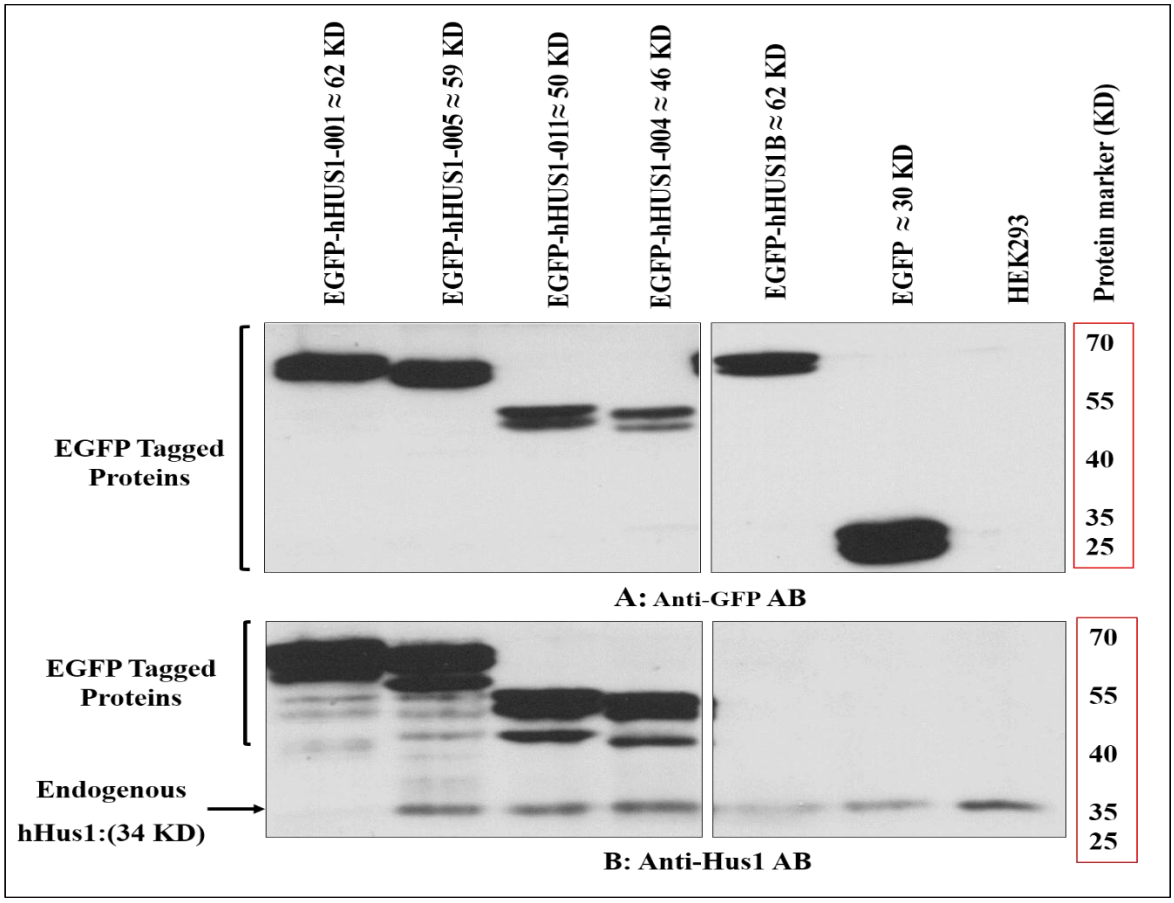

Figure 6-13: Whole cell extracts of EGFP-hHUS1B, full-length hHUS1 and its splice variants. The proteins were extracted at 20hr post induction with doxycycline. Western blot membranes were probed with either the monoclonal anti-HUS1 antibody or the anti-GFP antibody. (The predicted protein sizes are mentioned between two brackets, please refere to the protein marker for the observed protein size).

To know the stability of the recombinant proteins post doxycycline removal, I induced the cells for 16 hour, followed by washing the cells twice with 1xPBS to remove the antibiotic residues. Total protein extracts were prepared at 0, 4, 8, 24 and 53 hours post the removal of the antibiotic, and analyzed by SDS-PAGE and Western blot (Figure 6-14). This experiment showed that the recombinant proteins were stable up to 53 hours, which may related to the stability of the proteins or may be because the cells needed to be split to remove the already expressed proteins. The cells in this experiment were not split. An alternative explanation could be the imperfect switch off the Tetracycline repressor system after the removal of the inducer, or that not all inducer was removed from the cells.

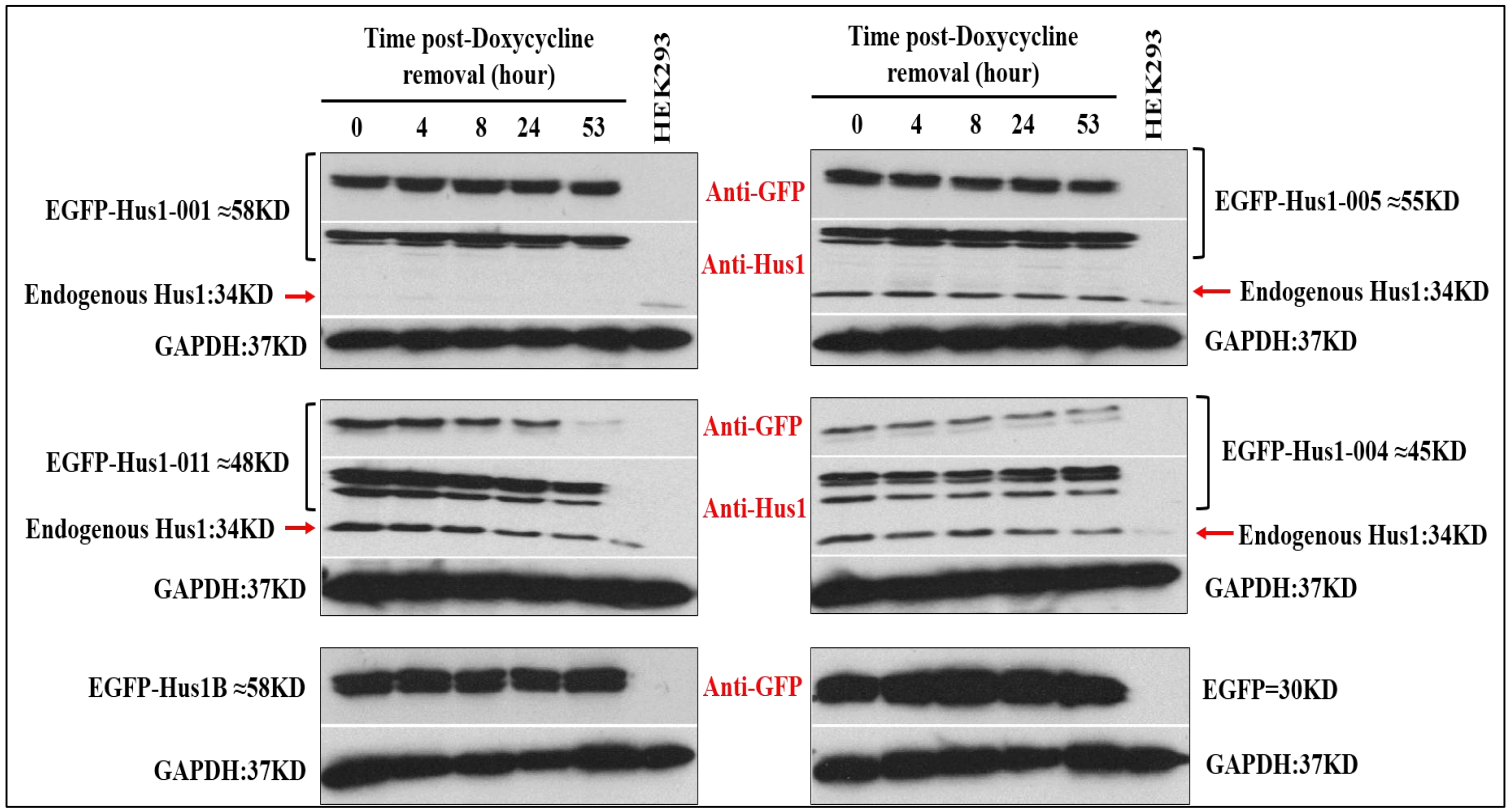

Figure 6-14: Stability of the induced recombinant proteins after the removal of doxycycline. The constructed stable cell lines were treated with doxycycline (2µg/ml) for 16hr followed by the removal of the antibiotic by washing the cells twice with 1xPBS. Whole cell extracts were prepared at the indicated time points, analyzed by SDS-PAGE and Western blot and compared with the expression level of the GAPDH protein. It seems that the induced proteins are stable up to 53 hours post removal of the doxycycline. (Please refere to Figure 6-13 for the predicted & observed protein sizes).

6.2.4 hHUS1, its splice variants and hHUS1B form large protein complexes with other cellular proteins

In addition to the previous analysis of the recombinant proteins (hHUS1-001, hHUS1-005, hHUS1-011, hHUS1-004 and hHUS1B), I fractionated total protein extracts using Size Exclusion Chromatography (Figure 6-15) to find out whether they interact with 9-1-1 complex, which appears to have a molecular weight that ranges between 200-500 kDa in *S.pombe* (Caspari, et.al. 2000). All hHUS1 recombinant proteins (hHUS1-001, hHUS1-005, hHUS1-011 and hHUS1-004) showed a molecular weight that range between 200-700 kDa. Using antibodies against hRAD9, hRAD1 and hHUS1, I could detect the endogenous 9-1-1 complex in untreated HEK293 cells (Figure 6-15, bottom panels). Interestingly, while hRAD9 and hHUS1 eluted in the high molecular weight section (200-700kDa), hRAD1 showed two elution peaks, one at 700kDa and a second, smaller peak at 150kDa. Interestingly, all hHUS1 variants eluted with a molecular size, which is above their monomeric size, suggesting that they assemble in larger protein complexes. While all hHUS1 proteins showed a wide elution peak, hHUS1B eluted in a sharp peak in fractions 8-10 (Figure 6-15). CDC2 kinase and the p21WAF1/CIP1 proteins were used as a loading control. CDC2 eluted as an approximately 100KD protein, which is consistent with the molecular weight of the CDK1-CyclinB (CDC2-CyclinB) complex (CDC2=32KD and CyclinB= 48-60KD, total is 82-94KD). The CDK inhibitor p21 WAF1/CIP1 peaked between 500-200KD.

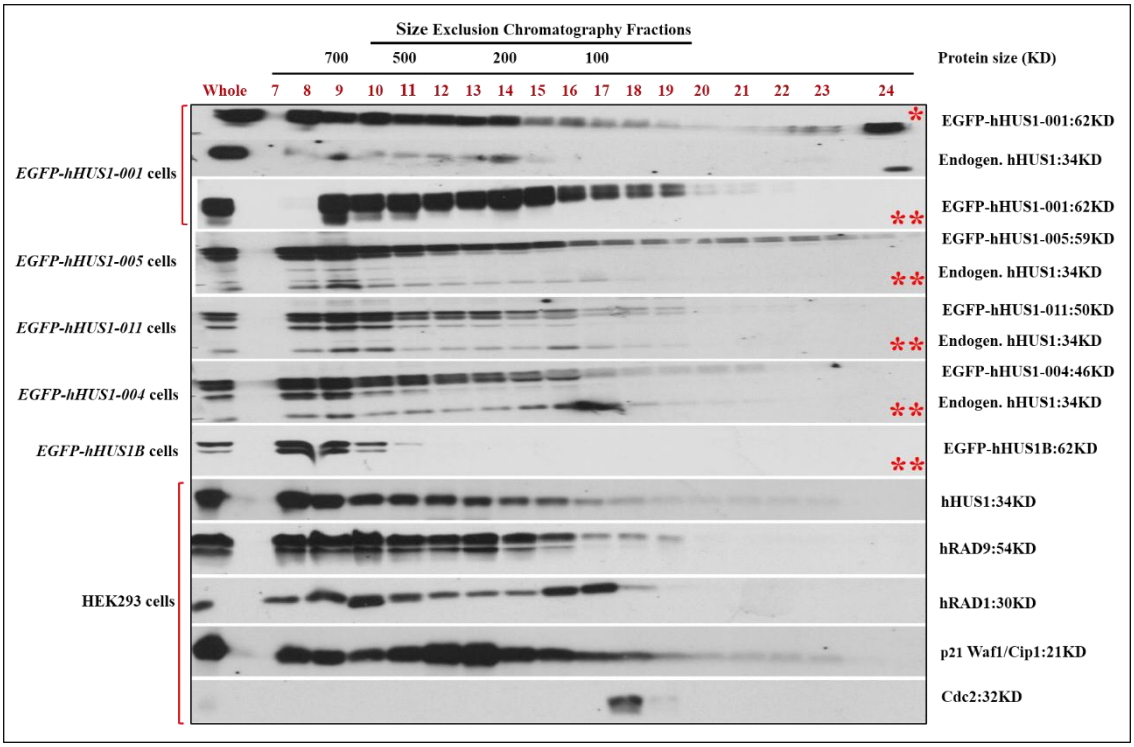

Figure 6-15: hHUS1, its variants and hHUS1B recombinant proteins contribute to high molecular weight complexes. *hHUS1* and its variants, and *hHUS1B* cell lines were induced with Doxycycline (2µg/ml) for either 8 or 24 hours, followed by extracting the total cellular proteins, which were fractionated on a Superdex200 HR column. hHUS1 and its alternative splice variants seemed to contribute to large protein complexes ranging from 200-700 kDa. In contrast, hHUS1B eluted in a sharp peak at around 600-700kDa. CDC2 kinase and the CDK inhibitor p21 WAFI/CIPI were used as a loading control. **(*):** cells were induced for 8hr with doxycycline. **(**):** cells were induced for 24hr with doxycycline.

6.2.5 The cellular localization of hHUS1, its splice variants and hHUS1B

To analyze the cellular localization of the N-terminally EGFP fusion proteins, I started by staining the cells with Propidium Iodide (DNA stain) only. As in the case of the C-terminally GFP tagged proteins (Figure 6-8), the EGFP signal was very low (Figure 6-16). The only exceptions were EGFP-hHUS1B and EGFP. Interestingly, the EGFP-hHUS1B protein appeared to be in the cytoplasm and a defined region within the nucleus, which could be the nucleolus (Figure 6-16). EGFP was present in the cytoplasm and the nucleus, but did not show the nucleolar signal. A nucleolar localization of hHUS1B

would be consistent with the nucleolar localization of recombinant Rad9B (Pe´rez-Castro & Freire, 2012).

To enhance the fluorescent green signal of the EGFP-tagged proteins in the transfected cells, I incubated the fixed cells first with an anti-GFP primary antibody in combination with a secondary anti-mouse Alexa-Flouro488 antibody in addition to the Propidium Iodide stain. Cells were stained in parallel with either the monoclonal anti-hHUS1 or the polyclonal anti-hHUS1B primary antibodies in a combination with a secondaryAlexa-Flouro633 antibody to detect both endogenous and exogenous hHUS1 and hHUS1B proteins, respectively (Figures 6-17 & 6-18). Staining the cells with the anti-GFP antibody first did slightly improve the EGFP fluorescent signal and showed that all hHUS1 proteins are mainly in the cytoplasm in untreated HEK293 cells (Figure 6-17). In contrast, staining the cells with the anti-hHUS1 (Figure 6-17) and anti-hHUS1B antibodies (Figure 6-18) produced much stronger signals, which overlapped with the EGFP signal in all transfected cells. While full-length EGFP-hHUS1 and the endogenous hHUS1 were present in the cytoplasm and to a lesser extent in the nucleus, the cytoplasmic signal was much stronger when cells expressed the truncated variants EGFP-hHUS1-005, EGFP-hHUS1-011 or EGFP-hHUS1-004 (Figure 6-17). This implies that the variants reside mainly in the cytoplasm. This conclusion is supported by the cell fractionation experiments conducted with the C-terminal GFP fusion proteins (Figure 6-7, B). As observed in my first set of experiments using only the DNA dye Propidium Iodide, recombinant EGFP-hHUS1B was present in the cytoplasm and the nucleoli (Figures 6-16, 6-18). This nucleolar staining was not evident in untransfected HEK293 cells suggesting that it is linked with the over-expression of the EGFP-hHUS1B fusion protein. Normal cell may have hHUS1B in the nucleolus, but the amount may be much lower. A very similar link between over-expression and nucleolar staining was reported for hRAD9B (Pe´rez-Castro & Freire, 2012).

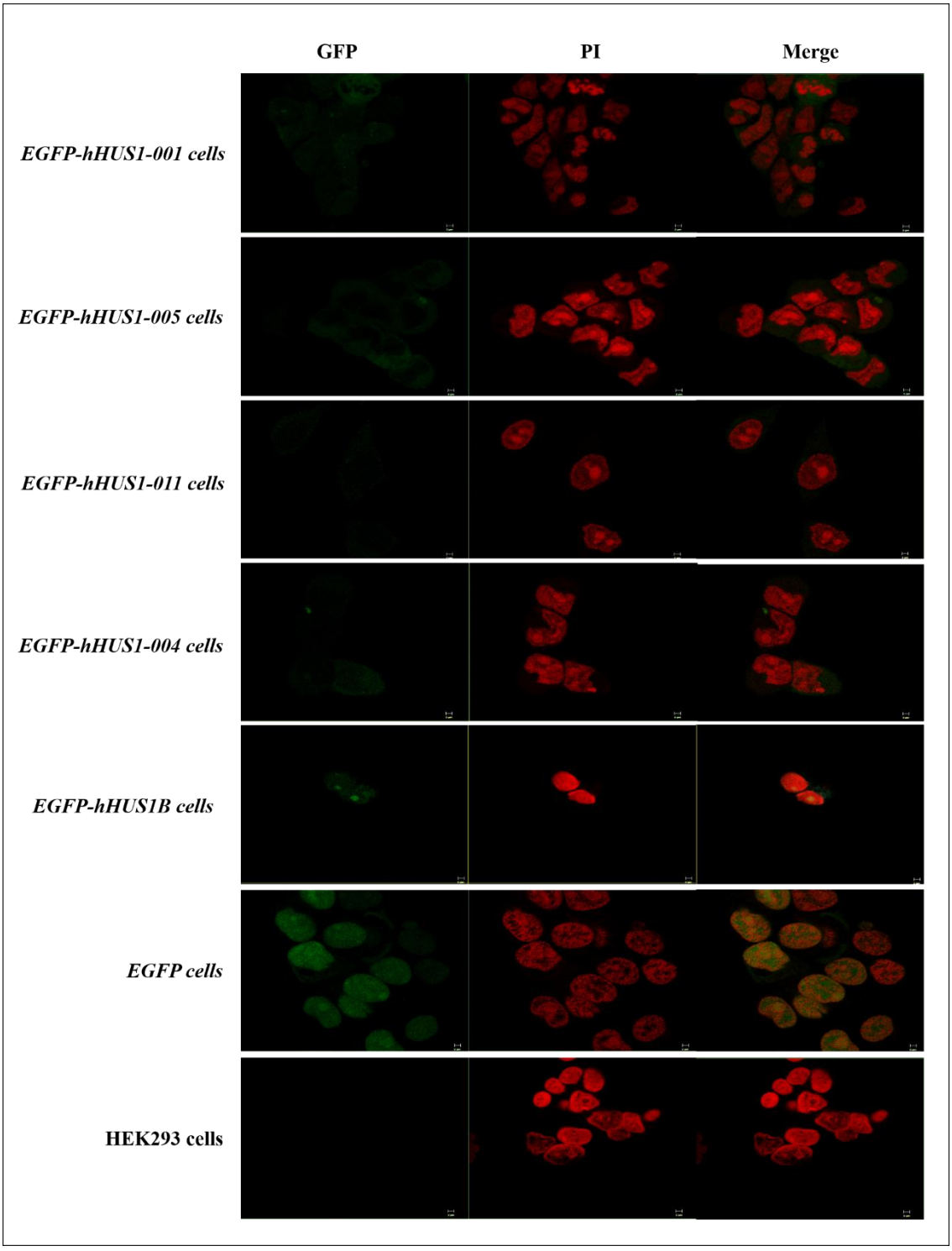

Figure 6-16: Immune staining of *EGFP tagged-hHUS1* and *hHUS1B* stable cell lines and non-transfected HEK293 cells with Propidium Iodide only. Cells were grown on cover slips for overnight, fixed with 4% paraformaldehyde (PFA) and stained with the DNA dye Propidium Iodide only. All cells were slightly fluorescent except the EGFP and hHUS1B clones were the EGFP signal was clearly visible. While EGFP was present in the cytoplasm and the nucleus, hHUS1B was present in the cytoplasm and in a defined region within the nucleus. hHUS1 and its splice variants seemed to reside mainly in the cytoplasm but the EGFP signal was very low. (Scale bar= 2µm). (Images were obtained by Zeiss LSM710 Confocal Microscope with a 63× objective, and analyzed by Zen2010 software and processed by Photoshop (Adobe)).

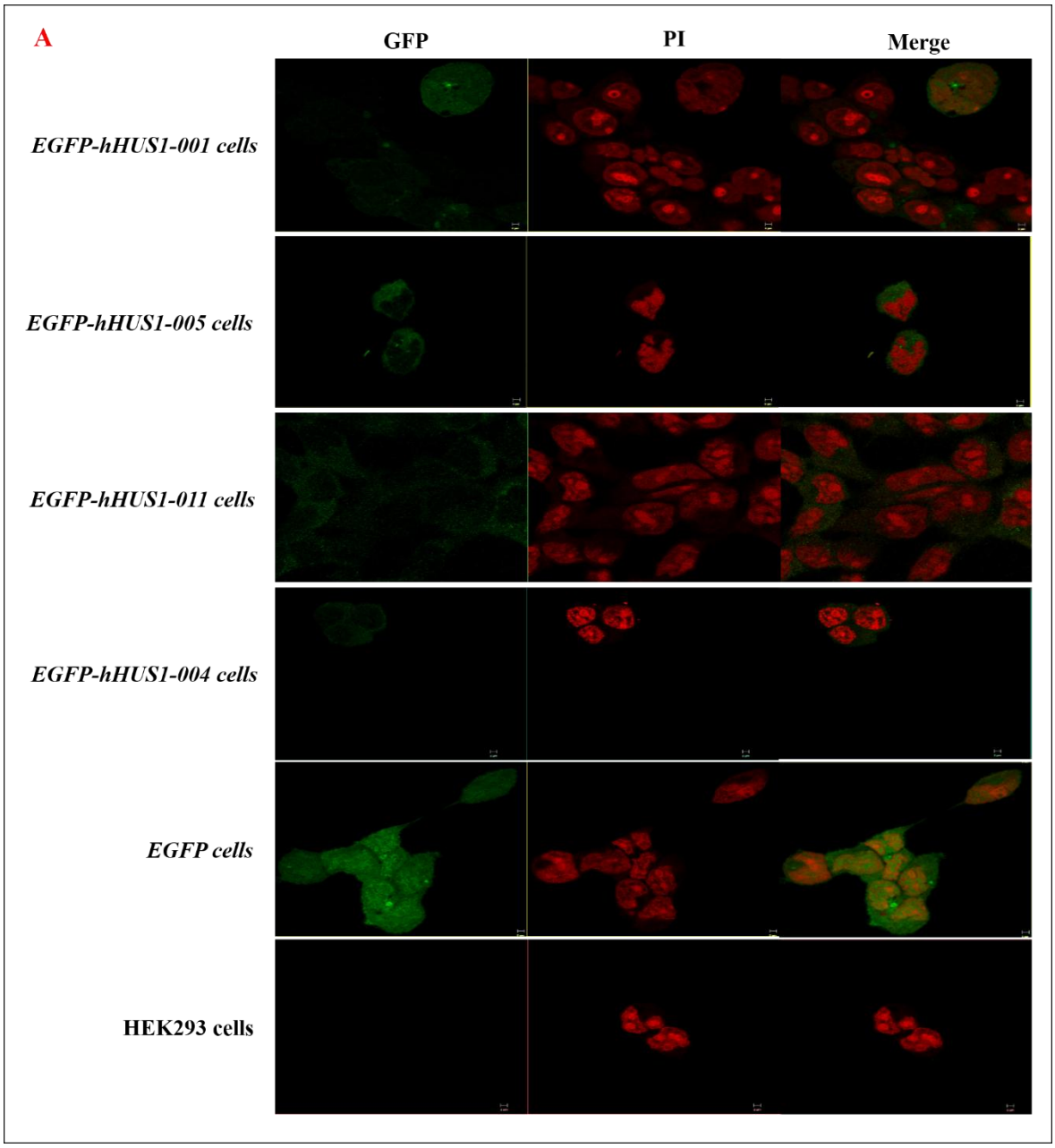
A
GFP
PI
Merge
EGFP-hHUS1-001 cells
EGFP-hHUS1-005 cells
EGFP-hHUS1-011 cells
EGFP-hHUS1-004 cells
EGFP cells
HEK293 cells

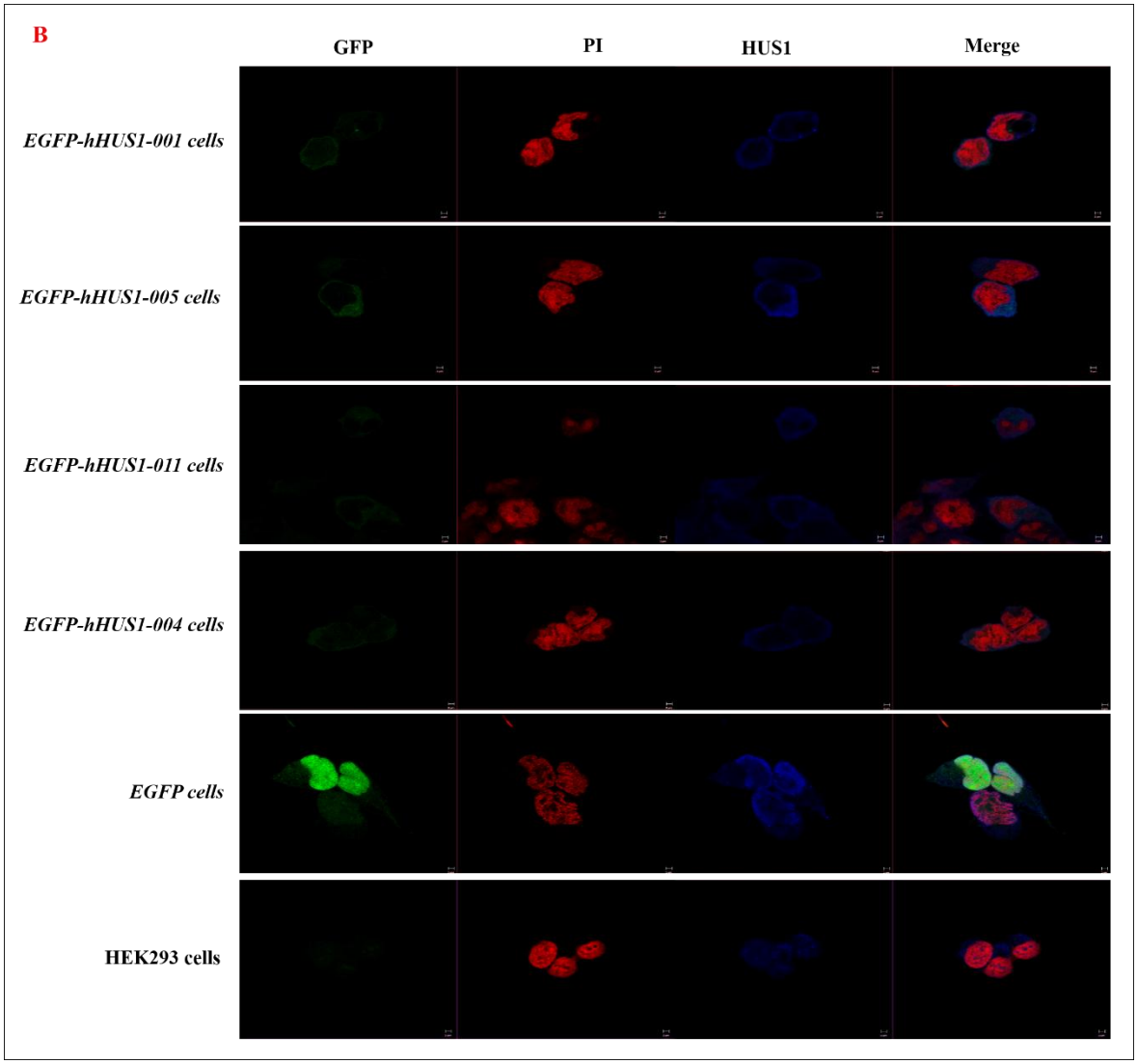

Figure 6-17: Immune-staining of *EGFP tagged-hHUS1* stable cell lines and non-transfected HEK293 cells with GFP & HUS1 antibodies. Cells were grown onto coverslips for overnight, then fixed with 4%PFA and stained with either anti-GFP antibody and Alexa Fluro488 (A) or anti-hHUS1antibody and Alexa Fluro633(B) in addition to Propidium Iodide. The EGFP signal was not enhanced significantly after the GFP staining in all cell lines with exception of *EGFP* cells, since I needed to use higher settings of 488nm laser light. (Scale bar = 10µm). (Images were obtained by Zeiss LSM710 Confocal Microscope with a 63× objective, and analyzed by Zen2010 software and processed by Photoshop (Adobe)).

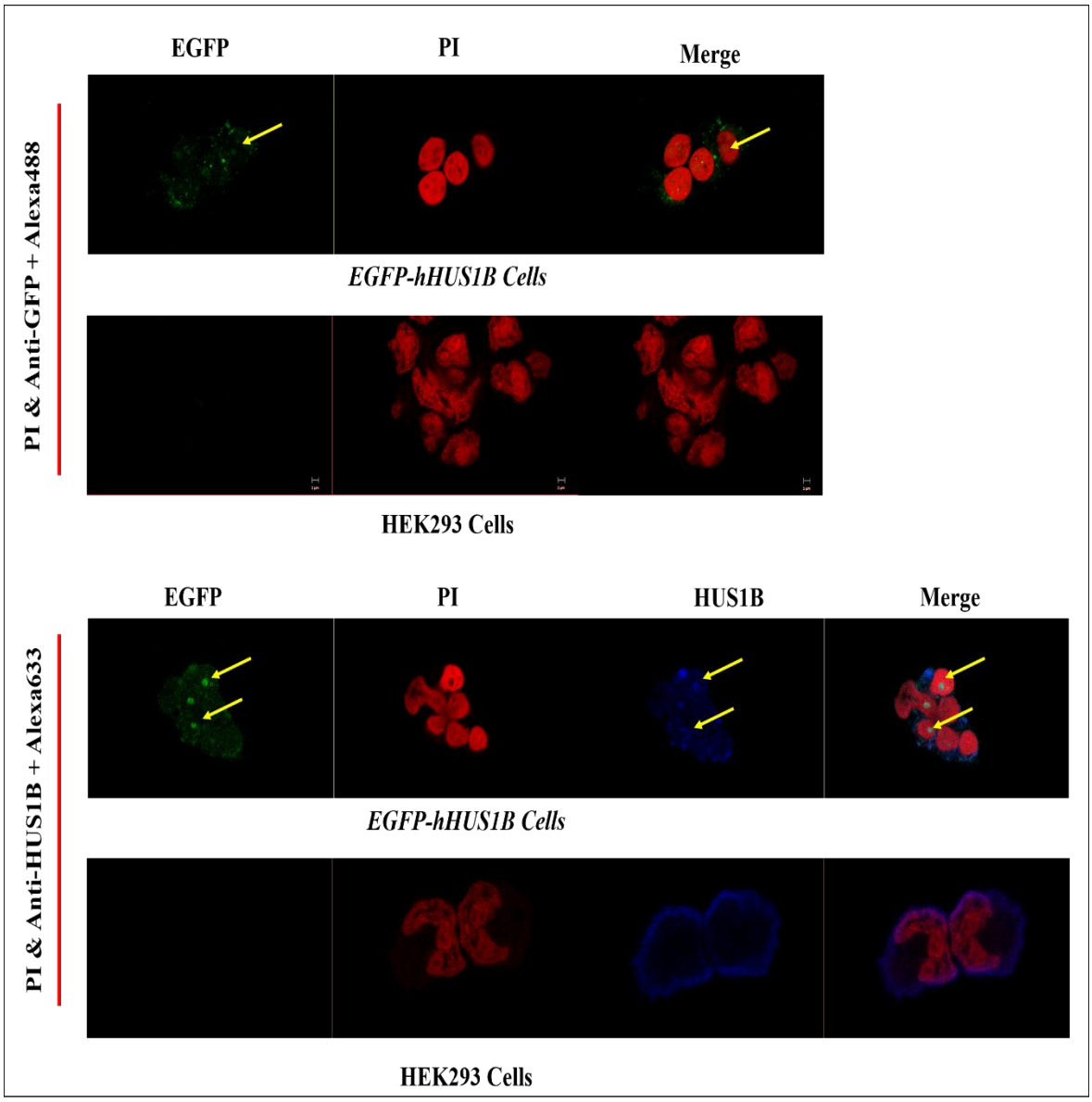

Figure 6-18: Immune staining of the EGFP tagged-hHUS1B protein and non-transfected HEK293 cells with either anti-GFP or anti-hHUS1B antibodies. Cells were grown on cover slips for overnight, fixed with 4% PFA and stained with either the anti-GFP antibody in combination with Alexa-Fluro488 (top panels) or the anti-hHUS1B antibody in combination with Alexa-Fluro633 (bottom panel) in addition to Propidium Iodide stain. The EGFP signal was not significantly enhanced after the anti-GFP staining since I needed to use higher settings of the 488nm laser intensity to obtain a signal. The anti-hHUS1B signal was much stronger. Interestingly, recombinant hHUS1B was resides in the nucleoli (yellow arrows), while this was not very evident in the non-transfected HEK293 cells (Scale bar = 2µm). (Images were obtained by Zeiss LSM710 Confocal Microscope with a 63× objective, and analyzed by Zen2010 software and processed by Photoshop (Adobe)).

6.2.6 hHUS1 and hHUS1B may contribute to the DNA damage response upon UV treatment

To find out whether the recombinant proteins respond to DNA damage, cells expressing EGFP-hHUS1, its isoforms and EGFP-hHUS1B cells were induced with Doxycycline for 16 hours, exposed to UV light at 40J/m^2 and left to recover for 2 hours at 37^{o}C. Cells were fractionated for protein analysis or fixed with 4% PFA for immune staining. To have a control for the efficacy of the UV treatment, I used an anti-phospho Chk1 antibody, which detects the DNA damage induced modification of the checkpoint kinase at serine-345 (Liu, et.al. 2000). The effectiveness of the UV treatment was evidenced by the change of the cellular localization of the S-345 phosphorylated Chk1 kinase. As reported previously (Wilsker, et.al.2008), S-345 phosphorylated Chk1 in the nucleus in untreated cells, which may be linked with its essential replication function. However, in the response to UV damage, the signal became much stronger and it was found in the cellular fraction since the activated Chk1 kinase is known to relocate to the cytoplasm to regulate Cdc25 phosphatase (Sanchez, et.al. 1997; Zeng, et.al. 1998; Mailand, 2000; Oe, et.al. 2001). Regarding the recombinant proteins, there were no differences in the fractionation pattern upon UV treatment since EGFP-hHUS1 and EGFP-hHUS1B were present in both cytoplasmic and nuclear fractions. EGFP-hHUS1-005, EGFP-hHUS1-011 and EGFP-hHUS1-004 were mainly in the cytoplasmic fraction, and EGFP was restricted to the cytoplasm. Interestingly, immune staining of the cells showed some noticeable differences from Western blot results. While EGFP-hHUS1-011 and EGFP-hHUS1-004 showed no changes upon the treatment with UV, EGFP-hHUS1-001 relocated to the nucleus (Figure 6-20, top panels). This change in cellular localization was very clear when the anti-GFP antibody was used to detect the recombinant protein. It was however less obvious when the anti-HUS1 antibody was used. The latter could indicate that the hHUS1 moiety of the fusion protein is not accessible to the antibody when the 9-1-1 complex relocated to the nucleus. Given the structure of the 9-1-1 ring, the EGFP part of the fusion protein may protrude from the ring thereby allowing for easy detection. The re-localization of EGFP-hHUS1-001 is consistent with its incorporation into the 9-1-1 ring and loading of the ring onto damaged DNA. Recombinant EGFP-hHUS1-005, which lacks the first 21 amino acids of the hHUS1 protein (Figure 6-4), showed an

unusual nuclear localization in long filaments running through the nuclear matrix (Figure 6-20, lower panels). The intensity of these structures seemed to increase in the response to UV light.

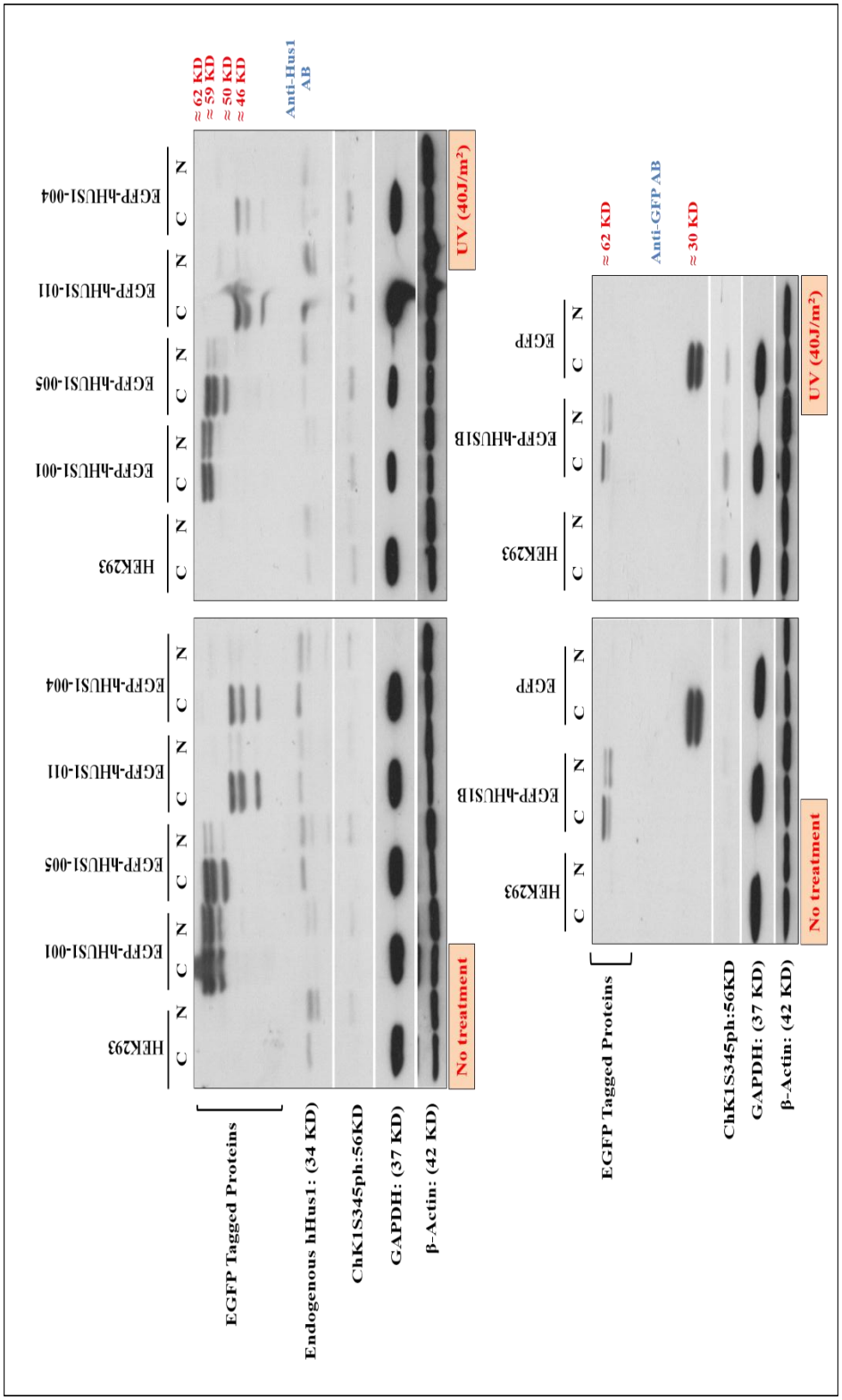

Figure 6-19: UV treatment of EGFP tagged *hHUS1* and *hHUS1B* cell lines. Cells were induced with doxycycline for 16 hours prior to their exposure to 40J/m^2 of UV light. Cells were left to recover for 2 hours at 37ºC. Protein extracts were prepared at the end of the recovery time and subjected to the cell fractionation protocol. The Western blot results revealed that there were no differences in the cellular fractionation pattern for the recombinant proteins upon the UV treatment. Please note that the serine-345 phosphorylated Chk1 kinase relocated to the cytoplasmic fraction post UV treatment. (The predicted protein sizes are mentioned, please refere to the Figure 6-13 for the observed protein size).

Cells immune staining showed variations for some proteins localization that are different from what was explained by Western blot. Figure 6-20 showed nuclear re-localization of EGFP-hHUS1-001 as a DNA damage response that caused by UV exposure. Whereas, the localization of EGFP-hHUS1-005 protein was consistent with the Western blot profile. Interestingly, EGFP-hHUS1-005 protein showed a unique distribution in the nucleus as a network of unknown structures, which exists independently from the exposure to a DNA damage agent.

While EGFP-hHUS1-011 remained in the cytoplasm, EGFP-hHUS1-004 did show a low number of nuclear spots upon UV treatment but remained largely in the cytoplasm (Figure 6-21). In combination with the Western blot data, these observations imply that both short hHUS1 variants reside largely in the cytoplasm independently of UV-induced DNA damage.

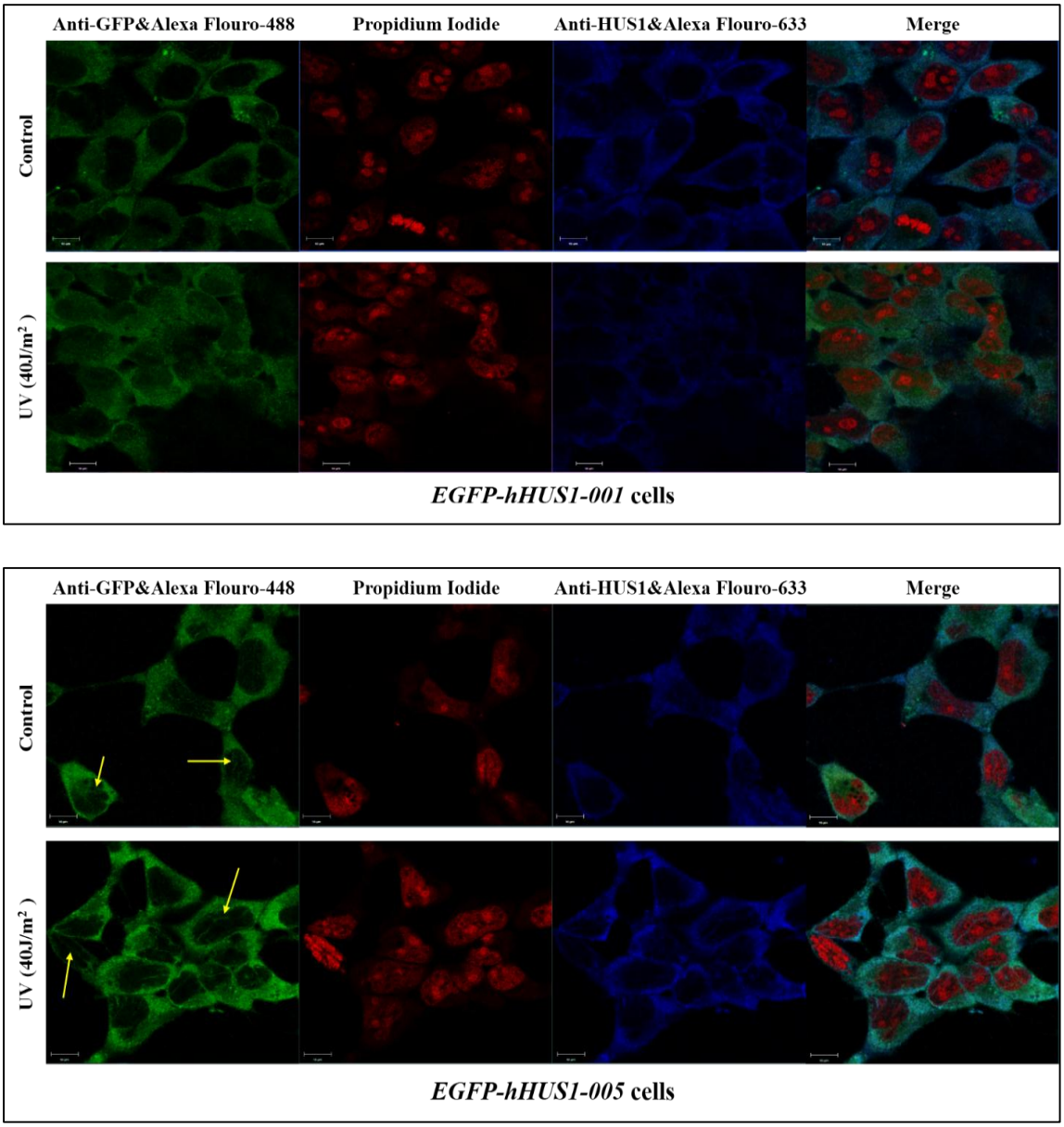

Figure 6-20: Cell localization of EGFP-hHUS1-001 and EGFP-hHUS1-005 proteins upon UV treatment. Cells were treated as for the protein extraction (Figure 6-19). EGFP-hHUS1-001 showed nuclear re-localization in the response to UV light, which was very evident when the anti-GFP antibody was used. It was however less obvious when the anti-HUS1 antibody was used. Interestingly, EGFP-hHUS1-005 was present in the nucleus in thin filaments, the intensity of which slightly increased after UV treatment, (yellow arrows). (Scale bar=10µm). (Images were obtained by Zeiss LSM710 Confocal Microscope with a 63× objective, and analyzed by Zen2010 software and processed by Photoshop (Adobe)).

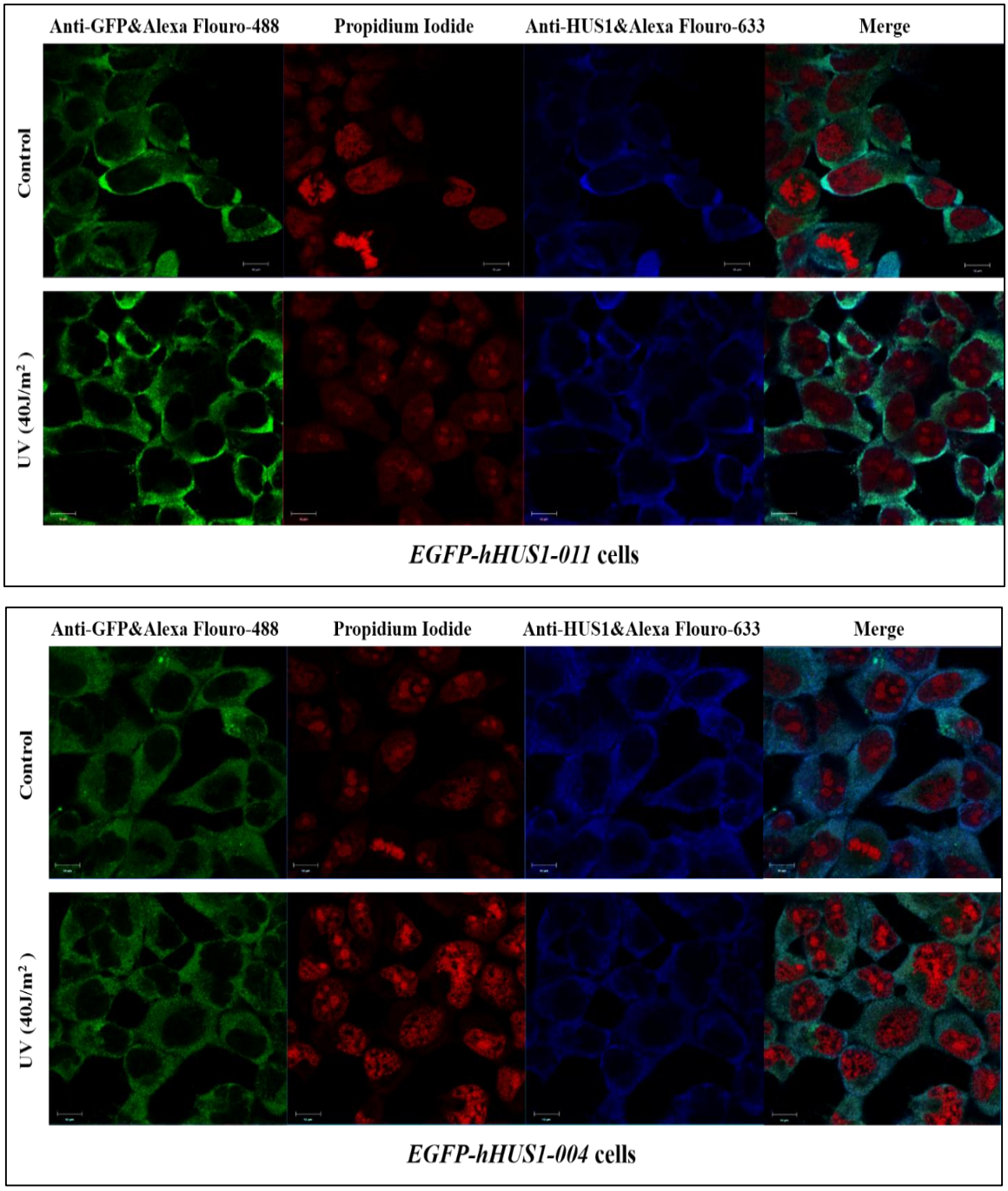

Figure 6-21: Cell localization of EGFP-hHUS1-011 and EGFP-hHUS1-004 proteins upon UV treatment. While EGFP-hHUS1-011 remained in the cytoplasm, EGFP-hHUS1-004 did show a low number of nuclear spots upon UV treatment but remained largely in the cytoplasm. (Scale bar=10μm). (Images were obtained by Zeiss LSM710 Confocal Microscope with a 63× objective, and analyzed by Zen2010 software and processed by Photoshop (Adobe)).

The EGFP protein without a hHUS1 fusion partner was present in the nucleus and cytoplasm and did not change in the response to UV light (Figure 6-22, top panels). Untransfected HEK293 cells showed no GFP signal (Figure 6-22, lower panels). As in the previous experiments, the endogenous hHUS1 protein was mainly detectable in the cytoplasm under both conditions.

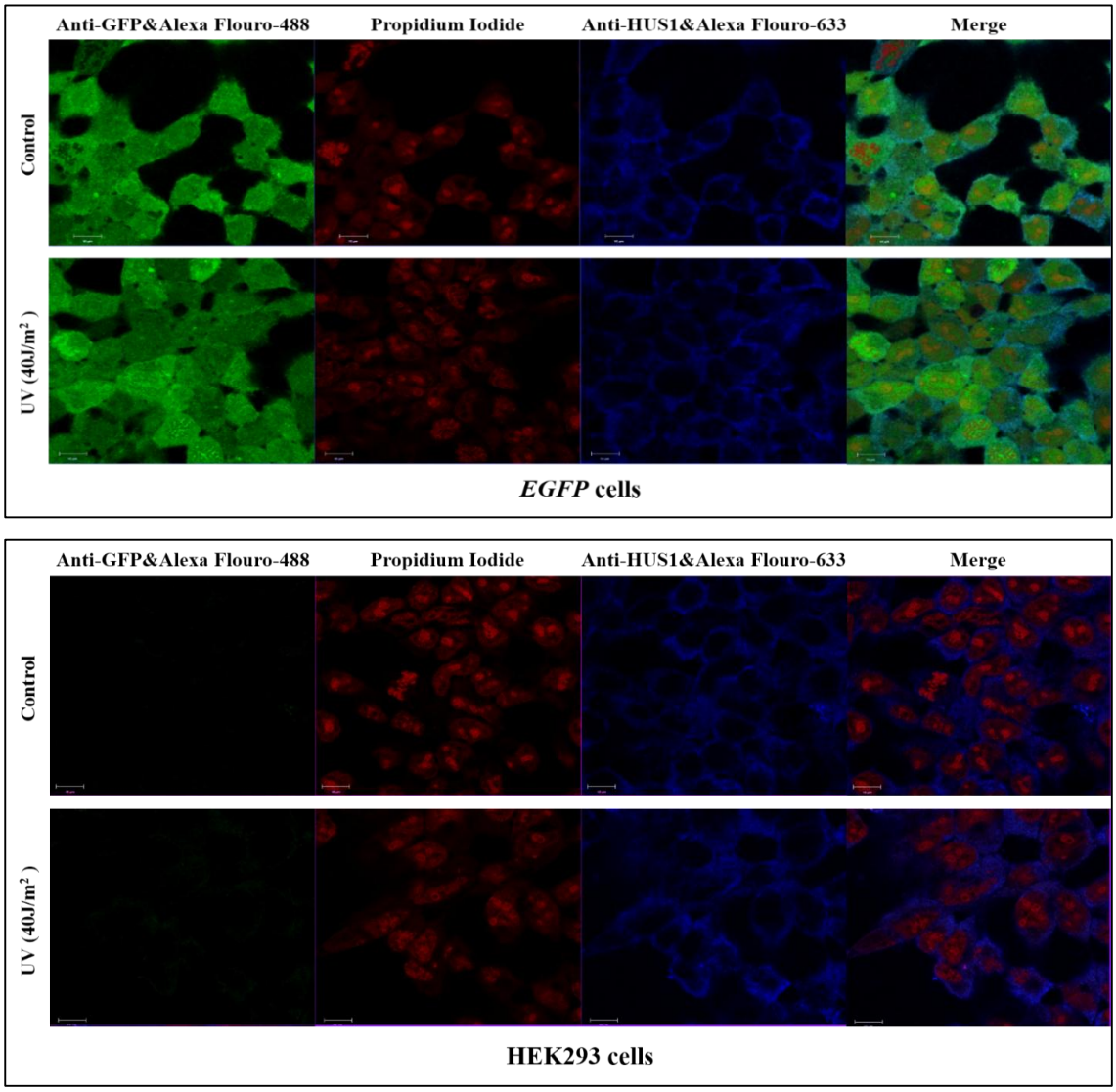

Figure 6-22: Cell localization of the EGFP protein and the endogenous hHUS1 in non-transfected HEK293 cells upon UV treatment. Cells localization did not show any changes of EGFP and endogenous hHUS1 proteins post-UV exposure. (Scale bar=10µm). **(**Images were obtained by Zeiss LSM710 Confocal Microscope with a 63× objective, and analyzed by Zen2010 software and processed by Photoshop (Adobe)).

EGFP-hHUS1B was detectable in both, the cytoplasm and in the nucleus (Figure 6-23). In contrast to the earlier experiments, no nuclear signal was evident. The localization of EGFP-hHUS1B was not affected by UV light. As in the case of hHUS1, the detection of EGFP-hHUS1B with the anti-hHUS1B antibody was reduced in the nucleus although a faint nuclear signal could be detected especially after UV treatment (Figure 6-23). The difference between the anti-GFP and anti-HUS1 antibodies indicates that the HUS1 part of the fusion protein may not be accessible to the anti-HUS1 antibodies when the protein is in the nucleus. Unfortunately, I could not use the anti-HUS1B antibody in Western blots as it failed to detect denatured hHUS1B protein. The results obtained with the anti-GFP antibody in the protein fractionation experiment is, however, consistent with a largely cytoplasmic localization of hHUS1B (Figure 6-19).

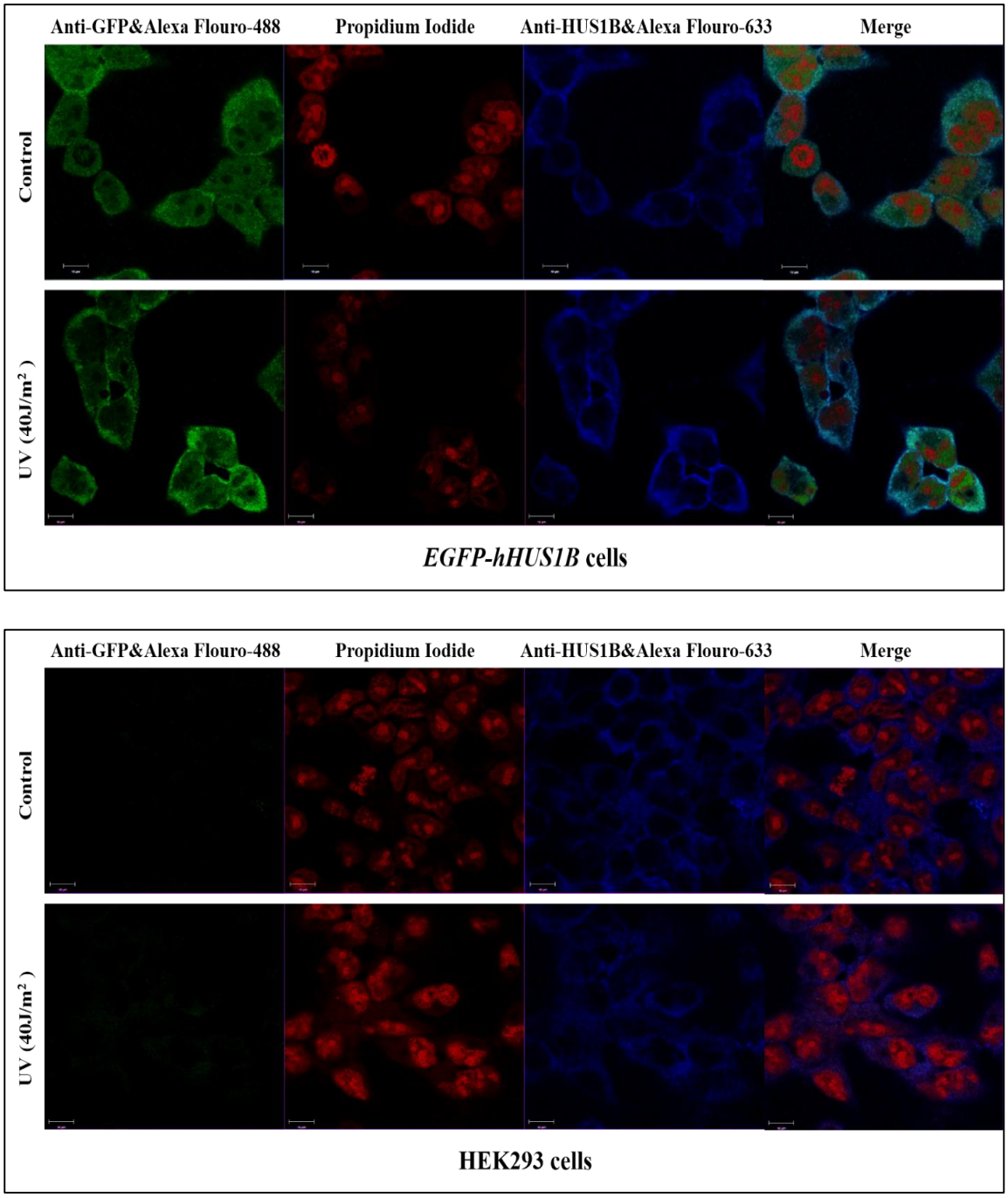

Figure 6-23: Cell localization of EGFP-hHUS1B and the endogenous one in HEK293 cells upon UV treatment. EGFP-hHUS1B showed overall cellular localization in untreated and UV treated cells with nucleoli localization upon UV treatment. Predicted endogenous hHUS1B protein did not show any changes upon UV treatment. (Scale bar=10µm). (Images were obtained by Zeiss LSM710 Confocal Microscope with a 63× objective, and analyzed by Zen2010 software and processed by Photoshop (Adobe)).

6.3 Discussion

The main findings in this chapter are: **(1):** The endogenous hHUS1 protein underwent posttranslational modifications and degraded when HEK293 cells express either full-length hHUS1-001-GFP or EGFP-hHUS1-001. While expression of hHUS1-005-GFP triggers some of these modifications, the endogenous protein is not degraded. None of the other recombinant variants triggers a similar response. **(2):** EGFP-hHUS1-001 is present in the cytoplasmic and nuclear fractions, whereas all truncated variants are mainly in the cytoplasmic fraction. **(3):** Only EGFP-hHUS1-001 re-localizes to the nucleus after UV inflicted DNA damage. **(4):** EGFP-hHUS1-005 localizes to thin filament-like structures in the nucleus largely independent of UV-induced DNA damage. **(5)**: EGFP-hHUS1B localizes to the nucleus independently of UV induced DNA lesions and it is sometimes observed in the nucleolus. I will discuss each point separately in the following paragraphs.

6.3.1 hHUS1 over-expression interferes with the endogenous hHUS1 protein differently depending on the length of the recombinant HUS1 protein

Endogenous hHUS1 underwent posttranslational modifications depending on the composition of the overexpressed hHUS1 fusion protein. When the full-length hHUS1 protein was C-terminally fused to the GFP protein (*hHUS1-001-GFP*), the endogenous hHUS1 protein underwent a series of yet unknown modifications resulting in a molecular weight higher than that of the normal protein (Figure 6-7). Only over-expression of the slightly shorter hHUS1-005-GFP protein resulted in similar modifications, but to a lesser extent. The type of modifications is not known yet. However, Hirai and colleagues (2004) showed that hHUS1 is an unstable protein, which can be degraded via the ubiquitin-proteasome pathway. Taken together, the engineered hHUS1-GFP full-length protein may replace the endogenous hHUS1 protein as a subunit of the 9-1-1 ring, thereby exposing the unstable hHUS1 protein to post-translational modifications including its ubiquitinylation and degradation. Since this effect was most obvious when the full-length protein was over-

expressed, it is very likely that the truncated variants are much less efficient in replacing hHUS1 in the 9-1-1 ring.

Interestingly overexpression of EGFP-hHUS1 had a different impact on the endogenous hHUS1 protein as the levels of the endogenous hHUS1 protein declined without the detection of modified forms when the induction time exceeded to more than 12 hours. While both observations imply that the recombinant hHUS1-001 protein competes with the endogenous hHUS1 protein in the 9-1-1 ring, the reason may the C-terminal fusion stabilizes the modified forms, which may be precursors of the degradation process is not known.

6.3.2 The EGFP-hHUS1 protein and its splice variants function differently from each other

One important outcome of the over-expression of hHUS1-001 and its truncated isoforms was that they function differently inside the cell. While the full-length EGFP-hHUS1-001 protein re-localised to the nucleus in the response to UV light (Figure 6-20) and was present in the nuclear fraction of treated and untreated cells (Figure 6-19), all truncated variants are mainly in the cytoplasm. One interesting exception is EGFP-hHUS1-005, which lacks the first 21 amino acids, as this variant was present inside the nucleus in these filament-like structures, which may be open sub-domains in the chromatin (Figure 6-20). The nature of these sub-domains is currently unknown, considering the previous finding of the ability of the EGFP-hHUS1-001 protein to substitute for the endogenous protein in the 9-1-1 ring; none of the truncated variants may act as part of this ring complex. This conclusion is consistent with the idea that the truncated variants adopt a different protein fold from the full-length protein given the extend of amino acids which are missing from the N-terminus of the variants (Figure6-4).

6.3.3 hHUS1B shows some variations from hHUS1

The engineered EGFP-hHUS1B protein showed several variations from EGFP-hHUS1 protein. Firstly, EGFP-hHUS1B eluted in a much sharper peak in the range of 600-700kDa

from the Superdex-200 column compared to the much wider elution profile of hHUS1 (Figure 6-15) had no impact on the endogenous hHUS1 protein (6-15). Secondly, EGFP-hHUS1B localized to the nucleus in untreated cells whereas EGFP-hHUS1 did this in the response to UV-induced DNA damage (Figures 6-20, 6-23).

These findings are consistent with previous reports showing that recombinant HUS1-HA localizes to the cytoplasm and the nucleus when over-expressed and that HUS1 shuttles between both cellular compartments (Cai, et.al. 2000; Hopkins, et.al. 2003; Madabushi, et.al. 2010). While little is known about hHUS1B, the previous finding that human HUS1B directly interacts with RAD1, but not RAD9 or HUS1 (Hang, et.al. 2002) supports the differences between both HUS1 isoforms. Why EGFP-hHUS1B localises to the nucleolus in some experiments but in others is still unclear. A nucleolar localisation is, however, consistent with the same localisation of hRAD9B when over-expressed in human cell lines (Perez-Castro & Freire, 2012).

Chapter 7: General Discussion

The current study focused on the expression of *hus1* gene variants in both fission yeast and human cells. As a summary, my work revealed the following key findings:

1. Leaky ribosome scanning enables *S. pombe* cells to express two N-terminally truncated variants, Hus1-32 and Hus1-46, starting at the internal methionine codons 32 and 46, respectively (both variants form a double band, which was previously identified as Hus1C (Caspari, et. al. 2000) (Chapter 3).
2. Both variants act upstream of Chk1 kinase and are required for its activation when DNA replication forks break in the presence of the ribonucleotide reductase inhibitor hydroxyurea in cells devoid of Cds1 kinase (Chapter 3);
3. The yeast Hus1 variants may be conserved in human cells, which are expressing alternative transcripts of the hHUS1 gene. Expression of the corresponding mRNA variants was detected in cell lines and different human tissues. The corresponding proteins could not be all detected. The exception may be hHUS1-005, which may form a double band with the full-length hHus1 protein. hHUS1-005 lacks the first 21 amino acids and may correspond to the *S.pombe* Hus1-H32 variant. (Chapter 4 & 5).
4. While the full-length hHUS1 protein was located in the cytoplasm and the nucleus, the variant hHUS1-005 was found in filamentous structures in the nucleus independently of DNA damage. EGFP fusion proteins of the remaining hHUS1 variants localize all to the cytoplasm (Chapters 5 &6).
5. A short open reading frame (sORFs) was discovered between the first AUG codon and a premature stop codon upstream of the hHUS1-005 & hHUS1-004 transcript. Provisional results suggest that this very short mRNA may be expressed in human cell lines (Chapter4).

7.1 Identification of *S.pombe* Hus1-H32 and Hus1-H46 as N-terminally truncated variants

According to the previously published data by Caspari, et.al. (2000), that the *S. pombe hus1* gene expresses four isoforms. However, the underlying process and their biological roles were unknown. I successfully identified that one of that four isoforms, Hus1C, is expressed by leaky ribosome scanning (Kochetov, 2008), and the subsequent biochemical characterisations revealed that it is composed of two protein variants, which I designate as Hus1-H32 and Hus1-H46. Interestingly, the expression of these two variants is constitutive but restricted to dividing cells.

Kochetov, (2008) has reviewed that eukaryotic mRNA translation occurs as linear scanning process by ribosomes in a 5'to 3' direction. Most ribosomes initiate translation at the first start site (AUG-1), which has an optimal nucleotide context. However, if the context is suboptimal, some ribosomes will scan further down the mRNA and initiate translation from an internal AUG triplet with a suitable DNA context to produce an N-terminally truncated protein. In *S.cereviseae,* the AUG utilization efficiency varies depending on the nucleotide at position -3 upstream of the start codon (A>G>C>U; consensus: AAAAAAAAAUGUC). If this consensus sequence were applied to the *S.pombe hus1* mRNA sequence, it would be clear that the first AUG is in the optimal context which explains the higher abundance of the full-length Hus1B protein (Fig. 3-11). Figure 7-1 shows the consensus around the ATG codons in the *hus1* gene sequence. While the two internal ATG codons 32 and 46 do not share this optimal upstream sequence, codon ATG 46 has an adenine base at position -3 while ATG 32 has a cytosine base at this position. This would explain why the abundance of both variants is much lower compared to the full-length protein. Interestingly, mutation of the first ATG codon to an alanine triplet strongly increases the levels of the variants (Figure 3-11), which is consistent with the idea that ribosomes can scan past the first ATG codon. The efficiency with which ribosomes initiate at a given AUG codon could of course also depend on the secondary structures adopted by the mRNA. Leaky ribosome scanning is not only restricted to yeast cells. Bab, et.al. (1999) showed that expression of the human Pre- Osteogenic growth peptide (PreOGP)), which has a similar C-

terminal sequence to histone H4 between residues 90-103 , is translated from the internal AUG codon at position 85 of the *histone H4* mRNA sequence by leaky ribosomal scanning.

Recent work has identified a second checkpoint gene in *S.pombe* from which an N-terminally truncated variant is produced. Janes at al., 2012 have shown that AUG-50 in the *rad9* mRNA acts also as an internal initiation codon for leaky ribosome scanning. However in contrast to the *hus1* gene, initiation at this codon occurs mainly in the response to heat stress suggesting that internal initiation by ribosomes in fission yeast is a regulated process. Interestingly, the *rad9* and *hus1* genes do have introns (three in the case of *rad9* and four in the case of *hus1*) which would allow cells to use alternative splicing as in human cells for the production of protein variants. Why fission yeast uses leaky ribosome scanning instead of alternative splicing is not yet known.

Figure 7-1: First ATG in *S.pombe hus1* DNA sequence has an optimal context to initiate the HUS1 full-length protein expression. Methionines number 1, 32 and 46 are highlighted in blue and the nucleotide at position -3 is shown in yellow. The 5`- and 3`-untranslated regions are highlighted. (Pombase, accessed on June 2014) (http://www.pombase.org/spombe/download/sequence/SPAC20G4.04c/sequence.fasta).

7.2 Hus1-32 and Hus-46 act upstream of Chk1 kinase when DNA replication forks break in *cds1* deficient cells

The DNA replication checkpoint is a surveillance mechanism, which is initiated when the replication machinery stops in the response to a reduction in the nucleotide pool or breaks when it encounters unrepaired DNA lesions or proteins cross-linked to the DNA (Xu, et.al, 2006; Palermo & Walworth, 2007). It is well known that *S. pombe* Cds1 is responsible to maintain the structural integrity of the replication fork when the nucleotide pool is depleted by the ribonucleotide inhibitor hydroxyurea (HU) (Boddy, et.al.2003; Kai, et.al. 2005). The second DNA damage checkpoint kinase Chk1 remains silent during such arrests, but is activated when replication forks collapse in HU medium in the absence of Cds1 (Lindsay, et.al., 1998) or when the replication fork collapses for a different reason (Chen & Sanchez, 2004). Since Cds1 and Chk1 kinase act both down-stream of Rad3 kinase and the Rad9-Rad1-Hus1 ring complex (Xu, et.al., 2006), only cells deficient of both are completely checkpoint deficient in the presence of HU. Whereas loss one of one kinase allows the cells to arrest in G2 phase (Figure 3-22) (Lindsay et al., 1998). How Chk1 is activated at broken replication forks is not fully understood. My results show that either the simultaneous methionines 32 and 46 modification to alanine or the combined deletion of the Hus1 variants H32 and H46 in *cds1* deficient cells abolishes the Chk1-dependent G2 arrest in HU medium (Figure 3-22). The *Δcds1-hus1.Myc-M32AM46A* cells are as checkpoint deficient as the *Δcds1- Δchk1* strain demonstrating that the loss of both variants has an extremely negative effect on activation of the Chk1 pathway when forks are damaged. This implies that both variants act up-stream of Chk1 under these conditions. Consistent with this conclusion, the *Δchk1-hus1.Myc-M32AM46A* strain is as checkpoint deficient as the *hus1.Myc-M32AM46A* strain (Figure 3-22). There is, however one key difference between *Δchk1* and *hus1.Myc-M32AM46A* cells as cells without *Chk1* kinase fully arrest in HU medium whereas the *hus1.Myc-M32AM46A* strain possesses a partial loss of the checkpoint. As shown in Figure 3-22, these cells exit the G2 arrest too early. This suggests that these variants may have also a link to the Cds1 pathway since the *hus1.Myc-M32AM46A* strain behaves like a partial loss of *Cds1* and *Chk1* mutant. Work by another student in the group has revealed that Hus1-H46 associates with Chk1 in pull-down assays and co-fractionates with the kinase in gel

filtration experiments (Lawes & Caspari, unpublished). These observations are in line with my findings and imply that the Hus1 variants form a complex with Chk1 kinase.

Consistent with previous work, mutation of the first *hus1* AUG codon abolishes the DNA damage checkpoint in the presence of HU (Figure 3-21) resembling a *hus1* deletion strain (Kostrub, et.al, 1997; Volkmer & Karnitz, 1999; Humphrey, 2000). This is in agreement with the conclusion that full-length Hus1-B assembles with Rad1 and Rad9 in the 9-1-1 ring. Interestingly, expression of the shorter variants in the *hus1.Myc-M1A* strain fails to restore a checkpoint response strongly suggesting that they cannot substitute for the full-length protein. A similar ring-independent activity was found for the Rad9-M50 variant (Janes, et. al. 2012). Taken together, this might suggest that the variants act outside of the normal 9-1-1 pathways. The only other treatment beside HU to which the *hus1.Myc-M32AM46A* cells are slightly sensitive was the DNA methylation with methyl-methanesulfonate (MMS) (Figure 3-13, 3-17). This implies that they may also be required for the regulation of the Chk1 pathway when the DNA template becomes modified.

The only other *S.pombe* mutant known to have a partial loss of the G2 arrest in HU medium is the *rad9-T412A* mutant (Furuya, et. al. 2004). Threonine 412 within the C-terminus of Rad9 becomes phosphorylated by Rad3 kinase while undamaged cells progress through S phase. Although it is not yet known whether this *rad9* mutation and the *hus1.Myc-M32AM46A* double mutation act in the same pathway, it implies that Rad3 targets an alternative Rad9-Hus1 complex in S phase to respond to activate Chk1 when replication forks are damaged.

One question, which is currently unanswered, is why *S.pombe* cells need two Hus1 variants to target Chk1. In human cells, activation of Chk1 by ATR kinase requires the presence of single-stranded DNA (ssDNA) (Zou & Elledge, 2003). Since the same applies to the activation of *S.pombe* Chk1 by Rad3 kinase (Edwards, et.al. 1999), it is likely that Chk1 activation at damaged forks requires the presence of ssDNA. Work in *S.cerevisiae* has shown that two parallel pathways are involved in the generation of ssDNA at broken chromosome. One pathway utilizes Exonuclease 1 (Exo1), whereas the second pathway depends on Sgs1 DNA helicase and endonuclease Dna2 (Cejka, et.al. 2010; Mimitou & Symington, 2011).The corresponding enzymes in *S.pombe* are Exo1 and Rqh1 DNA helicase. The existence of two parallel pathways may explain why two Hus1 variants are

necessary to activate Chk1 when DNA replication forks break. May be the Hus1 variants mediate activation of Chk1 with Exo1 and Rqh1during the formation of ssDNA at broken forks? This idea is supported by the formation of large protein complexes by both variants (Figure 3-18). Similar large complexes have been found for Chk1 and Rqh1 (Mahyous, et.al. 2014). Further work is however required to establish whether this model explains why two Hus1 variants are required.

What is also interesting to note is that the up-regulation of Rad9 variant correlates with the heat-induced de-phosphorylation of Chk1 at serine-345 (Janes, et.al. 2012). This raises the possibility that Chk1 is one of the key targets of the Hus1 and Rad9 variants. Over the last few years, more isoforms of other checkpoint proteins were identified. For example, the *S.pombe cds1* gene produces an N-terminal short splice variant, which contains the SQ/TQ and fork-head-associated domains but lacks the kinase domain (Lemaire, et.al. 2004). The same group reported also a similar variant of human Chk2/Cds1 (Lemaire, et.al. 2004). Pabla, et.al. (2012) revealed recently the existence of a short splice variant of the human Chk1 protein that plays a role in cell cycle regulation and DNA damage checkpoints.

7.3 The three splice variants of the human *HUS1* gene

Investigation of the *hHUS1* mRNA using RT-PCR revealed the existence of up to three alternative splice variants (*hHUS1-005, hHUS1-011 & hHUS1-004*) in different human tissues (fetal brain, heart, kidney, fetal liver and uterus) and cell lines (HeLa and HEK293). Since the DNA sequences of these variants are very similar (Figure 6-3, Appendix 2) the design of variant-specific primers was difficult. The DNA sequences from the cloned *hHUS1* variants was the same sequence as curated at the Ensembl database with exception of *hHUS1-011*, which has an in-frame deletion of 19 amino acids in the middle of the ORF sequence (Figure 6-10).

The hHUS1 variants expression was investigated on both mRNA (chapter 4) and protein level (chapter 5). The RT-PCR results showed a variation in the hHUS1 transcripts expression on mRNA level as shown in figure 4-5 and table 7-1. On the other hand, I could not find their proper expression conditions on protein level using variety of techniques (cell cycle arrest, cells senescence or DNA damage-mediated expression). However, the exposure of HEK293, and for less extent, HeLa cells to either HU (DNA replication fork arrest) or

UV and MMS (slow down the replication machinery) induced the expression of another smaller band, which is predicted to represent hHUS1-005 variant.

Table 7-1: hHUS-001 and its splice variants expression level on selected mRNAs of human tissues and cell lines. (+ very low, ++ low expression, +++ moderate expression, ++++high expression).

Variant	*hHUS1-001*	*hHUS1-005*	*hHUS1-011*	*hHUS1-004*
mRNA source				
Fetal brain tissue	+++	++++	+++	+++
Heart tissue	+++	++++	+++	+++
Kidney tissue	++	+++	++	++
Fetal liver tissue	++	+++	++	++
Uterus tissue	++	++	++	+
HeLa cell line	+++	++++	++++	++++
HEK293 cell line	+++	+++	+++	+++

The variant, which is best supported by the results, is *hHUS1-005*. This variant is only 21 amino acids shorter than the full-length protein and may run jointly as a double band with the longer HUS1 protein on a normal SDS gel (Figure 5-9, 5-11, 5-12, and 6-13). The primers which used to test for the presence of the *hHUS1-005* mRNA were also specific to the 5`-region (Appendix 2 & Figure 4-5). Taken together, it is very likely that human cells do express this variant.

Expression of the different variants fused to the EGFP protein (Enhanced Green Fluorescence Protein) had quite distinct effects on the stability of the endogenous hHus1 protein. While induction of EGFP-hHUS1-011 and EGFP-hHUS1-004 had no effect on the endogenous protein, over-expression of EGFP-hHUS1-001 triggered its degradation (Figure 6-12 and 6-13). The degradation was not so obvious when the C-terminal GFP fusion, hHus1-001-GFP was induced, but the appearance of higher molecular weight bands indicate post-translational modifications of the endogenous hHUS1. Human HUS1 is degraded by the proteasome pathway upon its ubiquitinylation and its association with hRAD1, but not hRAD9, protects the protein from this modification (Hirai, et.al. 2004). This indicates that

over-expression of the full-length hHUS1-001 fusion proteins competes with the endogenous hHUS1 protein in the RAD9-RAD1-HUS1 ring and that the hHUS1 protein outside of the ring is degraded. Interestingly, induction of the N-terminally truncated variant hHUS1-005-GFP has only a moderate effect on the stability of the endogenous protein as indicated by the appearance of some higher molecular bands (Figure 6-7). This indicates that the shorter variant has some effect on hHUS1 turnover, but fails to compete with hHUS1 as a subunit of the 9-1-1 ring. Unlike the full-length hHUS1 fusion protein, which is detectable in the cytoplasm and nucleus, the EGFP-hHUS1-005 fusion protein localizes to filamentous like structures in the HEK293 cells nuclei (Figure 6-20). In summary, these findings are in line with the finding in yeast suggesting a different role of the N-terminally truncated variant outside of the normal 9-1-1 ring.

7.4 Very short Open reading frames in the *hHUS1-005* and *hHUS1-004* transcripts

Interestingly, I noticed that the N-terminal regions of the *hHUS1-005* and *hHUS1-004* encode for very short open reading frame in front of the longer N-terminally truncated ORF (Figures 4-8, 4-9 & 4-10). Such short ORFs, are well studied that can produce short peptides with biological activities (Calvo, et.al. 2009). For example, the 5' leader region of mammalian *beta 2 adrenergic* receptor mRNA contains a short ORF and that encoded peptide regulates the expression of the beta 2 receptor (Parola & Kobilka, 1994). However, further work is, required to find out whether the two short ORFs that located upstream of the longer ORFs of hHUS1-004 and hHUS1-005 produce the corresponding peptides, which differ in their potential C-terminal sequence. If they exist, this may explain why the variants evolved as it would allow human cells to express two novel proteins from the same splice variant. Similar short peptides are also detected in *S.cerevisiae* (Werner, et.al. 1987) and it may explain the presence of a short N-terminal fragment of *S.pombe* Cds1 kinase (Lemaire, et. al. 2004).

7.5 Human cells overcome the low expression of hHUS1 protein to survive

The down-regulation of mammalian HUS1 either by knock down of the gene or by the use of interfering RNAs (siRNA) was reported previously in order to investigate its cellular role (Kinzel, et.al. 2002; Meyerkord, et.al. 2008; Lyndaker, et.al. 2013).

Kinzel et.al. (2002) down regulated *hHUS1* mRNA in human H1299 non-small lung carcinoma cells using antisense oligonucleotides. Analysing the mRNA level 24 hours post-transfection using Quantitative PCR technique revealed variations in the efficiency of the down-regulation, which varied between 30% and 80%. Interestingly, the HUS1 protein levels were not analysed in this study. They showed however, that *hHUS1* mRNA down-regulation had no effect on cells viability but rendered cells sensitive to the DNA damaging agent Cisplatin. I did find it very difficult to reduce the protein levels of hHUS1 by interfering RNAs using different systems. Only the combination of up to four different down-regulation plasmids with different target sequences (HUSH shRNA, Origene) resulted in a significant decrease in hHUS1 protein levels (Figure 4-15). This implies the requirement of targeting the *hHUS1* mRNA at more than one site to achieve proper down regulation. Interestingly, the effect of the down-regulation was only transient as it disappeared at later time points (Figure 4-15). This might suggests that cells have to keep a minimum hHUS1 protein level to maintain their viability, which is consistent with the loss of viability mouse embryos upon knockdown of the *Hus1* gene (Kinzel, et.al. 2002; Weiss, et.al. 2003).

7.6 Final conclusion

The main outcome of this project is that the N-terminally truncated variants of the DNA damage checkpoint protein Hus1 are conserved between yeast and human cells, and that they act outside of the normal Rad9-Rad1-Hus1 ring complex to regulate, at least in fission yeast, the DNA damage checkpoint kinase Chk1 when replication forks break in S phase.

References:

Alao, John P.; Gamble, Simon C.; Stavropoulou, Alexandra V.; Pomeranz, Karen M.; Lam, Eric W-F.; Coombes, R. Charles & Vigushin, David M. (2006). The Cyclin D1 proto-oncogene is sequestered in the cytoplasm of mammalian cancer cell lines. Molecular cancer, 5:7. 1-11.

Al-Khodairy, Fahad & Carr, Antony M. (1992). DNA repair mutants defining G2 checkpoint pathways in *Schizosaccharomyces pombe*. The EMBO Journal, 11 (4):1343 – 1350.

Al-Khodairy, F.; Fotou, E.; Sheldrick, K. S.; Griffiths, D. J.; Lehmann, A. R. & Carr A. M. (1994). Identification and characterization of new elements involved in checkpoint and feedback controls in fission yeast. Mol Biol Cell. 5(2):147-160.

Ampatzidou, E.; Irmisch, A.; O'Connell, M. J. & Murray, J. M. (2006). Smc5/6 is required for repair at collapsed replication forks. Mol Cell Biol. 26(24):9387-9401.

Andersen, Parker L.; Xu, Fang & Xiao, Wei (2008). Eukaryotic DNA damage tolerance and translesion synthesis through covalent modifications of PCNA. Cell Research, 18:162-173.

Andreassen, Paul R.; Ho, Gary P.H. & D'Andrea, Alan D. (2006). DNA damage responses and their many interactions with the replication fork. Carcinogenesis, 27(5): 883–892.

Evans, T.; Rosenthal, E. T.; Youngblom, J.; Distel, D. & Hunt, T. (1983). Cyclin: a protein specified by maternal mRNA in sea urchin eggs that is destroyed at each cleavage division. Cell. 33(2):389-396.

Bab, Itai; Smith, Elisheva; Gavish, Hanna; Attar-Namdar, Malka; Chorev, Michael; Chen, Yu-Chen; Muhlrad, Andrash; Birnbaumi, Mark J.; Stein, Gary & Frenkel, Baruch (1999). Biosynthesis of Osteogenic Growth Peptide via Alternative Translational Initiation at AUG85 of Histone H4 mRNA. J. Biol. Chem., 274:14474-14481.

Baldin, V.; Lukas, J.; Marcote, M.J.; Pagano, M. & Draetta, G. (1993). Cyclin D1 is a nuclear protein required for cell cycle progression in G1. Genes Dev., 7:812-821.

Balogun, F. O.; Truman, A. W. & Kron, S. J. (2013). DNA resection proteins Sgs1 and Exo1 are required for G1 checkpoint activation in budding yeast. DNA Repair (Amst), 12(9):751-760.

Banflavi, Gasper. (2011). Overview of cell synchronization. In: Cell cycle checkpoint control protocols. Lieberman, H.B. (Ed.). Methods in Molecular Biology. 241: 11-16. Humana Press Inc., Totowa.

Bartek, Jiri & Lukas, Jiri (2001). Mammalian G1- and S-phase checkpoints in response to DNA damage. Current Opinion in Cell Biology, 13:738–747.

Bartek, J. & Lukas, J. (2007). DNA damage checkpoints: from initiation to recovery or adaptation. Current Opinion in Cell Biology, 19: 238-245.

Blagosklonny, Mikhail V. (2011).Cell cycle arrest is not senescence. Aging, 3(2):94-101.

Blanco, Francisco J.; Grande, Maria T.; Langa, Carmen; et.al. (2008). S-Endoglin Expression Is Induced in Senescent Endothelial Cells and Contributes to Vascular Pathology. Circ Res.; 103:1383-1392

Boddy, M. N.; Shanahan, P.; McDonald, W. H.; Lopez-Girona, A.; Noguchi, E.; Yates III, J. R. & Russell, P. (2003). Replication checkpoint kinase Cds1 regulates recombinational repair protein Rad60. Mol Cell Biol. 23(16):5939-46.

Bøe, C. A.; Krohn, M.; Rødland, G. E.; Capiaghi, C.; Maillard, O.; Thoma, F.; Boye, E. & Grallert, B. (2012). Induction of a G1-S checkpoint in fission yeast. Proc Natl Acad Sci U S A. 109(25):9911-9916.

Branzi, D. & Foiani, M. (2009). The checkpoint response to replication stress. DNA repair, 8:1038-1046.

Bree, R. T.; Neary, C.; Samali, A. & Lowndes, N. F. (2004). The switch from survival responses to apoptosis after chromosomal breaks. DNA Repair 3: 989-995.

Brondello, Jean-Marc; Boddy, Michael N.; Furnari, Beth & Russel, Paul (1999). Basis for the Checkpoint signal specificity that regulates Chk1 and Cds1 protein kinases. Mol. Cell. Biol., 19(6):4262- 4269.

Brummelkamp, Thijn R.; Bernards, Rene´ & Agami, Reuven (2002). A system for stable expression of short interfering RNAs in mammalian cells. SCIENCE, 296:550-553.

Buis, J.; Stoneham, T.; Spehalski, E. & Ferguson, D. O. (2012). Mre11 regulates CtIP-dependent double-strand break repair by interaction with CDK2. Nat Struct Mol Biol. 19(2):246-252.

Burma, S.; Chen, B.P.; Murphy, M.; Kurimasa, A. & Chen D. J. (2001). ATM phosphorylates histone H2AX in response to DNA double-strand breaks. J Biol Chem. 276(45):42462- 42467.

Burova, Elena; Borodkina, Aleksandra; Shatrova, Alla & Nikolsky, Nikolay (2013). Sublethal Oxidative Stress Induces the Premature Senescence of Human Mesenchymal Stem Cells Derived from Endometrium. Oxidative Medicine and Cellular Longevity, 2013: 1-12.

C´mielova´, Jana & R˘eza´c˘ova´, M. (2011). p21 Cip1/Waf1 Protein and its Function Based on a Subcellular Localization. Journal of Cellular Biochemistry 112:3502–3506.

Cai, Richard L.; Yan-Neale, Yan; Cueto, Maria A.; Xu, Hong and Cohen, Dalia. (2000). HDAC1, a Histone Deacetylase, Forms a Complex with Hus1 and Rad9, Two G2/M Checkpoint Rad Proteins. The Journal of Biological Chemistry, 275(36), Issue: September 8: 27909–27916.

Calvo, S. E.; Pagliarini, D. J. & Mootha, V. K. (2009). Upstream open reading frames cause widespread reduction of protein expression and are polymorphic among humans. PNAS, 106(18):7507-7512.

Capasso, H.; Palermo, C.; Wan, S.; Rao, H.; John, U. P.; O'Connell, M. J. & Walworth NC. (2002). Phosphorylation activates Chk1 and is required for checkpoint-mediated cell cycle arrest. J Cell Sci., 115(Pt 23):4555-4564.

Carr, A. M.; Moudjou, M.; Bentley, N. J. & Hagan, I. M. (1995). The chk1 pathway is required to prevent mitosis following cell-cycle arrest at 'start'. Curr Biol. 5(10):1179-1190.

Caspari, Thomas; Dahlen, Maria; Kanter-Smoler, Gunilla; Lindsay, Howard D.; Hofmann, Kay; Papadimitriou, Konstantinos; Sunnerhagen, Per & Carr, Antony M. (2000). Characterization of *Schizosaccharomyces pombe* Hus1: a PCNA-Related Protein That Associates with Rad1 and Rad9. Mol. Cell. Biol., 20(4):1254- 1262.

Cejka, P.; Cannavo, E.; Polaczek, P.; Masuda-Sasa, T.; Pokharel, S.; Campbell, J. L. & Kowalczykowski, S. C. (2010). DNA end resection by Dna2-Sgs1-RPA and its stimulation by Top3-Rmi1 and Mre11-Rad50-Xrs2. Nature. 467 (7311): 112-116.

Chan, Timothy A.; Hermeking, Heiko; Lengauer, Christoph; Kinzler, Kenneth W. & Vogelstein, Bert. (1999). 14-3-3σ is required to prevent mitotic catastrophe after DNA damage. Nature, 401: 616-620.

Chandler, Dawn S.; Singh, Ravi K.; Caldwell, Lisa C.; et.al. (2006). Genotoxic stress induces coordinately regulated alternative splicing of the p53 modulators MDM2 and MDM4. Cancer Res., 66: 9502-9508.

Chang, Debbie J. & Cimprich, Karlene A. (2009). DNA Damage Tolerance: When it's OK to Make Mistakes. Nat Chem Biol., 5(2): 82-90.

Chen, Jun & Goligorsky, Michael S. (2006). Premature senescence of endothelial cells: Methusaleh's dilemma. Am J Physiol Heart Circ Physiol. 290: 1729–1739.

Chen, L.; Liu, T. H. & Walworth, N. C. (1999). Association of Chk1 with 14-3-3 proteins is stimulated by DNA damage. Genes Dev., 13(6):675-685.

Chen, Wei-Ta; Alpert, Amir; Leiter, Courtney; Gong, Fade; Jackson, Stephen P. & Millera, Kyle M. (2013). Systematic Identification of Functional Residues in Mammalian Histone H2AX. Molecular and Cellular Biology, 33: 111–126.

Chen, Yinhuai & Sanchez, Yolanda (2004). Chk1 in the DNA damage response: conserved roles from yeasts to mammals. DNA Repair, 3: 1025–1032.

Cimprich, K. A. & Cortez, D. (2008). ATR: an essential regulator of genome integrity. Nat. Rev. Mol. Cell Biol., 9(8): 616-627.

Cimprich, Karlene A.; Shin, Tae Bum; Keith, Curtis T. & Schreiber, Stuart L. (1996). cDNA cloning and gene mapping of a candidate human cell cycle checkpoint protein. Proc. Natl. Acad. Sci. USA, 93:2850-2855.

Conrad, Sandro; Künzel, Julia & Löbrich, Markus. (2011). Sister Chromatid exchanges occur in G2-irradiated cells. Cell Cycle, 10(2): 222-228.

Costanzo, Vincenzo; Robertson, Kirsten; Ying, Carol Y.; Kim, Edward; Avvedimento, Enrico; Gottesman, Max; Grieco, Domenico & Gautier, Jean. (2000). Reconstitution of an ATM-Dependent Checkpoint that Inhibits Chromosomal DNA Replication following DNA Damage. Molecular Cell, 6: 649–659.

Coudreuse, D. & Nurse, P. (2010). Driving the cell cycle with a minimal CDK control network. Nature. 468 (7327):1074-1079.

Cunningham, B. C. & Wells, J. A. (1989). High-resolution epitope mapping of hGH-receptor interactions by alanine-scanning mutagenesis. Science. 244 (4908):1081-1085.

D'Adda di Fagagna, Fabrizio (2008). Living on a break: cellular senescence as a DNA-damage response. Nature Reviews Cancer 8, 512-522.

D'Adda di Fagagna, Fabrizio; Reaper, Philip M.; Clay-Farrace, Lorena; Fiegler, Heike; Carr, Philippa; von Zglinicki, Thomas; Saretzki, Gabriele; Carter, Nigel P. & Jackson, Stephen P. (2003). A DNA damage checkpoint response in telomere-initiated senescence. Nature 426, 194-198.

Darzynkiewicz, Zbigniew; Halicka, H. Dorota; Zhao, Hong & Podhorecka, Monika (2011). Cell synchronization by inhibitors of DNA replication induces stress and DNA damage response: Analysis by Flow Cytometry. In: cell cycle synchronization. Banfalvi, G. (Ed.). Methods in Molecular Biology, 761: 85-96. Springer Science+ Business Media.

de la Torre, J.; Gil-Moreno, A.; Garcia, A.; Rojo, F.; Xercavins, J.; Saldo, E.; and Freire, R. (2008). Expression of DNA damage checkpoint protein Hus1 in epithelial ovarian tumors correlates with prognostic markers. Int J Gynecol Pathol., 27(1):24-32.

Dean, Frank B.; Lian, Lubing & O'Donnell, Mike. (1998). cDNA Cloning and Gene Mapping of Human Homologs for *Schizosaccharomyces pombe* rad17, rad1, and hus1 and Cloning of Homologs from Mouse, *Caenorhabditis elegans*, and *Drosophila melanogaster*. GENOMICS, 54: 424-436.

Deng, Chuxia; Zhang, Pumin; Harper, J. Wade; Elledge, Stephen J.; & Leder, Philip (1995). Mice Lacking p21Cip1/Waf1 Undergo Normal Development, but Are Defective in Gl Checkpoint Control. Cell, 82: 875-884.

Diffley, John F. X. (2004). Regulation of Early Events in Chromosome Replication. Current Biology, 4: R778–R786.

Dischinger, S.; Krapp, A.; Xie, L.; Paulson, J.R. & Simanis, V. (2008). Chemical genetic analysis of the regulatory role of Cdc2p in the *S. pombe* septation initiation network. . J Cell Sci. 15; 121(Pt 6):843-53.

Dore´, Andrew S.; Kilkenny, Mairi L.; Rzechorzek, Neil J. & Pear, Laurence H. (2009). Crystal Structure of the Rad9-Rad1-Hus1 DNA Damage Checkpoint Complex-Implications for Clamp Loading and Regulation. Molecular Cell, 34: 735-745.

Edwards, R. J.; Bentley, N. J. & Carr AM. (1999). A Rad3-Rad26 complex responds to DNA damage independently of other checkpoint proteins. Nat Cell Biol. 1(7):393-398.

Ekholm, Susanna V & Reed, Steven I. (2000). Regulation of G1 cyclin-dependent kinases in the mammalian cell cycle. Current Opinion in Cell Biology, 12:676–684.

Elliott, David and Ladomery, Michael (2011). Molecular biology of RNA. Oxford university press Inc., New York.

Enoch, Tamar; Carr, Anthony M. & Nurse, Paul (1992). Fission yeast genes involved in coupling mitosis to completion of DNA replication. Genes Dev., 6: 2035-2046.

Esashi, F. & Yanagida, M. (1999). Cdc2 phosphorylation of Crb2 is required for reestablishing cell cycle progression after the damage checkpoint. Mol Cell. 4(2):167-174.

Escribano-Díaz, C.; Orthwein, A.; Fradet-Turcotte, A.; Xing, M.; Young, J. T.; Tkáč, J.; Cook, M. A.; Rosebrock, A. P.; Munro, M.; Canny, M. D.; Xu, D. & Durocher D. (2013). A cell cycle-dependent regulatory circuit composed of 53BP1-RIF1 and BRCA1-CtIP controls DNA repair pathway choice. Mol Cell. 49(5):872-883.

Evans, T.; Rosenthal, E. T.; Youngblom, J.; Distel, D. & Hunt, T. (1983). Cyclin: a protein specified by maternal mRNA in sea urchin eggs that is destroyed at each cleavage division. Cell. 33(2):389-396.

Filippov, Valery; Filippova, Maria & Duerksen-Hughes, Penelope J. (2007). The Early Response to DNA Damage Can Lead to Activation of Alternative Splicing Activity Resulting in CD44 Splice Pattern Changes. Cancer Res., 67(16): 7621-7630.

Fleck, O. & Nielsen, O. (2004). DNA repair. Journal of Cell Science, 117: 515-517.

Forsburg, S.L.; Rhind, N. (2006). Basic methods for fission yeast. Yeast, 23: 173–183.

Fox, Michael H. (2004). Methods for synchronizing Mammalian cells. In: Cell cycle checkpoint control protocols. Lieberman, H.B. (Ed.). Methods in Molecular Biology. 241: 11-16. Humana Press Inc., Totowa.

Friedberg, E. C.; Walker, G.C.; Siede, W.; Wood, R. D.; Schultz, R. A. & Ellenberger, T. (2006). DNA repair and mutagenesis. 2nd ed. ASM Press, Washington, D.C.

Friedberg, E.C. (2003). DNA damage and repair. Natural, 421: 436-440.

Friedberg, E.C.; Walker, G.C. & Siede, W. (1995). DNA repair and mutagenesis. Washington, D.C.: ASM Press.

Furusawa, Y.; Iizumi, T.; Fujiwara, Y.; Zhao, Q.L.; Tabuchi, Y.; Nomura, T. & Kondo T. (2012). Inhibition of checkpoint kinase 1 abrogates G2/M checkpoint activation and promotes apoptosis under heat stress. Apoptosis, 17(1):102-112.

Furuya, K. & Carr, A.M. (2003). DNA checkpoints in fission yeast. J Cell Sci. 116: 3847-3848.

Furuya, K.; Poitelea, M.; Guo, L.; Caspari, T. & Carr A.M. (2004). Chk1 activation requires Rad9 S/TQ-site phosphorylation to promote association with C-terminal BRCT domains of Rad4TOPBP1. Genes Dev. 18(10):1154-1164.

Graves, Paul R.; Lovly, Christine M.; Uy, Geoffrey L. & Piwnica-Worms, Helen. (2001). Localization of human Cdc25C is regulated both by nuclear export and 14-3-3 protein binding. Oncogene, 20: 1839-1851.

Guo, Y.; Yang, K.; Harwalker, J.; Nye, J.M.; Mason, D.R.; Garrett, M.D.; Hitomi, M. & Stacey, D.W. (2005). Phosphorylation of cyclin D1 at Thr286 during S phase leads to its proteasomal degradation and allows efficient DNA synthesis. Oncogene. 24: 2599-2612.

Hang, H.; Zhang, Y.; Dunbrack, R.; Wang, C.; Lieberman, H.B. (2002). Identification and Characterization of a Paralog of Human Cell Cycle Checkpoint Gene HUS1. Genomics, 79(4): 487-492.

Hang, Haiying & Lieberman, Howard B. (2000). Physical Interactions among Human Checkpoint Control Proteins HUS1p, RAD1p, and RAD9p, and Implications for the Regulation of Cell Cycle Progression. Genomics, 65:24-33.

Harper, Jane V. (2005). Synchronization of cell population in G1/S and G2/M phases of the cell cycle. In: cell cycle control. Humphrey, T. & Brooks, G. (Ed.). Methods in Molecular Biology. 296: 157-166. Humana Press Inc., Totowa.

Harper, Jane V. & Brooks, G. (2005). The mammalian cell cycle, an overview. In: cell cycle control. Humphrey, T. & Brooks, G. (Ed.). Methods in Molecular Biology, 296: 113-153. Humana Press Inc., Totowa.

Hiom, K. (2000). Homologous recombination. Current Biology, 10 (10): R359-R361.

Hirai, Itaru; Sasaki, Terukatsu & Wang, Hong-Gang (2004). Human hRad1 but not hRad9 protects hHus1 from ubiquitin–proteasomal degradation. Oncogene 23:5124–5130.

Hochegger, H. & Takeda, S. (2006). Phenotypic analysis of cellular responses to DNA damage. In: reviews and protocols in DT40 research (eds. JM. Buerstedde. & S. Takeda): 313 -325.Springer.

Hochwagen, A. & Amon, A. (2006).Checking your breaks: surveillance mechanisms of meiotic recombination. Current Biology, 16: 217-228.

Hopkins, Kevin M.; Wang, Xiaojin; Berlin, Ana; Hang, Haiying; Thaker, Harshwardhan M. and Lieberman, Howard B. (2003). Expression of Mammalian Paralogues of HRAD9 and Mrad9 Checkpoint Control Genes in Normal and Cancerous Testicular Tissue. Cancer Research 63(September 1): 5291–5298.

Hu, J.; Sun, L.; Shen, F.; Chen, Y.; Hua, Y.; Liu, Y.; Zhang, M.; Hu, Y.; Wang, Q.; Xu, W. Sun, F. Ji, J.; Murray, J. M.; Carr, A. M. & Kong, D. (2012). The intra-S phase checkpoint targets Dna2 to prevent stalled replication forks from reversing. Cell. 149(6):1221-1232.

Humphrey, Tim (2000). DNA damage and cell cycle control in Schizosaccharomyces pombe. Mutation Research, 451:211–226.

Huschtscha, Lily I. & Reddel, Roger R. (1999). p16INK4a and the control of cellular proliferative life span. Carcinogenesis.20 (6): 921–926.

Ishii, H.; Mimori, K.; Inoue, H.; Inageta, T.; Ishikawa, K.; Semba, S.;, Druck, T.; Trapasso, F.; Tani, K.;, Vecchione, A.; Croce, C.M.; Mori, M. & Huebner, K.(2006). Fhit modulates the DNA damage checkpoint response. Cancer Res., 66(23):11287-11292.

Ishikawa, Kazuhiro; Ishii, Hideshi; Saito, Toshiyuki & Ichimura, Keiichi (2006). Multiple Functions of Rad9 for Preserving Genomic Integrity. Current Genomics, 7: 477-480.

Janes, S.; Schmidt, U.; Ashour, Garrido K.; Ney, N.; Concilio, S.; Zekri, M. & Caspari, T. (2012). Heat induction of a novel Rad9 variant from a cryptic translation initiation site reduces mitotic commitment. J.CellSci. 1; 125:4487-4497.

Jeggo, P. A. & Lobrich, M. (2006). Contribution of DNA repair and cell cycle checkpoint arrest to the maintenance of genomic stability. DNA Repair, 5: 1192-1198.

Johansen, Kristen M. & Johansen, Jørgen (2006). Regulation of chromatin structure by histone H3S10 phosphorylation. Chromosome Research.14:393–404.

Ju, Zhenyu; Choudhury, Aaheli Roy & Rudolph, K. Lenhard (2006). A Dual Role of p21 in Stem Cell Aging. Ann. N.Y. Acad. Sci. 1100: 333–344.

Kai, M.; Boddy, M. N.; Russell, P. & Wang, T. S. (2005). Replication checkpoint kinase Cds1 regulates Mus81 to preserve genome integrity during replication stress. Genes Dev., 19 (8):919-932.

Karnoub, Antoine E. & Weinberg, Robert A. (2008). Ras oncogenes: split personalities. Nature Reviews Molecular Cell Biology. 9: 517-531.

Karran, Peter (2000). DNA double strand break repair in mammalian cells. Current Opinion in Genetics & Development, 10:144-150.

Kastan, M. B. & Bartek, J. (2004). Cell-cycle checkpoints and cancer. Nature, 432: 316-323.

Kaufmann, W. K. & Paules, R. S. (1996). DNA damage and cell cycle checkpoints. The FASEB Journal, 10: 238-247.

Kiang, L.; Heichinger, C.; Watt, S.; Bähler, J. & Nurse, P. (2009). Cyclin-dependent kinase inhibits reinitiation of a normal S-phase program during G2 in fission yeast. Mol Cell Biol. 29(15):4025-4032.

Kinzel, B.1.; Hall, J.; Natt, F.; Weiler, J. & Cohen, D. (2002). Downregulation of Hus1 by antisense oligonucleotides enhances the sensitivity of human lung carcinoma cells to cisplatin. Cancer. 94(6):1808-1814.

Knobel, Philip A. & Marti, Thomas M. (2011). Translesion DNA synthesis in the context of Cancer research. Cancer Cell International, 11:39.

Kochetov, Alex V. (2008). Alternative translation starts sites and hidden coding potential of eukaryotic mRNAs. BioEssays, 30:683–691.

Kostrub, C.F.; al-Khodairy, F.; Ghazizadeh, H.; Carr, A.M. & Enoch, T. (1997). Molecular analysis of hus1+, a fission yeast gene required for S-M and DNA damage checkpoints. Mol Gen Genet. 254(4):389-399.

Kostrub, Corwin F.; Knudsen, Karen; Subramani, Suresh & Enoch, Tamar (1998). Hus1p, a conserved fission yeast checkpoint protein, interacts with Rad1p and is phosphorylated in response to DNA damage. The EMBO Journal, 17(7):2055–2066.

Krohn, M.; Skjølberg, H. C.; Soltani, H.; Grallert, B. & Boye E. (2008).The G1-S checkpoint in fission yeast is not a general DNA damage checkpoint. J Cell Sci., 121(Pt 24):4047-4054.

Kuilman, Thomas; Michaloglou, Chrysiis; Mooi, Wolter J. & Peeper, Daniel S. (2013). The essence of senescence. GENES & DEVELOPMENT, 24:2463–2479.

Lambert, S.; Watson, A.; Sheedy, D. M.; Martin, B. & Carr, A. M. (2005). Gross chromosomal rearrangements and elevated recombination at an inducible site-specific replication fork barrier. Cell. 121(5):689-702.

Lee, J. H. & Paull, T. T. (2004). Direct activation of the ATM protein kinase by the Mre11/Rad50/Nbs1 complex. Science. 304 (5667):93-96.

Lee, Joon; Kumagai, Akiko & Dunphy, William G. (2001). Positive regulation of Wee1 by Chk1 and 14-3-3 proteins. Molecular Biology of the Cell, 12: 551–563.

Lee, Melanie & Nurse, Paul (1988). Cell cycle control genes in fission yeast and mammalian cells. Trends in Genet, 4(10): 278-290.

Lemaire, M.; Prime, J.; Ducommun B, Bugler B. (2004). Evolutionary conservation of a novel splice variant of the Cds1/Chk2 checkpoint kinase restricted to its regulatory domain. Cell Cycle, 3(10):1267-1270.

Lieber, Michael R. & Karanjawala, Zarir E. (2004). Ageing, repetitive genomes and DNA damage. Nature Reviews Molecular Biology, 5: 69-75.

Lieberman, Howard B. (2006). Rad9, an evolutionarily conserved gene with multiple functions for preserving genomic integrity. J. Cell. Biochem. 97:690–697.

Lieberman, Howard B.; Hopkins, Kevin m.; Nass, Monica; Demetrick, Douglas & Davey, Scott. (1996). A human homolog of the Schizosaccharomyces *pombe* rad9^{+} checkpoint control gene. Proc. Natl. Acad. Sci. USA, 93:13890–13895.

Limbo, O.; Porter-Goff, M. E.; Rhind, N. & Russell, P. (2011). Mre11 nuclease activity and Ctp1 regulate Chk1 activation by Rad3ATR and Tel1ATM checkpoint kinases at double-strand breaks. Mol Cell Biol. (3):573-583.

Lindsay, Howard D.; Griffiths, Dominic J.F.; Edwards, Rhian J.; Christensen, Per U.; Murray, Johanne M.; Osman, Fekret; Walworth, Nancy & Carr, Antony M. (1998). S-phase-specific activation of Cds1 kinase defines a subpathway of the checkpoint response in Schizosaccharomyces pombe. GENES & DEVELOPMENT, 12:382–395.

Liu, Q.; Guntuku, S.; Cui, X.S.; Matsuoka, S.; Cortez, D.; Tamai, K.; Luo, G.; Carattini-Rivera, S.; DeMayo, F.; Bradley, A.; Donehower, L.A. & Elledge, S.J. (2000). Chk1 is an essential kinase that is regulated by ATR and required for the G2/M DNA damage checkpoint. Genes Dev., 14(12):1448-1459.

Löbrich. M. Jeggo, P.A. (2007). The impact of a negligent G2/M checkpoint on genomic instability and cancer induction. Nat Rev Cancer, 7 (11): 861-869.

Lopez-Girona, A.; Furnari, B.; Mondesert, O. & Russell P. (1999).Nuclear localization of Cdc25 is regulated by DNA damage and a 14-3-3 protein. Nature, 397(6715):172-175.

Lou, Zhenkun & Chen, Junjie (2005). Mammalian DNA damage response pathway. In: Genome instability in cancer development. (ed: E.A. Nigg). 425-455. Springer.

Lyndaker, A.M.; Lim, P. X.; Mleczko, J. M.; Diggins, C. E.; Holloway, J. K.; Holmes, R. J.; Kan, R.; Schlafer, D. H.; Freire, R.; Cohen, P. E. & Weiss, R. (2013). Conditional Inactivation of the DNA Damage Response Gene Hus1 in Mouse Testis Reveals Separable Roles for Components of the RAD9-RAD1-HUS1 Complex in Meiotic Chromosome Maintenance. PLoS Genet, 9(2):1371- 1392.

Ma, Hoi Tang & Poon, Randy Y.C. (2011). Synchronization of HeLa cells. In: cell cycle synchronization. Banfalvi, G. (Ed.). Methods in Molecular Biology, 761: 151-161. Springer Science+ Business Media.

Ma, J.; Ward, C.C.; Jungreis, I.; Slavoff, S.A.; Schwaid, A.G.; Neveu, J.; Budnik, B.A.; Kellis, M. & Saghatelian, A. (2014). Discovery of Human sORF-Encoded Polypeptides (SEPs) in Cell Lines and Tissue. J Proteome Res., 13:1757−1765.

Madabushi A, Gunther RC, Lu AL. HUS1 (HUS1 checkpoint homolog (S. pombe)). Atlas Genet Cytogenet Oncol Haematol. September 2010.

Mahyous, Saeyd S. A.; Ewert-Krzemieniewska, K.; Liu, B. & Caspari, T. (2014). Hyperactive Cdc2 kinase interferes with the response to broken replication forks by trapping S.pombe Crb2 in its mitotic T215 phosphorylated state. Nucleic Acids Res. 2014 May 26. pii: gku452. [Epub ahead of print].

Mailand, Niels; Falck, Jacob; Lukas, Claudia; Syljuasen, Randi G.; Welcker, Markus; Bartek, Jiri & Lukas, Jiri. (2000). Rapid Destruction of Human Cdc25A in Response to DNA Damage. Science, 288: 1425- 1429.

Malumbres, Marcos & Barbacid, Mariano (2005). Mammalian cyclin-dependent kinases. TRENDS in Biochemical Sciences, 30 (11):630-641.

Manolis KG1, Nimmo ER, Hartsuiker E, Carr AM, Jeggo PA, Allshire RC. (2001). Novel functional requirements for non-homologous DNA end joining in Schizosaccharomyces pombe. EMBO J. 20 (1-2):210-221.

Mansilla, Sabrina F.; Soria1, Gasto´ n; Vallerga, Marı´a Bele´ n; Habif, Martı´n; Martı´nez-Lo´ pez, Wilner; Prives, Carol & Gottifredi, Vanesa (2013). UV-triggered p21 degradation facilitates damaged-DNA replication and preserves genomic stability. Nucleic Acids Research: 1–10.

Matsuoka, Shuhei; Huang, Mingxia & Elledge, Stephen J. (1998). Linkage of ATM to Cell Cycle Regulation by the Chk2 Protein Kinase. SCIENCE, 282: 1893-1897.

Matsuoka, S.; Rotman, G.; Ogawa, A.; Shiloh, Y.; Tamai, K. & Elledge, S. J. (2000). Ataxia telangiectasia-mutated phosphorylates Chk2 in vivo and in vitro. Proc Natl Acad Sci U S A. 97(19):10389-94.

Mattia, Melissa; Gottifredi, Vanesa; McKinney, Kristine & Prives, Carol (2007). p53-Dependent p21 mRNA Elongation Is Impaired when DNA Replication Is Stalled. Molecular and Cellular Biology, 27 (4): 1309–1320.

Mazin, A., Mazin, A., Olga, M.; Bugreev, D. V. & Rossi, M. J. (2010). RAD54, the motor of homologous recombination. DNA Repair, 9: 286-302.

Mazón, G. & Symington, L. S. (2013). Mph1 and Mus81-Mms4 prevent aberrant processing of mitotic recombination intermediates. Mol Cell. 52(1):63-74.

Meyerkord, C.L.; Takahashi1, Y.; Araya1, R.; Takada1, N.; Weiss, R.S. and Wang1 H-G. (2008). Loss of Hus1 sensitizes cells to etoposide-induced apoptosis by regulating BH3-only proteins. Oncogene 27: 7248–7259.

Mickle, K., Oliva, A., Huberman, J. and Leatherwood, J. (2007). Checkpoint effects and telomere amplification during DNA re-replication in fission yeast. BMC Mol. Biol. 8, 119.

Mimitou, E.P. & Symington, L. S. (2011). DNA end resection--unraveling the tail. DNA Repair 10: 344–348.

Moore, C. W. (1988). Internucleosomal Cleavage and Chromosomal Degradation by Bleomycin and Phleomycin in Yeast. Cancer Res., 48(23):6837-6843.

Morgan, David O. (2007). The cell cycle principles of control. New Science Press Ltd.

Morita, T.; Tsutsui, Y.; Nishiyama, Y.; Nakamura, H. & Yoshida, S. (1982). Effects of DNA polymerase inhibitors on replicative and repair DNA synthesis in ultraviolet-irradiated HeLa cells. Int J Radiat Biol Relat Stud Phys Chem Med., 42(5):471-480.

Navadgi-Patil, V.M. & Burgers, P.M. (2009) .A tale of two tails: activation of DNA damage checkpoint kinase Mec1/ATR by the 9-1-1 clamp and by Dpb11/TopBP1. DNA Repair 8(9):996-1003).

Niida, H. & Nakanishi, M. (2006). DNA damage checkpoints in mammals. Mutagenesis, 21(1):3-9.

Nilssen, E. A.; Synnes, M.; Kleckner, N.; Grallert, B. & Boye, E. (2003). Intra G1 arrest in response to UV irradiation in fission yeast. Proc Natl Acad Sci U S A., 100(19):10758-10763.

Nurse, Paul (1975). Genetic control of cell size at cell division in yeast. Nature. 256(5518):547-551.

Nurse, Paul (1990). Universal control mechanism regulating onset of M-phase. Nature, 344: 503-508.

Nyberg, Kara A.; Michelson, Rhett J.; Putnam, CharlesW. & Weinert, Ted A. (2002). Toward maintaining the genome: DNA damage and replication checkpoints. Annu. Rev. Genet., 36:617–656.

Oe, Tomoya, Nakajo, Nobushige; Katsuragi, Yoshinori; Okazaki, Kenji & Sagata, Noriyuki (2001). Cytoplasmic Occurrence of the Chk1/Cdc25 pathway and regulation of Chk1in Xenopus Oocytes. Developmental Biology, 229: 250–261.

Ohtsubo, Motoaki; Theodoras, Anne M.; Schumacher, Jill; Roberts, James M. & Pagano, Michele (1995). Human Cyclin E, a nuclear protein essential for the G1-to-S phase transition. Molecular and Cellular Biology, 15(2): 2612–2624.

Okada, T.; Sonoda, E.; Yoshimura, M.; Kawano, Y.; Saya, H.; Kohzaki, M. & Takeda, S. (2005). Multiple roles of vertebrate REV genes in DNA repair and recombination. Molecular and Cellular Biology, 25(14): 6103-6111.

Ong, S.T.; Fong, K.M.; Bader, S.A.;, Minna, J.D.; Le Beau, M.M.; McKeithan, T.W. & Rassool, F.V. (1997). Precise localization of the FHIT gene to the common fragile site at 3p14.2 (FRA3B) and characterization of homozygous deletions within FRA3B that affect FHIT transcription in tumor cell lines. Genes Chromosomes Cancer, 20(1):16-23.

Pabla. N.; Bhatt, K. & Dong, Z. (2012). Checkpoint kinase 1 (Chk1)-short is a splice variant and endogenous inhibitor of Chk1 that regulates cell cycle and DNA damage checkpoints. Proc Natl Acad Sci U S A., 109(1):197-202.

Palermo, Carmela & Walworth, Nancy C. (2007). Yeast as model system for studying cell cycle checkpoints. In: Yeast as tool in cancer research. J.L.Nitiss & Joseph Heitman (eds.) 179-189.

Parker, Andrew E.; Van de Weyer, Inez; Laus, Marc C.; Oostveen, Inge ; Yon, Jeff ; Verhasselt, Peter &. Luyten, Walter H. M. L. (1998). A Human Homologue of the Schizosaccharomyces pombe rad1+ Checkpoint Gene Encodes an Exonuclease. The Journal of Biological Chemistry, 273(29):18332–18339.

Parola, A. L. & Kobilka, B. K. (1994). The Peptide product of a 5' leader Cistron in the B2 adrenergic receptor mRNA inhibits receptor synthesis. J Biol Chem., 269(6):4497-4505.

Parrilla-Castellar, Edgardo R.; Arlander, Sonnet J.H. & Karnitz, Larry (2004). Dial 9–1–1 for DNA damage: the Rad9–Hus1–Rad1 (9–1–1) clamp complex. DNA Repair, 3: 1009-1014.

Paulovich, A. G.; Toczyski, D. P. & Hartwell, L. H. (1997). When checkpoints fail. Cell, 88: 315-321.

Pe´rez-Castro, Antonio Jesu´ s & Freire, Raimundo (2012). Rad9B responds to nucleolar stress through ATR and JNK signalling, and delays the G1–S transition. J. Cell Sci., 125: 1152–1164.

Pero, R.W.; Roush, G.C.; Markowitz, M.M. & Miller, D.G. (1990). Oxidative stress, DNA repair, and cancer susceptibility. Cancer Detect Prev., 14(5):555-561.

Pichiorri, F.; Ishii, H.; Okumura, H.; Trapasso, F.; Wang, Y. & Huebner, K. (2008). Molecular parameters of genome instability: roles of fragile genes at common fragile sites. J Cell Biochem, 104(5):1525-33.

Pommier, Yves; Leo, Elisabetta; Zhang; HongLiang & Marchand, Christophe. (2010). DNA Topoisomerases and Their Poisoning by Anticancer and Antibacterial Drugs. Chemistry & Biology, 17: 421-433.

Pospelova, Tatyana V.; Demidenko, Zoya N.; Bukreeva, Elena I.; Pospelov, Valery A.; Gudkov, Andrei V. & Blagosklonny, Mikhail V. (2009). Pseudo-DNA damage response in senescent cells. Cell Cycle, 8(24): 4112-4118.

Qu, M.; Rappas, M.; Wardlaw, C. P.; Garcia, V.; Ren, J. Y.; Day, M.; Carr, A. M.; Oliver, A. W.; Du, L. L. & Pearl, L. H. (2013). Phosphorylation-dependent assembly and

coordination of the DNA damage checkpoint apparatus by Rad4TopBP. Mol Cell. 51(6):723-736.

Rainey, M.D.; Zachos, G. & Gillespie, D.A.F. (2006). Analysing the DNA damage and replication checkpoints in DT40 cells. In: reviews and protocols in DT40 research (eds. J.M. Buerstedde and S Takeda): 313 -325.Springer.

Raji, Hayatu & Hartsuiker, Edgar (2006). Double-strand break repair and homologous recombination in *Schizosaccaromyces pombe.* Yeast, 23: 963-976.

Rauen, M.; Burtelow, M. A.; Dufault, V. M. & Karnitz LM. (2000). The human checkpoint protein hRad17 interacts with the PCNA-like proteins hRad1, hHus1, and hRad9. J Biol Chem. 275(38):29767-29771.

Reinhardt, H. Christian & Yaffe, Michael B. (2009). Kinases that control the cell cycle in response to DNA damage: Chk1, Chk2, and MK2. Current Opinion in Cell Biology, 21:245–255.

Rhind, N. & Russell, P. (2000). Chk1 and Cds1: linchpins of the DNA damage and replication checkpoint pathways. J Cell Sci., 113 (Pt 22):3889-3896.

Rufini, A.; Tucci, P.; Celardo, I. & Melino, G. (2013). Senescence and aging: the critical roles of p53. Oncogene, 1–15.

Russell, P. & Nurse, P. (1986). cdc25+ functions as an inducer in the mitotic control of fission yeast. Cell. 45(1):145-153.

Russell, P. & Nurse P. (1987). Negative regulation of mitosis by wee1+, a gene encoding a protein kinase homolog. Cell. 49(4):559-567.

Ryan, A.J.; Squires, S.; Strutt, H.L. & Johnson, R.T. (1991). Camptothecin cytotoxicity in mammalian cells is associated with the induction of persistent double strand breaks in replicating DNA. Nucleic Acids Res., 19(12):3295-3300.

Saka, Y.; Esashi, F.; Matsusaka, T.; Mochida, S. & Yanagida, M. (1997). Damage and replication checkpoint control in fission yeast is ensured by interactions of Crb2, a protein with BRCT motif, with Cut5 and Chk1. Genes Dev. 11(24):3387-3400.

Sale, J. E.; Ross, A. & Simpson, L. J. (2006). Analysis of DNA replication damage bypass and its role in immunoglobulin repertoire development. In: reviews and protocols in DT40 research (eds. J.M. Buerstedde and S Takeda), pp.271-294.Springer.

Sancar, Aziz; Lindsey-Boltz, Laura A.; U¨nsal-Kacmaz, Keziban & Linn, Stuart. (2004). Molecular mechanisms of mammalian DNA repair and the DNA damage checkpoints. Annu. Rev. Biochem., 73:39–85.

Sanchez, Yolanda; Wong, Calvin; Thoma, Richard S.; Richman, Ron; Wu, Zhiqi; Piwnica-Worms, Helen & Elledge, Stephen J. (1997). Conservation of the Chk1 checkpoint pathway in mammals: linkage of DNA Damage to Cdk regulation through Cdc25. Science, 277: 1497- 1501.

Sarbajna, S.; Davies, D. & West, S. C. (2014). Roles of SLX1-SLX4, MUS81-EME1, and GEN1 in avoiding genome instability and mitotic catastrophe. Genes Dev. 28 (10):1124-1136.

Schärer, Orlando D. (2003). Mechanisms of DNA Repair, Chemistry and Biology of DNA Repair. Angew. Chem. Int. Ed., 42: 2946-2974.

Schmidt, M. W.; Houseman, A.; Ivanov, A. R. & Wolf, D. A. (2007). Comparative proteomic and transcriptomic profiling of the fission yeast Schizosaccharomyces pombe. Mol. Syst. Biol, 3, 79.

Shackelford, R. E.; Kaufmann, W. K. & Paules, R. S. (1999). Cell cycle control, checkpoint mechanisms, and genotoxic stress. Environmental Health Perspectives, 107: 5-24.

Shkreta, Lulzim; Michelle, Laetitia; Toutant, Johanne; Tremblay, Michel L. & Chabot, Benoit. (2011). The DNA damage response pathway regulates the alternative splicing of the Apoptotic mediator Bcl-x. J. Biol. Chem., 286: 331-340.

Shrivastav, M.; De Haro, L. P. & Nickoloff, J. A. (2008). Regulation of DNA double-strand break repair pathway choice. Cell Research, 18: 134-147.

Siede, W.; Friedberg, A. S. & Friedberg, E. C. (1993). RAD9-dependent G1 arrest defines a second checkpoint for damaged DNA in the cell cycle of Saccharomyces cerevisiae.Proc Natl Acad Sci U S A., 90(17):7985-7989.

Slavoff, S.A.; Heo, J.; Budnik, B.A.; Hanakahi, L.A. & Saghatelian, A. (2014). A Human Short Open Reading Frame (sORF)-encoded Polypeptide That Stimulates DNA End Joining. J Biol Chem., 289(16):10950-7.

Sohn, S.Y & Cho, Y. (2009). Crystal structure of the human Rad9-Hus1-Rad1 clamp. J. Mol. Biol. 390:490-502.

Sonoda, E.; Sasaki, M.S.; Morrison, C.; Yamaguchi-Iwai, Y.; Takata, M. & Takeda, S. (1999). Sister chromatid exchanges are mediated by homologous recombination in vertebrate cells. Molecular and Cellular Biology, 19(7): 5166-5169.

Sonoda, E.; Morrison, C.; Yamashita, Y.M...; Takata, M. & Takeda, S. (2001, a). Reverse genetic studies of homologous DNA recombination using the chicken B-lymphocyte line, DT40. Phil. Trans. R. Soc. Lond B. 356: 111-117.

Sonoda, E.; Takata, M.; Yamashita, Y. M.; Morrison C. & Takeda, S. (2001, b). Homologous DNA recombination in vertebrate cells. PNAS, 98(15): 8388-8394.

Sonoda, E.; Okada, T.; Zhao, G. Y.; Tateishi, S. Araki, K.; Yamaizumi, M.; Yagi, T.; Verkaik, N. S.; Gent, D. C.v.; Takata, M. & Takeda, S. (2003). Multiple roles of REV3, the catalytic subunit of polζ in maintaining genome stability in vertebrates. The EMBO Journal, 22(12): 3188-3197.

Štorcelová, M.; Vicián, M.; Reis, R.; Zeman, M., and Herichová, I. (2013). Expression of cell cycle regulatory factors hus1, gadd45a, rb1, cdkn2a and mre11a correlates with expression of clock gene per2 in human colorectal carcinoma tissue. Mol Biol Rep., 40(11):6351-61.

Synnes, M.; Nilssen, E. A.; Boye, E. & Grallert, B. (2002). A novel chk1-dependent G1/M checkpoint in fission yeast. J Cell Sci. 115(Pt 18):3609-3618.

Tanaka, K. & Russell, P. (2001). Mrc1 channels the DNA replication arrest signal to checkpoint kinase Cds1. Nat Cell Biol. 3(11):966-972.

Terada, Yasuhiko; Tatsuka, Masaaki; Jinno, Shigeki & Okayama, Hiroto. (1995). Requirement for tyrosine phosphorylation of Cdk4 in Gl arrest induced by ultraviolet irradiation. Nature, 376: 358-362.

Thomas, Philip & Smart, Trevor G. (2005). HEK293 cell line: A vehicle for the expression of recombinant proteins. Journal of Pharmacological and Toxicological Methods, 51:187 – 200.

Tvegård, T.; Soltani, H.; Skjølberg, H. C.; Krohn, M.; Nilssen, E. A.; Kearsey, S. E.; Grallert, B. & Boye, E. (2007). A novel checkpoint mechanism regulating the G1/S transition. Genes Dev., 21(6):649-654.

Udell, Christian M.; Lee, Sabrina K. & Davey, Scott. (1998). HRAD1 and MRAD1 encode mammalian homologues of the fission yeast rad1+ cell cycle checkpoint control gene. Nucleic Acids Research, 26(17): 3971-3976.

Van Gent, D. C. & van der Burg, M. (2007). Non-homologous end joining, a sticky affair. Oncogene, 26:7731-7740.

Van Hooser, A.; Goodrich, D.W.; Allis, C.D.; Brinkley, B.R. & Mancini, M.A. (1998). Histone H3 phosphorylation is required for the initiation, but not the maintenance, of mammalian chromosome condensation. J Cell Sci., 111: 3497-3506.

Volkmer, Elias & Karnitz, Larry M. (1999). Human Homologs of Schizosaccharomyces pombe Rad1, Hus1, and Rad9 Form a DNA Damage-responsive Protein Complex. J Biol Chem, 274(2):567-570.

Walworth, N. C. & Bernards, R. (1996). rad-dependent response of the chk1-encoded protein kinase at the DNA damage checkpoint. Science. 271(5247):353-6.

Wang, Jean Y.J. (1998). Cellular responses to DNA damage. Current opinion in cell biology, 10: 240-247.

Wang, Lili; Kao, Richard; Douglas Ivey, F. & Hoffman, Charles S. (2004). Strategies for gene disruptions and plasmid constructions in fission yeast. Methods, 33:199–205.

Wang, X. & D'Andrea, A.D. (2004). The interplay of fanconi anaemia proteins in the DNA damage response. DNA Repair 3: 1063-1069.

Wang, X.; Hu, B.; Weiss, R.S. & Wang, Y. (2006). The effect of Hus1 on ionizing radiation sensitivity is associated with homologous recombination repair but is independent of nonhomologous end joining. Oncogene, 25: 1980–1983.

Watson, Adam T.; Garcia, Valerie; Bone, Neil; Carr, Antony M. & Armstrong, John (2008). Gene tagging and gene replacement using recombinase-mediated cassette exchange in Schizosaccharomyces pombe. Gene, 407:63–74.

Wei-Feng, L.; Shan-Shan, Y.; Guan-Jun, C. & Yue-Zhong, Li. (2006). DNA damage checkpoint, damage repair, and genome stability. Acta Genetica Sinica, 33(5): 381-390.

Weinert, T. A. & Hartwell, L. H. (1988). The RAD9 gene controls the cell cycle response to DNA damage in Saccharomyces cerevisiae. Science. 241(4863):317-322.

Weiss, Robert S.; Leder, Philip & Vaziri, Cyrus (2003). Critical Role for Mouse Hus1 in an S-Phase DNA Damage Cell Cycle Checkpoint. Molecular and cellular biology, 23(3): 791–803.

Weiss, R. S.; Matsuoka, S.; Elledge, S. J. & Leder, P. (2002). Hus1 acts upstream of Chk1 in a mammalian DNA damage response pathway. Curr Biol., 12(1):73-77.

Werner, M.; Feller, A.; Messenguy, F. & Piérard, A. (1987). The leader peptide of yeast gene CPA1 is essential for the translational repression of its expression. Cell. 49(6):805-813.

Wilsker, Deborah; Petermann, Eva; Helleday, Thomas & Bunz, Fred (2008). Essential function of Chk1 can be uncoupled from DNA damage checkpoint and replication control. PNAS, 105 (52): 20752–20757.

Wilson III, D. M. & Thompson, L.H. (2007). Molecular mechanisms of sister-chromatid exchange. Mutation Research, 616:11–23.

Wohlbold, Lara & Fisher, Robert P. (2009). Behind the wheel and under the hood: Functions of cyclin-dependent kinases in response to DNA damage. DNA Repair, 8: 1018–1024.

Wood, Richard D.; Mitchell, Michael, Lindahl, Tomas. (2005). Human DNA repair genes, 2005. Mutation Research, 577:275–283.

Wu, X.; Shell, S. M. & Zou, Y. (2005). Interaction and colocalization of Rad9/Rad1/Hus1 checkpoint complex with replication protein A in human cells. Oncogene. 24(29):4728-4735.

Wyman, Claire & Kanaar, Roland (2006). DNA Double-Strand break repair: All's well that ends Well. Annu. Rev. Genet., 40:363–83.

Wyman, Claire; Risticb, Dejan & Kanaar, Roland (2004). Homologous recombination-mediated double-strand break repair. DNA Repair, 3: 827–833.

Xie, Suqing; Wu, Huiyun; Wang, Qi; Cogswell, John P.; Husain, Intisar; Conn, Chris; Stambrook, Peter; Jhanwar-Uniyal, Meena & Dai, Wei. (2001). Plk3 Functionally Links DNA Damage to Cell Cycle Arrest and Apoptosis at Least in Part via the p53 Pathway The Journal of Biological Chemistry, 276(46): 43305–43312.

Xu, Y. J.; Davenport, M. & Kelly, T.J. (2006). Two-stage mechanism for activation of the DNA replication checkpoint kinase Cds1 in fission yeast. Genes Dev., 20 (8):990-1003.

Yamamoto, K.; Kobayashi, M. & Shimizu, H. (2006). ATM, A paradigm for a stress-responsive signal transducer in higher vertebrate cells. In: reviews and protocols in DT40 research (eds. J.M. Buerstedde and S. Takeda): 32713 -339.Springer.

Yamashita, Y. M.; Okada, T.; Matsusaka, T.; Sonoda, E.; Zhao, G. Y.; Araki, K.; Tateishi, S.; Yamaizumi, M. & Takeda, S. (2002). RAD18 and RAD54 cooperatively contribute to maintenance of genomic stability in vertebrate cells. The EMBO Journal, 21(20): 5558-5566.

Yang, K.; Hitomi, Masahiro & Stacey, Dennis W. (2006). Variations of Cyclin D1 levels through the cell cycle determine the proliferative fate of a cell. Cell Division.1 (32): 1-8.

Yata, Keiko & Esashi, Fumiko (2009). Dual role of CDKs in DNA repair: To be, or not to be. DNA repair, 8: 6–18.

You, Z.; Kong, L. & Newport, J. (2002). The role of single-stranded DNA and polymerase alpha in establishing the ATR, Hus1 DNA replication checkpoint. J Biol Chem, 277: 27088-27093.

Zachos, G.; Rainey, M.D. & Gillespie, D.A. (2005). Chk1-dependent S-M checkpoint delay in vertebrate cells is linked to maintenance of viable replication structures. Mol Cell Biol., 25(2):563-574.

Zarzov, P.; Decottignies, A.; Baldacci, G. & Nurse P. (2002). G (1)/S CDK is inhibited to restrain mitotic onset when DNA replication is blocked in fission yeast. EMBO J., 21(13):3370-3376.

Zdanov, Stephanie; Remacle, Jose & Toussaint, Oliver (2006). Establishment of H2O2-induced premature senescence in human fibroblasts concomitant with increased cellular production of H2O2. Ann. N. Y. Acad. Sci., 1067: 210-216.

Zeng, Y. & Piwnica-Worms H. (1999). DNA damage and replication checkpoints in fission yeast require nuclear exclusion of the Cdc25 phosphatase via 14-3-3 binding. Mol Cell Biol., 19(11):7410-9.

Zeng, Yan; Forbes, Kristi Chrispell; Wu, Zhiqi; Morenok, Sergio; Piwnica-Worms, Helen & Enoch, Tamar (1998). Replication checkpoint requires phosphorylation of the phosphatase Cdc25 by Cds1 or Chk1. Nature, 395: 507-510.

Zhao, Hui & Piwnica-Worms, Helen (2001). ATR-mediated checkpoint pathways regulate phosphorylation and activation of human Chk1. Mol Cell Biol., 21(13):4129-4139.

Zhu, Min & Weiss, Robert S. (2006). Increased Common Fragile Site Expression, Cell Proliferation Defects, and Apoptosis following Conditional Inactivation of Mouse Hus1 in Primary Cultured Cells. Molecular Biology of the Cell, 18:1044-1055.

Zimmermann, M.; Lottersberger, F.; Buonomo, S. B.; Sfeir, A. & de Lange T. (2013). 53BP1 regulates DSB repair using Rif1 to control 5' end resection. Science, 339(6120):700-704.

Zou, L. & Elledge, S.J. (2003). Sensing DNA damage through ATRIP recognition of RPA-ssDNA complexes. Science, 300(5625):1542-1548.

Zou, L.; Cortez, D. & Elledge, S. J. (2002). Regulation of ATR substrate selection by Rad17-dependent loading of Rad9 complexes onto chromatin. Genes Dev. 16(2):198-208.

Websites:

Clustal Omega:

(http://www.ebi.ac.uk/Tools/msa/clustalo/).

Ensembl Fungi database, *hus1* gene, accessed on June 2014:

(http://fungi.ensembl.org/Schizosaccharomyces_pombe/Gene/Sequence?db=core;g=SPAC20G4.04c;r=I:4820987-4822706;t=SPAC20G4.04c.1).

Ensembl genome browser, *hHUS1* gene:

(http://www.ensembl.org/Homo_sapiens/Transcript/Summary?db=core;g=ENSG00000136273;r=7:48015252-48019150;t=ENST00000258774).

Flp-In™ T-REx™ Core Kit User Guide, Life Technologies:

(http://tools.lifetechnologies.com/content/sfs/manuals/flpintrex_man.pdf).

Flp-In™ System for Generating Stable Mammalian Expression Cell Lines by Flp Recombinase-Mediated Integration: Invitrogen:

(http://tools.lifetechnologies.com/content/sfs/manuals/flpinsystem_man.pdf).

Flp-In™ T-REx™ Core Kit for Generating Stable, Inducible Mammalian Expression Cell Lines by Flp Recombinase-Mediated Integration, Invetrogen:

(http://tools.lifetechnologies.com/content/sfs/manuals/flpintrex_man.pdf).

Growth and Maintenance of the Flp- In™ T-Rex™ Cell Line:

(http://tools.lifetechnologies.com/content/sfs/manuals/flpintrexcells_man.pdf).

Gene Cards website:

(http://www.genecards.org/cgi-bin/carddisp.pl?gene=HUS1).

H-DBAS - Human-transcriptome DataBase for Alternative Splicing:

(http://h-invitational.jp/h-dbas/index.js).

HUSH shRNA Plasmids (29-MER) manual, Origene:

(http://www.origene.com/assets/Documents/HuSH/AppGuideHuSH29.pdf).

IGD, Intronless gene database:

(http://www.bioinfo-cbs.org/igd/description1.php).

NEB High Efficiency transformation protocol:

(https://www.neb.com/protocols/1/01/01/high-efficiency-transformation-protocol-c3019).

Optimizing Restriction Endonuclease Reactions, New England BioLabs (NEB):

(https://www.neb.com/protocols/2012/12/07/optimizing-restriction-endonuclease-reactions).

Polyview 3D server:

(http://polyview.cchmc.org/polyview3d.html).

Pombase the scientific resource for fission yeast, *hus1* (SPAC20G4.04c):

(http://www.pombase.org/spombe/result/SPAC20G4.04c).

Promega protocol to prepare ES1301 *mut*S and JM109 Competent Cells:

(http://www.promega.com.cn/techserv/tbs/TM001-310/tm001.pdf).

psiRNA-h7SKGFPzeo kit manual, Invivogen:

(http://www.invivogen.com/PDF/psiRNA4-7SKGFPzeo_TDS.pdf)

RNA extraction: cells in culture:

(http://www.abcam.com/ps/pdf/protocols/RNA_isolation_cell_culture.pdf.)

siRNAWizard:

(http://www.sirnawizard.com/).

Appendices

1. *hus1.Myc-M32AM46A* mutantation sequence

```
hus1            ATGAGATTTAAAACAAGGATTAGCAACTTGTACACGTTGACGCGTAAGTTGGAAAAGATC 60
hus1M32AM46A    ATGAGATTTAAAACAAGGATTAGCAACTTGTACACGTTGACGCGTAAGTTGGAAAAGATC 60
                ************************************************************

hus1            AGCAGAAAGTTCGTTTACTAATCAAATTTAGGTCTTGTTCAGGCGCTAGATAAAATTGGA 120
hus1M32AM46A    AGCAGAAAGTTCGTTTACTAATCAAATTTAGGTCTTGTTCAGGCGCTAGATAAAATTGGA 120
                ************************************************************

hus1            AGATTTTGCTGGCTTCGTCTGATGCCTGAAACTGTAAATTTTGTGATAGTGCCAGATTTT 180
hus1M32AM46A    AGATTTTGCTGGCTTCGTCTGGCTCCTGAAACTGTAAATTTTGTGATAGTGCCAGATTTT 180
                ********************   ***********************************

hus1            AGGATGACTCAAGTTTGGTCGTAAGTGAAGATATTAAGCATTTAACGGTGAAAAAAATCA 240
hus1M32AM46A    AGGGCTACTCAAGTTTGGTCGTAAGTGAAGATATTAAGCATTTAACGGTGAAAAAAATCA 240
                ***   ******************************************************

hus1            CATTGTGAAACTAATAAAGAAACAGAGTTTTAGAAGTCGTATGATTAACTATCTTTTTCT 300
hus1M32AM46A    CATTGTGAAACTAATAAAGAAACAGAGTTTTAGAAGTCGTATGATTAACTATCTTTTTCT 300
                ************************************************************

hus1            ATTTGATTGCCCTAACTAACGTAAACGGAAAGGAAACAATATTTGAGGACTATGTCGTCC 360
hus1M32AM46A    ATTTGATTGCCCTAACTAACGTAAACGGAAAGGAAACAATATTTGAGGACTATGTCGTCC 360
                ************************************************************

hus1            AAAGCAATGCAGACAACGTGATAAATCTAGAAGTTCCTATAGATAATTTCTATAAAGCCT 420
hus1M32AM46A    AAAGCAATGCAGACAACGTGATAAATCTAGAAGTTCCTATAGATAATTTCTATAAAGCCT 420
                ************************************************************

hus1            TACGATCAGCGGCCAACGCTAGTGATTCTACTGTTCGTCTATCCAAGAAGAATAACCAGC 480
hus1M32AM46A    TACGATCAGCGGCCAACGCTAGTGATTCTACTGTTCGTCTATCCAAGAAGAATAACCAGC 480
                ************************************************************

hus1            CATTACTTTCGTTGTCTACCACTTGGAGTGGAAGGGCGTTTGGTTCGAATATTGTGACTC 540
hus1M32AM46A    CATTACTTTCGTTGTCTACCACTTGGAGTGGAAGGGCGTTTGGTTCGAATATTGTGACTC 540
                ************************************************************

hus1            ATAATATACCTGTTCGAGTACTATCACAATCATACGTGTCAGTTATTAAGGAACCAACTG 600
hus1M32AM46A    ATAATATACCTGTTCGAGTACTATCACAATCATACGTGTCAGTTATTAAGGAACCAACTG 600
                ************************************************************

hus1            CTCCTGAACCAGACTGTCATATATTCCTTCCACAACTGAATTTTCTAAGACACGTCGTGG 660
hus1M32AM46A    CTCCTGAACCAGACTGTCATATATTCCTTCCACAACTGAATTTTCTAAGACACGTCGTGG 660
                ************************************************************

hus1            ACAAATACAAGAGTCTTTCAGACCGTATTATAATGTCAGCCAACATGTCAGGCGAATTGC 720
hus1M32AM46A    ACAAATACAAGAGTCTTTCAGACCGTATTATAATGTCAGCCAACATGTCAGGCGAATTGC 720
                ************************************************************

hus1            AGTTATCGGTAAACATACCTTCAGCTAGAGTAAGCACAAAATGGAAAGGATTAGAGAATC 780
hus1M32AM46A    AGTTATCGGTAAACATACCTTCAGCTAGAGTAAGCACAAAATGGAAAGGATTAGAGAATC 780
                ************************************************************

hus1            CAGAGTTAGATCCTAGTCAAGTCGAAGACATCAGTCGACATCCCTCTCAAACAAGGGCAC 840
hus1M32AM46A    CAGAGTTAGATCCTAGTCAAGTCGAAGACATCAGTCGACATCCCTCTCAAACAAGGGCAC 840
                ************************************************************

hus1            CCGAAGAATTTGTTCACATGAGACTAGACAGCAAGGACTTAGTCAACATGTTAAAAATAT 900
hus1M32AM46A    CCGAAGAATTTGTTCACATGAGACTAGACAGCAAGGACTTAGTCAACATGTTAAAAATAT 900
                ************************************************************

hus1            CCAGTGTTGCAAAGCGTGTAATAGCGTGTATGTACTATGAGAGAATCCTTTTTATGACCA 960
hus1M32AM46A    CCAGTGTTGCAAAGCGTGTAATAGCGTGTATGTACTATGAGAGAATCCTTTTTATGACCA 960
                ************************************************************
```

```
hus1             CGAACTAACCTTTTTACATTACAGGTTTCTGTGAAGGACATGCGCTAGTACTTTATGTTT 1020
hus1M32AM46A     CGAACTAACCTTTTTACATTACAGGTTTCTGTGAAGGACATGCGCTAGTACTTTATGTTT 1020
                 ************************************************************

hus1             ATATAACAGATCCAGAAGATGAACATACGGCTGTTTTAACATACTACATTAGTACCTATG 1080
hus1M32AM46A     ATATAACAGATCCAGAAGATGAACATACGGCTGTTTTAACATACTACATTAGTACCTATG 1080
                 ************************************************************

hus1             TGGACTAAGGTTACTTCAATTTGTTTATGATT--TGATTTAATTAACGAATAATTGTTAT 1138
hus1M32AM46A     TGGACCGGATCCCCGGGTTAATTAACGGTGAACAAAAGCTAATCTCCGAGGAAGACTTGA 1140
                 *****        *       *              *  ****   ***  **   **

hus1             GAGTGACTAGCCACATTTTTAATGTACATTAAAATGAAAAGAGATTAATCAACATCTACC 1198
hus1M32AM46A     --ACGGTGAACAAAAATTAATCTCAG---------AAGAAGAC-TTGAACGGACTCGACG 1188
                     *   * * * * **    *             * ****  ** * *    ** **

hus1             ATGCTT-ATACTTATTTTCTCTCTCTTCCTTTATCGATCTTACCGTTCTT---TTTTATT 1254
hus1M32AM46A     GTGAACAAAAGTTGATTTCTGAAGAAGATTTGAACGGTGAACAAAAGCTAATCTCCGAGG 1248
                  **    * * **  *****          ** * ** *          **    *   *

hus1             TATTTT------ATACAGTTGTTGTAATCTCGGCAACTCA------------GTGTTTTA 1296
hus1M32AM46A     AAGACTTGAACGGTGAACAAAAATTAATCTCAGAAGAAGACTTGAACGGACTCGACGGTG 1308
                  *   *       *  *       ******* * *    *                 *

hus1             CTATTCCGTTGATATCTCTTAAAAGGATAACACCAAAAAGAAATATAATGTTCAAGTCAC 1356
hus1M32AM46A     AACAAAAGTTGATTTCTGAAGAAGATTTGAACGGTGAACAAAAGCTAATCTCCGAGGAAG 1368
                        ****** ***    **    * *      **  ***  **** * * **  *

hus1             AGAAAATCTGTTGATAAAATCCATATGTTTTCACGTTTTCAATGAGAGATACATACGATT 1416
hus1M32AM46A     ACTTGAACGGTGAACAAA----AATTAATCTCAGAAGAAGACTTGAACGGACTCGACGGT 1424
                 *    * * **  * ***    *  *  * ***       * *   *   **       *

hus1             AAACACAAACGTATGTTTTCAAGCAATTAACTTGAATATGAATAAACCTTGGTTCATCTT 1476
hus1M32AM46A     GAAC--AAAAGTTGATT-TCTGAAGAAGATTTGAACGGTGA---------------ACAA 1466
                  ***  *** **   ** **     *  *  *  *   ***               *

hus1             TCTTTAATCTTTTAGACAAGCAACTGTTCAGAAATCTATAAAGTCTCAATTGAA--CATT 1534
hus1M32AM46A     AAGCTAATCTCCGAGGAAGACTTGAACGGTGAACAAAAATTAATCTCAGAAGAAGACTTG 1526
                     ******   **  *  *         ***    *   * *****   ***  * *

hus1             TAAGTGCTCAATGGGAAATA-------TATACTTAATAAAAATTGAATATTTTAATCGTT 1587
hus1M32AM46A     AACGGACTCGACGGTGAACAAAAGTTGATTTCTGAAGAAGATTTGAACGGTGAACAAAAG 1586
                  * *  *** * **  ** *         * ** ** ** * *****   *  *

hus1             TT--------------TTT-- 1592
hus1M32AM46A     CTAATCTCCGAGGAGACTTGA 1607
                  *              **
```

Translation of Myc tag

End of Hus1

```
  1   V  L  T  Y  Y  I  S  T  Y  V  D  R  I  P  G  L  I  N  G  E
  1   GTTTTAACATACTACATTAGTACCTATGTGGACCGGATCCCCGGGTTAATTAACGGTGAA

 21    Q  K  L  I  S  E  E  D  L  N  G  E  Q  K  L  I  S  E  E  D
 61   CAAAAGCTAATCTCCGAGGAAGACTTGAACGGTGAACAAAAATTAATCTCAGAAGAAGAC

 41    L  N  G  L  D  G  E  Q  K  L  I  S  E  E  D  L  N  G  E  Q
121   TTGAACGGACTCGACGGTGAACAAAAGTTGATTTCTGAAGAAGATTTGAACGGTGAACAA

 61    K  L  I  S  E  E  D  L  N  G  E  Q  K  L  I  S  E  E  D  L
181   AAGCTAATCTCCGAGGAAGACTTGAACGGTGAACAAAAATTAATCTCAGAAGAAGACTTG

 81    N  G  L  D  G  E  Q  K  L  I  S  E  E  D  L  N  G  E  Q  K
241   AACGGACTCGACGGTGAACAAAAGTTGATTTCTGAAGAAGATTTGAACGGTGAACAAAAG

101    L  I  S  E  E  D  L  N  G  E  Q  K  L  I  S  E  E  D  L  N
301   CTAATCTCCGAGGAAGACTTGAACGGTGAACAAAAATTAATCTCAGAAGAAGACTTGAAC

121    G  L  D  G  E  Q  K  L  I  S  E  E  D  L  N  G  E  Q  K  L
361   GGACTCGACGGTGAACAAAAGTTGATTTCTGAAGAAGATTTGAACGGTGAACAAAAGCTA

141    I  S  E  E  D  L  N  G  E  Q  K  L  I  S  E  E  D  L  N  G
421   ATCTCCGAGGAAGACTTGAACGGTGAACAAAAATTAATCTCAGAAGAAGACTTGAACGGA

161    L  D  G  E  Q  K  L  I  S  E  E  D  L  N  G  E  Q  K  L  I
481   CTCGACGGTGAACAAAAGTTGATTTCTGAAGAAGATTTGAACGGTGAACAAAAGCTAATC

181    S  E  E  T  -
541   TCCGAGGAGACTTGA
```

2. Alignment of the four-hHUS1 cDNAs with diagrams illusitate the primers priming sites within the transcripts cDNA sequences and their PCR products:

2.1 Alignment of the four-*hHUS1* cDNAs as curated in the Ensembl database

The active ATG translation start codons are shown in blue. The location and sequence of the variant-specific forward primers is shown in colors. The common reverse primer is shown in grey. The last codon of each open reading frame is underlined and highlighted in green. The primer pair for the *hHUS1-tail* region is shown in red and dark green, respectively.

(The alignement was produced by Clustal Omega server: http://www.ebi.ac.uk/Tools/msa/clustalo/).

```
HUS1-001      ----------GCCGCGGCTGCGCCATCCGCGGCCATGAAGTTTCGGGCCAAGATCGTGGA     50
HUS1-005      ACAGAGGCCCGCCGCGGCTGCGCCATCCGCGGCCATGAAGTTTCGGGCCAAGATCGTGGA     60
HUS1-011      ------------------------------------------------AAGATCGTGGA     11
HUS1-004      ACAGAGGCCCGCCGCGGCTGCGCCATCCGCGGCCATGAAGTTTCGGGCCAAGATCGTGGA     60
                                                              ***********

HUS1-001      CGGGGCCTGTCTGAAC----------------------------------------------     66
HUS1-005      CGGGGCCTGTCTGAACCACTTCACACGTGAGCAGGGAGGCCGGAGAGGAGCGAGGGAGGA     120
HUS1-011      CGGGGCCTGTCTGAACCACTTCACACTA-----------------------------AT     41
HUS1-004      CGGGGCCTGTCTGAACCACTTCACACGTGAGCAGGGAGGCCGGAGAGGAGCGAGGGAGGA     120
              ****************

HUS1-001      --------------CACTTCACACGAATCAGTAACATGATAGCCAAGCTTGCCAAAACCT     112
HUS1-005      ACGGAAGGAAGCAGTGAGCGCGCGGAATCAGTAACATGATAGCCAAGCTTGCCAAAACCT     180
HUS1-011      TCCTTATTTTAACCCCTGCTTTAGGAATCAGTAACATGATAGCCAAGCTTGCCAAAACCT     101
HUS1-004      ACGGAAGGAA-----------GCAGAATCAGTAACATGATAGCCAAGCTTGCCAAAACCT     169
                                 . **********************************

HUS1-001      GCACCCTCCGCATCAGCCCTGATAAGCTTAACTTCATCCTTTGTGACAAGCTGGCTAATG     172
HUS1-005      GCACCCTCCGCATCAGCCCTGATAAGCTTAACTTCATCCTTTGTGACAAGCTGGCTAATG     240
HUS1-011      GCACCCTCCGCATCAGCCCTGATAAGCTTAACTTCATCCTTTGTGACAAGCTGGCTAATG     161
HUS1-004      GCACCCTCCGCATCAGCCCTGATAAGCTTAACTTCATCCTTTGTGACAAGCTGGCTAATG     229
              ************************************************************

HUS1-001      GAGGAGTGAGCATGTGGTGTGAGCTGGAACAGGAGAACTTCTTCAACGAATTTCAAATGG     232
HUS1-005      GAGGAGTGAGCATGTGGTGTGAGCTGGAACAGGAGAACTTCTTCAACGAATTTCAAATGG     300
HUS1-011      GAGGAGTGAGCATGTGGTGTGAGCTGGAACAGGAGAACTTCTTCAACGAATTTCAAATGG     221
HUS1-004      GAGGAGTGAGCATGTGGTGTGAGCTGGAACAGGAGAACTTCTTCAACGAATTTCAAATGG     289
              ************************************************************

HUS1-001      AGGGTGTCTCTGCAGAAAACAATGAGATTTATTTAGAGCTAACATCGGAAAACTTATCTC     292
HUS1-005      AGGGTGTCTCTGCAGAAAACAATGAGATTTATTTAGAGCTAACATCGGAAAACTTATCTC     360
HUS1-011      AGGGTGTCTCTGCAGAAAACAATGAGATTTATTTAGAGCTAACATCGGAAAACTTATCTC     281
HUS1-004      AGGGTGTCTCTGCAGAAAACAATGAGATTTATTTAGAGCTAACATCGGAAAACTTATCTC     349
              ************************************************************

                                        .
                                        .
HUS1-001      TGGTCCCAGATCCTGATGTTAGTATTTATTTACCAGTCTTGAAGACTATGAAGAGTGTTG     532
HUS1-005      TGGTCCCAGATCCTGATGTTAGTATTTATTTACCAGTCTTGAAGACTATGAAGAGTGTTG     600
HUS1-011      TGGTCCCAGATCCTGATGTTAGTATTTATTTACCAGTCTTGAAGACTATGAAGAGTGTTG     521
HUS1-004      TGGTCCCAGATCCTGATGTTAGTATTTATTTACCAGTCTTGAAGACTATC----------     579
              ************************************************

HUS1-001      TGGAAAAAATGAAAAACATCAGCAATCACCTTGTTATTGAAGCAAACCTAGATGGAGAAT     592
HUS1-005      TGGAAAAAATGAAAAACATCAGCAATCACCTTGTTATTGAAGCAAACCTAGATGGAGAAT     660
HUS1-011      TGGAAAAAATGAAAAACATCAGCAATCACCTTGTTATTGAAGCAAACCTAGATGGAGAAT     581
HUS1-004      ------------------------------------------------------------     579
```

```
HUS1-001      TGAATTTGAAAATAGAAACTGAATTAGTATGTGTTACAACTCATTTTAAAGATCTTGGAA     652
HUS1-005      TGAATTTGAAAATAGAAACTGAATTAGTATGTGTTACAACTCATTTTAAAGATCTTGGAA     720
HUS1-011      TGAATTTGAAAATAGAAACTGAATTAGTATGTGTTACAACTCATTT-------------     627
HUS1-004      ------------------------------------------------------------     579

HUS1-001      ATCCTCCATTAGCCTCTGAAAGCACCCATGAGGACAGAAACGTGGAACACATGGCTGAAG     712
HUS1-005      ATCCTCCATTAGCCTCTGAAAGCACCCATGAGGACAGAAACGTGGAACACATGGCTGAAG     780
HUS1-011      ------------------------------------------------------------     627
HUS1-004      ------------------------------------------------------------     579

HUS1-001      TGCACATAGATATTAGGAAGCTCCTACAGTTTCTTGCTGGACAACAAGTAAATCCCACAA     772
HUS1-005      TGCACATAGATATTAGGAAGCTCCTACAGTTTCTTGCTGGACAACAAGTAAATCCCACAA     840
HUS1-011      ------------------------------------------------------------     627
HUS1-004      ------------------------------------------------------------     579

HUS1-001      AGGCCTTATGCAATATTGTGAATAACAAGATGGTGCATTTTGATCTGCTTCATGAAGACG     832
HUS1-005      AGGCCTTATGCAATATTGTGAATAACAAGATGGTGCATTTTGATCTGCTTCATGAAGACG     900
HUS1-011      ------------------------------------------------------------     627
HUS1-004      ------------------------------------------------------------     579

HUS1-001      TGTCCCTTCAGTATTTCATCCCTGCGCTGTCCTAGCACCCTGTCGCTGGAGTTGGCATGC     892
HUS1-005      TGTCCCTTCAGTATTTCATCCCTGCGCTGTCCTAGCACCCTGTCGCTGGAGTTGGCATGC     960
HUS1-011      ------------------------------------------------------------     627
HUS1-004      ------------------------------------------------------------     579

HUS1-001      AGAGACTTTGTCAGGATGGGAGAGGCCGCAGGTGTTGTGTTCTGATCACTGGTCTGTGCC     952
HUS1-005      AGAGACTTTGTCAGGATGGGAGAGGCCGCAGGTGTTGTGTTCTGATCACTGGTCTGTGCC    1020
HUS1-011      ------------------------------------------------------------     627
HUS1-004      ------------------------------------------------------------     579

HUS1-001      CTCACAGCACCGCACATCGACACACTGTACTTATTTGTCCCTCTCTAACATTTTAACTAA    1012
HUS1-005      CTCACAGCACCGCACATCGACACACTGTACTTATTTGTCCCTCTCTAACATTTTAACTAA    1080
HUS1-011      ------------------------------------------------------------     627
HUS1-004      ------------------------------------------------------------     579

                                        .
                                        .
                                        .

HUS1-001       TGAATGGCTTAAGATTTTATCTTTGTGTAGAATGTGGCTAAAGAAACCTTAGTTGAGATT   2932
HUS1-005       ------------------------------------------------------------   1125
HUS1-011       ------------------------------------------------------------    627
HUS1-004      ------------------------------------------------------------    579

HUS1-001      CAA  2935
HUS1-005      ---  1125
```

```
HUS1-011      ---  627
HUS1-004      ---  579
```

2.2 Primers sequences and their PCR product sizes to amplify the short 5`-fragments of the *hHUS1* mRNAs (The colour code is the same as in 2.1)

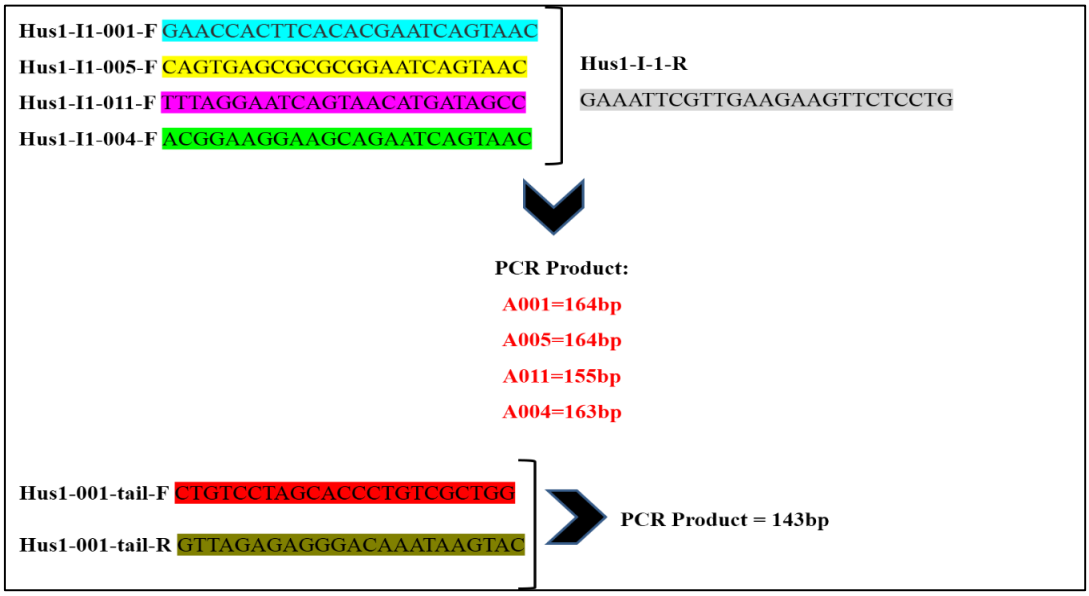

2.3 Primers used to amplify the full-length cDNA sequences of hHUS1 and its splice variants and their PCR product sizes (The colour code is the same as in 2.1)

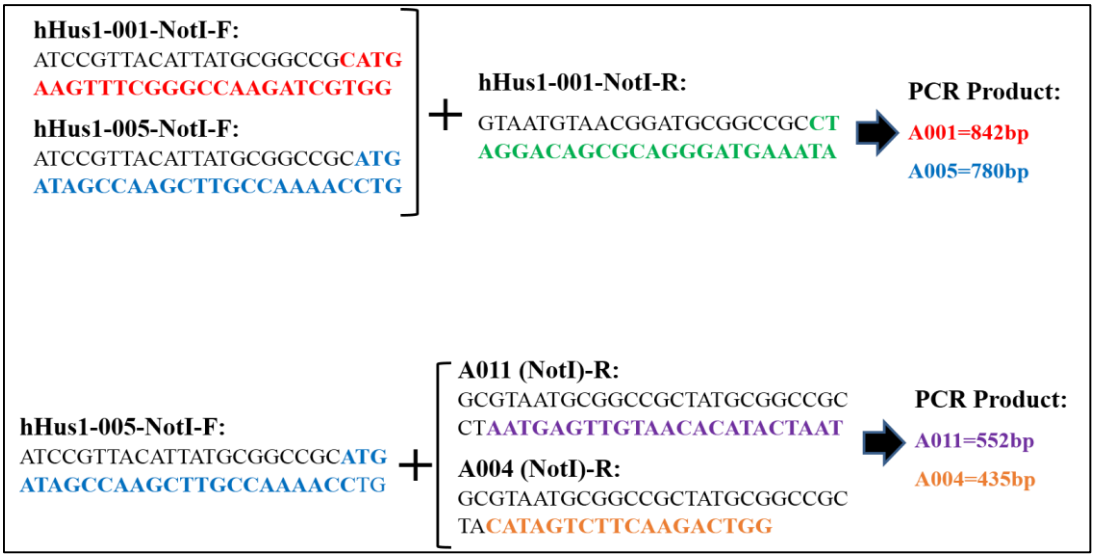

2.4 cDNA sequence of *hHUS1B*. (The start codon is shown in blue, the TAA stop codon is shown in green. The 3`-UTR is shown in yellow)

Hus1B:

```
   1 CTGCCTTCCCTGTGGCATCATGAAGTTTCGCGCCAAGATCACCGGCAAAGGCTGTCTAGA
  61 GCTGTTCATTCACGTCAGCGGCACCGTCGCGAGGCTAGCGAAGGTCTGCGTGCTCCGCGT
 121 GCGCCCTGACAGCCTGTGCTTCGGCCCCGCGGGTTCCGGCGGCCTCCACGAGGCCAGGCT
 181 GTGGTGCGAGGTGCGGCAGGGGGCCTTCCAGCAGTTTCGCATGGAAGGTGTCTCGGAAGA
 241 TCTCGATGAGATCCACCTGGAGCTGACGGCGGAGCACCTGTCCCGGGCGGCGAGAAGCGC
 301 AGCGGGCGCGTCCTCCCTGAAGCTGCAGCTGACCCACAAGCGCCGCCCCTCCCTCACGGT
 361 GGCGGTGGAGCTGGTCTCGTCCCTGGGCCGCGCTCGCAGCGTGGTGCACGATCTGCCCGT
 421 GCGGGTGCTTCCCAGGAGAGTGTGGCGGGACTGCCTGCCGCCCAGCCTGCGCGCCTCCGA
 481 CGCGAGCATCCGCCTGCCGCGCTGGAGGACGCTGAGGAGCATCGTGGAGAGGATGGCGAA
 541 CGTGGGCAGTCACGTGCTGGTGGAAGCAAACCTCAGTGGCAGGATGACCCTGAGTATAGA
 601 GACGGAGGTGGTGTCCATTCAAAGTTATTTTAAAAATCTTGGAAACCCTCCCCAGTCGGC
 661 TGTGGGTGTGCCTGAAAACAGAGACCTGGAGAGCATGGTGCAAGTGCGGGTGGACAATCG
 721 GAAGCTTCTGCAGTTTTTGGAGGGACAGCAAATACATCCTACGACGGCCCTGTGCAATAT
 781 TTGGGACAATACTCTTCTTCAGCTTGTTTTGGTTCAAGAAGATGTCTCTCTTCAGTATTT
 841 CATTCCTGCCTTGTAAAAATTCAGCCAGCTTAGATTTTTTTTTTAAGGTTTTGATCTTTT
 901 CAAAACTAAAACAGACCCTGAGTTAATTGGGTTGAAAATTTGGACCTTCACTGACTTATG
 961 CAGGGCGTATATTTTGTTGAGCCCTTCCTCCTTTGCAAAATTTATATTAAAGCATTGGTA
1021 AAACA
```

2.5 Primers to amplify the short and full-length *hHUS1B* fragments and their PCR product sizes (The colour code is the same as in 2.4)

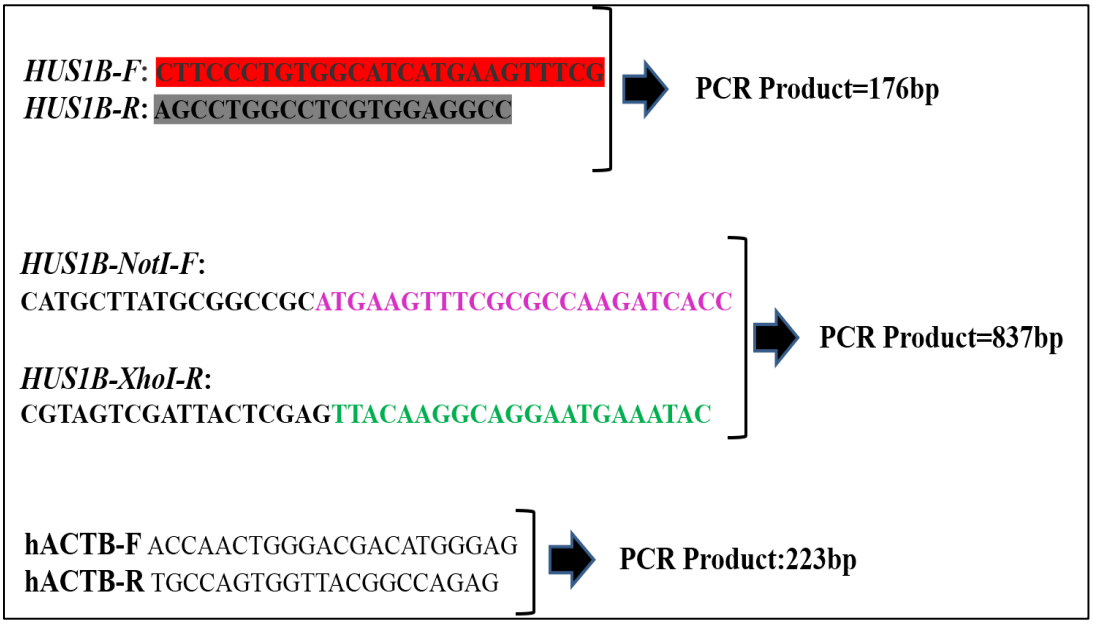

2.6 *hHUS1-001* as a short sequence that was amplified from human brain tissue (Figure 4-5)

```
A001sequenced      ------------------------------------------------------------
A001Ensemble       GCCGCGGCTGCGCCATCCGCGGCCATGAAGTTTCGGGCCAAGATCGTGGACGGGGCCTGT
A001sequenced      --GAACCACTTCACACGAATCAGTAACATGATAGCCAAGCTTGCCAAAACCTGCACCCTC
A001Ensemble       CTGAACCACTTCACACGAATCAGTAACATGATAGCCAAGCTTGCCAAAACCTGCACCCTC
                     ************************************************************
A001sequenced      CGCATCAGCCCTGATAAGCTTAACTTCATCCTTTGTGACAAGCTGGCTAATGGAGGAGTG
A001Ensemble       CGCATCAGCCCTGATAAGCTTAACTTCATCCTTTGTGACAAGCTGGCTAATGGAGGAGTG
                   ************************************************************
A001sequenced      AGCATGTGGTGTGAGCTGGAACAGGAGAACTTCTTCAACGAATTTC--------------
A001Ensemble       AGCATGTGGTGTGAGCTGGAACAGGAGAACTTCTTCAACGAATTTCAAATGGAGGGTGTC
                   *********************************************
A001sequenced      ------------------------------------------------------------
```

```
A001Ensemble       TCTGCAGAAAACAATGAGATTTATTTAGAGCTAACATCGGAAAACTTATCTCGAGCCTTG

A001sequenced      ------------------------------------------------------------

A001Ensemble       AAGACTGCCCAGAATGCCAGGGCTTTGAAAATCAAACTGACTAATAAACACTTTCCCTGC

A001sequenced      ------------------------------------------------------------

A001Ensemble       CTCACGGTCTCCGTGGAGCTGTTATCTATGTCAAGCAGTAGCCGCATTGTGACCCATGAC
```

GAACCACTTCACACGAATCAGTAAC forward primer

CAGGAGAACTTCTTCAACGAATTTC reverse primer

2.7 *hHUS1-005* as a short sequence that was amplified from human brain (Figure 4-5)

```
A005sequenced      ------------------------------------------------------------

A005Ensemble       ACAGAGGCCCGCCGCGGCTGCGCCATCCGCGGCCATGAAGTTTCGGGCCAAGATCGTGGA

A005sequenced      ------------------------------------------------------------

A005Ensemble       CGGGGCCTGTCTGAACCACTTCACACGTGAGCAGGGAGGCCGGAGAGGAGCGAGGGAGGA

A005sequenced      -----------CAGTGAGCGCGCGGAATCAGTAACATGATAGCCAAGCTTGCCAAAACCT

A005Ensemble       ACGGAAGGAAGCAGTGAGCGCGCGGAATCAGTAACATGATAGCCAAGCTTGCCAAAACCT

                           **************************************************

A005sequenced      GCACCCTCCGCATCAGCCCTGATAAGCTTAACTTCATCCTTTGTGACAAGCTGGCTAATG

A005Ensemble       GCACCCTCCGCATCAGCCCTGATAAGCTTAACTTCATCCTTTGTGACAAGCTGGCTAATG

                   ************************************************************

A005sequenced      GAGGAGTGAGCATGTGGTGTGAGCTGGAACAGGAGAACTTCTTCAACGAATTTC------

A005Ensemble       GAGGAGTGAGCATGTGGTGTGAGCTGGAACAGGAGAACTTCTTCAACGAATTTCAAATGG

                   ******************************************************

A005sequenced      ------------------------------------------------------------

A005Ensemble       AGGGTGTCTCTGCAGAAAACAATGAGATTTATTTAGAGCTAACATCGGAAAACTTATCTC

A005sequenced      ------------------------------------------------------------

A005Ensemble       GAGCCTTGAAGACTGCCCAGAATGCCAGGGCTTTGAAAATCAAACTGACTAATAAACACT
```

CAGTGAGCGCGCGGAATCAGTAAC forward primer

CAGGAGAACTTCTTCAACGAATTTC reverse primer

2.8 *hHUS1-004* as a short sequence that was amplified from human brain tissue (Figure 4-5)

```
A004sequenced      ------------------------------------------------------------
A004Ensemble       ACAGAGGCCCGCCGCGGCTGCGCCATCCGCGGCCATGAAGTTTCGGGCCAAGATCGTGGA
A004sequenced      ------------------------------------------------------------
A004Ensemble       CGGGGCCTGTCTGAACCACTTCACACGTGAGCAGGGAGGCCGGAGAGGAGCGAGGGAGGA
A004sequenced      ACGGAAGGAAGCAGAATCAGTAACATGATAGCCAAGCTTGCCAAAACCTGCACCCTCCGC
A004Ensemble       ACGGAAGGAAGCAGAATCAGTAACATGATAGCCAAGCTTGCCAAAACCTGCACCCTCCGC
                   ************************************************************
A004sequenced      ATCAGCCCTGATAAGCTTAACTTCATCCTTTGTGACAAGCTGGCTAATGGAGGAGTGAGC
A004Ensemble       ATCAGCCCTGATAAGCTTAACTTCATCCTTTGTGACAAGCTGGCTAATGGAGGAGTGAGC
                   ************************************************************
A004sequenced      ATGTGGTGTGAGCTGGAACAGGAGAACTTCTTCAACGAATTTC-----------------
A004Ensemble       ATGTGGTGTGAGCTGGAACAGGAGAACTTCTTCAACGAATTTCAAATGGAGGGTGTCTCT
                   ****************************************
A004sequenced      ------------------------------------------------------------
A004Ensemble       GCAGAAAACAATGAGATTTATTTAGAGCTAACATCGGAAAACTTATCTCGAGCCTTGAAG
A004sequenced      ------------------------------------------------------------
A004Ensemble       ACTGCCCAGAATGCCAGGGCTTTGAAAATCAAACTGACTAATAAACACTTTCCCTGCCTC
```

ACGGAAGGAAGCAGAATCAGTAAC forward primer

CAGGAGAACTTCTTCAACGAATTTC reverse primer

2.9 *hHUS1B* as a short sequence that was amplified from human brain tissue (Figure 4-5)

```
HUS1Bsequenced      ----CTTCCCTGTGGCATCATGAAGTTTCGCGCCAAGATCACCGGCAAAGGCTGTCTAGA
HUS1BEnsemble       CTGCCTTCCCTGTGGCATCATGAAGTTTCGCGCCAAGATCACCGGCAAAGGCTGTCTAGA
                        ********************************************************
HUS1Bsequenced      GCTGTTCATTCACGTCAGCGGCACCGTCGCGAGGCTAGCGAAGGTCTGCGTGCTCCGCGT
HUS1BEnsemble       GCTGTTCATTCACGTCAGCGGCACCGTCGCGAGGCTAGCGAAGGTCTGCGTGCTCCGCGT
```

```
                    ************************************************************

HUS1Bsequenced      GCGCCCTGACAGCCTGTGCTTCGGCCCCGCGGGTTCCGGCGGCCTCCACGAGGCCAGGCT

HUS1BEnsemble       GCGCCCTGACAGCCTGTGCTTCGGCCCCGCGGGTTCCGGCGGCCTCCACGAGGCCAGGCT

                    ************************************************************

HUS1Bsequenced      ------------------------------------------------------------

HUS1BEnsemble       GTGGTGCGAGGTGCGGCAGGGGGCCTTCCAGCAGTTTCGCATGGAAGGTGTCTCGGAAGA

HUS1Bsequenced      ------------------------------------------------------------

HUS1BEnsemble       TCTCGATGAGATCCACCTGGAGCTGACGGCGGAGCACCTGTCCCGGGCGGCGAGAAGCGC

HUS1Bsequenced      ------------------------------------------------------------

HUS1BEnsemble       AGCGGGCGCGTCCTCCCTGAAGCTGCAGCTGACCCACAAGCGCCGCCCCTCCCTCACGGT

HUS1Bsequenced      ------------------------------------------------------------

HUS1BEnsemble       GGCGGTGGAGCTGGTCTCGTCCCTGGGCCGCGCTCGCAGCGTGGTGCACGATCTGCCCGT

CTTCCCTGTGGCATCATGAAGTTTCG forward primer

GGCCTCCACGAGGCCAGGCT reverse primer
```

3. Confirmation of *hHUS1-001*, *hHUS1-005* and *hHUS1-011* existence in human cells using primers that are more specific (Figure 4-7)

3.1 Alignment of the four-*hHUS1* cDNAs as curated in the Ensembl database.

The new forward primers for *hHUS1-001, 005* and *011* are shown in blue, yellow and red, respectively. The previous reverse primers are shown in grey and the new reverse primer specific for the *hHUS1-001* 3`-UTR is shown in brown. The alignement was produced by Clustal Omega: (http://www.ebi.ac.uk/Tools/msa/clustalo/).

```
HUS1-001      ----------GCCGCGGCTGCGCCATCCGCGGCCATGAAGTTTCGGGCCAAGATCGTGGA     50
HUS1-005      ACAGAGGCCCGCCGCGGCTGCGCCATCCGCGGCCATGAAGTTTCGGGCCAAGATCGTGGA     60
HUS1-011      ------------------------------------------------AAGATCGTGGA     11
HUS1-004      ACAGAGGCCCGCCGCGGCTGCGCCATCCGCGGCCATGAAGTTTCGGGCCAAGATCGTGGA     60
                                                              ***********

HUS1-001      CGGGGCCTGTCTGAAC------------------------------------------     66
HUS1-005      CGGGGCCTGTCTGAACCACTTCACACGTGAGCAGGGAGGCCGGAGAGGAGCGAGGGAGGA     120
HUS1-011      CGGGGCCTGTCTGAACCACTTCACACTA----------------------------AT     41
HUS1-004      CGGGGCCTGTCTGAACCACTTCACACGTGAGCAGGGAGGCCGGAGAGGAGCGAGGGAGGA     120
              ****************

HUS1-001      --------------CACTTCACACGAATCAGTAACATGATAGCCAAGCTTGCCAAAACCT     112
HUS1-005      ACGGAAGGAAGCAGTGAGCGCGCGGAATCAGTAACATGATAGCCAAGCTTGCCAAAACCT     180
HUS1-011      TCCTTATTTTAACCCCTGCTTTAGGAATCAGTAACATGATAGCCAAGCTTGCCAAAACCT     101
HUS1-004      ACGGAAGGAA-----------GCAGAATCAGTAACATGATAGCCAAGCTTGCCAAAACCT     169
                                 . ***********************************

HUS1-001      GCACCCTCCGCATCAGCCCTGATAAGCTTAACTTCATCCTTTGTGACAAGCTGGCTAATG     172
HUS1-005      GCACCCTCCGCATCAGCCCTGATAAGCTTAACTTCATCCTTTGTGACAAGCTGGCTAATG     240
HUS1-011      GCACCCTCCGCATCAGCCCTGATAAGCTTAACTTCATCCTTTGTGACAAGCTGGCTAATG     161
HUS1-004      GCACCCTCCGCATCAGCCCTGATAAGCTTAACTTCATCCTTTGTGACAAGCTGGCTAATG     229
              ************************************************************

HUS1-001      GAGGAGTGAGCATGTGGTGTGAGCTGGAACAGGAGAACTTCTTCAACGAATTTCAAATGG     232
HUS1-005      GAGGAGTGAGCATGTGGTGTGAGCTGGAACAGGAGAACTTCTTCAACGAATTTCAAATGG     300
HUS1-011      GAGGAGTGAGCATGTGGTGTGAGCTGGAACAGGAGAACTTCTTCAACGAATTTCAAATGG     221
HUS1-004      GAGGAGTGAGCATGTGGTGTGAGCTGGAACAGGAGAACTTCTTCAACGAATTTCAAATGG     289
              ************************************************************

                                      .

                                      .

HUS1-001    CTCACAGCACCGCACATCGACACACTGTACTTATTTGTCCCTCTCTAACATTTTAACTAA    1012
HUS1-005    CTCACAGCACCGCACATCGACACACTGTACTTATTTGTCCCTCTCTAACATTTTAACTAA    1080
HUS1-011    ------------------------------------------------------------    627
```

```
HUS1-004     ------------------------------------------------------------    579
HUS1-001     AAGTTGATTCAACAACACACAGTTGGATAAACATATCACTTCATGTTGCTCATGTCTGTT    1072
HUS1-005     AAGTTGATTCAACAACACACAGTTGGATAAACATATCACTTCATG---------------    1125
HUS1-011     ------------------------------------------------------------    627
HUS1-004     ------------------------------------------------------------    579
HUS1-001     TTGCTTTGTTTTTAAGACACTGAAAAGAAAAGCTAGAATTTATTTATTCAGACTTTAAAG    1132
HUS1-005     ------------------------------------------------------------    1125
HUS1-011     ------------------------------------------------------------    627
HUS1-004     ------------------------------------------------------------    579

                                         .
                                         .

HUS1-001    TGAATGGCTTAAGATTTTATCTTTGTGTAGAATGTGGCTAAAGAAACCTTAGTTGAGATT    2932
HUS1-005    ------------------------------------------------------------    1125
HUS1-011    ------------------------------------------------------------    627
HUS1-004    ------------------------------------------------------------    579

HUS1-001      CAA  2935
HUS1-005      ---  1125
HUS1-011      ---  627
HUS1-004      ---  579
```

3.2 Sequences and expected PCR fragment sizes for the new primer combinations (The colour code is the same as in 3.2)

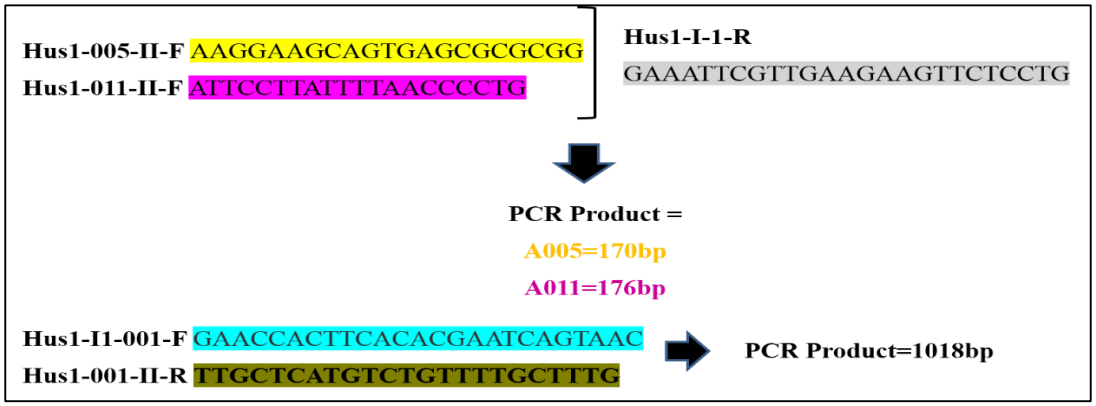

3.3 *hHUS1-005* sequence which was amplified using primers that are more specific (Figure 4-7)

```
A005sample      ------------------------------------------------------------
A005            ACAGAGGCCCGCCGCGGCTGCGCCATCCGCGGCCATGAAGTTTCGGGCCAAGATCGTGGA

A005sample      ------------------------------------------------------------
A005            CGGGGCCTGTCTGAACCACTTCACACGTGAGCAGGGAGGCCGGAGAGGAGCGAGGGAGGA

A005sample      --------AAGCAGTGAGCGCGCGGAATCAGTAACATGATAGCCAAGCTTGCCAAAACCT
A005            ACGGAAGGAAGCAGTGAGCGCGCGGAATCAGTAACATGATAGCCAAGCTTGCCAAAACCT
                        **************************************************

A005sample      GCACCCTCCGCATCAGCCCTGATAAGCTTAACTTCATCCTTTGTGACAAGCTGGCTAATG
A005            GCACCCTCCGCATCAGCCCTGATAAGCTTAACTTCATCCTTTGTGACAAGCTGGCTAATG
                ************************************************************

A005sample      GAGGAGTGAGCATGTGGTGTGAGCTGGAACAGGAGAACTTCTTCAACGAATTTC------
A005            GAGGAGTGAGCATGTGGTGTGAGCTGGAACAGGAGAACTTCTTCAACGAATTTCAAATGG
                ********************************************************
A005sample      ------------------------------------------------------------
A005            AGGGTGTCTCTGCAGAAAACAATGAGATTTATTTAGAGCTAACATCGGAAAACTTATCTC

A005sample      ------------------------------------------------------------
A005            GAGCCTTGAAGACTGCCCAGAATGCCAGGGCTTTGAAAATCAAACTGACTAATAAACACT
```

AAGGAAGCAGTGAGCGCGCGG forward primer

CAGGAGAACTTCTTCAACGAATTTC reverse primer

3.4 *hHUS1-011* sequence (band no.2) amplified with confirmative primers (Figure 4-7)

```
A011-2      ------------------------------------AATTCCTTATTTTAACCCCTGC

A011        AAGATCGTGGACGGGGCCTGTCTGAACCACTTCACACTAATTCCTTATTTTAACCCCTGC

                                                ********************

A011-2      TTTAGGAATCAGTAACTTGATAGCCAAGCTTGCCAAAACCAGCACCCTCCGCATCAGCCC

A011        TTTAGGAATCAGTAACATGATAGCCAAGCTTGCCAAAACCTGCACCCTCCGCATCAGCCC

            ***************:**********************:******************

A011-2      TGATAAGCTTAACTTCATCCTTTGTGACAAACTGGCTAATGGAGGAGTGAGCATGTGGTG

A011        TGATAAGCTTAACTTCATCCTTTGTGACAAGCTGGCTAATGGAGGAGTGAGCATGTGGTG

            ****************************.****************************

A011-2      TGAGCTGGAACAGGAGAACTTCTTCAACGAATTTC-------------------------

A011        TGAGCTGGAACAGGAGAACTTCTTCAACGAATTTCAAATGGAGGGTGTCTCTGCAGAAAA
```

```
                ***********************************

A011-2          ------------------------------------------------------------

A011            CAATGAGATTTATTTAGAGCTAACATCGGAAAACTTATCTCGAGCCTTGAAGACTGCCCA

AATTCCTTATTTTAACCCCTG forward primer

CAGGAGAACTTCTTCAACGAATTTC reverse primer
```

4. Investigation of a possible N-terminal variant of hHus1-005

Primers sequences and their PCR product size of the N-terminal very short hHUS1-005 transcript. The color code is the same as in Figure 4-8.